In vitro Studies on the Genotoxicity of Selected Pyrrolizidine Alkaloids

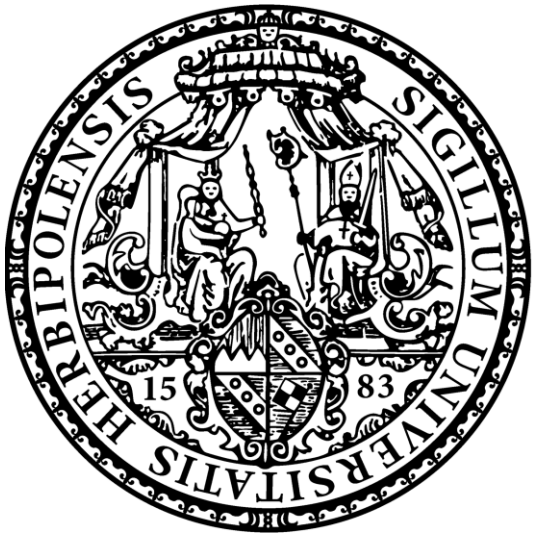

In-vitro-Studien zur Genotoxizität ausgewählter Pyrrolizidinalkaloide

Dissertation for Submission to a Doctoral Degree at the Graduate School of Life Sciences,

Julius-Maximillian-University of Wuerzburg, Germany

Section: Biomedicine

Department: Institute of Pharmacology and Toxicology

Submitted by:

Naji Said Aboud Hadi

From

Malindi, Kilifi County, Kenya

Wuerzburg, 2024

Submitted on: ……..……..

Office stamp

Members of Thesis Committee:

Chairperson: Prof. Dr. Uwe Gbureck

Primary Supervisor: Prof. Dr. Helga Stopper

Supervisor (Second): Prof. Dr. Leane Lehmann

Supervisor (Third): Prof. Dr. Markus Christmann

Date of Public Defense: ……..

Date of Receipt of Certificates: ……...

TABLE OF CONTENTS

LIST OF FIGURES

LIST OF TABLES

LIST OF ABBREVIATIONS

ALARA	As low as reasonable achievable
ATP	Adenosine triphosphate
BCRP	Breast cancer resistance protein
BfR	Bundesinstitut für Risikobewertung; Federal Institute for Risk Assessment
BfArM	Bundesinstitut für Arzneimittel und Medizinprodukte; Federal Institute for Drugs and Medical Devices
BSEP	Bile salt export pump
BN	Binucleated
$BMDL_{10}$	Benchmark dose lower confidence limit 10%
b.w.	Body weight
CBMN	Cytokinesis-Block Micronucleus Assay
CES	Carboxylesterases
CES1	Carboxylesterase subfamily type 1
CES2	Carboxylesterase subfamily type 2
CONTAM	EFSA Scientific Panel on Contaminants in the Food Chain
COT	Committee on Toxicity of Chemicals in Food, Consumer Products and the Environment
CYP 450	Cytochrome P450 enzyme
CYP3A	Cytochrome P450 isoform types 3A
CYP3A4	Cytochrome P450 isoform type 3A4 isoenzyme
CYP3A5	Cytochrome P450 isoform type 3A5 isoenzyme
CYP3A7	Cytochrome P450 isoform type 3A7 isoenzyme
DNA	Deoxyribonucleic acid
DSB	Double strand breaks
ED	Echimidine
EFSA	European Food Safety Authority
e.g.	For example
EMA	European Medicines Agency

ER	Endoplasmic reticulum
Ep	Europine
G:C	Guanine: Cytosine
GSH	Glutathione (γ-L-Glutamyl-L-cysteinylglycine)
GPx	Glutathione peroxidase
GSR	Glutathione reductase
GSSG	Glutathione disulphide
GST	Glutathione-S-transferase
g/mg/µg	Gram/Milligram/Microgram
HMTs	Hepatic membrane transporters
HSEC	Hepatic sinusoidal endothelial cells
HSOS	Hepatic sinusoidal obstruction syndrome
HVOD	Hepatic veno-occlusive disease
HMPC	Committee on Herbal Medicinal Products
H_2O_2	Hydrogen peroxide
IARC	International Agency for Research on Cancer
IPCS	International Programme on Chemical Safety
Las	Lasiocarpine
LOD	Limit of detection
LOQ	Limit of quantification
Ly	Lycopsamine
MDBK	Mardin-Darby bovine kidney epithelial cells
MDR 1	Multidrug resistance protein 1
MDR3	Multidrug resistance protein 3
M/mM/µM	Molar/Millimolar/Micromolar
mA	Milli amps
MN	Micronucleus
MNi	Micronuclei
MoE	Margin of exposure
MGE	Micro-gel electrophoresis

MRPs	Multidrug resistance-associated proteins
MRP1	Multidrug resistance-associated protein 1
MRP2	Multidrug resistance-associated protein 2
MRP3	Multidrug resistance-associated protein 3
MRP4	Multidrug resistance-associated protein 4
MRP5	Multidrug resistance-associated protein 5
MRP6	Multidrug resistance-associated protein 6
NATs	N-acetyltransferases
NaOH	Sodium hydroxide
NBUDs	Nuclear buds
NOAEL	No observed adverse effect level
NOEL	No observed effect level
NFR	Nelfinavir
NPBs	Nucleoplasmic bridges
NTCP	Sodium-dependent taurocholate co-transporting protein
NTP	National Toxicology Program of the U.S. Department of Health and Human Services
OECD	Organization for Economic Co-operation and Development
OCT	Organic cationic transporters
OCT1	Organic cationic transporters subtype 1
OCT2	Organic cationic transporters subtype 2
OCT3	Organic cationic transporters subtype 3
OATs	Organic anionic transporters
OAT2	Organic anionic transporters subtype 2
OAT7	Organic anionic transporters subtype 7
OATPs	Organic anion transporting polypeptides
OATP1B1	Organic anion transporting polypeptides subtype 1B1
OATP1B3	Organic anion transporting polypeptides subtype 1B3
OATP2B1	Organic anion transporting polypeptides subtype 2B1
O_2. -	Superoxide radicals’

.OH	Hydroxyl radicals
IARC	International Agency for Research on Cancer
IPCS	International Programme on Chemical Safety
PA	Pyrrolizidine alkaloid
PAs	Pyrrolizidine alkaloids
P-gp	P-glycoprotein
Q	Quinidine
REP	Relative potency factor
RT	Retrorsine
Rid	Riddelliine
RS	Reactive species
ROS	Reactive oxygen species
RNA	Ribonucleic acid
Rpm	Revolutions per minute
Sc	Seneciphylline
SCGE	Single cell gel electrophoresis
SSB	Single strand breaks
-SH	Sulfhydryl group
SULTs	Sulfotransferases
TDI	Tolerable daily intake
TTC	Threshold of Toxicological Concern
T: A	Thymine: Adenine
UDS	Unscheduled DNA synthesis
UGT	Uridine diphosphate glucuronyltransferase
V	Voltage

CHAPTER ONE

1 INTRODUCTION

1.1 Background to the study

Recently, pyrrolizidine alkaloids (PAs) have been receiving massive attention globally due to their widespread occurrence in several plant species which are relevant for human and animal consumption, their toxicological effects and pharmacological properties **[1]**. PAs are naturally present in plants as ester alkaloids and are considered among the most hepatotoxic substances that affect humans, livestock and wildlife. In humans, most PAs can cause recurring episodes of hepatotoxicity. For example, numerous case reports worldwide have been reported on human consumption of PA-containing products causing hepatotoxicity **[1, 2]**. PAs require metabolic activation in the liver to induce hepatic toxicity through essential hepatic abundant metabolic enzymes, mainly of the cytochrome P450 (CYP 450) family **[3]**. There are hundreds of different PAs and their derivatives which are known. To-date new PAs continue to be identified in both new and previously studied plant species.

Generally, PAs are found as cross-contaminants in various human consumption products such as spices, honey, wheat, botanicals and botanical preparation products including herbal teas, herbal medicines and herbal food supplements which are widely marketed all over the world. Notably, the human consumption of these botanical products is increasingly high and various reported cases of adverse effects upon consumption of botanicals and botanical preparation products are also on the rise globally **[4]**.

To date, there are no human epidemiological data regarding the carcinogenicity of PAs to humans, yet several PAs have been classified as possibly carcinogenic to humans (group 2B) (IARC, 1976) based on various experimental animal studies. Due to the fact that there is a further increase in the production, manufacturing and consumption of these botanical and botanical preparation products, there is concern that contamination of PAs to humans may become more rampant and serious. Although in most cases their levels are insufficient to cause

acute poisoning, they are frequently consumed in quantities that exceed the maximum daily intake suggested by various regulatory authorities **[5-10]**, which can be a contributory factor to hepatotoxicity. Thus, it is important for human risk assessment to further the investigation of PAs to combat these toxic effects associated with PAs.

PAs occurs in thousands of plant species, mainly in Asteraceae, Boraginaceae, Orchidaceae, and Fabaceae families **[11-13]**. PAs are esters of four necine bases including retronecine-type, heliotridine-type, otonecine-type and platynecine-type. Retronecine-type, heliotridine-type and otonecine-type PAs contain unsaturated necine bases and are toxic, while platynecine-type PAs possess a saturated necine base and are considered to be none or less toxic **[14-19]**. PAs can be classified as monoesters (for example europine, lycopsamine), cyclic-diesters (for example riddelliine, retrorsine) and open-diesters (for example lasiocarpine, echimidine) based on their esterification at the necic acid moiety. The esters of the unsaturated PAs necine base which have 1, 2-double bond are considered to be toxic **[20, 21]**. They require metabolic activation in the liver hepatocytes by CYP 450 enzymes (mainly of the CYP 450-3A4 isoenzyme) to form reactive pyrrolic-metabolites, which can bind to cellular proteins to form pyrrole-protein adducts and cause cytotoxicity **[22-24]**. These reactive metabolites can also bind to cellular DNA to form pyrrole-DNA adducts and induce genotoxicity **[25-27]** or conjugate with the reduced form of glutathione to form pyrrole-GSH conjugates which are then excreted via urinary or biliary way **[14, 28]** or may contribute further to genotoxicity. Certain active metabolites of the unsaturated PAs (1, 2-Dehydro-PAs) are postulated to be the main cause for the toxic effects. For example, in recent in-vitro studies, the genotoxicity of a larger number of PAs has been reported **[29, 30]**. They cause chromosomal damage detected as micronucleus formation and DNA strand breaks detected as enhanced yH2Ax level **[30]**.

PAs-specific (geno-) toxicity has been demonstrated showing considerable structure dependence among the PAs. Due to the strong indication of chemical-structure relationship and toxic potency then, the concept of relative toxic potency (REP) factors was proposed, where PA variants have been divided into four different sub-groups based on their toxic potencies and structural features. However, at the moment there is limited data on the relative toxic potencies of individual PA variants due to poor comparability between studies on various endpoints used.

In addition, due to the genotoxicity and carcinogenicity effects exhibited in the chronic animal studies, there is a perception of no safe PAs threshold concentrations. For example, at first it was suggested to minimize or avoid the exposure of PAs **[31, 32]**. Later, the ``Margin of exposure (MoE) ´´ approach was used, where a reference dose of benchmark dose lower confidence limit 10% (BMDL10; 10% increase in the tumor incidence in the animal experiments) combined with an MoE >10,000 (low level of concern) was used in order to come up with a tolerable daily intake of toxic PAs **[33-35]**. Currently, the risk assessments are mainly based on the rat bioassay carcinogenicity associated with riddelliine, which is assumed to be the most potent PA-variant. Hence, the assumption was made that the toxic potency of all other PAs is equal and shares the same mechanism of toxicity as that of riddelliine. Since, recent in vitro and animal experimental studies have demonstrated that the toxic potencies of PAs may be likely differing by orders of magnitude. Normally, PAs are classified based on their chemical structure and it has become evident that the ester type is relevant for their (geno-) toxicity **[30, 36]**. Therefore, over- or underestimating the risks of the individual PAs in botanical or botanical preparation products could possibly mislead which could easily contribute to their excessive intake or restrict their intake. Hence, a suitable evaluation of individual PAs potency and threshold concentrations could assists the human risk assessment and contribute immensely to guarantee the safety of marketed PA-containing food and herbal products.

1.2 Genomic damage and Carcinogenicity

Genomic damage is one of the major driving forces of carcinogenesis mainly due to deleterious effects to the cellular genetic material in the cells. Genomic damage can be induced by a variety of physical and chemical agents such as xenobiotics and endogenous reactive oxygen species (ROS) that accumulate in cells due to natural metabolic processes **[37]**. Genotoxicants also referred to as genotoxic substances or genotoxins, are agents that have the capability of inducing DNA or chromosomal damage **[38]**. Broadly, genotoxins can be classified as clastogens or aneugens. Clastogens are chemicals or substances that can cause breaks in chromosomes, leading to sections of the chromosomes being deleted, added, or rearranged. Aneugens are chemicals or substances that affect the mitotic spindle apparatus or mitotic machinery, causing

a daughter cell to have an abnormal number of chromosomes. In contrary to clastogens, aneugens do not damage the physical structure of the chromosome, but represent a deletion or insertion of an additional copy of a whole chromosome with an intact centromere **[39]**. One of the sources of DNA damage is exogenous substances such as xenobiotics and phytotoxins; which can induce DNA replication stress or generate free radicals, induce DNA structural changes such as single strand (SSB) or double strand breaks (DSB) in DNA through base modification, helix-distorting bulky lesions, or can induce cross-link of DNA strands **[40]**. In totality, genomic damage can be induced in a cell via DNA adduct formation, DNA cross-links, DNA strand breaks, DNA oxidation and replicative errors **[41]**.

1.2.1 Mitosis and Mitotic defects

In human life, it is important for human cells to divide in order to create new functional cells to replace those that have been damaged. Normally, to undergo this, cells progress through a cell cycle where DNA and cellular components replicate, mature, and finally they divide via a process commonly referred to as mitosis and cytokinesis.

In general, mitosis is a division of the cellular genetic material in a cell into two equal parts while cytokinesis is a division of the cytoplasm of a cell into two roughly equal parts. Mitosis is a dynamic and fundamental process to human life. It is carried out precisely in cells to protect against any errors which can lead to imbalances in chromosomal copy number or rearrangements, or loss of whole/fragments chromosomes. When such errors occur in human cells then tissue homeostasis and development can be disrupted easily leading to diseases such as cancer **[42]**.

Henceforth, it is vital to analyze mitotic defects in cells in order to understand how some xenobiotics or phytotoxins may affect cell division in cells, and hence contribute to genomic damage leading to carcinogenesis. Also, analysis of mitotic defects is critical in providing detail insight as to how certain mitotic disruption can affect the precision of the cell division and how specific cellular structures, molecules, and enzymatic activities contribute to the accuracy of cell division.

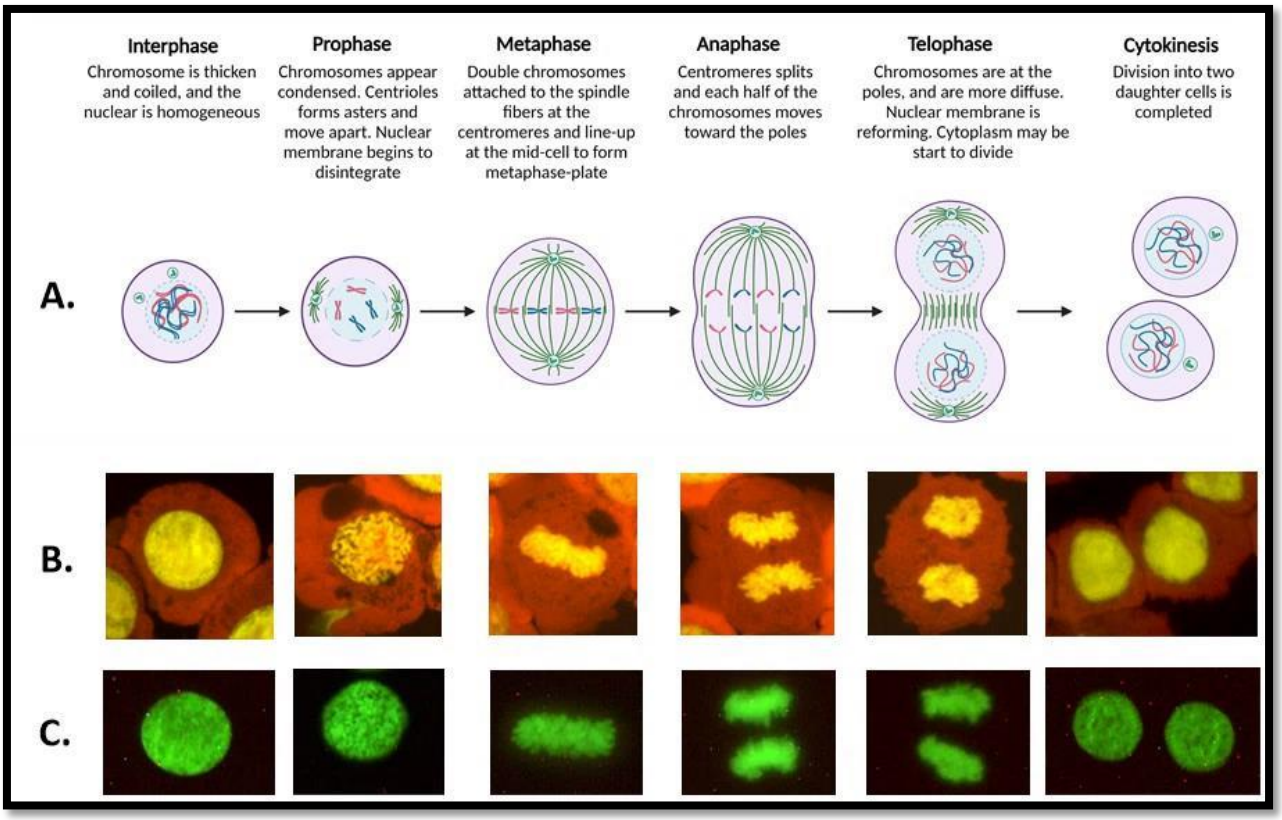

Figure 1: Schematic illustration of the normal cell division cycle (mitosis) **(A)**. Representative images of mitosis process in HepG2 cells **(B)**, while **(C)** is the representative images of mitosis process in HeLa H2B-GFP cells. The schematic illustration was own created using BioRender.com and ChemDraw version 20.1.

Several categories of mitotic defects have been reported. We can have spindle formation defects such as multipolar or chromosomal distribution, and separation defects such as non-congression, chromatin bridges, and lagging chromosomes/chromatids **[42]**.

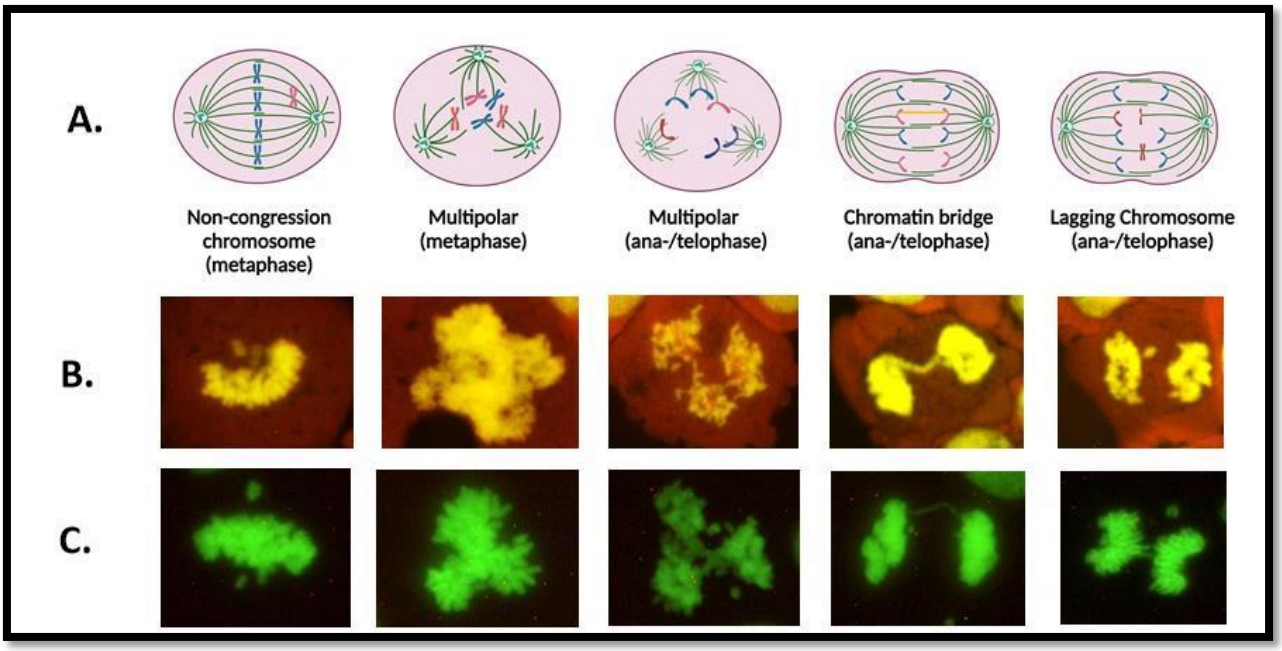

Figure 2: Examples of the common mitotic disturbances. Schematic illustration of the mitotic disturbance **(A)** and their representative images in HepG2 cells **(B)** and HeLa H2B-GFP cells **(C)**. Non-congression chromosome(s) represent a failure of one or more than one chromosome to align in the metaphase-phase during metaphase. Multipolar metaphase represents a display of more than two spindle poles during metaphase. Multipolar Ana-/telophase more than two spindle poles in a cell and chromosome may be segregating in more than two groups during anaphase or chromosome have segregated in more than two groups during telophase. Chromatin Bridge represents a DNA stretched between the two groups of segregating chromosomes in an anaphase or telophase cell. Lagging chromosome is represented as one or more chromosomes position in proximity of the spindle equator (in the middle of the cell) instead of within the main mass of segregating or segregated chromosomes in anaphase or telophase, respectively. The schematic illustration was own created using BioRender.com and ChemDraw version 20.1.

1.2.2 Oxidative stress and Reactive oxygen species

Oxidative stress can cause serious cell damage in humans through formation of reactive species (RS) of various types formed in vivo. These reactive species are very short-lived in cells and they have powerful oxidizing effects capable of damaging DNA in cells leading to serious diseases such as cancer **[43]**. Reactive oxygen species (ROS) are one of the most common reactive species in cells and they include superoxide radicals ($O_2^{\cdot -}$), hydroxyl radicals (.OH), and hydrogen peroxide (H_2O_2). Normally, ROS are important for several human physiological processes, but due to their high reactive oxidizing nature, pathophysiological elevated levels of ROS are capable of damaging DNA and proteins within cells **[44-46]**.

Generally, ROS are produced either as normal by-products of aerobic metabolism or upon xenobiotic stress **[44]** or can be generated at different cell organelles. The main sites of ROS

production are mitochondria, the endoplasmic reticulum (ER), plasma membrane and cytosol; where mitochondria generate almost 90% of the total ROS in the cells hence, making mitochondria the primary source in the cells **[47, 48]**. The mitochondrion is a membrane-bound cell organelle and generates most of the chemical energy (ATP) needed to power the cell's biochemical reactions.

The mitochondrial membrane potential is a crucial marker for mitochondrial health and it is the main driving force for the generation of ATP by the mitochondria. It consists of a proton gradient generated by the mitochondrial respiratory chain complexes which is the main source of ROS formation in mitochondria. This makes the mitochondria a primary source for oxidative stress through ROS formation leading to genomic damage induction **[47, 49, 50]**. For example, various studies have shown ROS play a key role in the development of carcinogenesis via damaging DNA and also acting as tumor promoter **[43, 51, 52]**.

Under normal situation, all living cells have a powerful endogenous anti-oxidative system. There are enzymatic and non-enzymatic anti-oxidative defense mechanisms to combat the effects of oxidative stress. The three major classes of anti-oxidant enzymes are superoxide dismutase, catalases and glutathione peroxidases, while non-enzymatic anti-oxidative defense consists of endogenous molecules such as glutathione (GSH) **[53]**. Also, many synthetic compounds such as N-acetyl cysteine (NAC) and many natural food compounds such as anthocyanins, vitamins and flavonoids show anti-oxidative properties **[54]**. The anti-oxidant defense system controls the levels of ROS formed as a result of normal metabolism or pathological conditions hence preventing the damage that might occur due to ROS **[55, 56]**. Normally, in living organism, there is a balance between the rate of ROS formation and elimination. This balance is commonly referred to as oxidative balance which is important to prevent the living cells from being affected by free radicals; therefore, when the production of ROS in cells exceeds its deactivation with endogenous anti-oxidative system then the oxidative stress manifest in cells leading to genomic damage or cell death **[44, 57]**.

1.2.3 Thiols and importance of thiol as anti-oxidants

In human biological system, thiol plays a vital biological role in the coordination of anti-oxidant defense system in cells due to its strong reducing effects when reacting with ROS. Thiols are a member of the organic compounds commonly referred to as biological mercaptans. They contain sulfhydryl group (-SH) which consist of sulfur atom and hydrogen atom attached to a carbon atom **[58-60]**. Thiols are highly reactive, where the –SH group can readily be oxidized or reduced in the presence of a catalyst. In case of oxidation in the living cells due to ROS; then, the thiol will have the capacity to receive excess electrons and form a disulphide bond. This makes the anti-oxidant ability of thiol-disulphide homeostasis very important in detoxification and as well as enzymatic reactions **[61-63]**. Thiol has been shown in various studies to play an important role in the pathogenesis and prevention of oxidative stress-mediated diseases including cancers. For example, studies have shown that interference of thiol/disulphide homeostasis may act as part in the pathogenesis of various cancers including gastric, endometrial, cervical, breast, prostate and lung **[64-67]**. In addition, it has been exhibited that higher oxidative stress level may cause advanced disease such as cancer to become widespread and aggressive **[67]**. Therefore, based on these facts, it is thought that intervention that can improve thiol status or capacity may highly contribute to the prevention of oxidative stress-related genomic damage diseases such as carcinogenicity.

1.2.4 Glutathione and importance of GSH in anti-oxidant system

Glutathione (GSH) is a tripeptide of low molecular weight intracellular thiol-containing compound. It is made up of three amino acids such as cysteine, glycine, and glutamate. Its main function in human cells is to act as a regulator of intracellular redox homeostasis. GSH is mainly synthesized in the liver and can also be found in all cells within the human body **[68]**. In human cells, it occurs mainly in the cytosol where it plays an important role in the detoxification of xenobiotics and as well as in the anti-oxidant defense system.

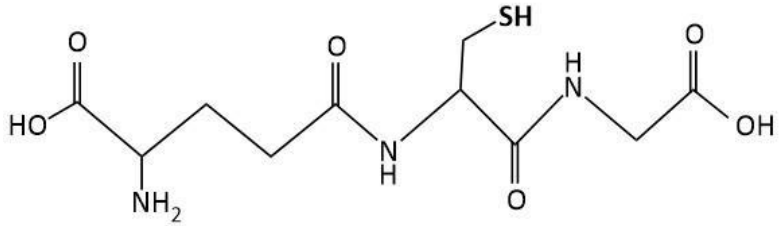

Figure 3: Chemical structure of glutathione (GSH; created using ChemDraw version 20.1)

Usually, there are two forms of GSH in the living human cells: the reduced form glutathione (GSH) and oxidized form glutathione (GSSG). Normally, the presence of GSH inside human cells is primarily in the reduced form which is stored mainly in the nucleus, endoplasmic reticulum, and mitochondria within a cell **[69-71]**. The reduced form GSH accounts for approximately 90-95% of the total GSH inside a cell. The remainder is present in oxidised form (glutathione disulphide, GSSG). And it is the thiol moiety which is inside the side chain of cysteine included in the tripeptide of GSH that plays the main role in anti-oxidant defence, xenobiotic metabolism, and regulation of the cell cycle and gene expression **[72-80]**.

Typically, the thiol group (-SH) of glutathione reduces the number of free radicals such as ROS, via binding to unpaired electrons of free radicals which have been formed due to oxidative stress **[69-71]**. For example, when a cell is under stress; the thiol content changes by being consumed in reactions that protect the cell by removing the harmful compounds, and then it is replaced through either enzymatic reduction of disulphide or by *de novo* synthesis. Hence, these changes in thiol content and metabolism in a cell can interfere with defense signalling pathways **[81]**. Therefore, the intracellular GSH status appears to be a sensitive indicator of the overall health of a cell and its ability to resist toxic challenges. GSH is also important for mitochondrial functioning and the maintenance of mitochondrial DNA **[82]**.

Consequently, GSH can be oxidized by electrophilic substances such as reactive oxygen (ROS) or electrophilic metabolites of the xenobiotics to glutathione disulfide (GSSG). Normally, various toxic substance metabolites bind with GSH covalently in order to form readily excreted mercapturic acid conjugates which are then excreted from the cells through glutathione-S-conjugate transporter **[69]**; this is considered as one of the most vital detoxification pathways. Therefore, in the case when GSH is exhausted or deficient the reactive toxic metabolites cannot

be eliminated by this pathway. Hence, the reactive metabolites will bind covalently to macromolecular components such as DNA and proteins leading to cytotoxicity or genomic damage**[83, 84]**.

In addition, GSH is not only a direct ROS scavenger but also an anti-oxidant that has a key role in the regulation of the intracellular redox status via the glutathione system. Generally, the glutathione system acts as the first line of cellular defense mechanism against ROS. This GSH system consists of glutathione peroxidase (GPx), glutathione reductase (GSR), and glutathione (GSH). Usually, GSH retains its antioxidant ability in its reduced form while GPx catalyzes the reduction of hydrogen peroxide (H_2O_2) to water using GSH as a co-substrate. Thereafter, the GSSG is then reduced to GSH by GSR using NADPH. This cycle between two states of GSH prevents ROS and toxic xenobiotic metabolism. Therefore, the ratio of GSH/GSSG can be considered as a sign of the redox state and relative oxidative stress level in a living organism. So, when a living organism is capable to regenerate GSH through the synthesis of GSH or through reduction of GSSG then this means that the cells in a living organism are successful to counteract and withstand oxidative stress **[44, 69, 85]**.

1.3 Genotoxicity and importance of Genotoxicity testing

In the field of toxicology, genotoxicity is defined as a harmful effect in cells genetic material such as DNA, which can result in affecting the cell´s integrity and function. . The primary effects of genotoxins in living organisms including humans can be mutation, teratogenic or cancer. The genotoxic substance mainly induces cell damage to the genetic material in the human living cells through interaction with the DNA sequence or structure.

Consequently, genotoxicity testing is an important toxicological end point which can assess sufficiently through the safety assessment process of natural toxins and their metabolites. Mostly it is applied widely at an early screening phase of botanical and botanical preparation products such as herbal medicines and supplements, drugs, food additive, pesticides, and chemical development in order to signal the presence and possibly the levels of potentially carcinogenic or mutagenic effects. It is of these reasons genotoxicity test analysis plays a crucial

role as the major contributor in the testing for carcinogenic potential and identification of natural toxins which are important for regulatory purposes in the human consumption products and industrial applications. Henceforth, genotoxicity testing has become a main requirement for all new xenobiotics or chemicals due to a major public concern on carcinogenicity associated with these xenobiotics or chemicals and their metabolites **[86-88]**.

In general, genotoxicity testing consists of a wider spectrum of endpoints which includes DNA damage, and it is based on in vitro and in vivo approaches. These approaches identify damages of DNA, gene, and chromosomes in order to entail possible human carcinogens and mutagens. The in vitro tests are suitable for assessing primary genotoxicity and there are various genotoxicity test endpoints to examine the genotoxic effects, examples of these test are the micronucleus test, the comet assay, and the analysis of chromosome aberrations.

1.3.1 Micronucleus test

The micronucleus (MN) test is one of the most popular and frequent technique used in genotoxicity testing due to easy and fast scoring of the genomic marker known as micronucleus. The micronucleus was discovered towards the end of 19th century when Howell and Jolly found small inclusions in the blood obtained from cats and rats. These small inclusions were then referred to as `Howell-jolly bodies´ and were then further observed in the erythrocytes of peripheral blood from severely anemic human patients **[89, 90]**. These micronuclei are mainly formed during anaphase from either a whole chromosomes or chromosomal/chromatid fragments that failed to be incorporated in the daughter nuclei due to not attaching correctly with the mitotic spindle during the chromosomal segregation **[91, 92]**.

In addition to misattachment of tubulin, also the defects in kinetochore proteins or in kinetochore assembly, late replication, epigenetic modification of histones, nucleoplasmic bridge formation and gene amplification can also play an important role in the formation of micronuclei **[93]**. Eventually, the dislocated whole chromosomes or chromosomal fragments are then covered with a nuclear membrane and are morphologically similar to the nucleus except that are in smaller sizes when stained with a standard nuclear staining **[94]**.

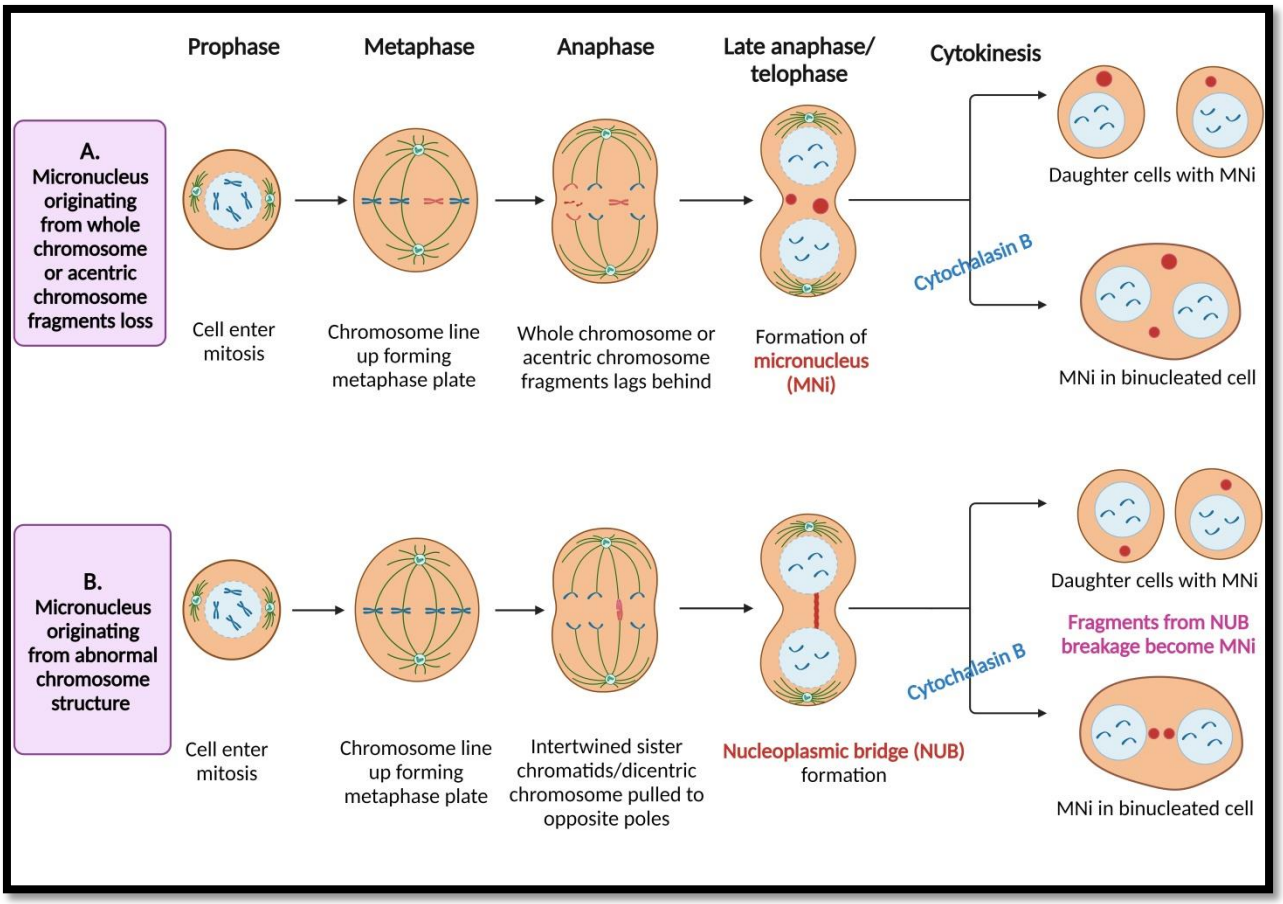

Figure 4: Visual summary of the most common mechanisms that cause micronucleus formation and nucleoplasmic bridge formation. **(A)** Micronucleus formation caused by either a lagging whole chromosome or an acentric chromosome fragments, due to microtubule or kinetochore malfunction **(B)** Nucleoplasmic bridge formation caused by a dicentric chromosome with centromeres pulled to opposite poles of the cell; the nucleoplasmic bridge may break at more than one point and the resulting fragments may become micronuclei. The images were self-created using BioRender.com and ChemDraw version 20.1.

In summary, a micronucleus is an extra-nuclear structure that contains chromosomal fragments and/or whole chromosomes surrounded by nuclear membrane. These chromosomal whole/fragments remnants forming micronuclei can be induced by natural toxins and their reactive metabolites through DNA damage, DNA cross-link, mitotic defects, chromosomal aberrations and oxidative stress. The micronucleus (MN) test can be applied in in vitro and in vivo approaches and in both approaches the tests are rapid and highly reliable. They have the capability to identify a wide range of DNA damage at the chromosomal level **[95]**.

Moreover, the MN assay is also considered the only method among the genotoxicity tests to detect aneuploidy induced by xenobiotics or genotoxins **[96]**. Furthermore, the development of

the cytokinesis-block technique with the application of the cytokinesis inhibitor cytochalasin B in the micronucleus test has led to a comprehensive system for measuring DNA damage, cytostasis and cytotoxicity. This technique (CBMN) has limited micronucleus scoring to cells that have divided once since test substances were added. In this technique, DNA damage events are scored specifically in once-divided binucleated (BN) cells and include (a) micronuclei (MNi), a biomarker of chromosome breakage and/or whole chromosome loss, (b) nucleoplasmic bridges (NPBs), a biomarker of DNA misrepair and/or telomere end-fusions, and (c) nuclear buds (NBUDs), a biomarker of elimination of amplified DNA and/or DNA repair complexes **[97]**.

1.3.2 Comet assay

The comet assay is also one of the most commonly used techniques in genotoxicity testing to detect DNA damage at individual cell levels. It is also commonly referred to as single cell gel electrophoresis (SCGE) or micro-gel electrophoresis (MGE). It was first developed by Ostling and Johansson in 1984 and was then later revised by Singh et al. in 1988 **[98, 99]**. Its principle is based on damaged DNA which migrates more rapidly than the intact DNA during electrophoresis through an agarose gel matrix.

Normally, in this assay the single-cell suspension is covered in agarose on a glass slide and then lysed in high salt and detergent in order to eliminate soluble cell components, membranes, and histones. This result in DNA to be left as nucleoids, consisting of supercoiled DNA loops bound to a matrix. Thereafter, during electrophoresis in the presence of an electric current normally at high PH, DNA breaks relax the supercoiling and relaxed loops of DNA extend in the agarose gel forming a ´comet tail´, which can easily be observed by fluorescence microscopy when stained with a suitable dye. The scoring of the comet tails is time efficient as it is evaluated by using automatized image-analysis software.

The DNA break frequency is then determined by the intensity of ´comet tail´ formed. Due to time efficient, simplicity, sensitivity, versatility, and affordability, the comet assay is increasingly used for genotoxicity testing studies **[100-102]**. Its application has contributed immensely in understanding the mechanism of genotoxicity of xenobiotics and their active metabolites and in performing risk assessment **[103-105]**.

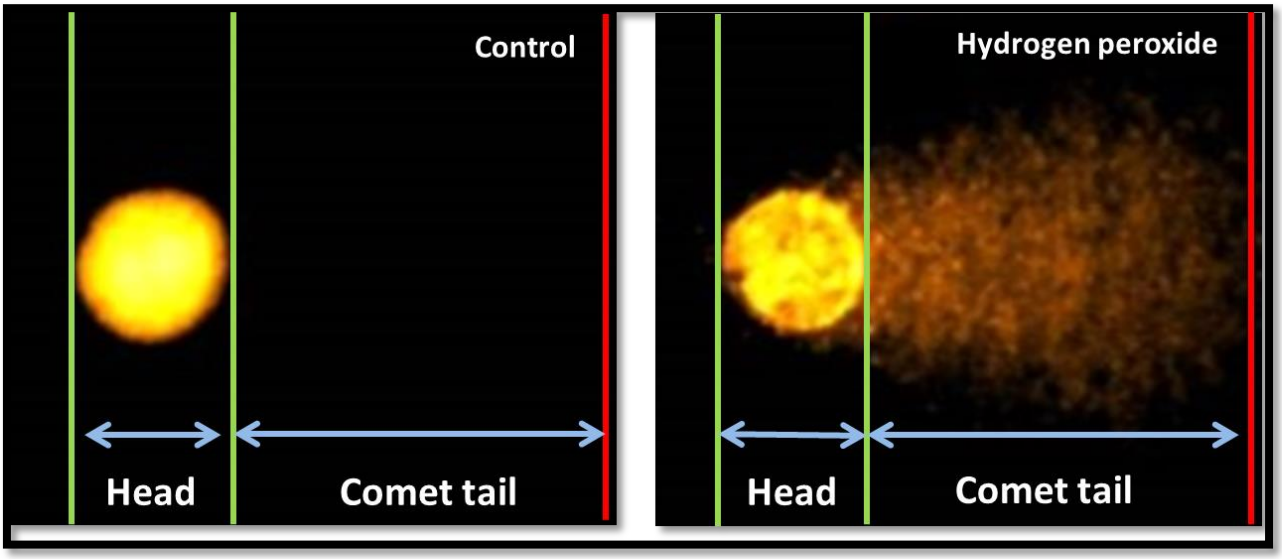

Figure 5: Representative Images of agarose embedded cells under fluorescence microscope. An example for a cell with intact nuclear DNA **(a)** and an example for a cell with DNA damage **(b)**. The comet assay is based on the migration of small DNA fragments (single or double strand breaks) in an electric field. The cells with a damaged DNA, more DNA can migrate than from cells with intact nuclear DNA. The 'Head' part indicates the intact DNA, while the 'Comet tail' indicates the DNA in tail which is damaged. DNA damage is then quantified with specialized software and expressed as percent of DNA in tail.

Consequently, understanding of the DNA migration process and comet formation can clearly suggest the type of the DNA lesions detection under different electrophoresis conditions **[106]**. For example, under alkaline conditions of a standard comet assay protocol, a wide spectrum of DNA lesions can be detected such as single or double strands break as well as alkali-labile sites. In addition, comet assay can also entail the damage DNA bases, DNA crosslinks or direct DNA strands breaks **[107]**. Therefore, several modifications of the comet assay can be designed and employed to reveal a particular type of DNA lesions, extending the range of comet assay utility. For example, modified versions of the standard comet assay protocol can detect oxidized DNA bases and may be used to reveal sites of DNA base loss, and DNA interstrand crosslinks.

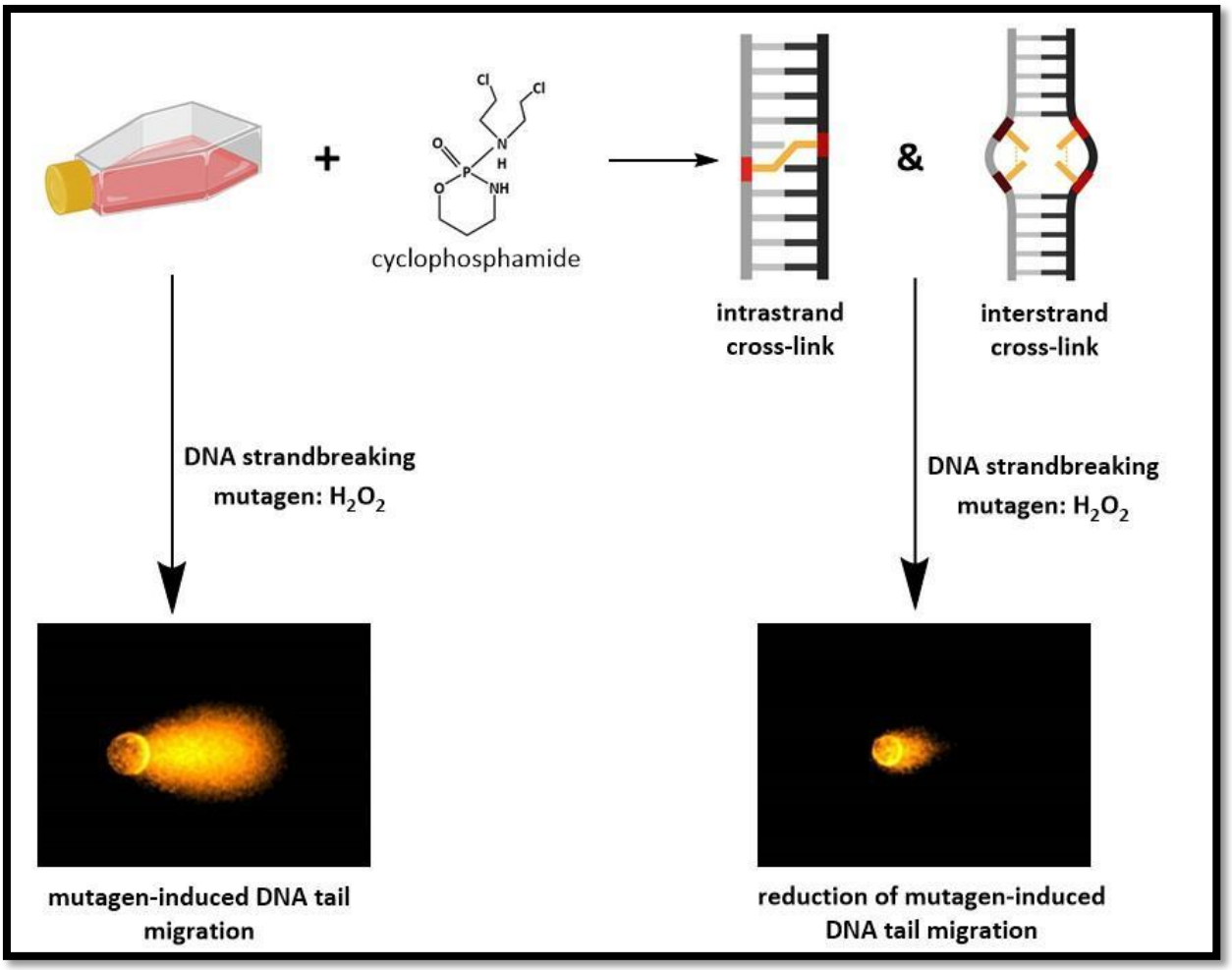

Figure 6: Detection of DNA cross-links by a modified version of standard comet assay. Cross-linked DNA results in bigger fragments after treatment with DNA strand breaking mutagen. The bigger DNA fragments move slower in the electrical field thus, resulting into smaller comets after DNA-staining. The schematic illustration and chemical structure were self-created using BioRender.com and ChemDraw version 20.1.

1.4 Hepatic metabolism and membrane transporters in liver toxicity

Liver is the major target organ for xenobiotics and toxins due to its unique role in drug metabolism, bio activation and detoxification **[108]**. The elucidation of metabolic and transport pathways through which xenobiotic are processed in the liver can contribute a better understanding of liver hepatotoxicity mechanisms. Therefore, a detailed assessment of drug metabolism and transport represents an important approach for better understanding of the

toxicological profile of specific xenobiotics and their metabolites which can also aid in managing risks associated with their potential to cause liver toxicity in humans.

1.4.1 Hepatic drug metabolism in liver

Liver accounts for more than 70% of drug metabolism **[109, 110]**. It is known that approximately 80% of the blood enters the liver via the portal vein and the remaining 20% enters the liver via the hepatic artery. The major cells and basic functional unit in the liver are hepatocytes **[111]**. These hepatocytes are the parenchymal liver cells and occupy almost 80% of the total liver volume and 60% of the total number of liver cells **[112]**. The non-parenchymal liver cells such as endothelial cells and other liver cells accounts for only 6.5% of the liver volume. Liver sinusoidal endothelial cells form a continuous lining of the liver sinusoids which separates hepatocytes and other hepatic cells such as hepatic stellate cells, from sinusoidal blood. Hepatic endothelial cells of liver sinusoids (HSEC) differ in many structural and functional aspects from other endothelial cells of the body. HSEC do not have regular basement membrane, and are often embraced by the cytoplasmic processes hepatic stellate cells. HSEC represent an important filtration barrier between macromolecules and blood cells present in the sinusoidal lumen and hepatocytes that prevents their direct contact, and also determines the exchange of various substances. HSEC also actively participate in the immunological functions of the liver **[112]**.

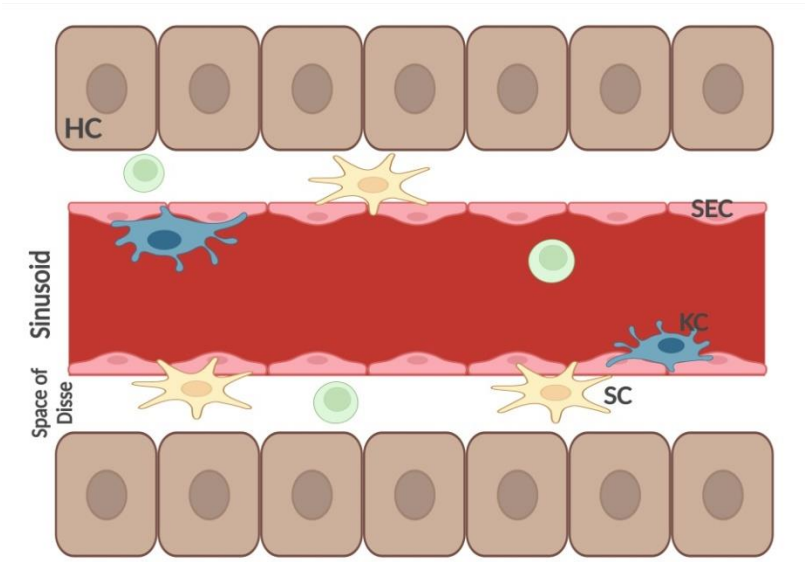

Figure 7: Schematic illustration of the liver. Hepatic sinusoids are composed of sinusoidal endothelial cells (SEC). Hepatic sinusoidal endothelial cells (HSEC) have a critical role in maintaining immune homeostasis within the liver and in mediating the immune response during acute and chronic liver injury. Blood circulates within the sinusoids in the liver. The Space of Disse is a location in the liver between hepatocytes (HC) and a sinusoid. It contains the blood plasma. Microvilli of hepatocytes extend

into this space, allowing proteins and other plasma components from the sinusoids to be absorbed by the hepatocytes. Kupffer cells (KC) are resident liver macrophages and play a critical role in maintaining liver functions; are located to the hepatic sinusoid and are in proximity to other cells in the sinusoid, including sinusoidal endothelial cells (SEC), natural killer and natural killer T cells. Hepatic stellate cells (SC) are located in the space of Disse between the hepatic sinusoidal endothelial cells and hepatocytes; and they play vital roles in liver physiology and fibrogenesis. The schematic figure is self-created using BioRender.com.

In general, drug metabolism in the liver involves breakdown and safe elimination of a parent drug through detoxification pathways. However, under certain conditions these reactions may result in the generation and build-up of harmful reactive metabolites which are more toxic that the parent drug. Normally, drug metabolism involves two phases: Phase I metabolism which mainly involves bio activation or toxification of xenobiotics reactions and Phase II metabolism mainly involves on detoxification of xenobiotics reactions. During phase I reactions, usually the parent drugs undergo biotransformation through addition of functional hydroxyl, carboxyl, amino, or thiol groups which are necessary for the next phase of detoxification, and which makes the compound more hydrophilic.

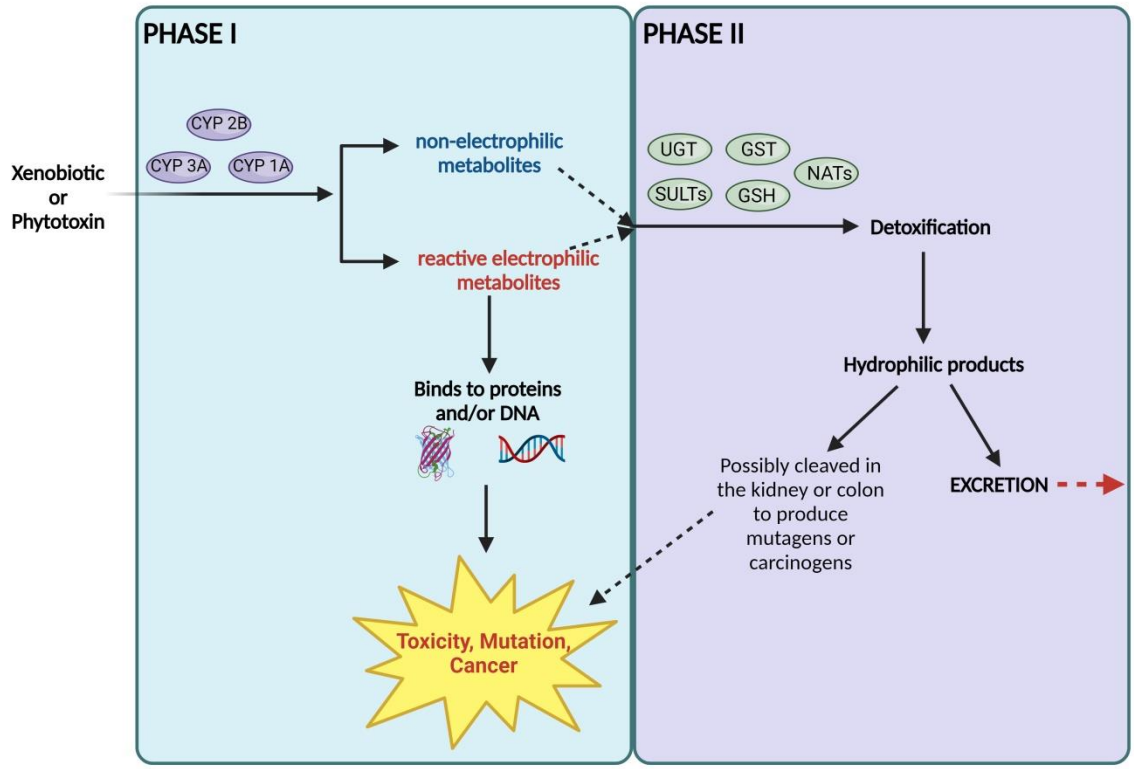

Figure 8: Diagrammatic representation of phase I and phase II xenobiotic metabolizing enzymes and risk of developing cancer. The diagram is self-created using BioRender.com.

The main metabolic enzymes associated with Phase I reactions belong to the cytochrome P450 superfamily, which contributes immensely to the metabolism of a wide range of xenobiotics and endogenous compounds. Phase II metabolism reactions mainly involve conjugation with small endogenous substances, which can further increase hydrophilicity enabling metabolites to be exported into sinusoidal circulation for renal clearance, or into bile. Here, the major enzymes involved include uridine diphosphate glucuronyltransferase (UGT), N-acetyltransferases (NATs), glutathione-S-transferase (GST) and sulfotransferases (SULTs), which conjugate glucuronic acid, acetate, glutathione (GSH) and sulfate, respectively **[113]**.

These Phase II enzymes can also catalyze the formation of reactive metabolites **[114-116]**. For example, it has been reported that carboxylic acid- containing drugs, which have been associated with drug toxicity, can undergo phase II reaction via glucuronidation by UGTs. This results in the formation of reactive acyl glucuronides that may covalently bind to endogenous macromolecules such as DNA and proteins, thus contributing to toxicity **[117-120]**. Reactive metabolites can irreversibly bind to and modify many cellular components including DNA, RNA and proteins. For example, reactive metabolites can bind to hepatic proteins to forms adducts, which can result in an immune response **[116]**. Also, reactive metabolites can lead to depletion of GSH, which may result in an oxidative stress.

i. Cytochrome P450 enzymes

Cytochrome P450 (CYP 450) enzymes are a group of heme monooxygenases which are membrane –bound predominately inside the hepatocytes and are known for their crucial role in metabolism or biotransformation of xenobiotics **[121, 122]**. In humans, CYP 450 enzymes are found and are highly concentrated in the liver cells (hepatocytes) mainly localized in the endoplasmic reticulum (ER) and the inner membranes of mitochondria. However, it has also been reported that CYP 450 can also be sited in the outer nuclear membrane, different Golgi compartments, peroxisomes and the plasma membrane **[123-128]**.

Several human CYP 450 isoenzymes have been identified in the liver **[129]**. Among CYP 450 isoenzymes, the subfamily CYP3A is the major and the main one responsible for the metabolism of about 60% of currently known therapeutic drugs **[130-135]**. For example, the CYP3A

subfamily in humans includes CYP3A4, CYP3A5 and CYP3A7 **[132]**, where the CYP3A4 is the most abundant among the isoenzymes in the human liver (~40%) and metabolizes more than half (>50%) of the currently available therapeutic drugs **[131, 136]**. CYP3A5 isoenzyme accounts for 5–50% of total CYP3A abundance **[137, 138]** and is present in appreciable amounts in about 25% of the human adult population **[139]**. CYP3A7 is the primary fetal isoform and is rarely detected in human adults **[140-147]**.

Notably, the expression levels of these CYP 450 isoenzymes have also been reported to be varying widely between individuals **[148]**. CYP 450s have necessary and important roles in the human body. In addition to bioactivating intermediates or metabolites, several studies have reported that hepatic CYP 450 mediated metabolism of xenobiotic can also generate ROS in the liver. This can increase oxidative stress and contribute to disease development such as carcinogenesis **[149]**. This so because it is known that ROS can modify DNA, which can create mutations and errors in replication **[150]**, and ROS is also known to play a major role in cancer development **[151]**. Henceforth, CYP 450s can play a predominant role in the metabolism of carcinogens that can mitigate cancer development. Thus, inhibitors or inducers of CYP 450 enzymes may potentially be informative in understanding the mechanism of PAs induced genomic damage.

ii. Carboxylesterases enzymes

Carboxylesterases (CES) are a multigene family of enzymes and exist as multiple isomers in humans. These enzymes are members of the serine hydrolase superfamily, in which a serine residue is capable of hydrolysis of ester, amide, or thioester bonds of numerous endogenous and exogenous substrates including phytotoxins and their metabolites **[152-154]**. In humans, CES are extensively distributed in various tissues, mainly in the liver and small intestine **[155]**.

Recently, genomic analysis clearly defined five distinct mammalian CES subfamilies based on genetic sequence and genomic structure **[152, 156]**, but CES1 and CES2 subfamily proteins are the most extensively studied **[157]**. These two forms are dominant in humans and their mRNA expression is highest in the liver **[158]**. Deficiency or abnormal amount of CES1 and/or CES2 is directly linked to human diseases such as cancer **[159, 160]**. Also, some studies have reported

that CES are up-regulated in many cancerous tissues such as pancreatic cancer **[155]**, colorectal cancer **[161]**, lung cancer **[162]** and neuroblastoma **[163]**. Human Hepatoma HepG2 cells have also been reported to express CES1 and CES2, but mainly CES2 in high concentrations **[164]**. They are known to be highly expressed and localized in endoplasmic reticulum (ER) **[165]**. Thus, this suggests an important role of CES in detoxification of xenobiotics and their metabolites **[152]** and could serve as a key determinant for toxicity of ester compounds such as PAs **[155]**.

Therefore, the application of selective inhibitors of this class of enzymes may have importance in modulating the metabolism, distribution and toxicity of agents that are subjected to enzyme hydrolysis **[166]**. Based on these facts, CES enzyme inhibition or induction may play a role in elucidating the mechanism of how the carcinogens or xenobiotics are being detoxified in the human body. Since PAs are ester alkaloids and might be detoxified by this group of CES enzymes, it would be relevant to investigate the involvement of CES in PA-induced genomic damage.

1.4.2 Hepatic membrane transporters in liver

Membrane transporters have a significant role in facilitating or preventing movements of xenobiotics and their metabolites **[167]**. In the liver, before cellular metabolism can occur, xenobiotics or drugs must first enter the hepatocytes where highly lipophilic xenobiotics can easily cross the sinusoidal membrane by a simple process known as passive diffusion. However, in the case of polar or ionized organic xenobiotics the passive diffusion process is not sufficient, hence hepatic transporters are required for the uptake into hepatocytes **[168-170]**. Hepatic transporters are membrane proteins that primarily facilitate nutrient and endogenous substrate transport into the cell via uptake transporters, or protect the cell by pumping out toxic chemicals via canalicular transporters. These transporters can also recognize and transport drugs that are structurally similar to their endogenous transporter substrates **[170]**. Hepatic membrane transporters (HMTs) are mainly distributed in parenchymal liver cells commonly referred to as hepatocytes. These transporters have an important effect in the liver on drug exposure and efficacy and they also play a key role in hepatotoxicity **[171, 172]**.

Consequently, in the liver, hepatic membrane transporters were identified on both the sinusoidal and canalicular membrane which have been shown to have either uptake or excretion function. The function of hepatic transport systems can be affected by interspecies differences and inter-individual variability such as polymorphism. Also, some drugs and disease can affect transporters by causing redistribution of hepatic transporters from the cell surface to the intracellular compartments, leading to changes of hepatic transporter expression and functions. Several studies have reported association of hepatic drug transporters with the liver toxicity due to drugs and active metabolites. Based on their function, these hepatic membrane transporters can be classified into influx and efflux transporters. Usually, the xenobiotic concentration in the liver is determined by the hepatic uptake and biliary excretion, which can further determine the chemical activation and clearance **[173]**. Therefore, actions of these transporters are one of the main determinants of toxicological effects of xenobiotics whose target is in the liver **[174, 175]**.

i. Hepatic Influx transporters

Hepatic influx transporters are also commonly referred to as uptake transporters which are mainly expressed in the basolateral or sinusoidal membrane of hepatocytes **[171, 176, 177]**. Their main function is to allow movement of specific molecules from blood stream in the body into hepatic cytosol of hepatocytes. Several hepatic influx transporters proteins have been identified which include polyspecific organic cationic transporters (OCTs) such as OCT subtype 1/2/3, organic anionic transporters (OATs) such as OAT subtype 2/7, organic anion transporting polypeptides (OATPs) such as OATP subtype 1B1, 1B3, and 2B1, and the sodium-dependent taurocholate co-transporting protein (NTCP).

The OATPs and OATs are mainly responsible for organic anion drug transport and the OCTs are specific transporters for organic cations. The NTCP recognizes drugs with similar structure to bile acid or drugs that bind to taurocholate **[170]**. Among these influx transporters, OATPs and OCTs mediate the uptake of a wide range of xenobiotics in the liver. For example, in humans OATP1B1/1B3 and OCT1/2/3 have been associated with transport of many xenobiotics **[178-185]**. Therefore, the influx hepatic transporters are believed to play a major role in hepatotoxicity through regulation of transport across both cellular and tissue membranes.

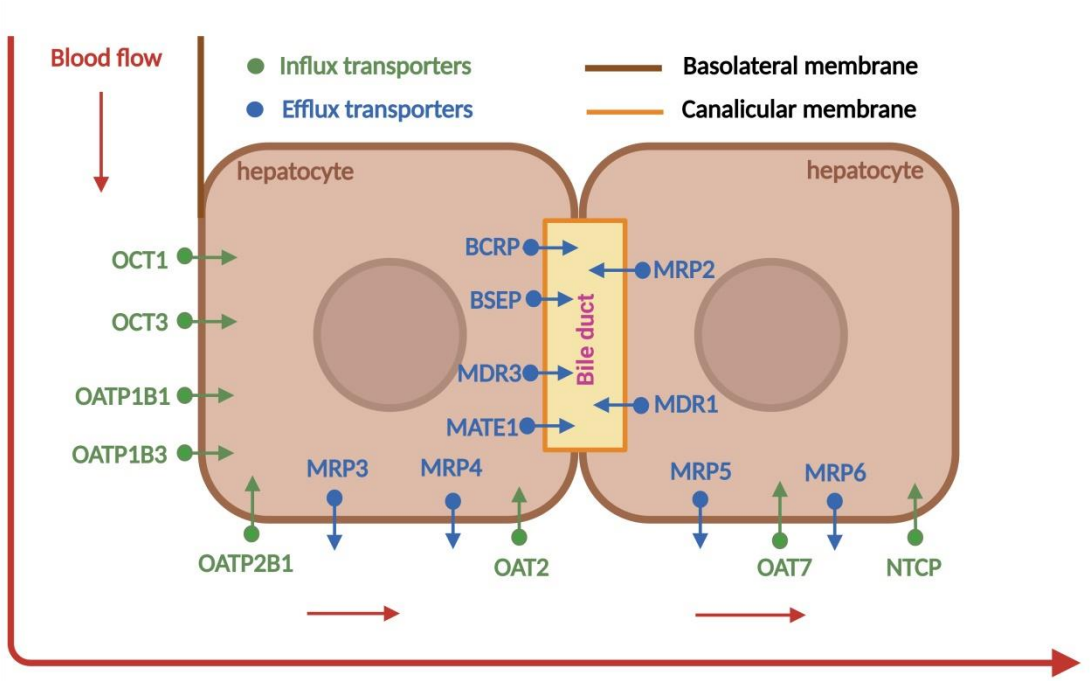

Figure 9: Membrane transporters (influx and efflux) expressed in hepatocytes. The diagrammatic representation was own created using BioRender.com.

ii. Hepatic Efflux transporters

The hepatic efflux transporters are also referred to as excretion transporters which are mainly located in the basolateral and canalicular membrane of hepatocytes. Their main function is to mediate excretion of xenobiotics and their metabolites that have been formed in the hepatocytes from hepatic cytosol to bloodstream in the sinusoids or bile in the bile canaliculi. On the basolateral membrane of hepatocytes, there are multidrug resistance-associated proteins (MRPs) including MRP 1, MRP3, MRP4, MRP5 and MRP6 **[186-188]** whose primary function is pumping drugs back into the blood circulation from the hepatocytes.

On the canalicular membrane, the transporters include P-glycoprotein (P-gp; also known as multidrug resistance protein 1, MDR 1), multidrug resistance-associated protein 2 (MRP2), multidrug resistance protein 3 (MDR3), breast cancer resistance protein (BCRP), multidrug and toxic compound extrusion subfamily 1 (MATE1) and the bile salt export pump (BSEP; mainly mediates the biliary excretion of substrates) **[189]**. Therefore, inhibition of the efflux transporters can play a key role in hepatotoxicity in the liver due to longer exposure of the xenobiotics or its reactive metabolites formed in the hepatocytes.

CHAPTER TWO

2 THEORETICAL FRAMEWORK ON PYRROLIZIDINE ALKALOIDS

2.1 Sources, occurrences and evolution

Pyrrolizidine alkaloids (PAs) are natural phytotoxins which can be found in more than 6000 plant species and almost 3% of the flowering plants worldwide. The main plant families are Asteraceae (mainly the tribes Eupatorieae and Senecioneae), Boraginaceae (most of the genera), Fabaceae (mainly the genus Crotalaria), and Orchidaceae (around ten genera). More than 95% of the PA-containing species which so far are being investigated belong to these four main families **[12, 13, 19, 190-197]**. Their main aim is to protect the plants against herbivores and also to protect plants effectively as insect-feeding deterrents **[19, 197, 198]**. However, these PAs can instigate harm to humans, livestocks and wildlife. In humans, they are usually found as cross-contaminants in human consumption products such as honey, spices, wheat, milk, meat, and botanicals and botanical preparation products such as herbal teas, herbal medicines and dietary supplements **[10, 15, 199-206]**.

Notably, different plant species in these families produce characteristic mixtures of PAs of different chemical features and in varying amounts **[207]**. That is to say, both, composition and concentration of PAs may fluctuate and usually depend on various factors such as species, age and part of plant, variety such as genotype or chemotype, season, location and other related factors **[197, 208, 209]**. Therefore, not all known PAs of PA-containing plants are necessarily present at the same time. The same plant species growing in different locations or in different seasons may contain different PAs **[20, 210]**. These toxins are mainly concentrated in the seeds and the flowering parts of the plant, with decreasing amounts in the leaves, stems and roots **[9, 209]**. For example, most plants species produce mixtures of PAs in varying concentrations ranging from less than 0.001% to 5% in certain plant seeds **[9]**.

In addition, some of these plants families containing PAs are used by humans as ground cover, soil improvers (Fabaceae), ornamental plants, and for animal feed. Also, for example

Boraginaceae family of plants is well appreciated for the quality of their honey **[9]**. Among these plants, the most commonly reported plants associated with food poisoning (excluding use of herbal teas and herbal medicines) in humans are Heliotropium in the family Boraginaceae, and Crotalaria in the family Fabaceae. For example, these occurred as weeds in cereal or legume crops where the seeds were mixed accidentally with the main crop harvest. Hence, the toxins survived the milling, and subsequent processes. This situation can also be aggravated by drought and other conditions that are advantageous to weed growth at the expense of the crop itself **[9]**.

PAs poisoning in animals has been reported and was attributed to Heliotropium, Trichodesma, Senecio, and Crotalaria species. In general, the grazing animals can avoid PA-bearing plants but they may have no choice in the situation of drought or when searching for food on over-grazed or otherwise depleted pastures. Also, if the weedy crops are used for the production of hay or silage the animals can no longer exercise discrimination when feeding because the toxins survive storage processes and are completely intermixed with the fodder. Hence, due to these facts the mortality of grazing animals has also been reported **[9]**.

2.2 Structural features and classification

Several hundred PAs have been isolated from plants and their chemical structures have been well characterized **[20]**. PAs are ester alkaloids composed of a necic acid and necine base moieties **[Figure 10]**.

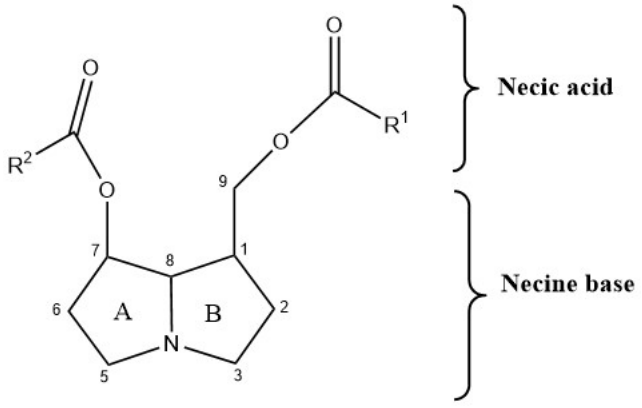

Figure 10: General schematic structure of pyrrolizidine alkaloids (ChemDraw version 20.1).

The necine base comprise of two saturated five-membered rings with a nitrogen atom between them, where sometimes displays a double bond in the 1, 2 position, which has been reported frequently as the main association with enhanced toxicity **[211]**. The necic acid moiety which is the esterified acids consists of one or two carboxylic ester arms at C-7 and/or C-9 positions.

PAs rarely occur in the free form as pyrrolizidine base but instead they are mostly found in the plants in form of tertiary bases or pyrrolizidine alkaloids N-oxides **[212, 213]**. The esters formed in these PAs consist of necine base containing amino alcohols and one or more necic acids, which are the main responsible for their structural diversity **[212]**. Based on these chemical structure necine base and esterification moieties, PAs can be classified diversely. According to the necine base, PAs can be categorized into four main groups such as retronecine, heliotridine, otonecine and platynecine **[Figure 11] [214]**.

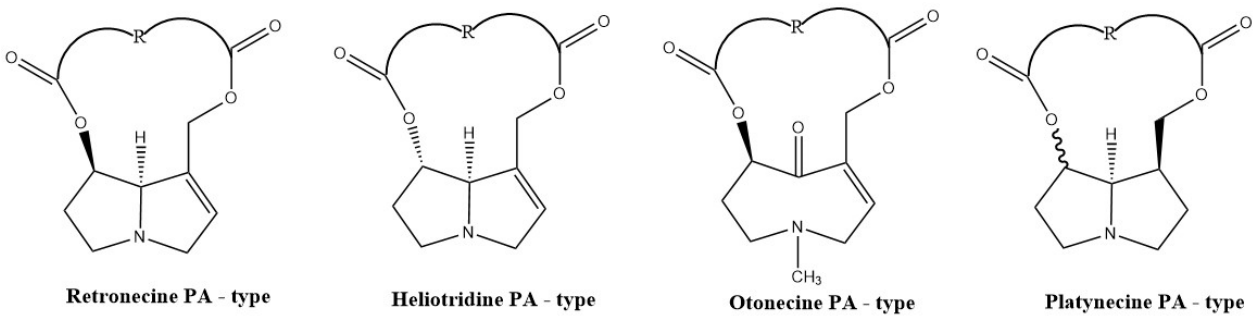

Figure 11: Structural classification of the selected pyrrolizidine alkaloids based on necine bases (ChemDraw version 20.1).

Retronecine-, heliotridine-, and otonecine-types have unsaturated bases at 1, 2 positions, while the platynecine-type is saturated **[215, 216]**. From a chemical structural point of view, otonecine-type is the most distinct among all types, because at position 8 (C-8) the carbon is oxidized and displays a monocyclic ring, thus it differentiates itself from the other groups, which displayed a bicyclic ring **[217-219]**.

In addition, retronecine and heliotridine are diastereomers, which shows a distinct orientation at position 7 (C-7) **[220, 221]**. The platynecine-type PAs does not contain a double bond in the necine base at position C1-C2. Thus, it has been widely been reported that the toxic PAs are esters of unsaturated necines having a 1, 2 double bond **[222, 223]**. The retronecine-type,

heliotridine-type, and otonecine-type PAs contain a C1-C2 double in their necine bases and are considered toxic, while the platynecine-type PAs with saturated necine base have been reported and considered to be non-toxic **[222, 223]**.

Nevertheless, the PAs can also be classified according to the esterification at the necic acid moiety such as monoesters and diesters. The diesters can be sub-grouped further into cyclic-diesters and open-chain diesters **[224, 225]**. It has become evident that the ester type is relevant for their (geno-) toxicity **[18, 196]**.

Table 1: Structural classification of the selected pyrrolizidine alkaloids based on necine base and esterification of the necic acid moieties. Chemical structure were created using Chem Draw software (version 2004).

Compound	PA type	Ester type	Chemical structure
Europine	Heliotridine-type	Monoester	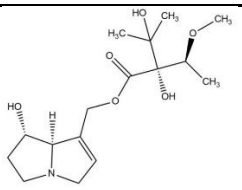
Lycopsamine	Retronecine type	Monoester	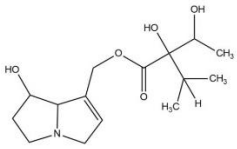
Retrorsine	Retronecine type	Cyclic diester	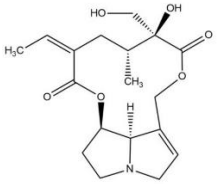
Riddelliine	Retronecine type	Cyclic diester	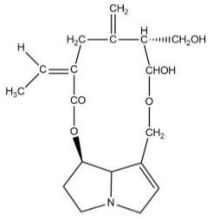
Seneciphylline	Retronecine type	Cyclic diester	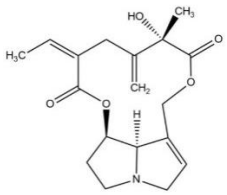

Echimidine	Retronecine type	Open diester	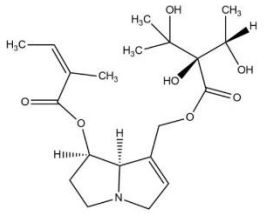
Lasiocarpine	Heliotridine-type	Open diester	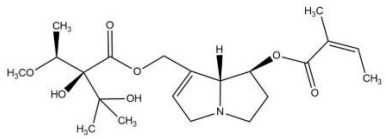

Naturally, hundreds of PAs and their N-oxides have been described up to now and it is assumed that about half of them are hepatotoxic **[11, 15, 195, 226]**. Because of their abundance and toxicities, including hepatotoxicity and carcinogenicity, the retronecine- and heliotridine-derived PAs have received the most attention **[21]**.

The term ``saturated PA´´ is sometimes used to emphasize the fact that there are no double bonds present. The terms ``1, 2-unsaturated´´ or ``1, 2-dehydro´´ PAs indicate that the alkaloids being referred to are modified PAs having a double bond between carbon 1 and 2. The term ``free base´´ means that the nitrogen lone pair electrons on the alkaloids are not protonated by acids or oxidized to N-oxides. The N-oxide forms of PAs occur naturally together with the parent PA molecules. In this thesis, the term ``PAs´´ used by itself refers to saturated and 1, 2-unsaturated PAs and their associated N-oxides. An overview of chemical structural formulae of PAs mention in this thesis is provided in **[Table 1]**.

2.3 Metabolic activation and toxicity

For many decades, the hepatic metabolism of PAs has been extensively studied, both in vitro and in vivo. PAs are generally considered pro-toxins, requiring metabolic activation primarily in the liver. They undergo biotransformation to introduce reactive or polar groups, enabling the formation of polar metabolites for excretion from the body. While the liver is the major organ for PA metabolism, studies have also identified metabolism in other tissues, such as the lungs

[227]. Upon ingestion, PAs are absorbed in the gut and transported to the liver, where hepatic enzymes and macromolecules act on them to facilitate their bioactivation and subsequent excretion.

Basically, there are three principal pathways for PA metabolism, including hydrolysis of PAs to release necine bases and necic acids, N-oxidation to form PA N-oxides, and oxidation of PAs to produce reactive pyrrolic ester metabolites (DHPA) **[Figure 12]**. When PAs are absorbed into tissues like the liver, some of them undergo hydrolysis at the C7-C9 ester bond into necine base and necic acid intermediate moieties. This hydrolysis is facilitated by non-specific esterase enzymes, mainly hepatic cytosolic carboxylesterases (CES). The resulting free necine base and necic acid intermediate moieties are not toxic and undergo further phase II metabolism conjugation to facilitate their excretion via the kidneys and urine **[20, 228-233]**. This metabolic pathway is a crucial detoxification route. For instance, studies have shown that rats are highly susceptible to the toxicity of PAs, partially if not totally, due to the lack of esterase activity in their livers. In contrast, guinea pigs possess marked resistance to the toxic effects of PAs because of their particularly high liver esterase activity **[234]**.

In addition, retronecine- and heliotridine-type PAs, at their necine bases, can undergo a N-oxidation process to form PA N-oxides, while otonecine-type PAs cannot form PA N-oxides because the nitrogen in their necine base is methylated, hindering the formation of PA N-oxides. The metabolism of PAs to their corresponding N-oxides is primarily catalyzed by the presence of both cytochrome P450 and flavin-containing monooxygenase enzymes **[235-237]**. Normally, PA N-oxides are considered detoxification products because these metabolites can be further conjugated for excretion **[238, 239]**. Hence, the process of PAs' metabolism to their corresponding N-oxides has been widely assumed as a detoxification pathway, implying that PA N-oxides are non-toxic or are much less toxic than their parent PAs **[229]**.

However, PA N-oxides can be metabolically converted back to their parent PAs, producing carcinogenic effects if the parent PAs are carcinogenic **[240-243]**. For instance, studies in rats have shown that retrorsine N-oxide and riddelliine N-oxide are toxic, inducing hepatic carcinogenesis and tumorigenesis, respectively **[244, 245]**. Additionally, Yang et al. (2017) **[246]**

demonstrated PA N-oxide-induced hepatotoxicity in mice, similar to its corresponding PAs but with much lower potency. The authors discovered that the toxic mechanism of senecionine N-oxide-induced hepatotoxicity in rats is via its biotransformation to the corresponding PAs followed by the metabolic activation to form pyrrole-protein adducts. Moreover, it was suggested that the low lipophilicity of PA N-oxides resulted in a lower extent of absorption through the cells, making them less toxic than their parent PAs. Thus, the differences in absorption and metabolism between PAs and PA-N-oxides were also attributed to their significant differences in hepatotoxicity potency.

Consequently, pyrrolic ester metabolites (DHPA) are produced through the hydroxylation of the necine base of retronecine- and heliotridine-type PAs at the C3 and C8 positions, forming 3- or 8-hydroxynecine derivatives followed by spontaneous dehydration. For otonecine-type PAs, pyrrolic ester metabolites are generated through oxidative N-demethylation of the necine base followed by ring closure and dehydration **[247]**. These processes to form pyrrolic ester metabolites are mainly catalyzed by cytochromes P-450, specifically CYP3A and CPY2B isoforms. For example, many animal studies have reported that hepatic CYP450, especially CYP3A and CYP2B isoforms, catalyze the metabolic activation of toxic PAs. While there is limited data indicating that human hepatic CYP3A4 isoenzymes mediate the metabolic activation of PAs, despite CYP3A4 being the major abundant CYP450 enzyme in the human liver **[235, 248-251]**. The pyrrolic ester PA metabolites are highly reactive and believed to be the primary metabolites responsible for causing human hepatotoxicity **[232, 252]**. These primary pyrrolic ester (DHPA) metabolites are extremely reactive, with very short half-lives, especially in aqueous environments **[229, 253]**, making these DHPA metabolites challenging to identify in in vivo and in vitro metabolic studies. Therefore, after formation in human hepatocytes, the DHPA ester metabolites can rapidly bind to one or two molecules of GSH to form GSH-conjugates, facilitating their excretion via the urinary or biliary pathways **[14, 28]**. However, He et al. (2017) **[254]** demonstrated that PA-derived GSH-conjugate adducts can bind to cellular DNA, suggesting they might still have some toxic potential.

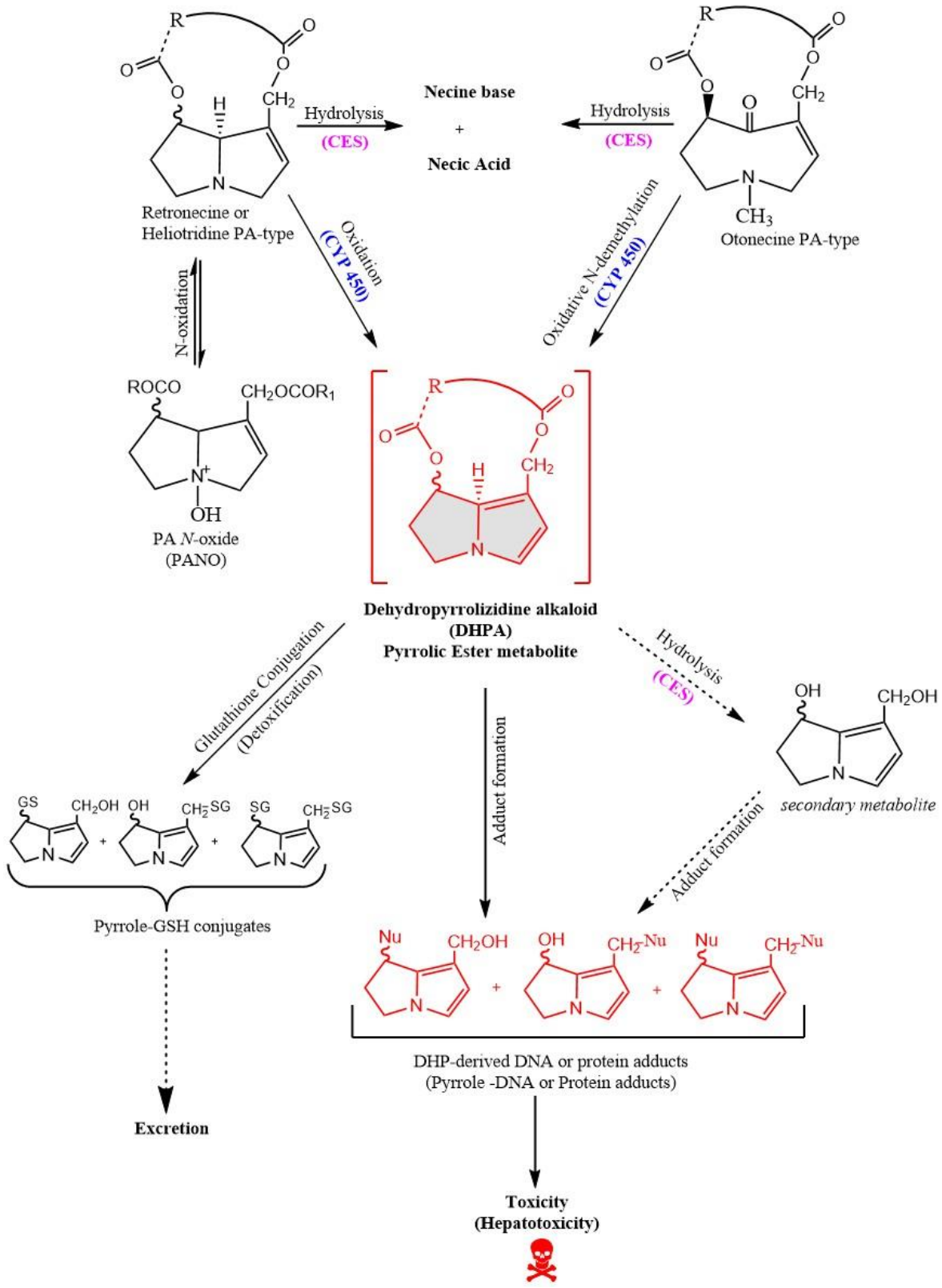

Figure 12: Proposed hepatic metabolic activation of PAs to form primary toxic pyrrolic esters that interact with glutathione (GSH) or DNA or Proteins to form conjugates or adducts (the figure was prepared using ChemDraw version 20.1).

Additionally, when GSH is exhausted in the detoxification of the DHPA pyrrolic ester metabolites, the DHPA ester metabolites will rapidly bind to nucleophilic functional groups such as sulfhydryl (-SH), amino (-NH), and hydroxyl (-OH) on DNA and proteins in the liver. This process produces mixtures of C7 and C9 mono- and di-DHP adducts, and also forms crosslinks between -SH, -OH, and -NH groups on different molecules or on the same macromolecules **[14, 20, 217, 229, 230, 235-237, 241, 255-260]**. It is for these reasons that the metabolic formation of pyrrolic ester (DHPA) metabolites has been considered the primary metabolic activation for the genotoxicity and carcinogenicity of PAs.

In addition, these primary DHPA metabolites can undergo further hydrolysis of pyrrolic esters with the aid of cytosolic carboxylesterases (CES) and be converted to a dehydronecine (DHP) metabolite. This metabolite is also toxic but to a lesser extent compared to the DHPA metabolite, and it has a longer lifespan in the human body. The formation of a DHP metabolite is considered a secondary toxic metabolite, and it has been reported to exhibit antimitotic, mutagenic, and carcinogenic effects **[247, 261]**. Although DHP is less reactive than the precursor DHPA esters, it is still capable of forming DHP adducts with nucleophilic targets in the liver and many extrahepatic tissues **[20]**. Some of the DHP adducts, linked to weaker nucleophilic groups, can also be released into the circulation or transferred to stronger nucleophiles **[20]**. Therefore, the DHP, which is associated with some circulating proteins and other substances such as GSH escaping from the liver, remains potentially active, thereby prolonging toxicity and leading to extrahepatic effects **[20, 262-268]**.

Limited information is available on the metabolism of saturated PAs; however, it is stipulated that the absence of the 1, 2-double bonds in the PAs means that they cannot be converted to DHPA esters or to DHP. Also, based on in vitro studies, it has been demonstrated that abdominal microorganisms are capable of metabolizing PAs, although the metabolites have not yet been clearly characterized **[269-272]**.

2.4 Human exposure and poisoning

Human PA-poisoning cases have been reported and documented in several countries worldwide, including Germany, Britain, Switzerland, China, Hong Kong, India, South Africa and the United States of America **[23]**. Due to numerous case studies reported on PAs; Health and Safety guidelines have been developed by many countries including Germany and international organizations, such as the world Health organization (WHO). However, the cases of PAs-induced poisoning reports are still on a rise.

The human case reports of PA-poisonings, including death cases due PA-containing herbal medicines and herbal teas have been reported to induce liver toxicity. Though, the amount of PA that resulted in the liver toxicity or disease in these reports is generally not well characterized. For example, the earliest case report of PAs to induce liver disease in form of HSOS was reported in 1920 in South Africa; which was mainly due to ingestion of bread made from wheat that was contaminated with Senecio seeds **[273]**.

The epidemic of hepatic veno-occlusive disease (HVOD) and other liver disorders have also been reported in parts of Central Asia, Afghanistan and India **[9]**. In the United States of America, two cases of poisoning were reported in infants following ingestion of infusion of herb known as Gordolobo Yerba by the Mexican American population and it is identified as Senecio longilobus **[203, 274, 275]**. One of the cases was a female 6-month infant (6 kg/body weight) diagnosed with hepatic veno-occlusive disease, which presented with portal hypertension and extensive hepatic fibrosis for over 2 months. Later in time, it was discovered that the PAs were present in plants that were used in the preparation of infusion taken by the infant and were to a large extent identified as riddelliine and the N-oxides of retrorsine, seneciphylline and senecionine. These PAs were largely present in the herb at a concentration of 3 g/Kg free alkaloid and 10 g/Kg N-oxides. Henceforth, it was estimated that the female infant received a total dose of between 70 and 147 mg of PAs for a period of 2 weeks, which corresponds to an intake of 0.8 to 1.7 mg/Kg **[207]**.

In South Africa, a 3.5-month old female infant was admitted in hospital due to diarrhea, vomiting and ascites after have been administered for short-time period treatment with a

traditional herbal remedy, which is commonly referred to as *Muti*. During admission, the infant developed peritoneal inflammation and septicemia and after 3 months of hospital admission the infant died. When the postmortem was done, liver histology confirmed the diagnosis of HVOD. Later, the extracts of the traditional remedy were analyzed using colorimetry and GC-MS. In GC-MS analysis, PAs mainly retrorsine, seneciphylline and platyphylline were identified in the herbal remedy. Meanwhile, in the colorimetric assay indicated a yield of 1 mg/g and 1.2 mg/g **[276]**.

Using the cell culture studies, the same traditional herbal remedy *Muti* indicated a dose-related toxicity with necrosis at high concentrations in human hepatoma cell lines. In comparable to that, a study was also carried out in two hospitals within South Africa, where twenty (20) children suffering from HVOD were identified and thought to be caused by administration of traditional herbal remedies known as *Muti* **[277]**. The age range of these children were 1 month to 7 years, where the mean age at admission in the hospitals was 2 years and 3 months while the female to male ratio was 1:1. The main clinical presentation was ascites of various magnitude and hepatomegaly. The histological findings in all of the biopsy specimens were relevant to veno-occlusive liver disease, where the majority manifest with centrilobular congestion with sinusoidal distension and dilatation. There was a high morbidity and mortality especially in the young infants. Previous consumption of *Muti* was confirmed or suspected in 15 out of the 20 patients and four of the cases on admission urine specimen were available. A simple colorimetric screening test was done on urine samples using a modified method of Birecka et al., **[278]** for the detection of PAs in plants and all the samples confirmed the presence of PAs **[207, 277]**.

In P.R. China, a 54-year-old female was admitted in a hospital in the city of Shanghai, complaining of abdominal distension and loss of appetite for over 4 months. Physical examination was done and revealed jaundice and ascites, while liver biopsy showed histological features indication a diagnosis of hepatic sinusoidal obstruction syndrome (HSOS). The female patient was treated with diuretics and fully recovered 3 months after discharge from the hospital **[205]**. Later it was noted that, before admission to the hospital, the female had consumed one to two cups of home-made herbal wine (*Tusanqi*) daily for about 3 months in

order to treat for traumatic injuries. This cultivated herb from the home of the patient was then identified as Gynura Segetum. Using HPLC-UV-MS analysis, the two hepatotoxic PAs seneciphylline and senecionine were identified in Gynura Segetum and its herbal wine. The concentrations of senecionine and seneciphylline were 1.13 and 0.83 µg/ml, respectively. An LC-MS-based analytical approach was also used to precisely determine serum PA-protein adducts. Hence, the same peak was depicted in the chemically derivative serum sample that was obtained from both the female patient with HSOS and rats administered with Gynura Segetum. In fact, the animals study showed a good correlation of liver injury with the ingestion of Gynura Segetum. The female patient had continuously ingested the home-made herbal wine for about 3 months, which was estimated to approximately 50-100 ml per day. Then, based on the quantitative analysis of PA content in the wine, PA dose was estimated to be approximately 98-196 µg per day (or 0.0016-0.0033 mg/Kg of body weight per day). Henceforth, the protein adduct derived from reactive metabolites of PAs has been suggested to play a key role in PA-induced liver toxicity. Hepatic tissue-bound PA metabolites, especially the pyrrole–protein adduct, appeared to be a reasonable biomarker of PA-induced HSOS **[205, 207]**.

In Germany, a 63-year-old female was admitted in hospital in the city of Munich with vomiting and abdominal pain, which started 3 hours after consumption of approximately 10 leaves (100g) of self-collected Petasites and Tussilago plants **[279]**. These plants belong to family of Asteraceae and the tribe Senecioneae, they are natively found in Europe and parts of western and central Asia. These plants have been reported to contain cyclic diesters hepatotoxic PAs including Senkirkine and Senecionine **[280-284]**. A liver biopsy was performed to a female patient at day 14 and found liver tissues with features of HVOD manifesting with intraluminal fibrin clots in the sinusoids. Three months later, a liver biopsy exhibited further progression of veno-occlusive disease of the liver **[207, 279]**. These human case reports and many other documented reports need to be put into consideration in order to provide reliable information to be used as the basis for human health risk characterization and health-based guidance values.

2.5 Toxicological studies

PAs, especially the 1, 2-unsaturated types have been found to exhibit acute toxicity, chronic toxicity, and genotoxicity. In acute poisoning with these 1, 2-unsaturated PAs, massive hepatic toxicity with hemorrhagic necrosis is observed. Chronic poisoning mainly occurs in liver, lungs, and blood vessels, and causes cell enlargement (megalocytosis), veno-occlusion in liver and lungs, fatty degeneration, nuclei enlargement with increasing nuclear chromatin, loss of metabolic function, inhibition of mitosis, proliferation of biliary tract epithelium, liver cirrhosis, nodular hyperplasia, and adenomas or carcinomas **[20]**.

In the cases of chronic or severe poisoning with PAs, the outbreak has resulted in a high mortality rate. The acute or short-term toxicity through consumption of food or herbal products containing high amount of PAs was commonly associated with hepatic sinusoidal obstruction syndrome (HSOS), which is also referred to as hepatic veno-occlusive disease (HVOD). This (HVOD) disease is mainly characterized by ascites and hepatomegaly, progressing to cirrhosis, which can even lead to mortality due to hepatic failure **[200, 285-288]**.

2.5.1 Acute toxicity

In the acute toxicity studies, the median lethal dose (LD_{50}), which entails half (50%) of lethality of PA in animal experiments, was investigated in animal models resulting in liver and lungs as the main organs affected. For instances, at an acute level, lasiocarpine, riddelliine and retrorsine were reported to induced liver damage inform of necrosis and megalocytosis and other biochemical changes in the organelles such as endoplasmic reticulum (ER) **[289-295]**.

Lasiocarpine, riddelliine, retrorsine, seneciphylline and senecionine, are among the acute toxic PA with lethality LD_{50} less than 100 mg/kg body weight. For example, senecionine oral LD_{50} was reported in mice at 57 mg/kg body weight while the oral LD_{50} for retrorsine, echimidine and heliotrine were determined in rats, where the oral LD_{50} for retrorsine was at 34-38 mg/Kg body weight, echimidine at 518 mg/Kg bodyweight, and for heliotrine at 510 mg/Kg body weight **[289, 296-298]**. The LD_{50} values of PAs in animal experiments after intraperitoneal (i.p) or intravenous (i.v) administration of PAs are also reported. Echimidine showed acute toxicity with lethality of LD_{50} between 200 to 350 mg/Kg of bodyweight **[9, 291]**. Meanwhile, lycopsamine

with the lethality of LD_{50} 1500 mg/Kg of body weight and europine with lethality of LD_{50} >1000 mg/Kg of body weight **[9, 291, 299]**.

Nonetheless, the 1, 2-saturated PAs such as platyphylline and cynaustraline were also investigated in rats, where for platyphylline at LD_{50} 118 mg/kg of body weight and cynaustraline at LD_{50} 67 mg/Kg of body weight was reported after intraperitoneal administration and at these LD_{50} values caused rapid deaths without hepatotoxicity **[300]**. In another two experimental rats animal studies, it was reported that platyphylline at LD_{50} of 252 mg/Kg body weight and cynaustraline at LD_{50} of 260 mg/Kg of body weight **[9, 294]**. Based on the LD_{50} animal studies, it was deduced that diesters PAs of heliotridine and retronecine were about four times more toxic than the respective monoesters PAs, and heliotridine esters were more toxic than retronecine esters **[301]**.

2.5.2 Sub-acute toxicity

A number of individual 1, 2-unsaturated PAs were investigated in mice and rats. Examples of PAs conducted were lasiocarpine, echimidine, retrorsine, retrorsine N-oxide, riddelliine, riddelliine N-oxide, and monocrotaline. Hepatotoxicity was depicted as the most common toxic effect of repeated doses of these 1, 2-unsaturated PAs. Pulmonary toxicity has also been observed with monocrotaline; here the metabolites produced by hepatocytes caused the toxicity in the lung **[302]**. However, the initial target appeared to the endothelial cells in the blood vessels **[295, 303]**.

Riddelliine was studied for 13-week in rats, which was administered by gavage. The no observed adverse effect level (NOAEL) was 0.24 mg/Kg of body weight per day however, histopathological changes in the liver were observed at a dose 0.71 mg/Kg of body weight per day **[304, 305]**.

Another study was conducted in rats which tested lasiocarpine and echimidine for 28-days **[296]**. The study reported no toxic effects at the highest tested dose of echimidine (2.5 mg/Kg of body weight per day), which was similar to lowest observed adverse effect level (LOAEL) for lasiocarpine at 2.8 mg/Kg of body weight per day and the NOAEL was 1.2 mg/Kg per day. This indicates that echimidine might be less toxic than lasiocarpine.

2.5.3 Chronic toxicity

The long-term exposure of 1, 2-unsaturated PAs to the animal studies has been considered to result in carcinogenicity as a critical end-point. Also, long-term PAs exposure studies in experimental animal toxicity have reported megalocytosis in the liver. For example, studies were conducted in rats administered with PAs such as lasiocarpine, riddelliine, retrorsine, and senecionine, and on crude plant extracts containing PAs, for long-term exposure and the end-results depicted in rats were tumors in multiple tissues mainly liver, lungs and blood vessels **[9, 306]**.

European Food Safety Authority (EFSA) and International Programme on Chemical Safety (IPCS) evaluated lasiocarpine and riddelliine for long-term carcinogenicity studies, in which it was observed that lasiocarpine was carcinogenic in Fischer 344 rats producing hepatocellular tumors and angiosarcomas of the liver in both sexes and hematopoietic tumors in female animals. For riddelliine, it was clearly observed that it induced carcinogenicity in male B6C3Fmice based on an increased incidence of hemangiosarcoma in the liver and clear evidence of carcinogenic activity in female B6C3F mice based on increased incidences of alveolar/bronchiolar neoplasms **[9, 307]**.

Based on detailed experimental animals studies on 1, 2-unsaturated PAs for lasiocarpine and riddelliine, the International Agency for Research on Cancer IACRC **[5, 308-310]** classified lasiocarpine and riddelliine as being possibly carcinogenic to humans (group 2B) **[5, 309, 310]**. For echimidine, retrorsine, seneciphylline, europine and lycopsamine not much data is available to-date in experimental animals and hence, IARC attributed them to the category that has limited evidence for the carcinogenicity to experimental animals (not classifiable as to its carcinogenicity to humans, group 3) **[309, 310]**.

2.6 Hepatotoxicity, Genotoxicity and Carcinogenicity

PA-induced hepatotoxicity is considered to be caused due to the formation of pyrrole –protein adducts in the liver resulting in the damage with the normal functions of specifics proteins in the liver. For example, the pyrrole-protein adducts of 1, 2-unsaturated PAs have been

demonstrated in the liver of mice and in vitro studies using rat liver microsomes and the recombinant human CYP 450s **[36, 311]**.

Consequently, most of purified PAs have been indicated in various animal experiments to induce carcinogenesis, not only in the liver but also in other organs such as lung, kidney, pancreas, or even in the brain **[281, 312-318]**. Both the in vivo and in vitro studies have demonstrated a variety of genotoxic effects such as formation of micronuclei, DNA-DNA cross-linking, DNA-protein cross-linking, sister chromatid exchanges, chromosomal aberrations, mutations, or teratogenicity.

2.6.1 Formation of DNA adducts

DNA adducts of riddelliine were found in the liver of female F344 rats and B6C3F1 mice after feeding **[257, 319, 320]**. It is presumed that riddelliine-induced liver tumor could be mediated by dehydronecine-DNA adducts based on magnificent correlation between the level of the dehydronecine-derived DNA adducts and tumorigenic potencies **[257]**. It was also reported that the DNA-adducts, which possibly lead to hemangiosarcoma, were mainly generated in the liver significantly in the endothelial cells more than in the parenchymal cells (hepatocytes) **[319]**. In addition, Wang et al (2005) supported that these dehydronecine-derived DNA adducts might be responsible for PA-induced liver tumorgenicity and genotoxicity, where formation of the DNA adducts by oral gavages of retrorsine with a daily dose of 1.0 mg/Kg b.w for three consecutive days to F344 female rats or monocrotaline with a single orally dose of 10 mg/Kg b.w were determined **[215, 321]**. Dehydronecine-DNA adducts were also determined in the liver of the rats after oral gavage with lasiocarpine, retrorsine, riddelliine, monocrotaline, clivorine, and heliotrine. The di-ester PAs formed higher levels of DNA-adducts than the mono-esters PAs, hence it was indicated that the DNA-adducts could be potential biomarkers of PA-induced carcinogenicity **[25]**. Yang et al (2002) also reported PA-derived DNA adducts found in the blood of both female and male F344 rats after a single dose of riddelliine through gavage **[322]**.

2.6.2 Formation of unscheduled DNA synthesis

The unscheduled DNA synthesis (UDS) test measures the DNA repair synthesis after excision and removal of a stretch of DNA containing the region of damage induced by chemical or physical

agents. Therefore, this assay measures the repair of primary DNA damage like DNA adducts. Several studies have been done to measure primary DNA damage induced by PAs. For example, Mirsalis et al **[323, 324]** found that riddelliine induced significant elevation in unscheduled DNA synthesis (UDS) in rat liver **[323, 324]**. In hepatocytes from cultured male and female rats and mice, UDS was also depicted after riddelliine was administered by gavage for 5 or 30 days **[304, 305, 325]**. The UDS test was also used in primary cultures of rat hepatocytes treated with PAs including retrorsine, seneciphylline, senecionine, and 19-hydrodroxyl- senecionine, or PA-metabolites such as alkenals. All these PAs or PA-metabolites demonstrated positive dose-related response measured by auto-radiographic detection. Similar UDS response by PAs and alkenal PA-metabolites was reported and suggested that trans-4-OH-2-hexenal is a toxic metabolite of the PAs **[326]**. In addition, UDS was also found and reported in hepatocytes from different species caused by lasiocarpine, senecionine, seneciphylline, and monocrotaline **[327, 328]**.

2.6.3 Formation of DNA cross-links and DNA-protein cross-links

Different PA variants and their pyrrolic derivatives have been found to form DNA-DNA cross-links and DNA-protein cross-links **[256, 329-331]**. In an in vivo study, after adult male Sprague-Dawley rats were injected intraperitoneally with monocrotaline, DNA-DNA interstrand cross-linking and DNA-protein cross-linking were depicted and there was no evidence of DNA single-strand break **[332]**.

Consequently, using in vitro studies, Hincks et al (1991) **[255]** demonstrated the formation of DNA cross-link associated with PA-variants in the cultured mammalian Mardin-Darby bovine kidney (MDBK) epithelial cell line incubated for 2 hours with eight PA-variants in concentrations ranging from 50 to 500 µM in the presence of S9. All the PAs tested including retrorsine, riddelliine, seneciphylline, senecionine, monocrotaline and lasiocarpine, induced DNA cross-links with dissimilar potency which consisted of proteinase sensitive cross-links and DNA interstrand cross-links. None of the tested PAs induced detectable amounts of DNA single strand breaks **[255, 332]**. A comparable study of DNA cross-link in MDBK cells was also reported by Kim et al. (1999) **[331]**; the PAs tested were dehydrosenecionine, dehydromonocrotaline,

dehydroriddelliine, dehydroretronecine and indicine N-oxide. All induced DNA cross-link formation with at different magnitude **[256, 331]**.

The DNA-protein cross-linking potency of the PA- has also been found to correlate well with the known potency differences in animal toxicity **[256]**. Hence, it was proposed that DNA-protein cross-linking activity is probably involved in PA-induced liver disease leading to carcinogenicity. Since some of these PA have been reported to be carcinogenic, thus formation of DNA-DNA cross-linking or DNA-protein cross-linking may lead to cancer formation **[256, 258]**.

In addition, the PAs or their reactive metabolites have also been proved to induce DNA or protein cross-linking in human breast carcinoma cells, as well as DNA-DNA cross-linking in E.coli, M13, and pBR322 plasmid **[331, 333-336]**. In spite the fact that DNA strand breaks could not be exhibited using alkaline elution assay, some studies using comet assay have reported isatidine and monocrotaline to have an effect on human hepatoma (HepG2) cells and human glioblastoma (GL-15) cells, respectively **[337, 338]**. *Louisse et al* (2019) **[30]** also identified several PA to induce DNA strand break in HepaRG human liver cells using the γH2AX assay.

2.6.4 Chromosomal and chromatid alterations

The PA-induced chromosomal damage has been widely investigated. The results demonstrate that PAs can induce clastogenic effects after being appropriately metabolically activated producing micronuclei in hepatocytes, bone marrow erythrocytes, and peripheral blood cells. In vivo, the clastogenic damage in form of micronuclei formation was evaluated in the bone marrow of the adult mice and their fetal liver after exposure to heliotrine and monocrotaline **[339]**. In the in vitro studies, retrorsine, monocrotaline, and isatidine exhibited induction of micronuclei formation in primary rat hepatocytes **[340]**.

Using HepaRG cell line, Allemang et al. (2018) **[29]** found dose-dependent micronuclei formation with several PAs including lasiocarpine, retrorsine, riddelliine, echimidine, seneciphylline, lycopsamine, and europine, and their corresponding N-oxides. Takanashi et al. **[341]**, investigated PAs in V79 Chinese hamster cells, and found that lasiocarpine and senkirkine can induce chromatid gaps, while heliotrine and petasitenine caused inter-chromosomal exchanges.

In addition, sister chromatid exchange (SCE) induced by seneciphylline, senkirkine, heliotrine, and monocrotaline, was also demonstrated in V79 cells when co-cultured with primary chick embryo hepatocytes **[9]**. Most of these PAs induced chromosomal aberrations have been reported in human cell lines. There is limited information available for chromosomal damage by PAs in humans. However, the most important study which was reviewed by International Programme on Chemical Safety (IPCS) described chromosomal damage in the blood cells of children with veno-occlusive disease, which was highly suggested to be caused by a PA known as fulvine from seeds of Crotalaria fulva **[342]**.

2.6.5 Mutagenicity

Frequently, mutagenicity is followed by carcinogenicity. In the in vivo studies using liver and the *cII* gene of transgenic big blue rats, Mei et al. (2004) **[343, 344]** reported riddelliine can transverse mutational pattern mainly a G:C to T:A. Using standard or modified Ames test with pre-incubation, the PAs including lasiocarpine, retrorsine, seneciphylline, senkirkine and monocrotaline were found to be mutagenic or weakly mutagenic to the strain TA100 of *Salmonella typhimurium* in the presence of S9 metabolic activation system **[345, 346]**. For retrorsine, the mutagenic activity was also observed in the strains of TA1535 and 1537 **[347]**. Several studies have shown that a number of PAs are dose-dependent mutagens. These studies used *Drosophila melanogaster* and *Salmonella typhimurium* TA100 as the main model systems.

2.7 Role of kinetics as toxicity determinant in PAs toxicity

Toxicokinetics represents the details of the absorption, distribution, metabolism and excretion (ADME) characteristics of chemicals or toxins. These ADME characteristic properties influence the bioavailability, the detoxification and bioactivation, and thus define the toxicity of chemicals or toxins. This also contributes to the 1, 2-unsaturated PAs due to the fact that they require bioactivation to a dehydro-PAs to become toxic, while the conversion to their PA-N-oxides and hydrolysis to non-toxic necines and necic acid moieties is mainly considered to result in their detoxification **[1, 348, 349]**. Therefore, kinetics is considered as a key factor for PA toxicity.

The differences in ADME characteristics of PAs may largely alter the relative potency of PAs. Kinetics is of importance for the toxicity of 1, 2-unsaturated PAs because these PAs require bio activation to dehydroPAs to become toxic. Although the metabolic pathway for bio activation of PAs is similar, there appear to be distinct differences in kinetics between PAs resulting in significant variation in metabolic clearance and bioavailability. Therefore, this implies that metabolism and thus kinetics are crucial determinants in PA-induced toxicity.

ADME differences for PA have become evident during absorption in the gastrointestinal tract (GIT). A number of studies have pointed differences in the absorption of the PAs across the intestinal barrier. For example, the intestinal uptake of PA-N-oxide was reported to be less efficient than that of the corresponding parent PAs **[350]**. A study using Caco-2 monolayer cells have shown that the permeability coefficient values of tested PA-N-oxides was low to moderate compared to those of tested corresponding parent PAs **[351]**. Despite the fact that the absorption of PAs may proceed through passive diffusion, there may also be a role for active transport depending on the type of PA. For example, the organic transporters 1 (OCT1) has been shown to play a role in active transport of some PAs into the liver hepatocytes **[352]**. The substrates of OCT1 are known to be mainly organic cations, while some bases, non-charged compounds and anions are also transported **[353]**. For example, retrorsine and monocrotaline have been shown to be high affinity substrates of OCT 1 **[352, 354]**; where at low pH, monocrotaline is protonated to its corresponding cation. In fact, the transport by OCT1 appeared to be more dominant while the passive diffusion was relatively negligible **[352]**. Meanwhile, at higher pH values in the intestinal compartment, a significant part of monocrotaline would be neutral and transported via passive diffusion **[355, 356]**.

In addition, a study in rat hepatocytes has shown that at pH 7.4 the OCT1 mediated transport and passive diffusion may contribute equally to the intestinal absorption of monocrotaline **[352]**. So far in extensive studies on PA distribution differences have not been described. Yet, the differences in, for example, lipophilicity might cause variations in tissue distribution and protein binding, which can influence the unbound concentration of a PA available in the target tissue to induce toxicity. For example, the diester-types are known to be more lipophilic than their corresponding PA-N-oxides **[350]**. Lipophilicity being one of the characteristic properties

for potentially resulting in PAs variation distribution, it can also play a key role in the level of protein binding hence affecting the results of the excretion of PAs via glomerular filtration in the kidney **[351]**.

In addition to absorption, distribution and excretion, the metabolic properties could also play an important role in mediating the toxicity of PA through, for example, differences in bio activation and/or metabolic clearance. Usually, the bio activation of PAs to reactive pyrrolic ester metabolites occurs in the liver, while for PA-N-oxides reduction to their corresponding parent PA is by intestinal microbiota and in the liver as an initial important step for the bio activation pathway **[20]**. However, the contribution from the GIT microbiota to this PA-N-oxide reduction may be higher than that of the liver **[20, 357]**. Notably, the efficiency of the reduction by the GIT microbiota may vary with the PA-N-oxide of interest **[289, 357-361]**.

Regarding the parent PAs, some in vitro studies using either liver microsomal incubations or rat hepatocyte sandwich cultures have demonstrated a significant variation in metabolic clearance between the tested PAs **[362-364]**. Based on kinetic data from in vitro liver microsomal incubations, metabolic clearance of lasiocarpine was depicted to be about 10-fold more effective than that of riddelliine and 43-fold more effective than that of monocrotaline **[364]**. These outcomes were in line with the data from Lester et al (2019) **[363]**, who demonstrated the metabolic clearance of PAs in rat hepatocyte sandwich cultures and reported the in vitro metabolic clearance of the same three PAs in a decreasing manner (lasiocarpine > riddelliine > monocrotaline) **[363]**. Consequently, kinetics seems to play an important role in the PA or PA-N-oxide toxicity. However, only for a few of the 1, 2-unsaturated PAs and their N-oxides kinetic data are available, which are required for consideration for the human risk assessment especially in defining the relative potency of individual PAs. Regardless of whatever different testing strategies are applied, it is important to consider that the relative toxicity of PA will depend on both toxicokinetics and toxicodynamics.

2.8 Role of biochemical aspects on pyrrolizidine alkaloids

The 1, 2-unsaturated PAs have been investigated and reported to be rapidly and extensively absorbed. In in vitro studies, Hessel at al. (2014) **[365]** showed the role of active transport in the small intestine, which favors absorption of cyclic-diester PAs such as senecionine and senkirkine, and excretion of the open-diester PA echimidine, and of the monoester PA, heliotrine **[365]**. In addition, one of the in vitro studies noted a role of the P-glycoprotein (MDR1) in the efflux of diester PAs. The PA N-oxides when ingested are mainly reduced to PA free bases in the digestive tract, and to a lesser extent in the liver, and thus contribute to PA toxicity **[20]**. After absorption, PAs are distributed to the liver, red blood cells (RBCs), plasma, brain, lung and kidneys.

In addition, some evidence has suggested that uptake into the red blood cells (RBCs) could facilitate movement of monocrotaline to the other organs such as the lung **[8]**.The elimination of cyclic diesters such as riddelliine, retrorsine, monocrotaline, dehydromonocrotaline, senecionine, adonifoline, and retrorsine N-oxide was investigated in rats, mice, guinea pigs and hamsters. Of these PAs, monocrotaline was mainly excreted unchanged, while the other PAs were excreted mainly as metabolites. Generally, the main predominant route of excretion was in urine and there was significant evidence for enterohepatic recirculation, perhaps involving back-transformation of the N-oxides in the parent basic PA compounds **[8]**.

In humans, specific information on PAs absorption, distribution and elimination is not available. However, the reports of human poisoning have demonstrated that PAs are absorbed and excreted in urine. With regard to the metabolism of PAs, the in vitro studies have demonstrated that the metabolic routes are common among animal species and humans. The in vitro studies have also indicated that PAs can undergo glucuronidation at the nitrogen atom; however, the significance of this pathway in vivo has not been well established. The ester bonds in PAs are cleaved via catalysis with carboxylesterases leading to formation of non-toxic necines and necic acids. The significance of this pathway is determined by the level of hepatic esterase activity, which is lower in the rat than in other species such as guinea-pig. The rat hepatic esterase activity is more or less equivalent to that of humans **[366]**.

Consequently, the structure of the ester component of different PAs also has an influence, since steric hindrance impairs or reduces de-esterification of PAs with branched or bulky chain esters **[269]**. The N-oxygenation of PAs is mainly catalyzed by cytochrome P450s and flavin-containing monooxygenases. In general, this is considered a detoxification route since the N-oxides are more water soluble; hence making them more readily excreted **[215, 237, 242, 321, 367, 368]**. However, the N-oxidation can easily be reversed by the action of hepatic reductases; hence it does not prevent the formation of reactive metabolites **[269]**. Cytochrome P450s and among them mainly the CYP3A4 and CYP3A5 isoenzymes, are the major enzymes involved in the formation of DHPA esters from most of the 1, 2-unsaturated PAs, with the exception of monocrotaline, for which CYP 2A6 isoenzyme has been reported to be the major activating enzyme. It has been shown in in vitro studies that PA-reactive metabolite formation is relatively high in humans compared to other species, which is measured by the formation of GSH conjugate and dehydrogenation metabolites, and a low rate of demethylation metabolite formation.

2.8.1 Effects of metabolic enzymes on pyrrolizidine alkaloids

Several studies investigating the effects of enzymes involved in metabolizing PAs have been reported. In in vitro CYP 450 inhibition, Dai, Zhang and Zheng et al. **[369]** studied inhibition of individual human CYP 450 isoenzymes in vitro by retrorsine or monocrotaline, based on the dependence inhibition of the nicotinamide adenine dinucleotide phosphate (NADPH), and the ability of the substrate present during the incubation to block the in activation of the isoenzymes. The results in their assay on the addition of 100 µM monocrotaline or retrorsine showed that in the mechanistic manner retrorsine, but not monocrotaline, inhibited CYP 3A4, but not the other CYP 450 isoenzymes tested such as CYP 1A2, 2A6, 2B6, 2C9, 2C19, 2D6 and 2E1. Contrary to that, the in vivo CYP 450 induction study conducted by Gordon, Coleman & Grisham et al. **[370]** established that a single intraperitoneal dose of 30 mg/Kg b.w retrorsine in rats induced an increase in both the protein levels of CYP1A1/2, 2B1/2 and 2E1 and the mRNA levels in microsomes of CYP1A1, 2B1/2 and 2E1, which were obtained from the livers of these rats.

In addition to that, Luckert et al. **[371]** found that of the four tested PAs echimidine, senecionine, senkirkine, and heliotrine, only echimidine was able to activate the nuclear receptor –pregnane X receptor (PXR). Meanwhile, the analysis of protein and mRNA level in HepG2 cells supported that echimidine can induce CYP 3A4. Moreover, five additional PAs of different ester types monoester, open-chain diester or cyclic diester, were studied in order to investigate whether if only the open-chain diesters are able to activate PXR. Only the open-chain diesters' echimidine and lasiocarpine were able to activate PXR. The induction of the model PXR target gene CYP3A4 by PAs was also confirmed at the mRNA, protein and enzyme activity level **[372]**.

2.8.2 Effect of glutathione (GSH) on pyrrolizidine alkaloids

Studies have demonstrated effects on GSH levels in cell-based assays, perfused organs or in vivo studies following exposure to PAs. Using cultured human pulmonary artery endothelial cells, Reid et al. **[373]** found a 40% reduction in GSH level in cells exposed to 100 µM dehydromonocrotaline and a 25% reduction in GSH level in cells exposed to 100 µM dehydroretrorsine after 15 minutes of exposure. Yan and Huxtable et al. **[374]** found a significant increase of in vitro GSH synthesis rates in liver cytosol prepared from rats administered with 65 mg/kg b.w intraperitoneal monocrotaline or 15 mg/kg b.w trichodesmine 24 hours before being sacrificed, compared to the rates in cytosols prepared from control rats.

In addition to that, the enzyme activity involved in GSH metabolism was also compared in several organs of rats administered with 65 mg/kg b.w monocrotaline via the intraperitoneal route for 24 hours. In the liver and lung, the activity of glutamate cysteine ligase (previously called gamma-glutamylcysteine synthetase), GSH synthase, gamma-glutamyl transpeptidase, dipeptidase and microsomal GSH-S-transferase were significantly increased compared to controls. In the heart and kidney, gamma-glutamyl transpeptidase and cytosolic GSH-S-transferase were significantly increased **[375]**.

2.9 Other Toxicities associated with Pyrrolizidine alkaloids

2.9.1 Reproductive and development toxicity

Developmental studies in rats exposed with various PAs have exhibited maternal toxicity, especially at the lower concentrations than those resulting in fetal toxicity **[376, 377]**. The fetal toxicity effects primarily manifest as abnormalities in fetal development, increased intrauterine death, and behavioral changes in the adulthood. A study was conducted due to maternal toxicity, making it difficult to determine whether the effects on the fetus are secondary to maternal toxicity. The study indicated that exposure of pups to monocrotaline via lactation resulted in lung and kidney toxicity, whereas severe toxicity and mortality were detected in the offspring exposed to the same dose of monocrotaline during gestation and lactation **[378]**. However, some of the in vivo studies using rats indicated that, based on body weight, the fetus might actually be less sensitive to PA toxicity than the mother **[379, 380]**. This could be due to the fetal liver being less able to metabolize PAs to form the reactive pyrrole metabolites **[336]**.

2.9.2 Immune toxicity

Some studies have reported possible PA-associated immunotoxic effects. The studies were conducted in rats and mice, using monocrotaline and integerrimine N-oxide. In the studies of monocrotaline in rats, at exposure doses below the one that caused noticeable toxicity (7.0 mg/Kg b.w), Hueza et al. (2009) **[381]** found effects on macrophage function at lower doses (1.0 and 5.0 mg/kg b.w), whereas Benassi et al. (2011) **[382]** did not.

In addition, rats exposed to 2.07, 4.14, or 6.21 mg/kg b.w integerrimine N-oxide, obtained by ethanolic extraction from Senecio brasiliensis leaves and administered by oral gavage for 28 days, showed reduced weight gain compared to controls but did not exhibit immunotoxicity **[383]**. In mice exposed to monocrotaline, changes in body weight and immune organ weight were seen at doses higher than 75 mg/kg b.w and, for some measures, above 50 mg/kg b.w when also treated with an immune inducing agent. Both humoral and cell-mediated immune responses were diminished in some assays at or below the exposures causing general toxicity **[384, 385]**.

Immunosuppression has also been described in a study where dehydroheliotridine has been shown to selectively destroy or inactivate cells involved in the initial stages of antigen recognition and processing **[8]**.

2.9.3 Neurotoxicity

Limited data is available on human studies on neuro toxic effects associated with pyrrolizidine alkaloids. Yet it has been noted that central nervous system poisoning can be an effect of pyrrolizidine alkaloids intoxication in animals such as cattle, sheep, horses, pigs and including mice, rabbits and dogs **[8, 9]**. Coll et al. (2011) **[386]**, administered a single intraperitoneal dose of 0 or 60 mg/Kg b.w monocrotaline to male Wister rats and after 44 days the rats were euthanized and examined for their blood-brain barrier permeability. Prior to sacrifice, samples of cerebrospinal fluid were obtained for protein and glucose determination. Blood samples were also collected for determination of alanine transaminase (ALT), aspartate transferase (AST), alkaline phosphatase (ALP) activity and albumin concentration. The administration of trypan blue via intracardial perfusion and Evans blue via intravenous injection were used to determine brain permeability at necropsy. The results showed that the protein and glucose content in the cerebrospinal fluid in treated rats was significantly increased compared to the control rats, while the serum ALT, AST and ALP activities in treated rats were significantly decreased compared to the control rats. The albumin concentration and the portal pressure were significantly increased in the treated rats compared to the control rats. In addition, trypan blue was identified in the hippocampi of the treated rats whereas no staining was observed in the controls. Evans blue dye was also identified in an increased concentration within the brains of treated rats compared to those of the controls. Hence, the study suggested that the altered blood–brain barrier permeability accompanied by alteration in the cerebrospinal fluid content is associated with monocrotaline toxicity **[386]**.

2.9.4 Skin toxicity

PAs are also known to be secondary photosensitization agents leading to induction of skin cancer. Several studies on the photo-genotoxicity associated with PAs have been demonstrated in transformed epidermal human cells. Wang CC et al. (2014) **[387]**, have tested several PAs for photo-toxicity or photo-genotoxicity using human HaCaT keratinocytes. The human HaCaT

keratinocytes, which are transformed epidermal human cells, were exposed to monocrotaline, riddelliine, lycopsamine, heliotrine, dehydromonocrotaline, dehydroriddelliine or dehydroretronecine, at concentration 250-500 μM for duration of 1 hour, followed by ultraviolet A (UVA) irradiation treatment and incubation for 24 hours before being assayed. The cells were exposed to 1, 2 or 4 J/cm^2 of ultraviolet A (UVA) irradiation and reduction of cell viability at 250 or 500 μM was measured using an MTS assay or induction of LDH release. The relative photo-toxicity was observed at 500 μM of dehydromonocrotaline, dehydroretronecine > dehydroriddelliine >>> monocrotaline, riddelliine, control. UVA irradiation of HaCaT cells treated with dehydromonocrotaline, dehydroriddelliine, and dehydroretronecine resulted in increased release of lactate dehydrogenase and enhanced photo-cytotoxicity proportional to the UVA doses. UVA-induced photochemical DNA damage also increased proportionally with dehydromonocrotaline and dehydroriddelliine. UVA treatment potentiated the formation of 8-hydroxy-2'-deoxyguanosine DNA adducts induced by dehydromonocrotaline in HaCaT skin keratinocytes.

Additionally, using electron spin resonance (ESR) trapping, it was found that the UVA irradiation of dehydromonocrotaline and dehydroriddelliine generates reactive oxygen species (ROS), including hydroxyl radical, singlet oxygen, and superoxide, and electron transfer reactions, indicating that cytotoxicity and genotoxicity of these compounds could be mediated by ROS. DNA cleavage was observed only for dehydromonocrotaline and dehydroriddelliine in an assay for DNA single strand breaks, although the authors deduced the additional presence of DNA cross-linking formation. HaCaT cells treated with 250 μM dehydromonocrotaline had increased levels of 8-OHdG DNA adducts, which were further increased with exposure to 4 J/cm^2 UVA irradiation.

Comparable to that, Zhao et al.(2011) **[388]**, also demonstrated in in vitro studies PAs and PAs metabolites to initiate processes which may lead to skin cancer and/or PA-induced secondary photosensitization. The PAs and the PAs metabolites used were lasiocarpine, riddelliine, monocrotaline, heliotrine, retronecine, senkirkine, dehydromonocrotaline, dehydroheliotrine, dehydrolasiocarpine, dehydroretrorsine, dehydrosenecionine, dehydroseneciphylline, dehydroretronecine, monocrotaline N-oxide, riddelliine N-oxide, heliotrine N-oxide, retronecine

N-oxide, 7-glutathionyl-6,7-dihydro- 1-hydroxmethyl-5H-pyrrolizine (7-GSH-DHP) and 7-(deoxyguanosin-N2-yl) dehydrosupinidine (DHP-dG-1) at a 0.1mM concentration. The study indicated that only the dehydro-PAs and 7-GSH-DHP at 0-70 J/cm2 of UVA in the presence of a lipid, induced a significantly increased production of methyl linoleate hydroperoxide, which was increased in a UVA dose-responsive manner. When irradiation was performed in presence of superoxide dismutase (SOD) the level of lipid peroxidation was significantly decreased. Superoxide dismutase (SOD) is known for scavenging oxygen radicals or inhibiting lipid peroxidation. The results suggest that singlet oxygen is a photo-induced product. The formation of both singlet oxygen and superoxide anion radicals during photoirradiation was confirmed using electron spin resonance (ESR) spin trapping.

Consequently, based on these studies, the results indicate that UVA photoirradiation of dehydro-PAs generates reactive oxygen species (ROS) that mediate the initiation of lipid peroxidation. UVA irradiation of the parent basic PAs and other PA metabolites, including PA N-oxides, under similar experimental conditions did not produce lipid peroxidation. These studies clearly suggest that dehydro-PAs are the active metabolites responsible for skin cancer formation and PA-induced secondary photosensitization **[388]**.

2.10 Regulatory measures on PAs and PA-containing products

Due to limited data, the International Agency for Research on Cancer (IARC) has classified only lasiocarpine, riddelline, and monocrotaline as category 2B, indicating that they are possibly carcinogenic to humans. Other PAs were not classifiable due to a lack of supporting data **[5]**. However, in 2016, BfArM implemented a risk assessment that classified contamination with PA-producing plants into three risk categories: Category A - very low or no concern (amount of PAs in 90% of the measured samples below 0.1 µg/day or none more than 0.35 µg/day); Category B - low concern (amount of PAs in 90% of the measured samples below 0.35 µg/day or none more than 1.0 µg/day); Category C - relevant concern (no data available or classification to categories A and B is not possible) **[221]**. Moreover, it was later clarified that an upper limit of 1 µg/day was valid for the subsequent three-year transition period. Afterward, a limitation of 0.35 µg/day

proposed by the Committee on Herbal Medicinal Products (HPMC) should be applied **[221]**. The World Health Organization - International Programme on Chemical Safety (WHO-IPCS) affirmed that human PA poisoning might lead to acute HVOD **[389]**. For example, literature data on Symphytum plant poisoning for over 6 months estimated a PA dose of 0.01 mg heliotrine/kg b.w per day, which may lead to liver disease in humans **[389, 390]**. It was then stipulated that even low doses of PAs taken for an extended period could possibly induce health risks in humans. Moreover, the facts on the genotoxic effects observed in chronic animal studies were difficult to evaluate for human cancer risk. Therefore, WHO-IPCS suggested that exposure to PAs should be avoided or minimized **[32, 389]**.

Consequently, the German Federal Institute for Risk Assessment (BfR) emphasized that exposure to 1,2-unsaturated PAs from various foods should always be kept as low as possible, complying with the 'As Low As Reasonably Achievable (ALARA)' principle, and not exceed an intake of 0.007 µg/kg b.w per day **[221]**. This aligns with the value provided by the Committee on Toxicity of Chemicals in Food, Consumer Products and The Environment (COT) in 2008, which was based on a benchmark dose lower confidence limit for a 10% extra cancer risk ($BMDL_{10}$) of 73 µg/kg b.w per day. This $BMDL_{10}$ value was established from a long-term (2 years) animal carcinogenicity study of lasiocarpine in male rats (NTP, 1978) with the application of a margin of exposure (MOE) of 10,000 **[391]**.

The European Food Safety Authority (EFSA) panel on Contaminants in the Food Chain (CONTAM) went further and concluded that 1, 2-unsaturated PAs might act as genotoxic carcinogens in humans. Nonetheless, as it was impossible to estimate a tolerable daily intake (TDI) from food other than honey, the CONTAM Panel also ruled to implement the Margin of Exposure (MOE) approach, as recommended by COT **[34]**. In 2017, following the availability of more data on PAs in various food supplements, EFSA established a Benchmark Dose Lower Confidence Limit for a 10% extra cancer risk (BMDL10) of 237 µg/kg b.w per day for the induction of liver haemangiosarcomas in female rats exposed to riddelliine. This became the new reference point of departure (PoD) for assessing the cancer risk associated with PAs **[7]**.

To minimize the risk caused by PA-containing herbal medicinal products, the BfArM specified that exposure to medicinal products containing 1, 2-unsaturated PAs should not exceed 100 µg/day with external application and 1 µg/day if used internally. However, if the application period exceeds six weeks, these limits should be reduced to 10 µg and 0.1 µg per day, respectively **[221]**. Additionally, the package insert for orally used products must contain the warning notice 'do not use during pregnancy or lactation' **[8, 9, 392-394]**. Furthermore, in the public statement EMA/HMPC/893108/2011, the Committee on Herbal Medicinal Products (HMPC) extrapolated a short-term (maximum 14 days) acceptable daily intake of 1, 2-unsaturated PAs at 0.35 µg/day. This value was derived from a final product for a 50 kg person, with a permitted daily intake of 0.007 µg/kg body weight per day, as stated by COT and EFSA **[6, 34, 391]**.

In summary, the current risk assessment for PAs, utilizing the MOE approach as performed by COT, has been adopted by EFSA and HMPC. The regulatory limits established are generally based on the most potent PA variants, such as lasiocarpine or riddelliine. While the MOE approach is suitable for assessing genotoxic and carcinogenic substances, it is deemed inappropriate for estimating a tolerable daily intake (TDI). Instead, the Threshold of Toxicology Concern (TTC) concept has been proposed. This concept, based on lifelong exposure and an acceptable lifetime cancer risk of 10^{-5}, establishes the limits for PAs.

In the TTC concept, a TDI threshold of 1.5 µg/day is considered acceptable for compounds with toxicological concern but lacking available data on carcinogenicity. In cases where compounds exhibit a structural alert for genotoxicity, the threshold should be reduced to 0.15 µg/day. Unfortunately, this TTC concept cannot be applied to PAs, given their known genotoxic, mutagenic properties and available data on carcinogenicity.

To date, few regulatory guidance approaches have imposed limits on PA intake, either for PA-containing medicinal products or food supplements. These limits have often been estimated solely based on the most potent variants, such as lasiocarpine or riddelliine. However, it is recommended that appropriate and reasonable limit values be established, taking into account the more available data on the toxic potencies of individual PA variants.

2.11 Selected PA variants

2.11.1 Lasiocarpine (Las)

(Reference substance: lasiocarpine; CAS No.: 303-34-4; M.W.: 411.50 g/mol)

Lasiocarpine is isolated from plant material. It is an open-chain diester PA belonging to the heliotridine-PA type, mainly distributed in plant species of Boraginaceae and Asteraceae. Known to cause hepatotoxicity, genotoxicity, and carcinogenicity **[395]**, it has been classified as Class 2B due to its carcinogenicity **[5]**. In HepaRG cells, lasiocarpine at a concentration of 0.59 µM has been shown to significantly induce micronuclei compared to the solvent control **[29]**. Additionally, dehydronecine-derived DNA adducts involved in the metabolism of lasiocarpine to exert its genotoxicity were demonstrated in rat livers and liver microsomes after oral gavage **[25, 396]**.

2.11.2 Echimidine (ED)

(Reference substance: Echimidine; CAS No.: 520-68-3; M.W.: 397.47 g/mol)

Echimidine is isolated from plant material. It is an open-chain diester PA belonging to the retronecine-PA type, mainly distributed in plant species of Boraginaceae and in the Asteraceae family. In transcriptomic analyses using CYP3A4-overexpressing HepG2 clone 9 cells, only the highest concentration of echimidine exhibited a significant expression of DNA damage **[397]**.

2.11.3 Riddelliine (Rid)

(Reference substance: Riddelliine; CAS No.: 23246-96-0; M.W.: 349.38 g/mol)

Riddelliine is isolated from plant material and is a cyclic-diester PA belonging to the retronecine-PA type. It occurs mainly in plants of the genera Crotalaria and Senecio **[398]**. In vitro studies have shown that riddelliine induces chromosome aberrations (CA) in mouse bone marrow cells, and these aberrations have also been reported in blood cells of children suffering from veno-occlusive disease **[9]**. Additionally, riddelliine has been reported to produce sister chromatid exchange (SCE) in vitro in V79 cells **[9]**.

2.11.4 Retrorsine (RT)

(Reference substance: Retrorsine; CAS No.: 480-54-6; M.W.: 351.40 g/mol)

Retrorsine is isolated from plant material and is a cyclic di-ester PA belonging to the retronecine-PA type. It occurs mainly in plants of the Senecio genus **[232, 395]**. In HepaRG cells, a chromosomal aberration was indicated at 9.5 μM **[29]**. Additionally, retrorsine could induce DNA cross-linking at doses ranging from 50-500 μM in cultured bovine kidney epithelial cells when co-incubated for 2 h with an NADPH-generating system and rat liver S9 fraction **[255, 399]**.

2.11.5 Seneciphylline (Sc)

(Reference substance: Seneciphylline; CAS No.: 480-81-9; M.W.: 333.39 g/mol)

Seneciphylline is isolated from plant material of the genus Senecio in the family Compositae **[232, 395]**. It is a cyclic-diester PA of the retronecine-PA type and has been shown to induce chromosomal damage, as evidenced by the sister chromatid exchange assay in V79 Chinese hamster cells co-cultured with chick embryo hepatocytes **[400]**.

2.11.6 Lycopsamine (Ly)

(Reference substance: Lycopsamine; CAS No.: 10285-07-1; M.W.: 299.37 g/mol)

Lycopsamine is isolated from plant material mainly belonging to the Boraginaceae family **[232, 395]**. It is a monoester PA of the retronecine-PA type. Despite limited available data related to the toxicity of lycopsamine due to its low toxic potency, it has been reported to induce cytotoxicity in rat primary hepatocytes **[401]**.

2.11.7 Europine (Ep)

(Reference substance: Europine; CAS No.: 570-19-4; M.W.: 365.86 g/mol)

Europine is a monoester PA of the heliotridine-PA type and is isolated from plant material, mainly belonging to the Boraginaceae family **[232, 395]**. Due to its low toxic potency, there is not much available data related to the toxicity of europine.

CHAPTER THREE

3 AIMS AND OBJECTIVES

Lately, the genotoxicity of pyrrolizidine alkaloids (PAs) has been a focal point of extensive research worldwide due to their occurrence in several plant species relevant for human consumption. Hundreds of compounds belonging to PAs have been identified. Given that high doses of PAs can lead to liver damage, and some have been shown to be genotoxic or carcinogenic, there is a legitimate reason for concern. PAs undergo hepatic metabolism, after which they can induce hepatotoxicity, genotoxicity, and carcinogenicity. However, many aspects of the mechanisms underlying PAs' genotoxicity and carcinogenicity remain unclear and warrant thorough investigation.

The main aim of this study was to investigate the mechanism of genotoxicity induced by selected PAs of different ester type in in vitro systems. The human hepatoma HepG2 cells were chosen as main model. Also using HepG2, a co-culture consisting of the metabolically active HepG2 cells and non-metabolically active human cervical HeLa H2B-GFP cells, was employed.

First the genotoxicity of the seven (7) selected PAs of different ester type had to be investigated in vitro in HepG2 cells and the dose-response relationship of each PAs was important to provide insight on PA potency and possible threshold.

To elucidate the link between PAs of different ester type and DNA damage, stimulation of ROS production upon treatment of the HepG2 cells had to be analyzed and the source of ROS production (mainly mitochondria) had to be identified. Intracellular glutathione (GSH) plays an important role in the detoxification of xenobiotics or toxins in cells. Thus, the role of GSH in PA-induced genotoxicity and quantification of intracellular GSH depletion had to be assessed.

In vivo, hepatic sinusoidal epithelial cells (HSECs) are the primary target for PA-induced toxicity and carcinogenicity, but PA need to be activated before reaching these (HSECs) cells. HSECs are not thought to be metabolically active due to lack of metabolic enzymes (CYP 450 enzymes). Thus, the question as to whether and how PAs are taken up by hepatocytes and the metabolites

being excreted from hepatocytes, and then might reach the target cells (HSECs) had to be elucidated. For this, a model consisting of the human metabolically active HepG2 cells and the human non-metabolically active cervical epithelial HeLa H2B-GFP cells were used to detect genomic damage achievable in the HeLa H2B-GFP cells of the co-culture upon treatment with three (3) representative PAs of different ester type. Since metabolic enzymes and membrane transporters could play a role in PA-inducing genotoxicity this was to be investigated using chemical inhibitors in vitro in HepG2 cells as well as in the co-culture model.

To further the clarification of the mechanism of PA-induced genotoxicity, effects on the mitotic process in HepG2 cells as well as in the HeLa H2B-GFP cells of the co-culture represent another endpoint to be investigated after treatment with the three (3) representative PAs of different ester type. Finally, it was an open question whether additive, synergistic or antagonistic effects could be exerted by combination of PA regarding their genotoxicity and this had to be investigated in HepG2 cells as well as co-culture model.

CHAPTER FOUR

4 MATERIALS AND METHODS

4.1 Cell lines and co-culture model conditions

HepG2: human hepatoma cell lines (ATCCHB-8065) that exhibited epithelial-like morphology were cultured at 37 ◦C with 5% (v/v) CO_2 in Minimum essential medium eagle (MEM) supplemented with 10% (v/v) fetal bovine serum, 1% (v/v) L-glutamine, 1% (v/v) antibiotics (50 U/mL penicillin and 50 mg/mL streptomycin) and 1% (v/v) nonessential amino acids. The cells had doubling time of forty hours thus, were sub-cultured twice per week and were tested regularly for mycoplasmas with Hoechst 33342 staining.

HeLa-H2B-GFP: human immortalized cervical epithelial cell lines derived from the cervical adenocarcinoma of a female patient. These cells were stably transfected with the green fluorescence protein (GFP) at the histone 2B position hence, expresses the green fluorescence and were obtained from Noriaki Shimizu, Graduate School of Integrated Sciences for Life, Hiroshima University, Japan through working group of Prof. Dr. Hintzsche **[402-404]**. The cells were cultured in a monolayer at 37 ◦C with 5% (v/v) CO_2 in high glucose-Dulbecco minimum essential medium eagle (High-glucose DMEM) medium without phenol red but supplemented with 10% (v/v) fetal bovine serum, 1% (v/v) L-glutamine, 1% (v/v) sodium pyruvate solution, 1% (v/v) HEPES sodium salt solution and 1% (v/v) antibiotics (50 U/mL penicillin and 50 mg/mL streptomycin). The cells had doubling time of twenty hours thus, were sub-cultured thrice per week and were tested regularly for mycoplasmas with Hoechst 33342 staining.

Co-culture system: The co-culture was set up such that overgrowth of the faster proliferating HeLa H2B-GFP cells over HepG2 cells was prevented within the duration of the experiment. The applied conditions for co-culture were that HepG2 cells and HeLa H2B-GFP cells were both seeded together in a six-well plate at 40,000 HeLa H2B-GFP cells and 150,000 HepG2 cells per well with 3 mL of HepG2 culture medium, and then incubated at 37◦C with 5% (v/v) CO_2 overnight, to allow the cells to settle and attach to the plate. Notably, the two cell lines were

cultured separately with their own suitable medium but during experimental protocol the cell lines were brought into contact and cultured in a HepG2 cells medium.

4.2 Chemical and Reagents

PAs (europine (CAS# 570-19-4; assay 100%), lycopsamine (CAS# 10285-07-1; assay ≥ 99%), retrorsine (CAS# 480-54-6; assay ≥ 98%), riddelliine (CAS# 23246-96-0; assay ≥ 98%), seneciphylline (CAS# 480-81-9; assay ≥ 99%), echimidine (CAS# 520-68-3; assay ≥ 93%) and lasiocarpine (CAS# 303-34-4; assay 100%)) were obtained from PhytoLab (Vestenbergsgreuth, Bayern, Germany).

Cyclophosphamide (CAS# 6055-19-2; assay ≥97%) was from Alfa Aesar (Karlsruhe, Germany). Gel Green and Gel Red Nucleic Acid stain were obtained from Biotium (Darmstadt, Germany). Fluorescein diacetate (FDA; CAS# 596-09-8) was from Invitrogen (Germany). Dimethylsulfoximide (DMSO; ≥ 99.8%), bisbenzimide H33258 (CAS# 23491-45-4; assay ≥ 98%), diazabicyclo-octane (DABCO), ketoconazole (CAS# 65277-42-1; assay ≥ 98%), rifampicin (CAS# 13292-46-1; assay ≥ 97%), quinidine (CAS# 56-54-2; assay ≥ 97%), verapamil (CAS# 152-11-4; assay ≥ 99%), nelfinavir (CAS# 159989-65-8; assay ≥ 98%), benzbromarone (CAS# 3562-84-3; assay ≥ 95%), cytochalasin B (CAS# 14930-96-2), loperamide (CAS# 34552-83-5; assay ≥ 99%), N-acetyl-L-cysteine (NAC; CAS# 616-91-1; assay ≥99%), ethidium bromide (CAS# 1239-45-8; assay ≥95%) and sodium fluorescein (CAS# 518-47-8; assay ≥95%) were from Sigma-Aldrich (Steinheim, Germany).

Calcein-acetoxymethyl ester (Calcein-AM; CAS# 148504-34-1; assay ≥95%) was from Cayman Chemical Company (Germany). Cell culture media and reagents were all from Sigma-Aldrich (Steinheim, Germany), except fetal bovine serum, which was from Biochrom (Berlin, Germany).

4.3 Methodology

4.3.1 Mycoplasma test

Rationale and Theory: Mycoplasma tests were routinely conducted at intervals of every 4 to 6 weeks to prevent contamination in the cultured cells. Mycoplasmas are the smallest free-living organisms and are commonly considered to be the simplest form of bacteria, lacking a cell wall and distinct shape.

Cell preparation and fixation: For this purpose, the cells were trypsinized, harvested, and part of the cell suspension was subjected to cytospin (centrifugation) using the Cytospin3 centrifuge Thermo Shandon machine at program load 8, at 1000 Rpm for 5 minutes, to fix the cells on the microscopic slides (76×26×1 mm; Marienfeld GmbH & Co.KG). Subsequently, the slides were fixed in ice-cold methanol for at least 2 hours.

Staining: The fixed cells (moist spot) on the microscopic slides were stained with a drop of bisbenzimide (5µg/ml in PBS) and covered with a 21 x 26 mm coverslip for three minutes at room temperature. Subsequently, the coverslip was removed by washing using one time PBS, and the stained cell spot on the microscopic slide was then mounted with DABCO and covered again with a 21 x 26 mm coverslip.

Evaluation: Immediately, the slides were evaluated or checked for mycoplasma at 200- and also at 400-fold magnification of Eclipse 55i fluorescence microscope using ultraviolet (UV) filter (Nikon GmbH, Japan). At least three (3) slides were evaluated per cell type.

4.3.2 Fluorescent dye exclusion/activation vitality test

Rationale for the Test: This test was implemented to prevent the cytotoxic effects of chemical inhibitors and inducers used in our cell model. The concentrations of chemical inhibitors, such as ketoconazole, loperamide, quinidine, verapamil, and benzbromarone, as well as inducers like rifampicin, were determined based on published effective concentrations. Additionally, a dye exclusion/activation fluorescent vitality test was employed to confirm the effective concentration of a substance without inducing cytotoxic effects.

Theory of the test: The main principle of the test uses combination of two different dyes such as fluorescein diacetate (FDA) and GelRed. The rationale of the combination of the dyes is to determine the plasma membrane integrity and cellular enzymatic activity. FDA is a fluorogenic substrate, which can be hydrolyzed intracellularly by cellular esterase activity and leads to accumulation of green fluorescent fluorescein **[405]**. GelRed is a fluorescent nucleic acid stain, which is sensitive, stable and environmentally safe dye designed for staining DNA. Its chemical structure was designed in a way that it is incapable of crossing cell membranes. However, it enters into cells which do not have an intact plasma membrane and binds to the DNA to exhibit a bright red fluorescent color **[406-408]**.

Performance protocol: Based on this principle, 35 µl of cell suspension pre-treated with chemical inhibitors or inducers in HepG2 cells for 24 hours was mixed with 15 µl of staining solution (2µl Gel Red stock solution and 12µl fluorescein diacetate (FDA; 5mg/ml in acetone) in 2 ml PBS). Thereafter, 15 µl of this mixture was applied on the microscopic slide (76×26×1 mm; Marienfeld GmbH & Co.KG) and covered with a cover slip (21x26 mm).

Evaluation: A total of 200 cells (red and green stained) were counted at 200-fold magnification with an Eclipse 55i fluorescence microscope which was equipped with fluorescein isothiocyanate (FITC) filter (Nikon GmbH, Japan). The proportion in percentage of green cells (vital) to red cells (dead) was evaluated.

4.3.3 Cytokinesis-blocking micronucleus test

Theory and Rationale: The cytokinesis-block micronucleus (CBMN) assay is performed to measure genomic damage via detection of micronuclei formation in the cytoplasm of the interphase cells. Micronuclei are formed during mitosis from chromatin fragments or misalignment of the whole chromatids that are unable to migrate to the poles during the anaphase stage of cell division. This test detects the activity of clastogenic and aneugenic substances in cells that have undergone cell division during or after exposure to the test substance. The micronucleus test guideline **[91]** allows the use of protocols with and without the actin polymerization inhibitor cytochalasin B. Cytochalasin B allows for the identification and

selective analysis of micronucleus frequency in cells that have completed one cycle of mitosis, because such cells are binucleated. Therefore, cytokinesis-block micronucleus (CBMN) assay test guideline allows the use of protocols with cytokinesis block provided that there is evidence that the cell population analyzed has undergone mitosis **[91, 409]**.Therefore, by adding the cytokinesis inhibitor cytochalasin B, micronucleus scoring can be limited to cells that have divided once since test substances were added.

Cell preparation and treatments: In the standard assay, 150 000 cells of HepG2 per 3 mL medium were seeded in a 6 well-plate and incubated at 37◦C with 5% (v/v) CO_2 overnight. After 24 hours to allow cells to settle, the medium was discarded, fresh medium added, followed by treatment of cells with test substances or with solvent controls (final concentration in cell culture: 1% sterile water or DMSO) for 28 hours. Lasiocarpine, riddelliine, and retrorsine were dissolved in DMSO and the remaining PA was dissolved in water. Cyclophosphamide (CPA) was used as a positive control. After treatment, the medium was discarded, cells were washed twice with phosphate-buffered saline (1x PBS) and fresh medium was added. Then, cells were exposed and incubated for 42-48 hours with the cytokinesis inhibitor cytochalasin B (3µg/ml). Next, cells were harvested by discarding the medium, washing with 1x PBS and then trypsinizing. Afterwards, cells in each sample were counted using a hemocytometer under light microscope and then centrifuged for 5 minutes x 1000 Rpm.

Cytospin and Fixation: Thereafter, cells were resuspended in a calculated volume to obtain a suitable cell density following cytospin centrifugation. During cytospin, the cells were fixed on the microscopic slides (76×26×1 mm; Marienfeld GmbH & Co.KG) by centrifugation using Cytospin3 centrifuge Thermo Shandon machine at programme load 8 at 1000 Rpm for 5 minutes. For each test substance treatment at least 3 slides were prepared. Then, the slides were fixed in ice-cold methanol for at least 2 hours.

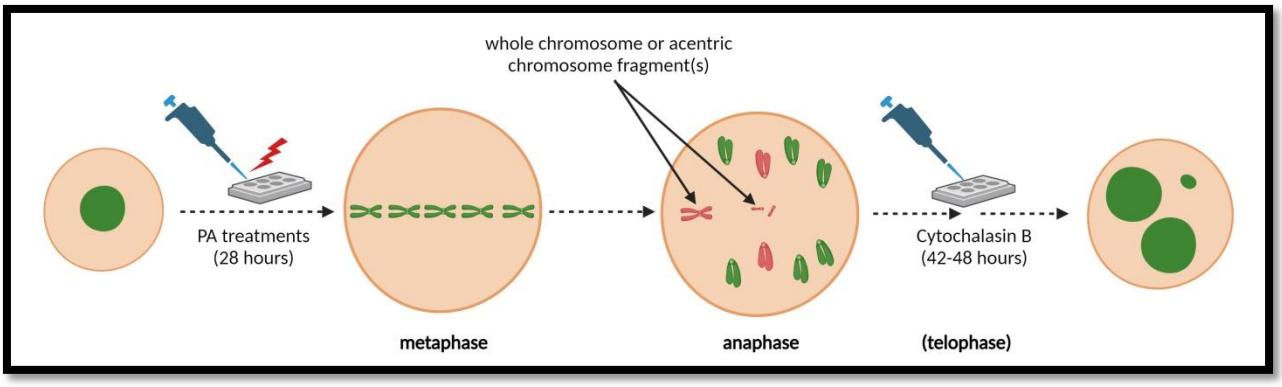

Figure 13: Schematic diagram on cytokinesis-blocking micronucleus test in HepG2 cells.

Gel Green Staining: Later the fixed cells on the slides were stained with 10µL Gel Green Nucleic Acid solution (1:100 dilutions in bi-distilled water) for 6-7 minutes in the dark, washed with one time PBS and then mounted with diazabicyclo-octane (DABCO) and covered with 18mm×18mm cover slips.

Evaluation: slides were coded and 1000 binucleated cells were evaluated at 400-fold magnification of Eclipse 55i fluorescence microscope using a fluorescein isothiocyanate (FITC) filter (Nikon GmbH, Japan). The number of mononucleated, binucleated, trinucleated, multinucleated, apoptotic and mitotic cells were recorded. Moreover, the number of micronuclei formation in 1000 binucleated cells was counted. The cytokinesis block proliferation was determined in 1000 cells that were counted for mononucleated cells (MN), binucleated cells (BN), trinucleated cells (TriN) and Tetra nucleated cells (TetraN) by using the equation as follows:

$$\mathrm{CBPI} = \frac{(1 \times \mathrm{MN}) + (2 \times \mathrm{BN}) + (3 \times \mathrm{TriN}) + (4 \times \mathrm{TetraN})}{\mathrm{MN} + \mathrm{BN} + \mathrm{TriN} + \mathrm{TetraN}}$$

For each experiment, 2 slides were analyzed. The average was calculated from 3 independent experiments. Often, the number of micronucleated cells per 1000 binucleated cells is chosen for presentation of the results because the cell is considered as the unit of damage. Here, we chose the number of micronuclei per 1000 cells for presentation to enable comparison with Allemang et al. (2018), who measured micronuclei using flow cytometry, which dissolves cellular

membranes, and then counts nuclei and micronuclei, not using the cell as the unit of damage, but providing a number for micronuclei per 1000 cells.

4.3.3.1 Confluency culturing of HepG2 cells

Studies have shown that the metabolic capacity (and expression of cytochrome P450s) in HepG2 cells is increased with prolonged (2 weeks) cultivation time without sub culturing, where the cells reach a pre-differentiated state **[410]**. For this, the cells were cultured for 2 weeks in a 6 well plate without sub culturing. Medium was replaced twice per week. Then, the cells were treated with a positive control (CPA) and lasiocarpine (Las) at different concentrations for 28 hours. Thereafter, cells were trypsinized, harvested again at a dilution 1:24 and allowed to settle for 24 hours before exposure with 3µg/ml of cytochalasin B for 42 to 48 hours. Afterwards the cells were handled as described above for exponentially growing HepG2 cells followed by standard protocol of CBMN assay.

4.3.3.2 Rifampicin pretreatment of HepG2 cells

Several in vitro studies have shown rifampicin (anti-bacterial drug) to be a potent inducer of CYP P450 expression and activity **[411-415]**. Based on this, cells were pretreated with 20µM rifampicin for 72 hours for induction of cytochrome P450 expression and activity, and after every 24 hours replacing medium with fresh medium containing fresh rifampicin. After that, cells were washed with PBS and the usual standard CBMN assay protocol was followed. The concentration of 20 µM rifampicin was based on Badolo, L., et al. (2015) **[411]** and Forsch, K., et al. (2018) **[414]** and also on our cytotoxicity vitality test results which are not shown here; indicating that 20 µM rifampicin treatment for 72 hours was tolerable. In addition, the interval of rifampicin pre-treatment in cells was also optimized, and the HepG2 cells were pretreated with rifampicin at 24 hours, 48 hours and 72 hours as pre-treatment. This was conducted using lasiocarpine 3.2 µM treatment (28 hours) after 20 µM rifampicin pre-treatment; the severity of the genotoxic effect was then assessed and analyzed using the cytokinesis-blocking micronucleus (CBMN) cytome assay. The 72 hours treatment with rifampicin (20 µM) showed the highest micronuclei formation, and thus, this interval was taken as a suitable pre-treatment duration for our further studies.

4.3.3.3 Inhibition of metabolic enzymes in HepG2 cells

Inhibition of enzymes that are involved in PA metabolism was performed with published effective concentrations of the carboxylesterase 2 inhibitor loperamide (2.5 µM, applied 15 min before and during lasiocarpine treatment) **[414]**, the cytochrome P450 3A4 inhibitor ketoconazole (1 µM; pretreatment for 24 hours **[416-419]**), and the cytochrome P450 1A2 inhibitor furafylline (1 µM; pretreatment for 24 hours **[419-422]**). Also, the effective inhibitor concentrations were confirmed using a fluorescent dye exclusion/activation vitality test as described earlier. After that, cells were washed with PBS and the usual standard CBMN assay protocol was followed.

4.3.3.4 Depletion of glutathione (GSH) in HepG2 cells

Glutathione is well known for detoxification of toxins. However, the role of glutathione in the toxicity associated with PAs is still unclear. L-Buthionine sulfoximine (BSO) is a specific and irreversible inhibitor of γ-glutamyl-cysteine synthetase; an enzyme involves in inhibiting glutathione synthesis and it has been shown in various experimental systems to deplete intracellular glutathione stores **[423-425]**. Based on this, 150,000 HepG2 cells were seeded in a 6-well plate with 3 mL medium and incubated at 37◦C with 5% (v/v) for 24 hours; to allow cells to settle and adhere. Then, medium was discarded and fresh medium added containing BSO (at final concentration 400µM) for 24 hours. The BSO concentration was based on the vitality test results (not shown here); which showed no cytotoxic effect in 150, 000 HepG2 cells treatment with BSO for 24 hour. After 24 hours of pre-treatment with BSO, the medium was discarded, cells washed twice with PBS. Then, fresh medium was added with lasiocarpine (at final concentration 3.2 µM in 3 mL medium) in the cells earlier pretreated with or without 400 µM BSO, and incubated at 37◦C with 5% (v/v) for 28 hours. Here, the lasiocarpine concentration of 3.2 µM was used based on our initial micronucleus test results which showed this to be the minimum lasiocarpine concentration inducing significant micronucleus formation. Next, medium was discarded and fresh medium added containing cytochalasin B (at final concentration 3 µg/ml) for 44 hours. Thereafter, the cells were harvested and the standard micronucleus test protocol and evaluation followed as described earlier.

4.3.3.5 Inhibition of CYP 450 activity and GSH depletion in HepG2 cells

Here, the rationale was to come up with the most sensitive protocol to test the genotoxic potencies of the selected PAs of different ester type in HepG2 cells. Hence, the combination effects of inhibition of CYP 450 and the depletion of GSH in HepG2 cells was tested under the same experimental conditions. Therefore, HepG2 cells were pretreated with 20 µM rifampicin for 72 hours and 400 µM BSO for 24 hours (at the last 24hours of rifampicin). Then the cells were treated with lasiocarpine 3.2 µM (Las3.2) for 28 hours. Thereafter, the cells were incubated with 3 µg/ml of cytochalasin B for 42 to 48 hours, followed by the standard CBMN assay protocol as described earlier.

4.3.3.6 Inhibition of membrane transporters in HepG2 cells

Transmembrane transporters may enhance or decrease PA mediated effects. Thus, representative transporters were inhibited with published effective concentrations of known inhibitors. The organic cationic transporter 1 (OCT1) influx transporter inhibitor quinidine (25 µM **[175]**), the organic anionic transporter protein 1B1 (OATP1B1) influx transporter inhibitor nelfinavir (2.5 µM; **[175]**), the multidrug resistance protein 1 (MDR1) inhibitor verapamil (50 µM; **[175, 426-428]**), and the multidrug resistance–associated protein 2 (MRP2) inhibitor benzbromarone (10 µM; **[429, 430]**) were applied as a pretreatment for 24 hours, after which a standard CBMN assay protocol with lasiocarpine treatment for 28 hours followed.

4.3.3.7 Combination of lasiocarpine and riddelline in HepG2 cells

Combination of 2 or more PAs is an important question in determining additive or synergistic effects. This depends on whether the same mechanism of action and target molecule is shared or more than one is affected. Lasiocarpine and riddelliine are PAs of different chemical structures. Lasiocarpine is an open diester or heliotridine PA-type, while riddelliine is a cyclic ester or retrenocine PA-type. HepG2 cells (150,000 cells/3mls) in a 6 well-plate were treated with a mixture of lasiocarpine and riddelliine and incubated at 37°C with 5% (v/v) CO_2 for 28 hours. Then, the cells were exposed and incubated with 3 µg/ml of cytochalasin B for 42 to 48hours. Afterwards, the standard micronucleus test protocol as described earlier was used to assess the genotoxic effects of PAs combinations.

Low and high concentrations of lasiocarpine and riddelliine were mixed, i.e., 1 µM lasiocarpine was combined with 10 µM riddelliine, and 10 µM lasiocarpine was combined with 100 µM riddelliine. These concentrations were obtained from preliminary test conducted in our laboratory by the author of this thesis, according to the low and high toxicity and genotoxicity of these PAs.

4.3.4 Standard alkaline comet assay

Theory and Rationale: The alkaline comet assay was implemented to determine if PAs of different ester types could induce DNA strand breaks. The comet assay was performed following the protocol by Tice et al. (2000) **[431]**. This technique is advantageous because it is simple and rapid to perform, offering sensitivity in detecting various forms of DNA damage at the individual cell level. The standard alkaline version of the comet assay is primarily used to detect DNA single-strand breaks, double-strand breaks, and the alkali-labile sites. The amount of migrated DNA in the tail region of the comet indicates the extent of DNA damage in the cell **[432]**. In our study, the concentrations of selected PAs that induced micronucleus formation in the CBMN assay were used to detect DNA strand breaks at both equimolar concentrations and high concentrations. At equimolar concentrations, all selected PAs of different ester types were at 10 µM, and the highest concentrations used to detect DNA strand breaks were 10 µM lasiocarpine, 100 µM riddelliine and retrorsine, and 320 µM echimidine, europine, and lycopsamine.

Cell preparation and treatment: 250,000 HepG2 cells were seeded in 12-well plate with 2 mL medium and incubated at 37◦C with 5% (v/v) CO_2 overnight; in order to allow the cells to settle and adhere to the bottom of the well-plate. Next, cells were treated with PAs of different ester type such as lasiocarpine, echimidine, riddelliine, retrorsine, europine and lycopsamine at equimolar and high concentrations for 28 hours. Then, the cells were harvested by washing with PBS, trypsinized and then centrifuged. Before the standard comet assay was carried out, the dye exclusion/activation fluorescent vitality test as described earlier was conducted in order to distinguish the cytotoxicity and genotoxicity associated with the PAs in test. The percentage of vital cells was >91% in all treatments using PAs.

*Embedding and lysis of cells***:** thereafter, 20 µl of cell suspension was mixed/embedded with 180 µl of 0.5% low melting point agarose at 37◦C. The embedding is required in order to immobilize the cellular DNA which helps in the formation of comet during electrophoresis **[433]**.Then, 45 µl of the cell-agarose mixture was placed on a fully frosted (pre-coated with 1.5% high-melting point agarose) microscopic slides and covered with a cover slip (21×26 mm) for at least 5 minutes to polymerize and solidify the mixture. Thereafter, the cover slips were gently removed and subsequently kept in a lysis solution for at least 1 to 2 hours in a dark at 4◦C in order to lyse the cells such as cell and nuclear membranes and to permit DNA unfolding **[433, 434]**. The lysis solution consisted of 89% lysis buffer (2.5 M NaCl, 100 mM Na_2EDTA and 10 mM Tris adjusted to pH 10) mixed with 1% Triton X-100 and 10% dimethyl sulfoxide (DMSO) protected from light.

*Electrophoresis***:** before running electrophoresis, the slides were washed gently with VE water and were then placed in the electrophoresis chamber that was filled with cold electrophoresis buffer solution (5 M NaOH and 0.2 M Na_2EDTA solution, pH 13) at 4◦C for 20 minutes in the dark; in order to allow DNA unwinding and expression of alkali labile sites **[435]**. Then, the electrophoresis was run where the electric current was applied for 20 minutes at 25 V and 300 mA, which was adjusted with the electrophoresis buffer solution. Thereafter, the slides were neutralized with a cold 1×PBS in a cuvette for 5 minutes and then fixed in a cold methanol (-20 °C) for 5 min. Later, the slides were left to dry under a fume hood for 10-20 minutes.

*GelRed® staining and Evaluation***:** 20 µl of GelRed nucleic acid gel stain (1:100)/diazabicyclo-octane (1:4) solution was added to each slide and one hundred randomly selected cell images at the middle of the slide (50 per replicate slide) were analyzed with a fluorescence microscope (Labophot-2; Nikon GmbH, Japan) at 200-fold magnification using a computer-aided image analysis software (Komet version 6, ANDOR™ Technology). At least three (3) independent experiments were carried out and the percentage of DNA in the tail was used to quantify the DNA damage.

4.3.5 Modified alkaline comet assay for DNA crosslink detection

Theory and Rationale: Crosslinks are an extremely toxic form of DNA damage that cells experience upon exposure to xenobiotics and their metabolites **[436]**. For example, interstrand crosslinks prevent the separation of the DNA strands, affecting the ability of vital processes such as replication or transcription of DNA to proceed **[437, 438]**. Crosslinking agents cause a reduction in mutagen-induced DNA migration after subsequent treatment with a strand break-inducing mutagen **[439]**. Based on these principles, the modified alkaline version of the standard comet assay was applied to assess and quantify the potency of PAs of different ester types in inducing DNA crosslinks using 100 µM hydrogen peroxide as a DNA strand-breaking mutagen in HepG2 cells.

Cells preparation and treatments: In this assay, 250,000-300,000 HepG2 cells were seeded in a 12 well-plate and incubated at 37◦C with 5% (v/v) CO_2 overnight. Then, cells were treated with PAs of different ester type, as well as with the crosslink positive control cyclophosphamide (CPA) for 24 hours. Thereafter, cells were washed with 1× PBS once and fresh medium added, followed by 100 µM hydrogen peroxide (H_2O_2) for 30 minutes to induce DNA strand breaks. Later, the cells were harvested by washing with PBS, trypsinized and then centrifuged. Before the DNA crosslinking comet assay was carried out, the dye exclusion/activation fluorescent vitality test as described earlier was conducted in order to distinguish the cytotoxicity and genotoxicity associated with the PAs in test. The percentage of vital cells was >88% in all treatments using PAs.

Embedding and lysis of cells, electrophoresis, GelRed staining and evaluation of the slides were performed as describe earlier for the standard alkaline comet assay.

4.3.6 Microscopic quantification of intracellular reactive oxygen species using Dihydroethidium – Assay

Theory and Rationale: In general, intracellular reactive oxygen species (ROS) are formed either due to the involvement of oxygen in cellular metabolic processes or upon cellular stress induced by xenobiotics and their reactive metabolites. Due to their highly reactive nature, ROS can

damage proteins, lipids, and DNA. Therefore, when the production of ROS exceeds its deactivation, it leads to oxidative stress **[44, 57, 440, 441]**. With the help of the red fluorescent dye dihydroethidium, the ROS formation of a cell can be detected microscopically. The Dihydroethidium (DHE) assay measures ROS directly in live cells. This assay uses DHE as a fluorescent probe for the detection of ROS generation and is specific for the superoxide radical ($O_2^{-\bullet}$) and hydrogen peroxide (H_2O_2) **[442]**. In this assay, ROS generation is represented as total DHE fluorescence.

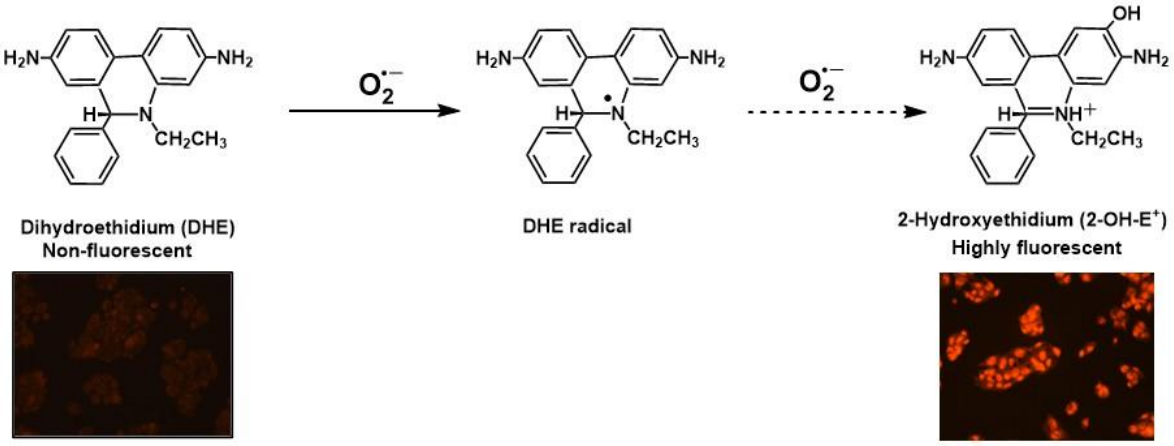

Figure 14: Schematic representation principle of dihydroethidium (DHE) fluorescent probe for detection of ROS generation. In presence of ROS, DHE is oxidized to form 2-hydroxyethidium (2-OH-E+) which will fluoresce (red-orange) under TRITC filter of fluorescence microscope. The figure and chemical structures in it was prepared using ChemDraw version 20.1.

The principal mechanism of the DHE assay is based on the oxidation of dihydroethidium by superoxide to form 2-hydroxyethidium (2-OH-E+) at excitation wavelengths of 500-530 nm and emission wavelengths of 590-620 nm, or by nonspecific oxidation by other sources of ROS to form ethidium ion (E+) at excitation wavelength 480 nm and emission wavelength 576 nm. Based on these facts, the cell-permeable fluorescent dye dihydroethidium (DHE) was used to detect intracellular ROS associated with PAs of different ester types at equimolar concentrations.

Experimental protocol: 300,000 HepG2 cells were seeded on 24 mm autoclaved cover slips in a 6-well plate with 3 mL medium and incubated at 37◦C with 5% (v/v) CO_2 overnight; in order to allow the cells to settle and adhere to the 24 mm cover slip. Next, cells were treated with the equimolar concentrations of PAs of different ester type such as 10 µM lasiocarpine, 10 µM

echimidine, 10 µM riddelliine, 10 µM retrorsine, 10 µM europine and 10 µM lycopsamine for 75 minutes. Then, in the last 15 minutes, 10 µM of DHE (final concentration in the culture per well) was added to the cells and incubated in dark at 37◦C with 5% (v/v) CO_2 for 15 minutes. Antimycin A was used a positive control at a final concentration 50 µM; which induces loss of mitochondrial membrane potential via inhibition of complex III of the electron transfer chain in the mitochondria. Thereafter, the cells were washed thrice with cold 1× PBS, and then the cover slips were inverted on to the microscopic slides (76×26×1 mm; Marienfeld GmbH & Co.KG).

Evaluation: cells in the microscopic slides were observed under Eclipse 55i microscope (Nikon GmbH, Düsseldorf, Germany) and images were taken randomly using a Fluoro Pro MP 5000 camera (Intas Science Imaging Instruments GmbH, Göttingen, Germany) at a 200-fold magnification with Tetramethyl Rhodamine Iso-Thiocyanate (TRITC) filter. All the images of the DHE staining were taken using the same exposure time. The quantification of DHE intensity was evaluated in 250 cells per treatment with ImageJ software (http://rsb.info.nih.gov/ij/). At least three (3) independent experiments were carried out.

4.3.7 Effect of N-acetylcysteine on PA-induced reactive oxygen species using Dihydroethidium – Assay

Theory and Rationale: N-acetyl-L-cysteine (NAC) is a synthetic precursor of intracellular cysteine, which is crucial in cellular glutathione synthesis **[443]**. It is also considered one of the main sources of sulfhydryl groups that act directly as free radical scavengers **[443, 444]**. Hence, its anti-ROS activity arises from its free radical scavenging properties, either directly through the redox potential of thiols or secondarily by increasing glutathione levels in cells **[445]**. Based on these facts, N-acetyl-L-cysteine (NAC) was used to confirm whether PAs induce ROS in HepG2 cells.

Here, the experimental protocol and evaluation of the DHE assay were performed as described earlier, with the addition of 5 mM NAC for a total of 2 hours. Specifically, after 1 hour of treatment with 5 mM NAC, equimolar concentrations of PAs of different ester types, such as 10 µM lasiocarpine, 10 µM riddelliine, and 10 µM europine, were added and incubated for an

additional 75 minutes. The choice of a final concentration of 5 mM N-acetyl cysteine (NAC) was based on vitality test results (not shown here), which demonstrated no cytotoxic effects in HepG2 cells after 24 hours of incubation.

4.3.8 Mitochondrial Membrane Potential using Tetramethylrhodamine-Ethyl-Ester – Assay

Theory and Rationale: Mitochondrial membrane potential is a crucial marker for mitochondrial health. It is the main driving force for the generation of ATP by the mitochondria and consists of a proton gradient generated by the mitochondrial respiratory chain complexes. Mitochondria generate roughly 90% of the total ROS in the cell and the mitochondrial electron transport chain is the central source of ROS formation. Thus, this makes mitochondria as a primary source for ROS formation causing oxidative stress leading to genomic damage induction **[446]**.

One of the most common fluorescent dyes used to quantifying changes in mitochondrial membrane potential in live cells by labelling the active mitochondria is known as tetramethylrhodamine ethyl ester (TMRE). TMRE is a lipophilic permeable cationic red-orange dye and due to its positively-charged it readily accumulates in active mitochondria due to their relative negative charge.

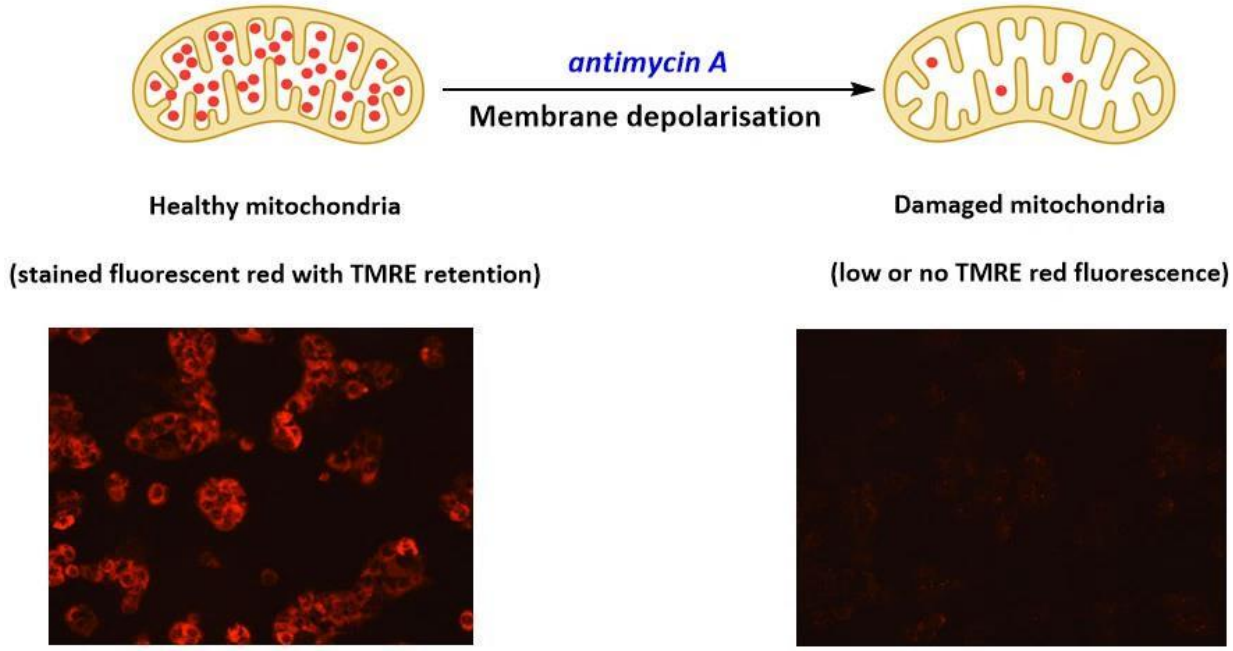

Figure 15: Schematic representation of the principle of tetramethylrhodamine ethyl ester (TMRE) fluorescent staining for quantification of the mitochondrial membrane potential. TMRE quantifies changes in mitochondrial membrane potential of live cells. TMRE is a cell permeable, positively charged dye that accumulates in active mitochondria (red-orange fluorescence) due to their relative negative charge. Inactive or depolarized mitochondria have decreased membrane potential and thus fail to retain the TMRE dye and as a result show low fluorescence signal. The figure was prepared by own using ChemDraw version 20.1.

Depolarized or inactive mitochondria have decreased membrane potential due to blockade of the electron transfer function leading to net positive charge. Hence, the depolarized mitochondria fail to sequester TMRE due to positively charged membrane where TMRE dye does not bind [465]. Therefore, here TMRE staining was used to demonstrate and clarify the source of the ROS-induced PAs of different ester type in HepG2 cells.

Experimental Protocol: Here, 300,000 HepG2 cells were seeded on a 24 mm autoclaved coverslip in a 6-well plate with 3 mL of medium and incubated at 37°C with 5% (v/v) CO2 overnight to allow the cells to settle and adhere to the 24 mm autoclaved coverslip. Next, the cells were treated with equimolar concentrations of PAs of different ester types, such as lasiocarpine 10 µM, riddelliine 10 µM, and europine 10 µM for 75 minutes. In the last 15 minutes, 30 nM of TMRE (final concentration in the culture per well) was added to the cells and incubated in the dark at 37°C with 5% (v/v) CO_2 for 15 minutes. Antimycin A was used as a

positive control at a final concentration of 50 µM, which induces loss of mitochondrial membrane potential via inhibition of complex III of the electron transfer chain in the mitochondria. Thereafter, the cells were washed thrice with cold one-time PBS, and then the coverslips were inverted onto the microscopic slides (76×26×1 mm; Marienfeld GmbH & Co.KG).

Evaluation: Later, cells were observed under the Eclipse 55i microscope (Nikon GmbH, Düsseldorf, Germany), and images were randomly taken using a Fluoro Pro MP 5000 camera (Intas Science Imaging Instruments GmbH, Göttingen, Germany) at a 200-fold magnification with TRITC filter. All the images of the TMRE staining were captured using the same exposure time. The quantification of DHE fluorescence intensity was evaluated in 250 cells per treatment with ImageJ software (http://rsb.info.nih.gov/ij/). Three (3) independent experiments were carried out.

4.3.9 Co-culture model system for mechanistic studies

4.3.9.1 Establishment of co-culture model system

Theory and Rationale: A co-culture model was applied in which non-metabolic active HeLa H2B-GFP cells were brought into contact with HepG2 human liver cells. This design was intended to mimic the hepatic environment with the metabolic active hepatocytes and the target cells for PA activity, HSECs, which lack functional cytochrome P450 enzymes required for metabolizing PAs. As a first step, a suitable cell ratio had to be obtained in order to prevent the over growth of HeLa H2B-GFP cells over HepG2 cells. It is known that the doubling time for HeLa H2B-GFP cells is 24 hours while that of metabolic active HepG2 cells is approximately 48 hours.

Performance protocol: HepG2 cells and HeLa H2B-GFP cells were seeded together in a 6-well plate at different cell ratio numbers and incubated for 24, 48 and 72 hours. Then, at time 0, 24, 48 and 72 hours the co-culture cells were harvested, put on the glass slides by cytospin centrifugation and fixed in cold methanol (-20◦C) for at least 2 hours.

Evaluation: Slides were stained with bisbenzimide H33342 (blue dye under UV filter) which stains the nuclei of all cells. The cell ratio was evaluated by counting cells in UV (all nuclei) and

FITC (GFP-labelled HeLa cells) filter at 200-fold magnification of Eclipse 55i fluorescence microscope (Nikon GmbH, Japan).

4.3.9.2 Cytokinesis-block micronucleus (CBMN) assay with Co-cultured cells

Rationale: The study of genomic damage was performed in the co-culture consisting of HeLa H2B-GFP cells and HepG2 cells. Additionally, the genomic damage was also assessed in a culture of only HepG2 and a culture of only HeLa H2B-GFP cells. The rationale here was to investigate if PAs induce genomic damage in non-metabolic active HeLa H2B-GFP cells after metabolic activation by HepG2 cells.

Experimental Protocol: The CBMN assay was carried out as described in section *4.3.3* of this thesis. However, here, 190, 000 of only HeLa H2B-GFP cells per 3 mL, 150, 000 of only HepG2 cells per 3 mL and for the co-culture 40,000 HeLa H2B-GFP and 150,000 HepG2 cells per 3 mL were seeded in a 6 well-plate. Later, cells were treated with solvent control (DMSO), 10 µM lasiocarpine, 100 µM riddelliine or 320 µM europine for 28 hours. Then, the medium was discarded, cells washed twice with PBS, followed by adding fresh medium with 3 µg/mL cytochalasin B for 20 hours in HeLa H2B-GFP cells and in the co-culture. In the well with only HepG2 cells the 3 µg/mL cytochalasin B exposure was for 44 hours. Thereafter, the cells were harvested and the standard CBMN assay as described earlier was continued. Notably, slides with co-culture cells and HeLa H2B-GFP cells were mounted only with DABCO to evaluate micronucleus formation in HeLa H2B-GFP cells, while slides with only HepG2 cells were stained with 10 µL Gel Green Nucleic Acid solution.

Evaluation: the slides were evaluated as described earlier, and three (3) independent experiments were conducted.

4.3.9.3 Inhibition of CYP 450-3A4 activity

In humans, understanding the role of CYP 450 enzymes is crucial for addressing issues such as achieving bioavailability and avoiding toxicity of xenobiotics and their metabolites **[447, 448]** . Therefore, the application of the chemical inhibitor ketoconazole for CYP 450-3A4 inhibition may influence the metabolism and toxicity of PAs that could be metabolized or bioactivated **[166]**. The impact of ketoconazole on PA-induced genomic damage was investigated in the co-

culture model using the CBMN assay, as described earlier. Based on the published effective concentration of ketoconazole, 1 µM was applied as a pretreatment for 24 hours **[416-419]**. The PAs tested in this study were 10 µM lasiocarpine, 100 µM riddelliine, and 320 µM europine.

Cells were pre-treated with 1 µM ketoconazole for 24 hours. Subsequently, the medium was discarded, and cells were washed with PBS. Fresh medium containing PAs was then added to the cells with or without ketoconazole pre-treatment for 28 hours. Cytochalasin B exposure (at a final concentration of 3 µg/mL) lasted for 20 hours, aligning with the doubling time of 24 hours for HeLa H2B-GFP cells in which micronucleus formation was determined. Following this, cells were harvested, and the standard protocol for the CBMN assay and evaluation was carried out as described earlier. Three (3) independent experiments were conducted.

4.3.9.4 Inhibition of efflux membrane transporters

Here, using the co-culture model, the chemical inhibitors of the multidrug resistance protein 1 (MDR1), verapamil (50 µM; **[175, 426-428]**), and of the multidrug resistance–associated protein 2 (MRP2), benzbromarone (10 µM; **[429, 430]**), were applied as a pretreatment for 24 hours. Next, the medium was discarded, cells were washed with PBS, and fresh medium containing PAs was added to the cells with or without chemical inhibitor pretreatment for 28 hours. Then, cytochalasin B (at a final concentration of 3 µg/ml) exposure was for 20 hours because the micronucleus formation was determined in HeLa H2B-GFP cells, which have a doubling time of 24 hours. Later, cells were harvested, and the usual standard protocol for the CBMN assay and evaluation was carried out as described earlier. Three (3) independent experiments were conducted.

4.3.9.5 Combination of lasiocarpine and riddelliine

Here, the co-culture model was treated with combination of low, medium and high concentrations of lasiocarpine and riddelliine for 28 hours. The low concentrations were 3.2 µM lasiocarpine and 10 µM riddelliine; medium concentrations were 5 µM lasiocarpine and 50 µM riddelliine; and high concentrations were 10 µM lasiocarpine and 100 µM riddelliine. After replacing the medium, cytochalasin B (at a final concentration of 3 µg/mL) was added for 20 hours. Subsequently, the standard protocol for cytokinesis-blocking micronucleus (CBMN) assay

and evaluation was carried out, as described earlier in sections *4.3.3* and *4.3.9.2*. Three (3) independent experiments were conducted.

4.3.9.6 Mitosis and Mitotic disturbance figure analysis

Genomic integrity relies on the co-ordination between DNA replication and chromosome segregation. Mitotic disturbances could potentially lead to imbalances in chromosomes copy number, chromosomal rearrangements, or loss of chromosomal fragments. These mitotic errors can easily disrupt normal tissue homeostasis and contribute to carcinogenesis **[42]**. As a first step, the characterization of the distribution of normal mitotic stages within cells in question was conducted.

Table 2: Characterization of mitotic stages (according to Baudoin et al., 2018)

Mitotic stage	Description
Interphase	DNA is decondensed and the nuclear appears homogenous.
Prophase	Chromosomes start to be identifiable and are still confined within a well delineated nuclear perimeter due to the presence of the nuclear envelope (**Figure 16b)**.
Prometaphase	Lack defined border around the chromosomes, indicative of complete nuclear envelope breakdown. Chromosomes can be recognized as having a more advanced stage of condensation, whereby they appear as distinct rod-like elements. Chromosomes not yet fully aligned. Chromosomes are oriented in a ring with chromosome arms extending outward away from the center of the ring. Chromosomes begin taking on the shape of metaphase plate with more chromosomes at the center of the mitotic spindle.
Metaphase	Chromosomes exhibited at the spindle equator (**Figure 16c**), forming metaphase plate.
Anaphase	The sister chromatids separated and appear as two masses of chromosomes positioned on the two sides of the spindle equator (**Figure 16d and e**).
Telophase	Chromosomes completed their movement to the spindle poles and a nuclear envelope starts to re-form around each of the two chromosome sets, while the chromosomes start to decondensed (**Figure 16d and e).**

The characterization of mitotic cells was described as in Baudoin et al, (2018) **[42]** and summarized in **Table 2.** Typical sample images of the normal mitotic cell stages in HeLa H2B-GFP cells and HepG2 cells were taken during this study; and are shown in **Figure 16.**

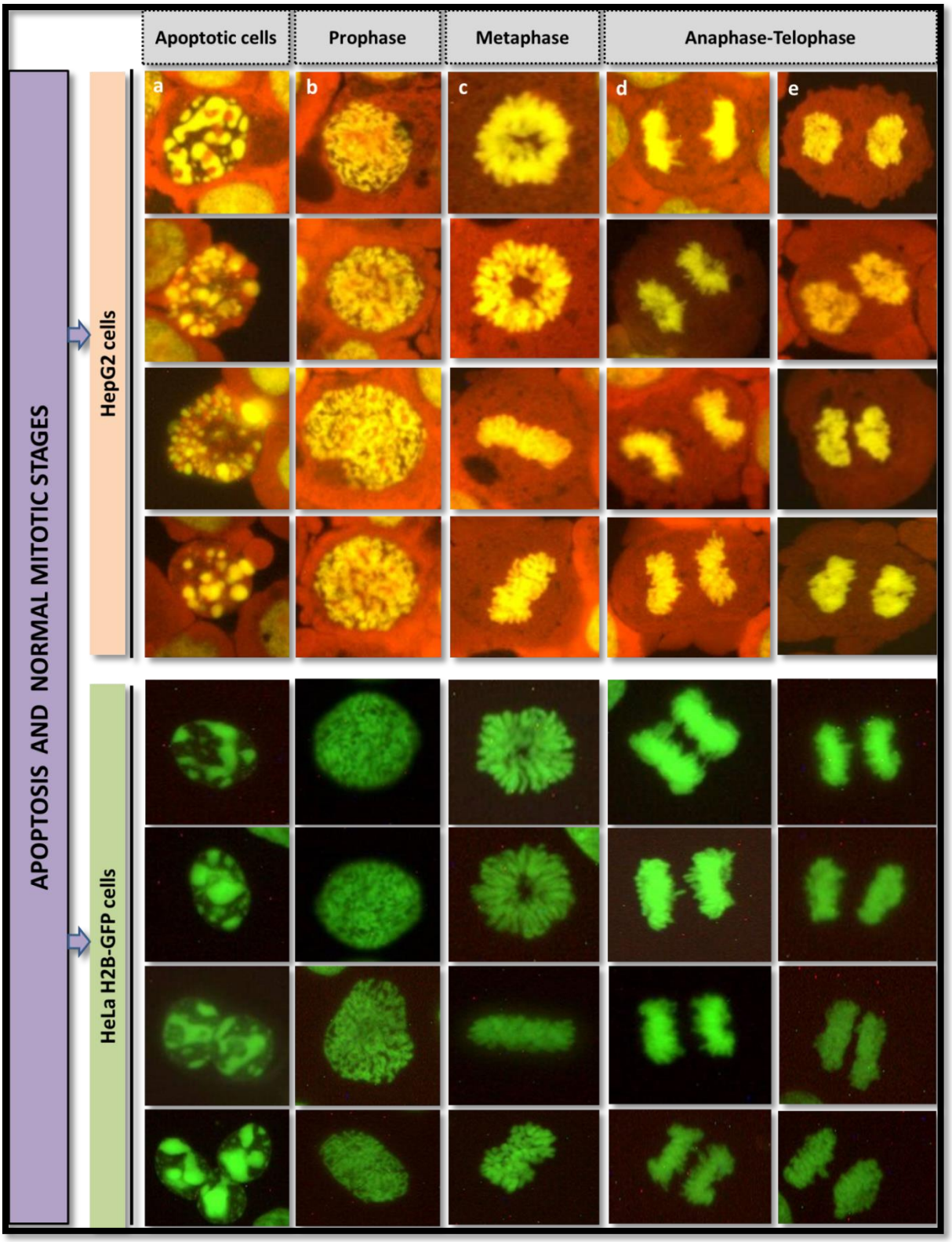

Figure 16: Representative images of HepG2 cells (orange-brown) and HeLa H2B-GFP cells (green) of the co-culture. Typical images of apoptotic cells (Images a) and mitotic cells at different stages such as prophase (Images b), metaphase (Images c), anaphase and telophase (Images d and e) are shown. The HepG2 cells (orange-brown) were stained with Gel Green while HeLa H2B-GFP cells (green) were mounted with DABCO; and all cells were viewed under a fluorescence microscope.

The analysis regarding numbers of cells in each of the mitotic stages as well as an assessment of disturbed arrangements in each of the stages was performed using cultures with only HepG2 cells, only HeLa H2B-GFP cells, and analyzing the HeLa H2B-GFP cells of the co-culture similar to the procedure described for micronucleus experiments. The seeded cells in a 6-well plate were incubated at 37◦C with 5% (v/v) CO2 for 20 hours. Then, cells were treated with lasiocarpine (10 µM), riddelliine (100 µM), europine (160 µM), vincristine 10 ng/ml (positive control for mitotic disturbance), and solvent controls, for 28 hours. Thereafter, cells were harvested and the microscopic slides prepared as described for micronucleus analysis but without using cytochalasin B.

The mitotic index (MI) was assessed by counting the number of mitoses at different stages such as prophase, metaphase, anaphase and telophase, in 1000 nuclei cells including apoptotic cells. The mitotic indexes in percentage (%) were calculated based on the following formulas:

$$\text{Mitotic Index } (\%) = \frac{\text{Nm}}{\text{Nt}} \times 100; \qquad \ldots\ldots\ldots\ldots equation\ 1$$

$$\text{Prophase Index } (\%) = \frac{\text{Nprophase}}{\text{Nm}} \times 100; \qquad \ldots\ldots\ldots\ldots equation\ 2$$

$$\text{Metaphase Index } (\%) = \frac{\text{Nmetaphase}}{\text{Nm}} \times 100; \qquad \ldots\ldots\ldots\ldots equation\ 3$$

$$\text{Anaphase Index } (\%) = \frac{\text{Nanaphase}}{\text{Nm}} \times 100; \qquad \ldots\ldots\ldots\ldots equation\ 4$$

$$\text{Telophase Index } (\%) = \frac{\text{Ntelophase}}{\text{Nm}} \times 100; \qquad \ldots\ldots\ldots\ldots equation\ 5$$

Where; N_m= total number of cells in mitotic division; N_t= total number of cells; $N_{prophase}$= number of cells in prophase; $N_{metaphase}$= number of cells in metaphase; $N_{anaphase}$= number of cells in anaphase; $N_{telophase}$= number of cells in telophase.

Normal mitotic figures were classified according to the definitions given by Baudoin et al., (2018) **[42]**. Disturbance mitoses were defined as mitoses deviating from the typical appearance

of normal mitoses and were assessed in 300 mitotic cells per slide. We classified the mitotic disturbance into the following categories:

i. Prophase disturbances
ii. Metaphase; no-spindle formation, non-congression, multipolar (tripolar and more than tripolar) and elongated chromosome/chromatid
iii. Anaphase; chromatin bridges, lagging chromosome(s), combination of chromatin bridges and lagging chromosome(s), and multipolar (tripolar and more than tripolar).
iv. Telophase; chromatin bridges, separate chromosome(s), and multipolar (tripolar and more than tripolar).
v. Other abnormal mitotic disturbance figures; atypical mitosis with a morphological appearance which was not reconcilable one of the above mentioned classes.

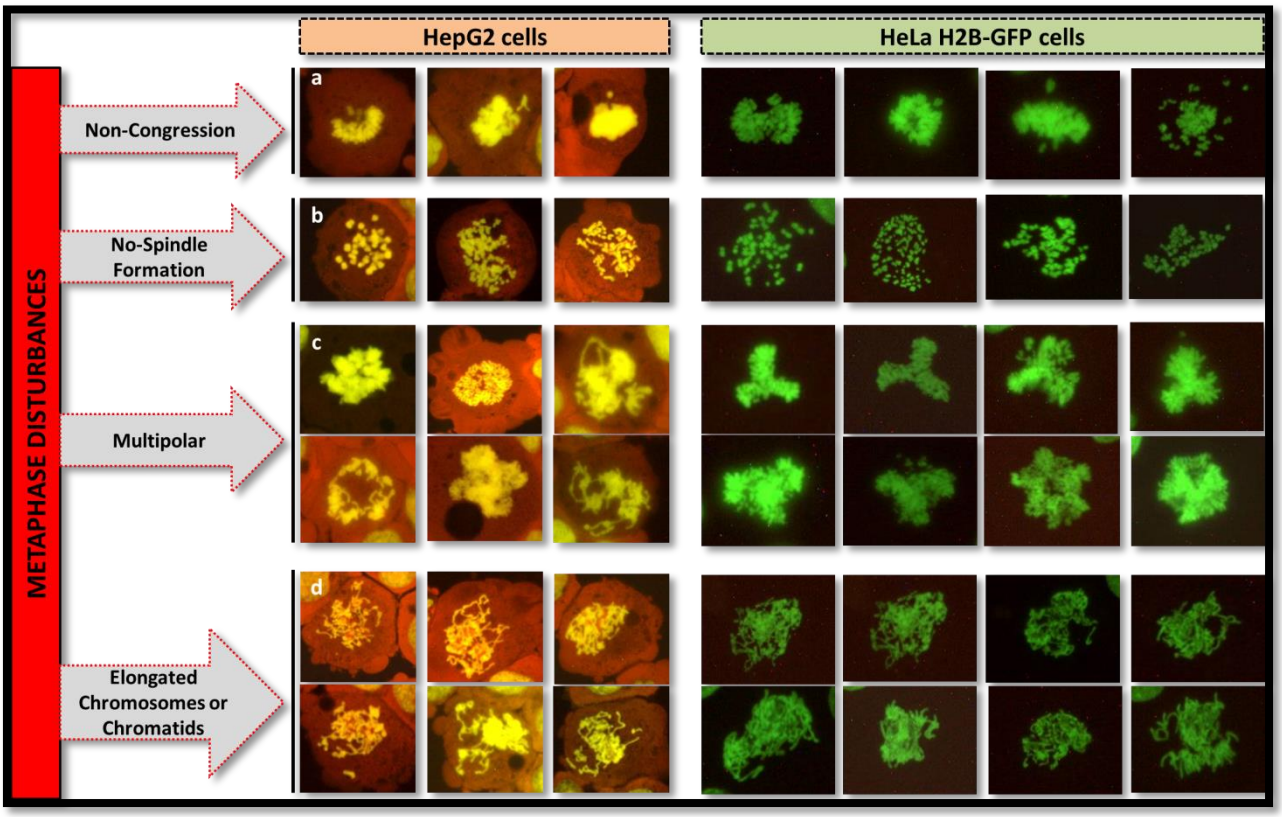

Figure 17: Representative images of metaphase disturbances of HepG2 cells (orange-brown) and of HeLa H2B-GFP cells (green) in the co-culture. The typical metaphase disturbances includes, non-congression (Images a), no-spindle formation (Images b), multipolar at metaphase (Images c), and elongated chromosomes or chromatids (Images d). HepG2 cells were stained with Gel Green, while HeLa H2B-GFP cells cultured alone or in co-culture were mounted with DABCO; all cells were viewed under fluorescence microscopy.

Typical sample images of metaphase disturbances in HepG2 cells cultured alone and that of HeLa H2B-GFP cells of the co-culture and HeLa H2B-GFP cells cultured alone were taken as shown in **Figure 17**.

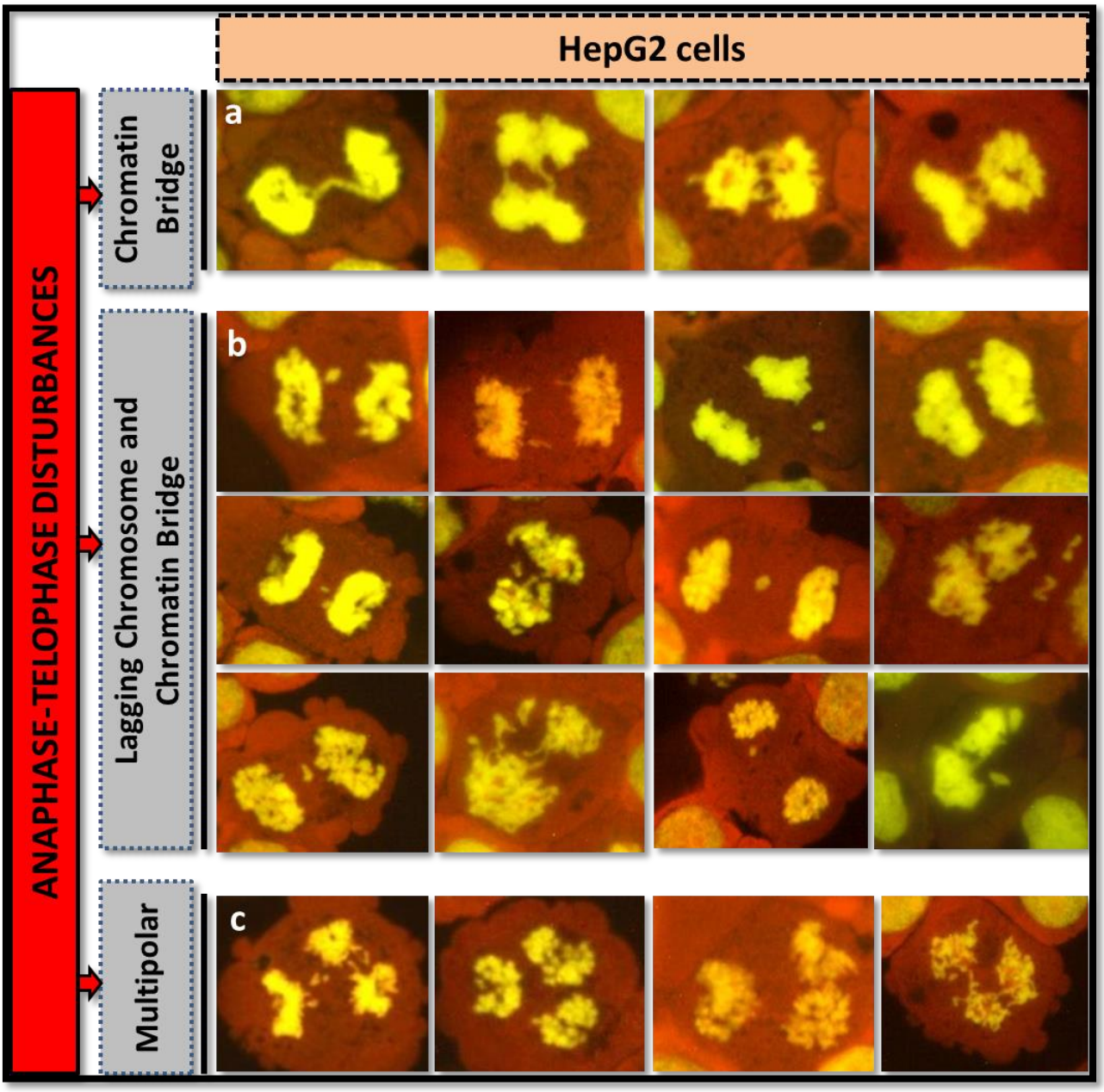

Figure 18: Representative images of HepG2 cells with anaphase-telophase disturbances. The anaphase-telophase disturbances include chromatin bridge (Images a), lagging chromosome (s) and chromatin bridge (Image b), and multipolar at anaphase or telophase (Images c). HepG2 cells were stained with Gel green and viewed under fluorescence microscopy.

Additionally, the typical sample images of anaphase-telophase disturbances in HeLa H2B-GFP cells of the co-culture and HeLa H2B-GFP cells cultured alone were taken as shown in **Figure 19**; and the Images from HepG2 cells are from a culture of only this cell type (**Figure 18**).

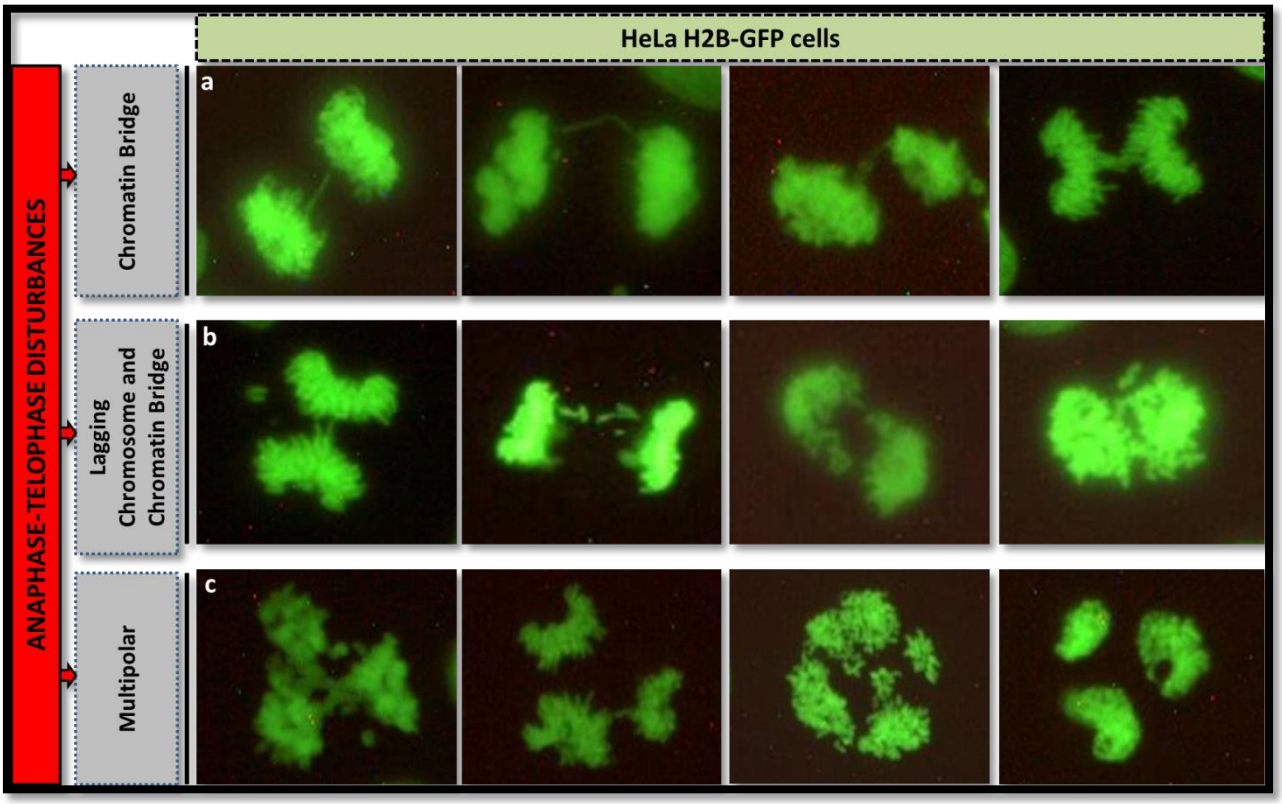

Figure 19: Representative images of HeLa H2B-GFP cells of the co-culture with HepG2 cells with anaphase-telophase disturbances. The anaphase-telophase disturbances include chromatin bridge (Images a), lagging chromosome(s) and chromatin bridge (Images b), and multipolar at anaphase or telophase (Images c). Co-culture cells were mounted with DABCO and viewed under fluorescence microscopy.

4.3.10 Analysis of metabolic enzymes and membrane transporter activities in HepG2 cells

4.3.10.1 Cytochrome P450 activity using GC/MS and UHPLC-MS/MS

Rationale and Theory: The metabolic activity of HepG2 cells after treatment with the chemical inhibitor ketoconazole (1 µM) and the chemical enzyme expression inducer rifampicin (20 µM) was analyzed using gas chromatography–mass spectrometry (GC/MS) and ultra-performance liquid chromatography-mass spectrometry (UHLC-MS/MS) at the Department of Food Chemistry, University of Wuerzburg, Germany, in collaboration with the author of this thesis.

The cells were treated and prepared by the author of this thesis, and GC/MS and UHPLC-MS/MS analyses were performed by the working group in the Department of Food Chemistry, following the procedure described in Kleider et al. (2022) **[449]**. Conclusions about the metabolic activity of HepG2 cells were drawn based on the metabolism of 17β-estradiol (E2) and estrone (E1).

Cell preparation and treatments: After pre-treatment of HepG2 cells with ketoconazole (1 µM; 24 hours) or rifampicin (20 µM; 72 hours), the cells were treated with 100 nM 17β-estradiol (E2) or 100 nM estrone (E1) for 28 hours. Following the 28-hour E1 or E2 treatment, the supernatant medium was collected. Subsequently, samples (E1 and E2) from the medium at time zero without HepG2 cells, samples from the medium incubated for 28 hours without HepG2 cells, and samples from the supernatant medium incubated for 28 hours using HepG2 cells pre-treated with ketoconazole or rifampicin were collected into 1.5 mL Eppendorf tubes, snap-frozen in liquid nitrogen, and then stored at -80◦C.

Transportation of samples: The frozen samples were then transported on dry ice to the Department of Food Chemistry for analysis using GC/MS and UHPLC MS/MS.

4.3.10.2 Carboxylesterase enzyme activity using Calcein-acetoxymethyl ester

Rationale and Theory: Intracellular carboxylesterase (CES) inhibition with loperamide (1 µM; 24 hours pre-treatment) in HepG2 cells was analyzed microscopically with calcein-acetoxymethyl ester (calcein-AM). Calcein-AM is a non-fluorescent and highly lipid soluble dye that rapidly diffuses through the plasma membrane into the cells. In the cytosol, this dye is metabolized by intracellular esterases by cleaving the ester bonds forming hydrophilic and green fluorescent calcein that cannot easily diffuse out of the cells. Hence, the green calcein formed is a fluorescent indicator with absorption and emission maximum wavelength of 494 nm and 517 nm, respectively, making this dye suitable for conventional fluorescence applications **[450-452]**. Thus, the accumulation of green fluorescent calcein can be used as indicator of intracellular carboxylesterase activity **[450, 453-455]**.

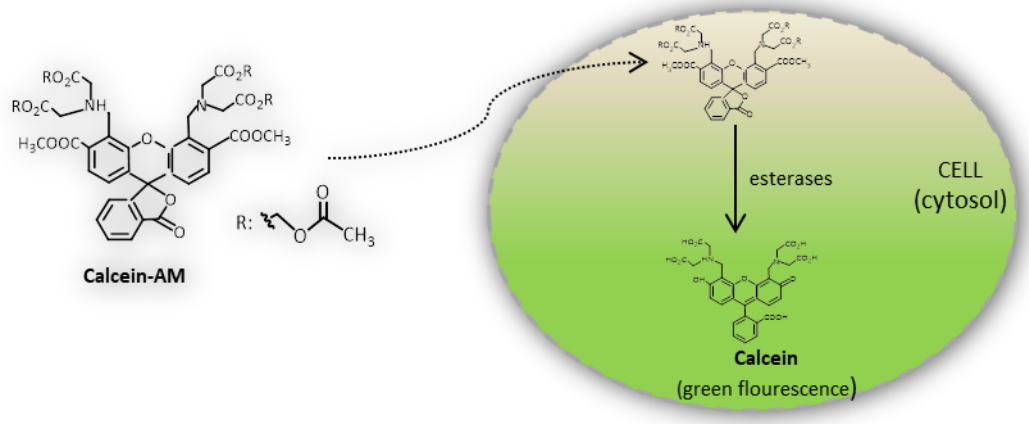

Figure 20: Calcein-acetoxymethyl ester (Calcein-AM) metabolized by esterases to form fluorescent green calcein in the cytosol of a cell. The diagram illustration was made using ChemDraw 20.1 software.

Microscopic analysis: CES inhibition with loperamide (1 µM) in HepG2 cells was analyzed using calcein-AM (100 nM) fluorescent dye under an Eclipse 55i fluorescence microscope using a fluorescein isothiocyanate (FITC) filter (Nikon GmbH, Japan) at 200-fold magnification. The green calcein fluorescence intensity in 250 cells was quantified using ImageJ software (http://rsbweb.nih.gov/ij) in cells with or without the CES inhibitor loperamide. Three (3) independent experimental analyses were conducted.

4.3.10.3 Influx membrane transporter activity using fluorescent dye-based transporter assays

Rationale and Theory: The chemical inhibitors nelfinavir (2.5 µM) for OATP1B1 influx transporter activity and the chemical inhibitor quinidine (25 µM) for OCT1 influx transporter activity were used in a fluorescent dye-based transporter assay. The activity of these two influx transporters was examined by measuring the intracellular accumulation of reference fluorescent dye substrates, namely sodium fluorescein (NaFLuo) for OATP1B1 influx transporter **[175, 456-458]** and ethidium bromide for OCT1 influx transporter **[175, 459, 460]**. Sodium fluorescein is a water-soluble fluorescent xanthene dye, for which several studies have demonstrated its use as a probe substrate for hepatic drug transport mediated through the OATP1B1 influx transporter **[457, 461]**. Ethidium bromide (EtBr) is a dark red, crystalline powder. In an aqueous solution, it has the capability to enter the cells and intercalate between the base pairs of DNA; upon

exposure to ultraviolet (UV) light, it fluoresces with a red-orange color. EtBr has been reported to be a suitable probe substrate for OCT1-mediated influx transporters **[175, 459, 460, 462]**.

Microscopic analysis: for OATP1B1 influx transporter activity, HepG2 cells were incubated at 37◦C with 20 µM EtBr for 30 minutes, in absence or presence of 2.5 µM nelfinavir (NFR) as OATP1B1 inhibitor **[175, 456-458]**; for OCT1 influx transporter activity, HepG2 cells were incubated with 5 µM NaFLuo for 1 hour, in absence or presence of 25 µM quinidine (Q), as OCT1 inhibitor **[175, 459, 460]**. Next, cells were washed thrice with PBS and then intracellular accumulation of fluorescent dye substrates was determined by taking images under an Eclipse 55i fluorescence microscope using a fluorescein isothiocyanate (FITC) filter (Nikon GmbH, Japan) at 200-fold magnification. Fluorescence intensity in 250 cells was quantified using ImageJ software (http://rsbweb.nih.gov/ij). The used excitation and emission wavelength for sodium fluorescein was 460 nm and 515 nm, respectively; while for ethidium bromide it was 360 nm and 590 nm in PBS, respectively. Three (3) independent experimental analyses were conducted.

4.3.10.4 Efflux membrane transporter activity using fluorescent dye-based transporter assays

Rational and Theory: The activities of MDR1- efflux transporter and that of MRP2- efflux transporter in human hepatoma HepG2 cells were analyzed through measuring intracellular accumulation or retention of a fluorescent probe substrate. Calcein-AM fluorescent dye was used as a probe substrate for MDR1- efflux transporter while calcein was used for MRP2- efflux transporter. Calcein-AM is a non-fluorescent, highly lipid soluble dye that can easily diffuse through the plasma membrane into the cells; and is well known as a probe substrate of MDR1-efflux transporter **[452]**. Once in the cytosol, calcein-AM dye is metabolized by intracellular esterases enzymes forming hydrophilic and green fluorescent calcein that cannot diffuse out of the cells passively. The free calcein formed in the hepatic cells can be easily effluxed out by MRP1 or MRP2, but not MDR1 **[463, 464]**. Thus, the only route for the free calcein (fluorescent) to be cleared out from the hepatic cells is via MRP1 or MRP2- mediated efflux transporters **[452]**. For example, studies have shown that calcein-AM (but not free calcein) serves as an excellent activator substrate for MDR1-ATPase in isolated cell membranes (Ka<1 µM). Additionally, it has been demonstrated that free calcein is not a substrate for export by MDR1 in

MDR1-expressing tumor cells **[465]**. Therefore, in principle, if calcein-AM is co-incubated with chemical inhibitor(s) of efflux-mediated transporters, calcein will increasingly be retained in the cells and thus the green fluorescence of the cells will increase. Therefore, the activity of the efflux-mediated transporters and their interaction with chemical inhibitors can easily be quantified by measuring the increase in the intracellular free calcein green fluorescence **[466]**.

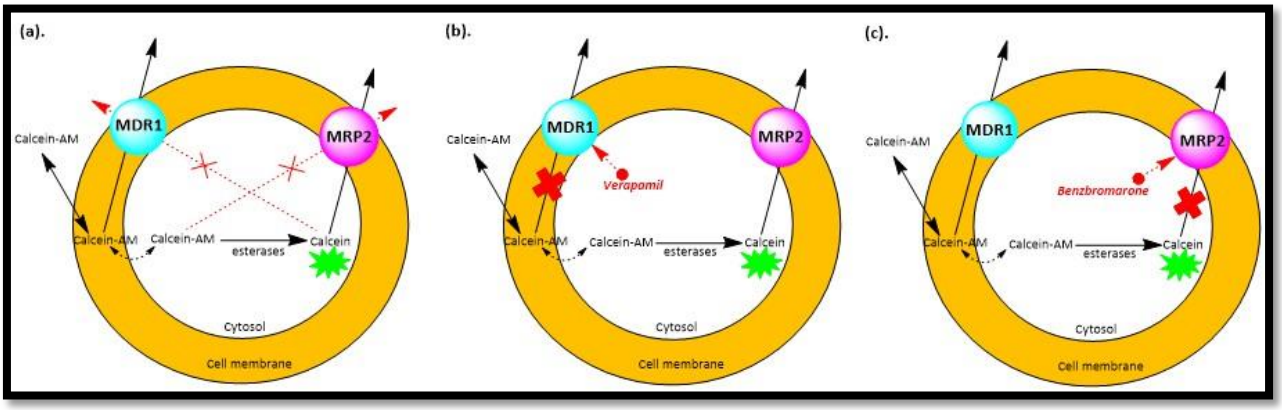

Figure 21: Calcein-acetoxymethyl ester (Calcein-AM) is a P-gp (MDR1) substrate and can be effluxed from the cell by MDR1 (a). Calcein is not effluxed by P-gp (MDR1) but can be effluxed by MRP2 (a). In the presence of a P-gp (MDR1) chemical inhibitor (verapamil), the efflux of Calcein-AM is reduced and more fluorescent Calcein is produced (b). In presence of MRP2 chemical inhibitor (benzbromarone), calcein efflux is reduced and is retained longer in the cytosol with green fluorescence (c). These diagram illustrations were made using ChemDraw 20.1 software.

Microscopic analysis: for MDR 1 (P-glycoprotein) efflux transporter activity, HepG2 cells were incubated with 100 nM calcein-AM for 15 minutes at 37◦C in the absence or presence of 50 µM verapamil, used here as a MDR 1-mediated efflux transporter inhibitor **[175, 426-428]**; for MRP2-mediated efflux transporter activity, HepG2 cells were first loaded with 100 nM calcein-AM for 15 minutes at 37◦C, then washed with one time PBS and re-incubated in calcein-AM free-medium for 120 minutes at 37◦C in the absence or presence of 10 µM benzbromarone, used here as a MRP2 efflux transporter inhibitor **[429, 430]**. Thereafter, cells were washed thrice with PBS and images of the cells were taken under an Eclipse 55i fluorescence microscope using a fluorescein isothiocyanate (FITC) filter (Nikon GmbH, Japan) at 200-fold magnification. Intracellular retention of fluorescent dye intensity was quantified in 250 cells for each treatment using ImageJ software (http://rsbweb.nih.gov/ij). The used excitation and emission wavelength for calcein-AM was at 485 nm and 515 nm, respectively. Three (3) independent experimental analyses were conducted.

4.3.10.5 Cross-reactivity of chemical inhibitor effects between metabolic enzymes and membrane transporters

The rationale was to analyze whether the used chemical inhibitors of metabolic enzymes had an effect on the studied membrane transporters. Because, based on a literature search, for example rifampicin (20 µM) was used as an inducer of cytochrome P450-3A4 **[411, 467-478]** in this study, however, it has also been reported to have an effect on inhibition of OATP1B1 (Ki=10 µM)-influx transporter **[479]** and induction on MDR1 and MRP2- efflux transporters **[411, 468, 477, 480]**; ketoconazole (1 µM) used as an inhibitor of cytochrome P450-3A4 **[417, 479, 481-491]**, has also been reported to inhibit MDR1- efflux transporter with IC_{50} >6 µM **[479, 492]**, OATP1B1- influx transporter with IC_{50}=1.8 µM **[479]**, and OCT1/2- influx transporters with IC_{50}= 0.13 µM and 0.89 µM, respectively **[479]**; for furafylline (1 µM) used as an inhibitor of cytochrome P450-1A2 **[419, 422, 481, 488-491]** no report was found regarding membrane transporters effects; loperamide (2.5 µM) used as an inhibitor of CES enzyme **[414, 493-496]** has been reported to inhibit MDR1- efflux transporter at a concentration of 20 µM **[497]**. Based on these literature reports, the author of this thesis performed an analysis to determine the effect on influx- and efflux-mediated transporters activities. The chemical inhibitors investigated here were rifampicin (20 µM), ketoconazole (1 µM), loperamide (2.5 µM), and furafylline (1 µM). These chemical inhibitors were analyzed using standard fluorescent dye-based transporter assays as described earlier in section *4.3.10.3* and *4.3.10.4*.

4.3.10.6 Depletion of intracellular glutathione using monochlorobimane dye

Rationale and Theory: In humans, glutathione (GSH) is present in all cells as the most abundant non-protein thiol that defends against oxidative stress. The biosynthesis of GSH takes place in the cytosol of all cells of the body; with the highest amount of GSH produced in liver cells. Part of the main determinants of GSH synthesis is the availability of the sulphur amino acid precursor, cysteine, and the activity of the rate-limiting enzyme, glutamate cysteine ligase (GCL) **[68, 498]**. The substance L-buthionine-sulfoximine inhibits glutamate-cysteine ligase, an enzyme that participates in GSH synthesis **[423, 425]**. Intracellular GSH in cells can be measured with monochlorobimane (MCBI) dye; MCBI readily enters the cells to form a fluorescent GSH-monochlorobimane (GSH-MCBI) adduct. The free, unbound probe shows very little

fluorescence, but when bound to reduced GSH in a reaction catalysed by glutathione-S-transferase (GST), its forms a highly and strongly fluorescent adduct **[498, 499]**. Here, L-buthionine sulfoximine (BSO; at final concentration 400 µM) was used for GSH depletion in HepG2 cells and GSH was determined by addition of MCBI using a plate reader at excitation and emission wavelengths of 380 nm and 490 nm, respectively.

Cell preparation, Treatments and Evaluation: 150,000 HepG2 cells were seeded in a 12-well plate with 2 mL medium and incubated at 37◦C with 5% (v/v) CO_2 for 24 hours. Then, medium was removed and cells were washed once with PBS and fresh 2 mL medium was added containing BSO at concentrations 0 µM, 200 µM, 400 µM and 800 µM, and incubated at 37◦C with 5% (v/v) CO_2 for 24 hours. Next, the medium was discarded and fresh medium added with monochlorobimane (MCBI; final concentration at 100 µM) for 30 minutes in dark at 37◦C with 5% (v/v) CO_2 incubation. Thereafter, cells were washed thrice with cold PBS and 1 mL of fresh PBS was added in the dark. The plate was then kept in the dark wrapped with aluminum foil and immediately the fluorescence intensity of the GSH-MCBI complex was determined using a plate reader (Ex/Em; 385 nm/490 nm). The amount of GSH in the cells correlates linearly with the fluorescence intensity, as the dye forms adducts with intracellular glutathione. Three (3) replicates were used per sample concentrations and three (3) independent experimental analyses were conducted.

4.3.11 Statistical analysis

All data are expressed as mean ± standard deviation (SD) from at least three (3) independent experiments. The independent sample *T*-test (Student´s T-test) was performed to check the significance compared to the control and one-way ANOVA analysis was used in comparison experiments with standard and inhibition/induction treatments. Graphs were created using GraphPad Prism version 10.0.1 (GraphPad Software, Inc, USA). Results were considered significant with $p\ value < 0.05$.

CHAPTER FIVE

5 RESULTS

5.1 Variation of micronucleus assay protocol in HepG2 cells

First, variations of the standard micronucleus protocol were attempted to increase the sensitivity of HepG2 cells to PA-induced genotoxicity. These modified protocols were tested using lasiocarpine as a model PA. The HepG2 cells were pre-differentiated for 2 weeks through culture in confluency and were then treated with lasiocarpine using the usual standard protocol. This protocol involved subculturing, thereby enabling cell proliferation and micronucleus formation even in confluent pre-cultured cells. The results were then compared with those obtained using the standard protocol (refer to **Figure 22a**). The findings showed that confluent pre-cultured cells exhibited increased sensitivity to the induction of micronuclei and cytotoxicity by lasiocarpine.

As a second option, the HepG2 cells were pre-treated with rifampicin for 72 hours to increase the expression and activity of cytochrome P450 enzymes **(Figure 22b)**. Then they were treated with lasiocarpine with the usual standard protocol. Compared to the standard protocol, rifampicin-pretreated cells were significantly more sensitive for the induction of micronuclei by lasiocarpine. There was no significant increase in cytotoxicity. The induction of CYP450 activity by rifampicin was analyzed based on the known metabolism of 17β-estradiol (E2) and estrone (E1) by CYP450 enzymes. This metabolism results in the formation of two major metabolites, 2-methoxy estrone (2-MeO-E1) and 16α-hydroxyl estrone (16α-HO-E1). As shown in **Figure 23**, a 72-hour pre-treatment with rifampicin significantly favoured the formation of estrone (E1) from 17β-estradiol (E2). Additionally, it led to a 3-fold increase in the formation of the major phase I metabolite 16α-hydroxyl estrone (16α-HO-E1), which, although not statistically significant l due to interexperimental variation, demonstrated a clear increasing trend. Moreover, rifampicin significantly increased the formation of the phase II metabolite estrone-3-glucuronide (E1-G) by 2-fold. Notably, there was a significant decrease in the levels of phase II metabolites, namely estradiol-3-sulfate (E2-3-S) and estrone sulfate (E1-S). Overall, rifampicin appeared to induce

CYP450 activity, as evidenced by the non-significant but clear increase in 16α-hydroxyl estrone (16α-HO-E1).

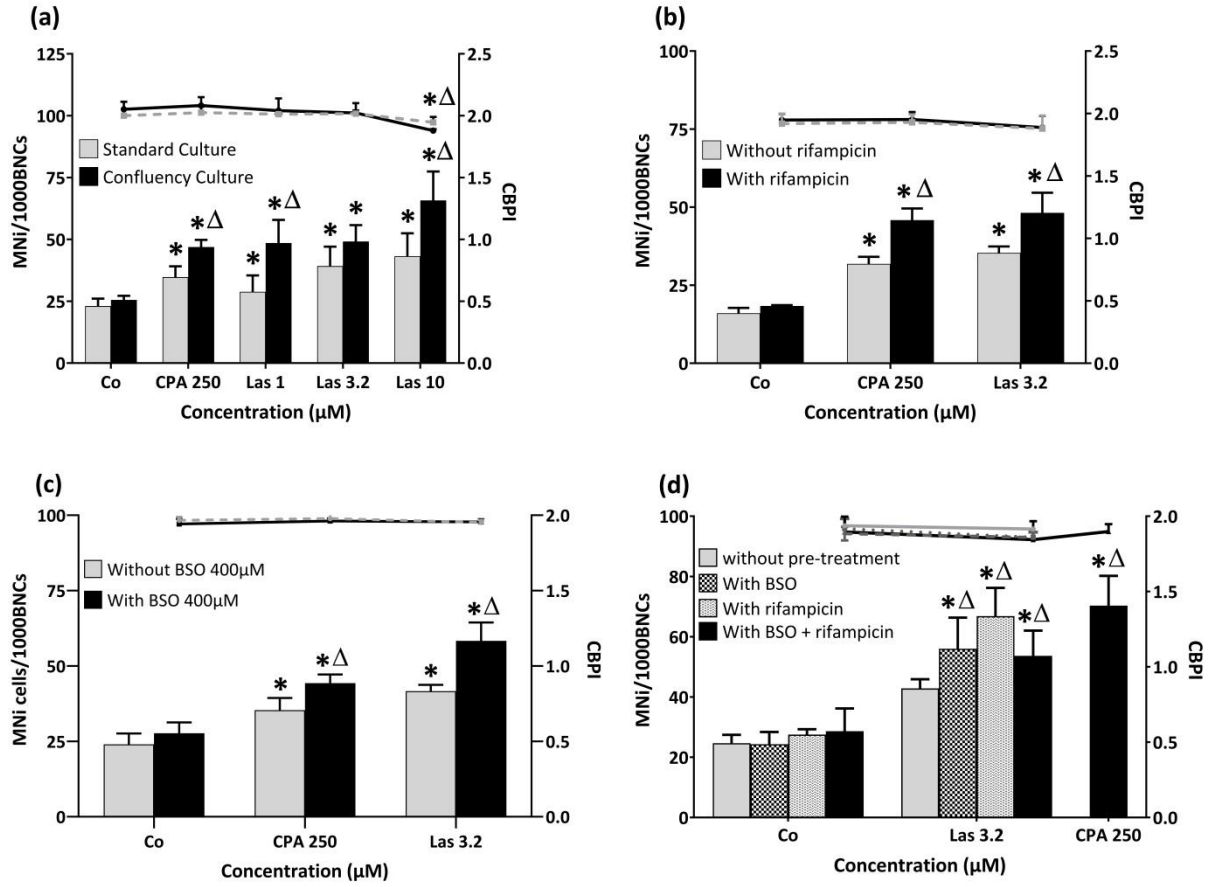

Figure 22: Micronucleus induction (columns) and proliferation index (CBPI, line) in pre-differentiated HepG2 cells (a); rifampicin-pre-treated HepG2 cells (b); L-buthionine sulfoximine (BSO) pre-treated HepG2 cells (c); and combination of rifampicin and BSO pre-treated HepG2 cells compared with the standard protocol (d). *p<0.05 compared to Co (solvent control) and Δp<0.05 compared with the respective undifferentiated/standard protocol cells. MNi= micronuclei; BNCs= binucleated cell; CBPI= cytokinesis-block proliferation index (cytotoxicity); CPA = cyclophosphamide (positive control); Las = lasiocarpine.

As a third option, HepG2 cells were pre-treated with 400 µM BSO for 24 hours to deplete GSH **(Figure 22c)**. Subsequently, lasiocarpine treatment followed using the standard protocol. In comparison to the standard protocol, the BSO-pretreated cells exhibited significantly higher sensitivity to the induction of micronucleus formation by lasiocarpine. There was no difference in the proliferation index (CBPI), indicating no cytotoxicity.

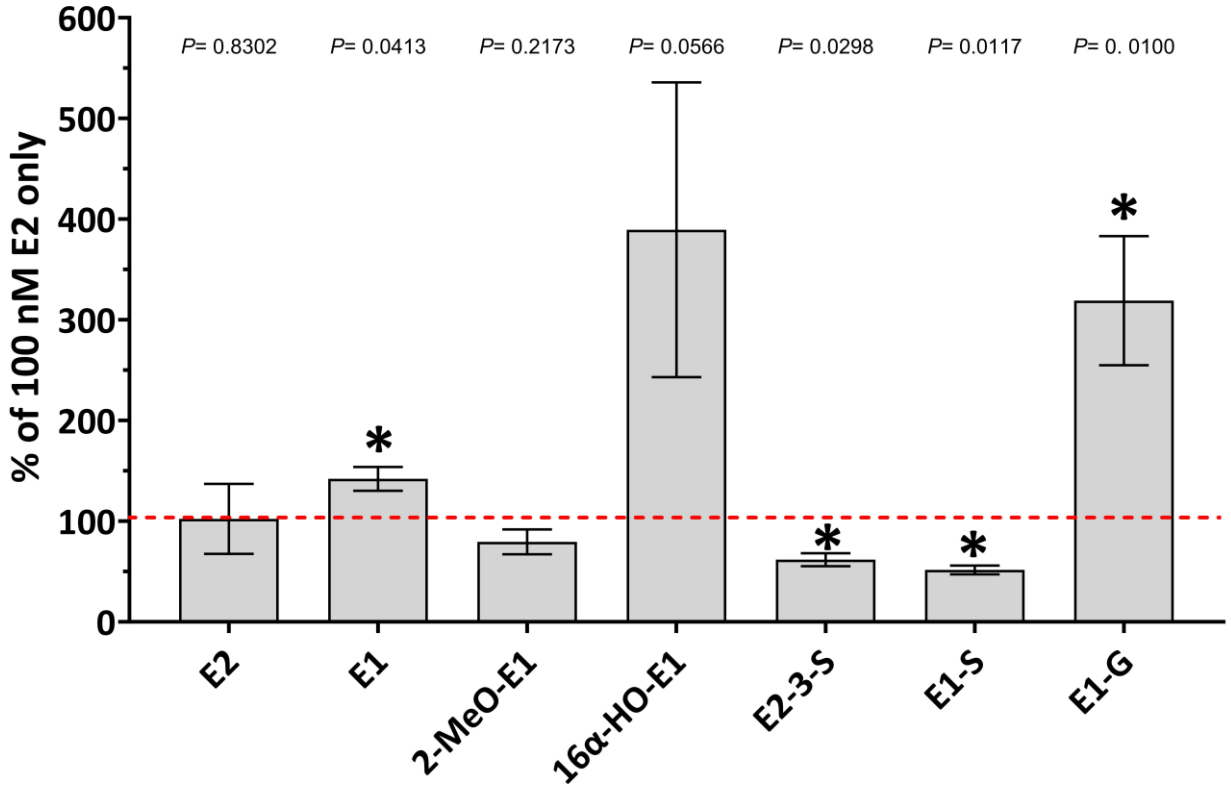

Figure 23: Percentage of levels of E2 and its metabolites (each related to the control 100 nM E2 set at 100%) detectable in the incubation media of cells pretreated with rifampicin for 72 hours and incubated with 100 nM E2 for 28 hours. Levels in the media of the control 100 nM E2 are in nmol/ml: 5.2 ± 1.6 (E2), 43.3 ± 8.4 (E1), 0.8 ± 0.5 (2-MeO-E1), 0.6 ± 0.08 (16α-HO-E1), 4.8 ± 0.6 (E2-3-S), 34.1 ± 3.5 (E1-S), and 0.3 ± 0.07 (E1-G). Statistical differences of levels in media with rifampicin treatment compared to the media of the control were determined using paired t-test and P values are given. Asterisks indicate a significant difference to the control. E2 refers to 17β-estradiol; E1 refers to estrone; 2-MeO-E1 refers to 2-methoxy estrone; 16α-HO-E1 refers to 16α- hydroxyl estrone; E2-3-S refers to Estradiol-3-sulfate; E1-S refers to Estrone sulfate; E1-G refers to estrone-3-glucoronide. Analysis performed by collaboration partners in the Department of Food Chemistry.

To confirm the depletion of GSH in HepG2 cells by BSO (400 µM), the analysis of BSO (400 µM) with MCBI showed a significant decrease in MCBI fluorescence intensity **(Figure 24)**. This reduction indicates a significant decrease in cellular GSH content by BSO. The vitality test results (not shown here) did not reveal any significant cytotoxicity compared to the solvent control for BSO up to 400 µM. However, at a concentration of 800 µM, the cells exhibited cytotoxicity. This suggests that the concentration of 400 µM BSO is suitable for the study, and with a 24-hour pretreatment, it confirms a significant depletion in cellular GSH content in HepG2 cells.

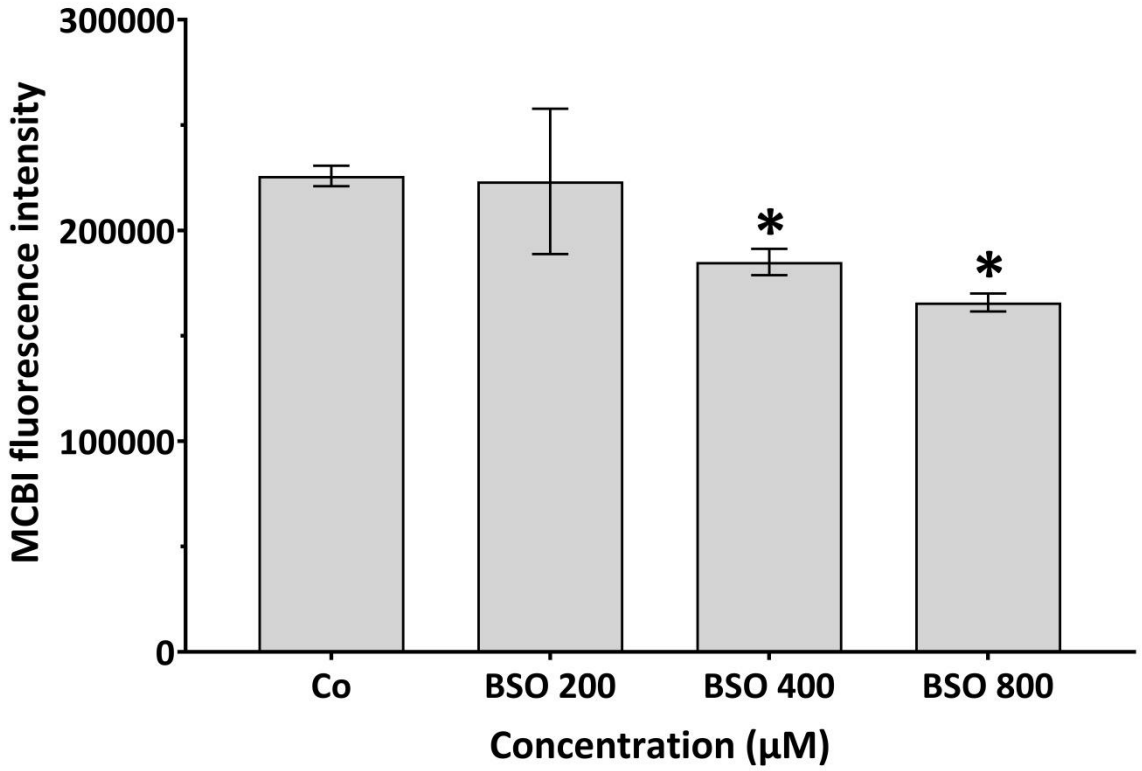

Figure 24: Effect of L-buthionine sulphoximine (BSO) in glutathione (GSH) depletion using monochlorobimane (mBCl) staining detection on different BSO doses for 24hours. BSO 200, 400, 800 = buthionine sulphoximine 200µM, 400µM, 800µM respectively. Where *p<0.05 compared with control (DMSO).

To optimize the protocol further, a fourth option was designed under same experimental conditions. HepG2 cells pre-treated with a combination of rifampicin and BSO were more sensitive for induction of micronucleus formation by lasiocarpine with no significant differences in proliferation index **(Figure 22d)** compared to solvent control. However, some floating cells (dead cells) were observed after lasiocarpine treatment; which indicates cytotoxicity. To compare the protocol options which were conducted again under the same experimental condition, the highest significant induction of micronuclei by lasiocarpine was observed in the rifampicin-pretreated HepG2 cells, compared to BSO-pretreated HepG2 cells and the combination of rifampicin and BSO pretreated HepG2 cells **(Figure 22d)**.

From these protocol variants, which all increased the sensitivity of HepG2 cells for the PA lasiocarpine, the more practical one was a 72-hour pretreatment with rifampicin for induction of cytochrome P450 activity. This protocol was then chosen for testing selected PAs.

5.2 Dose response relationships for selected PAs in rifampicin-pretreated HepG2 cells

After a pretreatment with rifampicin the selected PAs of different ester-type were added at different concentrations, and then a cytochalasin B treatment was performed in order to yield binucleated cells. The selected PAs were the monoesters europine (Ep) and lycopsamine (Ly), the cyclic-diesters retrorsine (RT), riddelliine (Rid) and seneciphylline (Sc), and the open-diesters echimidine (ED) and lasiocarpine (Las) **(Figure 25a-g)**.

Each of the tested PA yielded a significant induction of micronuclei. At least for one concentration, a significant induction was found in the absence of a significant reduction of cell proliferation. In each case, there was at least one lower concentration of PA at which no significant micronucleus induction was detected. The induction yielded a similar maximal increase for all PA in the range of 1.64-2.0 fold. Specifically, the increases were 1.99x for europine, 1.64x for lycopsamine, 1.99x for retrorsine, 2.0x for riddelliine, 1.8x for seneciphylline, 1.94x for echimidine and 1.97x for lasiocarpine. The lowest concentration at which significant induction of micronuclei was found was 3.2 µM for lasiocarpine and riddelliine, 32 µM for retrorsine and echimidine, and 100 µM for seneciphylline, europine and lycopsamine. The apoptotic and mitotic cells numbers, compared to the solvent control **(Appendix I)** were not critically altered in all the PA experiments with HepG2 cells, except for europine at 1000 µM, where a slight increase in apoptosis was detected, including observation of floating cells (dead cells) after europine 1000 µM treatment.

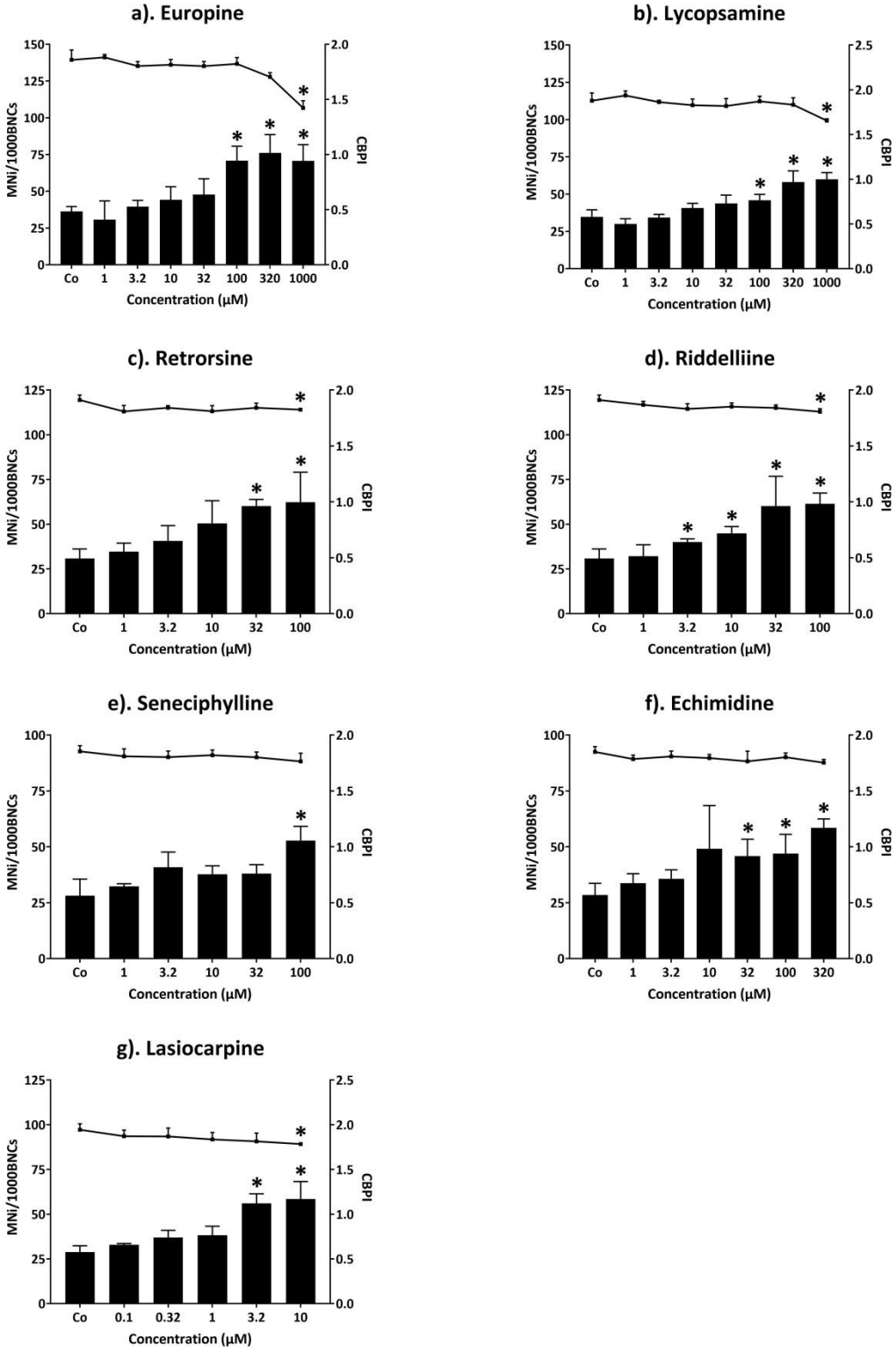

Figure 25: Micronucleus induction (columns) and proliferation index (CBPI; line) in rifampicin-pre-treated HepG2 cells with the indicated pyrrolizidine alkaloids. *p<0.05 compared to Co (solvent control). MNi= micronucleus; BNCs= binucleated cells; CBPI= cytokinesis-block proliferation index.

The lowest micronucleus inducing concentrations found in this thesis were compared with published literature concerning micronuclei and yH2Ax **(Table 3)**; which reveals a lower sensitivity of HepG2 used here compared to HepaRG for micronuclei, but similar sensitivity if compared with HepaRG yH2Ax.

Table 3: Comparison of the lowest significant pyrrolizidine alkaloid concentration with published literature.

	Study (endpoint, cell line)		
Compound	**Present study (micronuclei, HepG2)** **Lowest tested significant concentration**	**Allemang et al. (2018) (Micronuclei, HepaRG) Lowest tested significant concentration**	**Louisse et al. (2019) (yH2Ax, HepaRG)** **BMC_{50} (50% increase over background level)**
Lasiocarpine	3.2	0.59	5.3
Riddelliine	3.2	3.11	5.8
Echimidine	32	1.98*****	9.4
Retrorsine	32	9.5	6.4
Seneciphylline	100	Not tested	4.8
Europine	100	17.78	62
Lycopsamine	100	74.07	303

The study in this dissertation was based on micronucleus induction in human hepatoma cells HepG2 pretreated with rifampicin for 72 hours. *Louisse et al*. (2019) results were based on yH2Ax assay in HepaRG cells while *Allemang et al*. (2018) was based on micronucleus induction in HepaRG human liver cells. The concentrations of the present study and of *Allemang et al*. (2018) are based on lowest tested significant concentration, those of *Louisse et al*. (2019) are based on BMC_{50} (50% increase over background level). ***** received a different rank in the potency order when shape of dose response was also considered (see discussion). Concentrations of the compounds are in micromolar (μM).

5.3 Inhibitors of metabolic enzymes in HepG2 cells

For mechanistic investigation of PA induced genomic damage based on metabolic enzymes inhibition, lasiocarpine was chosen again as a model PA and HepG2 cells were used, applied with standard protocol. Carboxylesterase 2 enzyme (CES 2) is involved in the detoxification of PA. The CES 2 inhibitor loperamide yielded an increased formation of lasiocarpine-induced micronuclei in HepG2 cells **(Figure 26a)**, revealing a possible role of CES-mediated detoxification in the genotoxicity of lasiocarpine. There was no significant difference in cytotoxicity, as indicated by the proliferation index (CBPI).

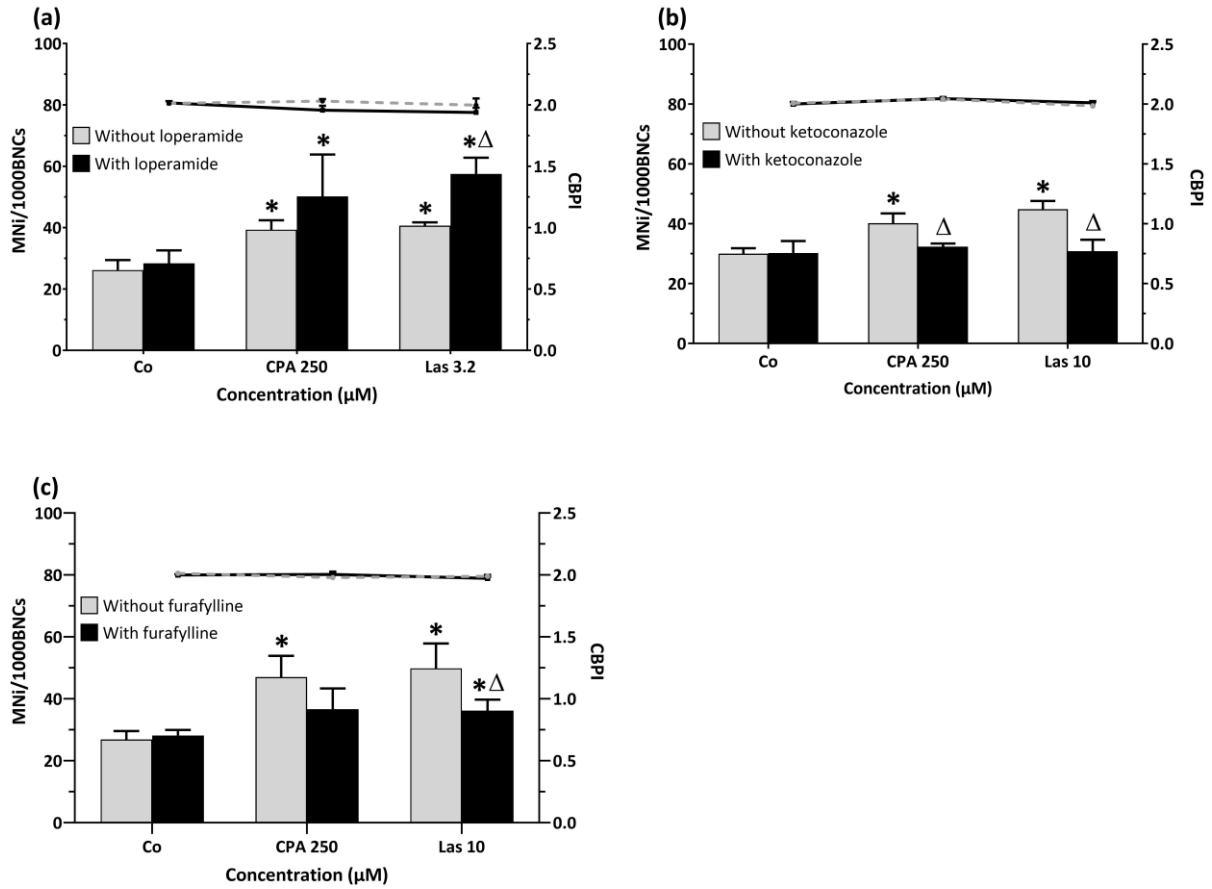

Figure 26: Micronucleus frequency (columns) and proliferation index (CBPI; line) in HepG2 cells pre-treated with inhibitors of metabolic enzymes, carboxylesterase-inhibitor loperamide (a), cytochrome P450 3A4 inhibitor ketoconazole (b) and cytochrome P450 1A2 inhibitor furafylline (c) compared with the standard protocol. *p<0.05 compared with Co (solvent control), Δp<0.05 compared with the respective dose without inhibitor pre-treatment. MNi= micronucleus; BNCs= binucleated cells; CBPI= Cytokinesis-block proliferation index; CPA = cyclophosphamide (positive control); Las = lasiocarpine; (n=3).

Regarding analysis of CES inhibition with calcein-AM, there was significant decrease in calcein green flourescence intensity in presence of loperamide (**Figure 27a-b**); which indicates less formation of calcein in the cytosol due to CES inhibition by loperamide. There was no cytotoxicity effect induced by loperamide (2.5 µM) in HepG2 cells, based on the vitality test (results not shown here) conducted by the author of this dissertation.

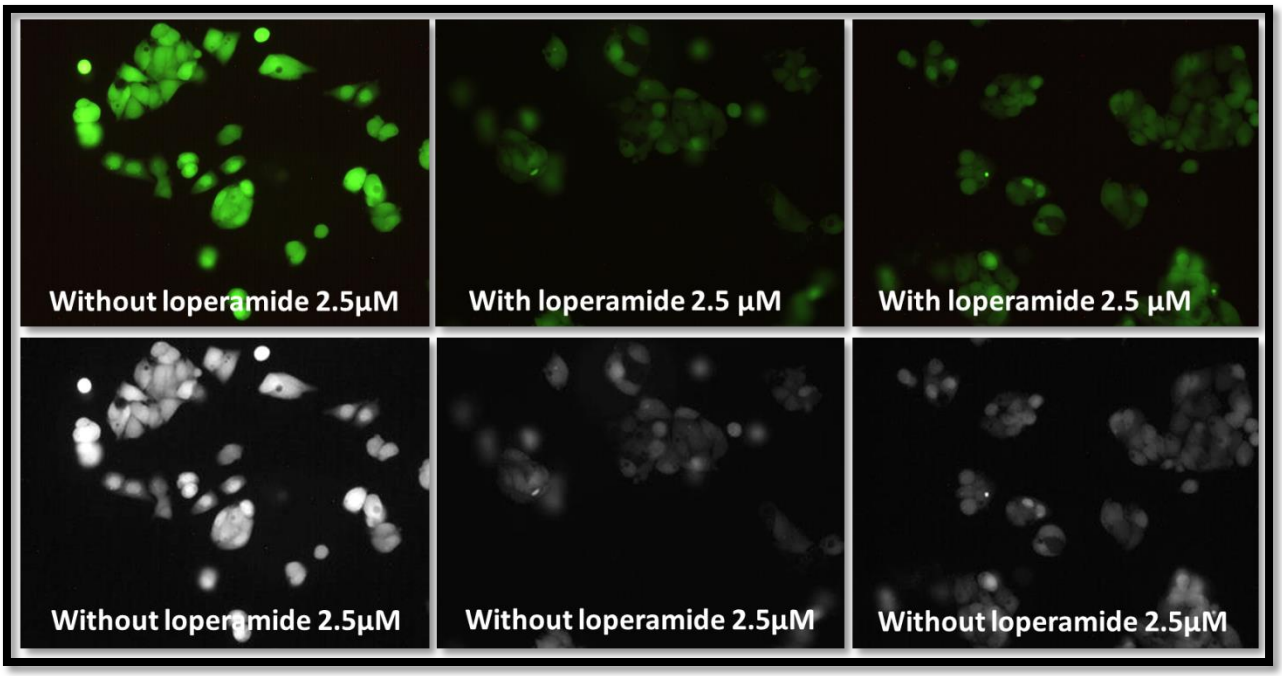

Figure 27a: Representative Images of HepG2 cells on the analysis of CES enzyme inhibition by loperamide (2.5 µM) using calcein-AM (100 nM) dye.

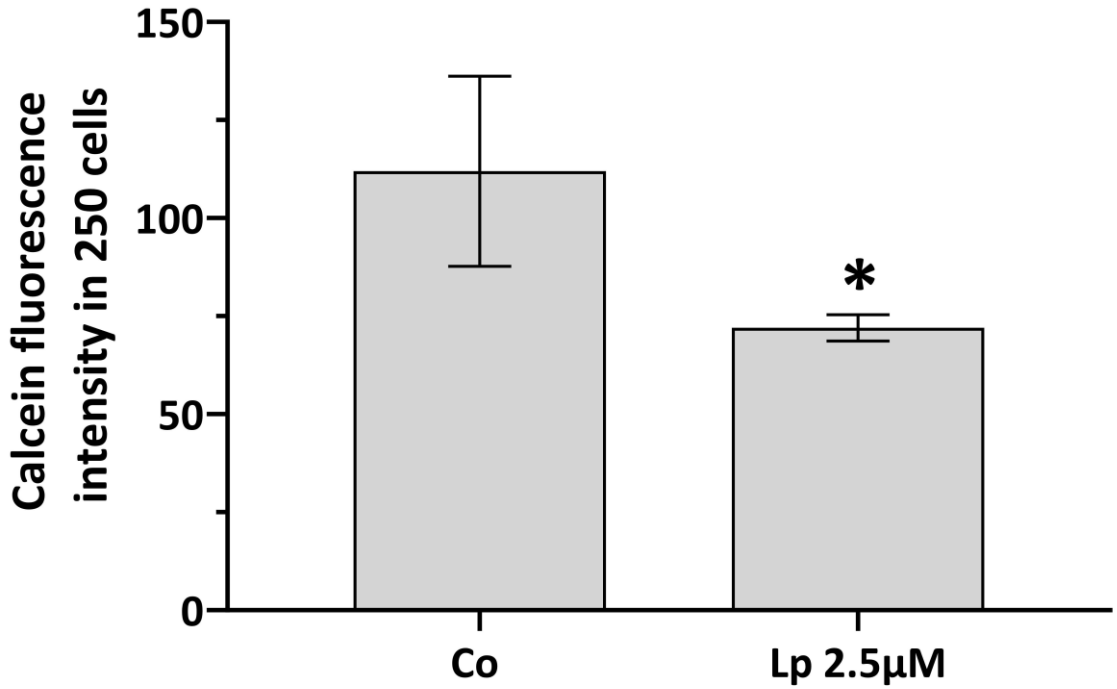

Figure 27b: Analysis of CES2 inhibition by loperamide using calcein-AM (100 nM) flourescence dye in HepG2 cells. Loperamide (2.5 µM) significantly reduce the calcein green flourescence intensity; indicating less calcein-AM is metabolized to calcein by CES enzyme in the cell cytosol. Images were taken under FITC filter of fluorescence microscope.

Cytochrome P450 enzyme activity is required for PA-induced effects. Ketoconazole is a cytochrome P450 inhibitor with a preference for cytochrome P450-3A4 isoenzyme. Ketoconazole prevented lasiocarpine-induced micronucleus formation completely **(Figure 26b)**.

The inhibition of the activity of the CYP450-3A4 isoenzyme by ketoconazole in HepG2 cells was also analyzed based on the metabolism of 17β-estradiol (E2) and estrone (E1) by CYP450 enzymes. Usually, mediated by the CYP450-3A4 isoenzyme, the two main metabolites, 2-methoxy estrone (2-MeO-E1) and 16α-hydroxyl estrone (16α-HO-E1), are formed. However, in the presence of ketoconazole, the formation of 2-methoxy estrone (2-MeO-E1) and 16α-hydroxyl estrone (16α-HO-E1) was significantly decreased **(Figure 28)**, indicating an inhibition of the CYP450-3A4 isoenzyme by ketoconazole.

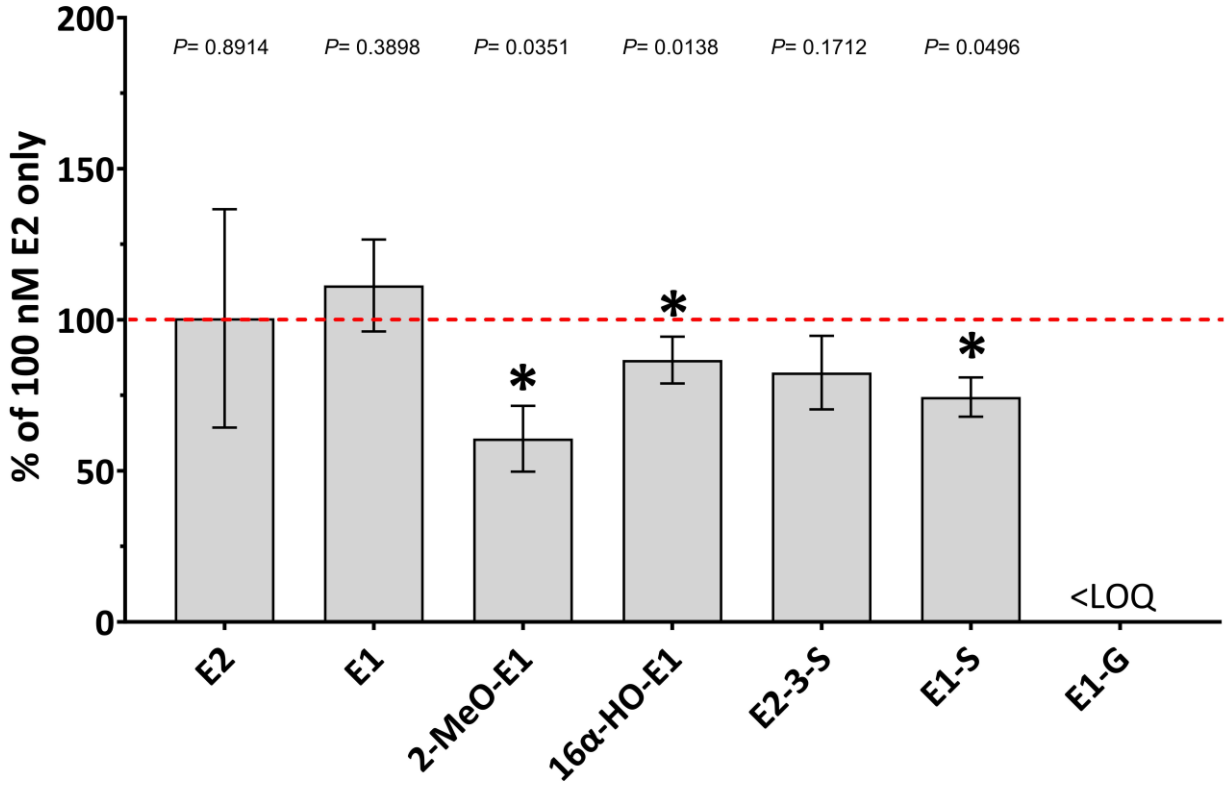

Figure 28: Percentage of levels of E2 and its metabolites (each related to the control 100 nM E2 set at 100%) detectable in the incubation media of cells pretreated with ketoconazole for 3days and incubated with 100 nM E2 for 28 hours. Levels in the media of the control 100 nM E2 are in nmol/ml: 4.0 ± 0.5 (E2), 69.6 ± 15.0 (E1), 0.8 ± 0.1 (2-MeO-E1), 0.7 ± 0.2 (16α-HO-E1), 1.7 ± 0.2 (E2-3-S), and 10.6 ± 2.5 (E1-S). E1-G levels were below limit of quantification (<LOQ). Statistical difference of levels in media with ketoconazole treatment compared to the media of the control was determined using paired T-test and P values are given. Asterisks indicate a significant difference to the control.

Furafylline is a cytochrome P450 inhibitor with a preference for cytochrome P450-1A2 isoenzyme. Furafylline reduced lasiocarpine-induced micronucleus formation, but did not abolish it completely **(Figure 26c)**. No significant differences in proliferation index (CBPI) occurred in ketoconazole or furafylline pre-treated cells, indicating the absence of cytotoxicity.

5.4 Inhibitors of membrane transporters in HepG2 cells

To further the mechanistic investigations, influx and efflux membrane transporters were studied using chemical inhibitors.Quinidine (Q) and nelfinavir (NFR) are OCT1 and OATP1B1 influx transporter inhibitors, respectively, which reduced micronucleus induction by lasiocarpine (only quinidine significantly), but not completely, pointing to a relevance of OCT1 for PA uptake in HepG2 cells **(Figure 29a-b)**.

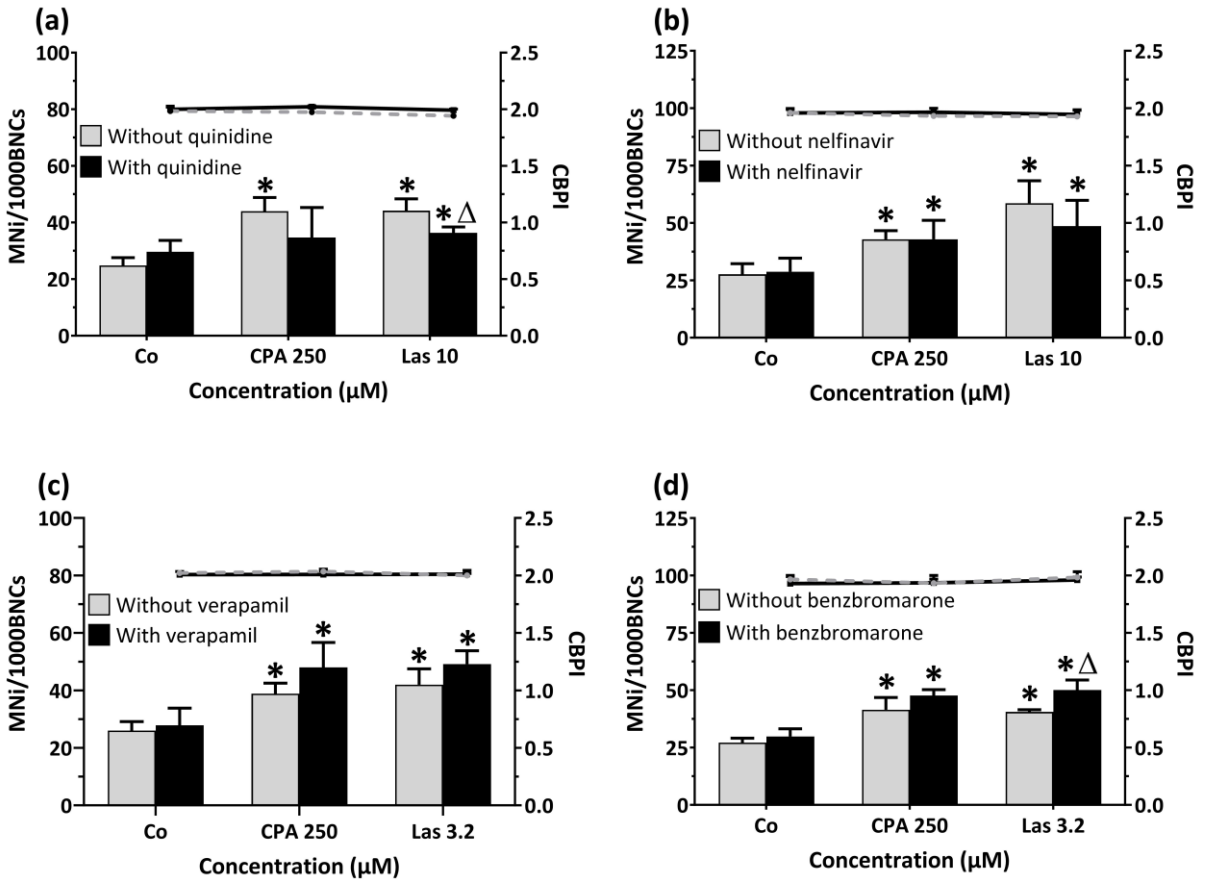

Figure 29: Micronucleus frequency (columns) and proliferation index (CBPI; line) in HepG2 cells pre-treated with inhibitors of transmembrane transporters, OCT1 influx transporter inhibitor quinidine (a),OATP1B1 influx transporter inhibitor nelfinavir (b),

MDR1 efflux transporter inhibitor verapamil (c), MRP2 efflux transporter benzbromarone (d), compared with the standard protocol. *p<0.05 compared with Co (solvent control), Δp<0.05 compared with the respective dose without inhibitor pre-treatment. MNi= micronucleus; BNCs= binucleated cells; CBPI= Cytokinesis-block proliferation index; CPA = cyclophosphamide (positive control); Las = lasiocarpine.

Verapamil (V) and benzbromarone (Bz) are MDR1 and MRP2 efflux transporter inhibitors, respectively, and they caused a slighly increased micronucleus induction by lasiocarpine (significant only for benzbromarone) in HepG2 cells **(Figure 29c-d)**.

The influx- or efflux- membrane transporter activities in HepG2 cells were analysed by using suitable reference probe substrate dyes and by measuring accumulation or retention of the dye in the cells. Accumulation of ethidium bromide (EtBr; OCT1 substrate) and that of sodium fluorescein (NaFLuo; OATP1B1 substrate) were significantly reduced in presence of quinidine (25 µM) and nelfinavir (2.5 µM), respectively **(Figure 31a-b)**; indicating the inhibition of OCT1-influx mediated transporter in cells by quinidine and OATP1B1-influx mediated transporter in cells by nelfinavir. The illustrated images of the accumulation of ethidium bromide (EtBr; OCT1 substrate) and sodium fluorescein (NaFLuo: OATP1B1 substrate) are shown in **Figure 30**.

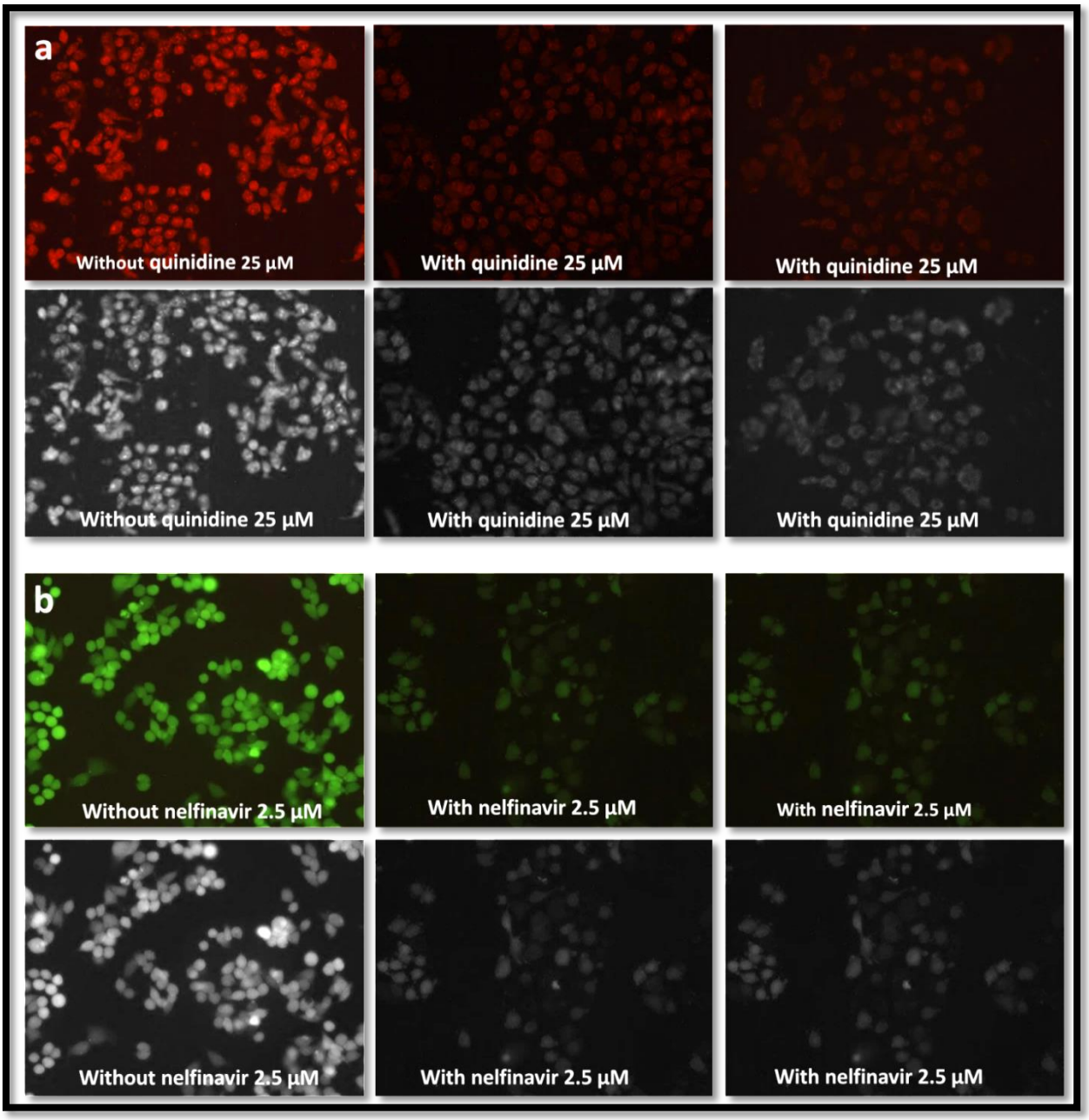

Figure 30: Representative Images of Uptake and Accumulation of Probe Substrate Dyes in HepG2 Cells. Images **(a)**: Analysis of OCT1 influx-mediated transporter inhibition by quinidine (25 µM) based on the uptake of the probe substrate dye ethidium bromide (20 µM). Images **(b)**: Analysis of OATP1B1 influx-mediated transporter inhibition by nelfinavir (2.5 µM) using the probe substrate dye sodium fluorescein (5 µM).

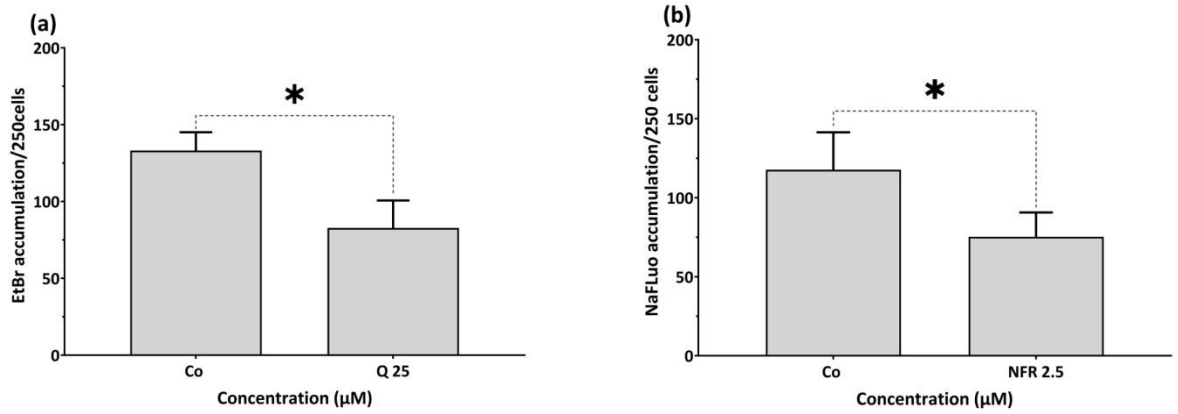

Figure 31: Uptake and Accumulation of the probe substrate dyes. Graph **(a)**: analysis of OCT1-influx mediated transporter based on the uptake of probe substrate dye ethidium bromide (EtBr; for OCT1); chemical inhibitor quinidine (Q; 25 µM) for OCT1-influx mediated transporter. Graph **(b)**: analysis of OATP1B1 -influx mediated transporters based on uptake of probe substrate dye sodium fluorescein (NaFLuo; for OATP1B1); chemical inhibitor nelfinavir (NFR; 2.5 µM) for OATP1B1-influx mediated transporter. Co= solvent control; NFR 2.5= nelfinavir 2.5 µM; Q 25= quinidine 25 µM.

Moreover, the increase in calcein green fluorescence was significantly higher in the presence of verapamil, indicating more retention and hydrolysis of calcein-AM to calcein in the cytosol due to the inhibition of MDR1-efflux transporter activity **(Figure 33b)**. In cells treated with benzbromarone, a significant increase in calcein green fluorescence was observed, demonstrating the effectiveness of benzbromarone in inhibiting MRP2-efflux transporter activity **(Figure 33a)**. Typical images illustrating the retention or accumulation of calcein in the presence or absence of benzbromarone or verapamil are shown in **Figure 32**.

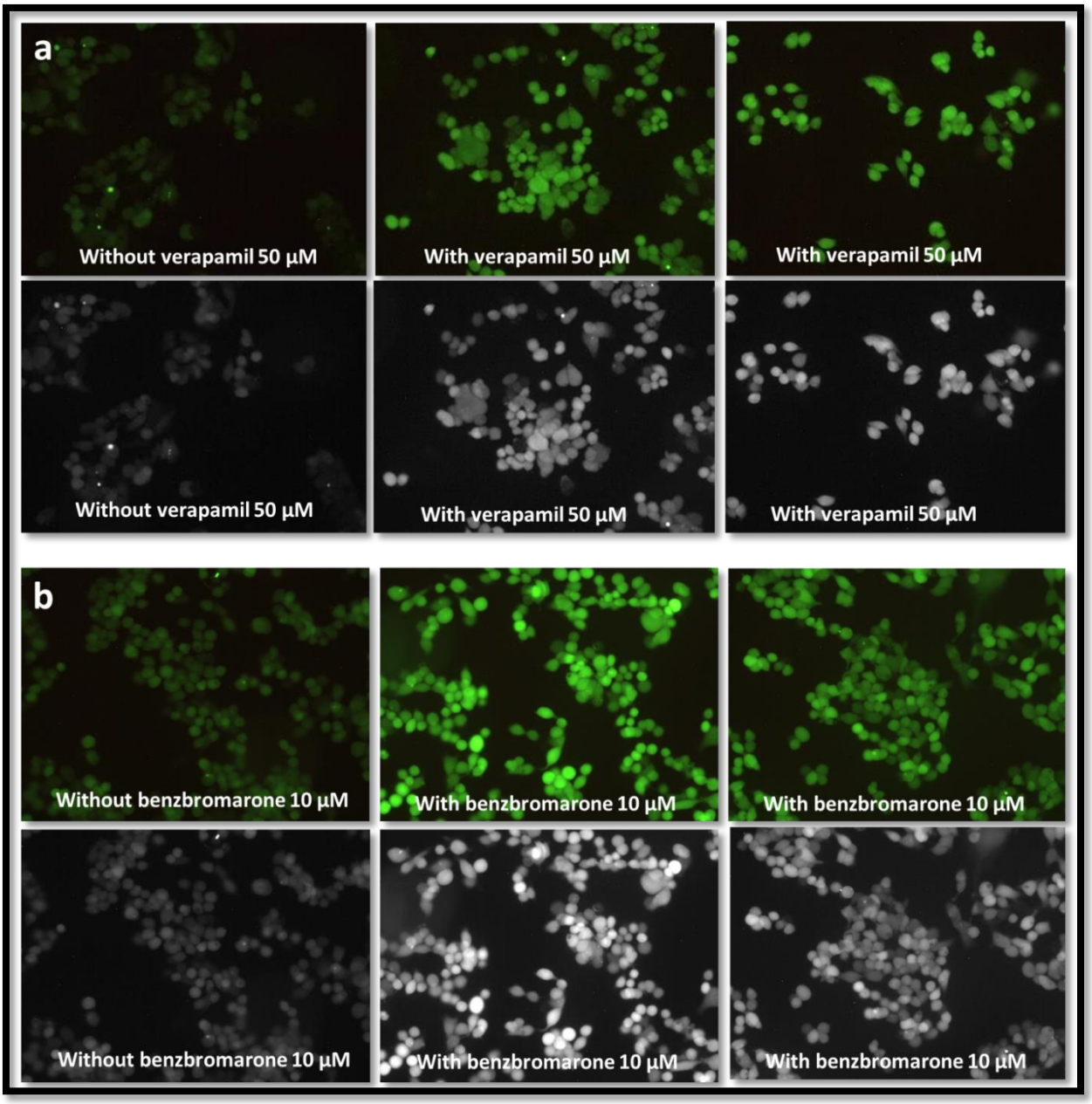

Figure 32: Representative Images on the analysis of MDR1-or MRP2 -efflux mediated transporters based on retention or accumulation of probe substrate dye calcein-AM (MDR1) or calcein (MRP2) in HepG2 cells; chemical inhibitor verapamil (50 µM) for inhibition of MDR1-efflux mediated transporter (Images **a**) and benzbromarone (10 µM) for the inhibition of MRP2-efflux mediated transporter (Images **b**).

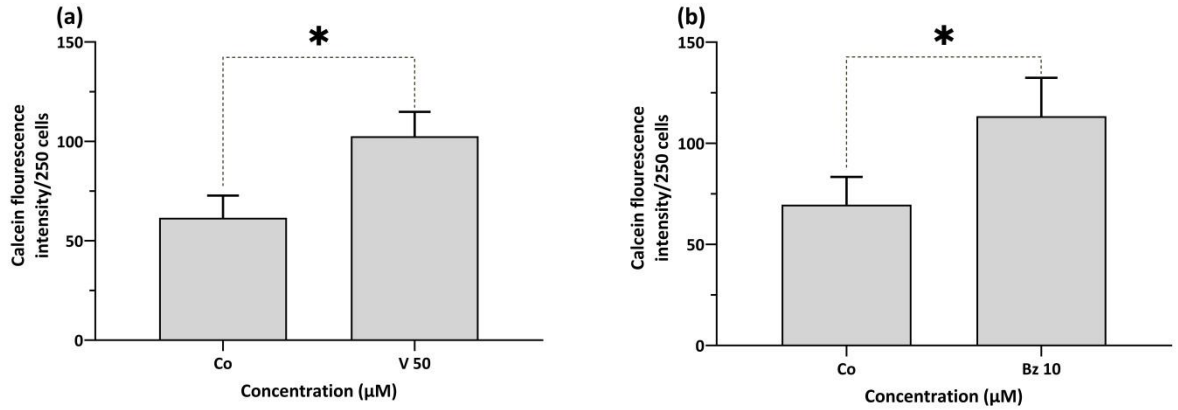

Figure 33: Accumulation and retention of the probe substrate dyes. Graph **(a)**: analysis of MDR1-efflux mediated transporter based on the accumulation of the probe substrate dye calcein-AM (MDR1); chemical inhibitor verapamil (V; 50 µM) for inhibiting MDR1-efflux mediated transporter. Graph **(b)**: analysis of MRP2-efflux mediated transporter based on the retention of the probe substrate dye calcein (for MRP2); chemical inhibitor benzbromarone (Bz; 10 µM) for inhibiting MRP2-efflux mediated transporter. Co = solvent control; Bz 10 = benzbromarone 10 µM, and V 50 = verapamil 50 µM.

The influence of chemical inhibitors (ketoconazole, furafylline, loperamide) and inducer (rifampicin) used in this dissertation were further analyzed regarding their effect on influx (OATP1B1 and OCT1) - and efflux (MDR1 and MRP2) - transporters in HepG2 cells. All these chemical inhibitors and inducer did not significantly interfere or have a significant effect on the influx or efflux- membrane transporters (results shown in **Appendix II**).

5.5 DNA cross-link comet assay

The cross-link comet assay was performed in HepG2 cells, and typical images are shown in **(Figure 34)**. The percentage of vital cells was more than eighty-eight percent (>88%) in all PA-treatments **(Figure 35a-b),** demonstrating the absence of cytotoxicity of the PA under the applied conditions.

The concentration of 10 µM yielded a significant reduction in the migration of the H_2O_2-induced DNA damage (tail DNA in %) in the case of lasiocarpine, echimidine, riddelliine, and retrorsine, while lycopsamine and europine did not reduce the tail DNA significantly **(Figure 35a)**; the open-diester lasiocarpine produced the strongest reduction in the tail DNA percentage. The equimolar concentration was chosen to enable comparison between the PA, but higher concentrations

were also tested. These high PA-concentrations were based on those that induce micronucleus formation. The high concentrations of the PAs lasiocarpine, echimidine, riddelliine, retrorsine, and europine significantly reduced the migration of tail DNA to the almost the same level despite the different ester-types **(Figure 35b)**.

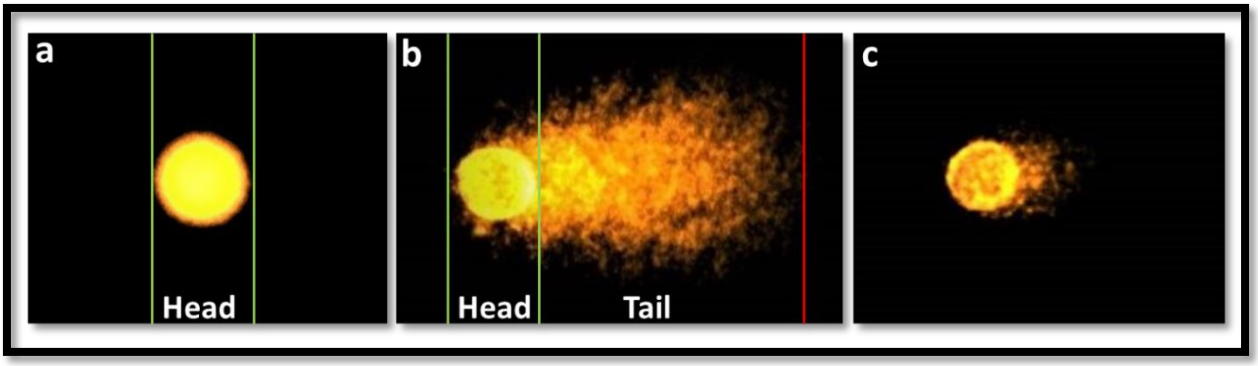

Figure 34: Representative photographs of HepG2 cells in the modified (crosslink) comet assay. Undamaged (intact DNA) HepG2 cells treated with solvent control without 100 µM H_2O_2 **(a)**; Damaged DNA in HepG2 cells treated with 100 µM H_2O_2 for 30 mins **(b)**; Reduced DNA damaged in HepG2 cells treated with lasiocarpine 10 µM for 24 hours with 100 µM H_2O_2 for 30 mins **(c)**.

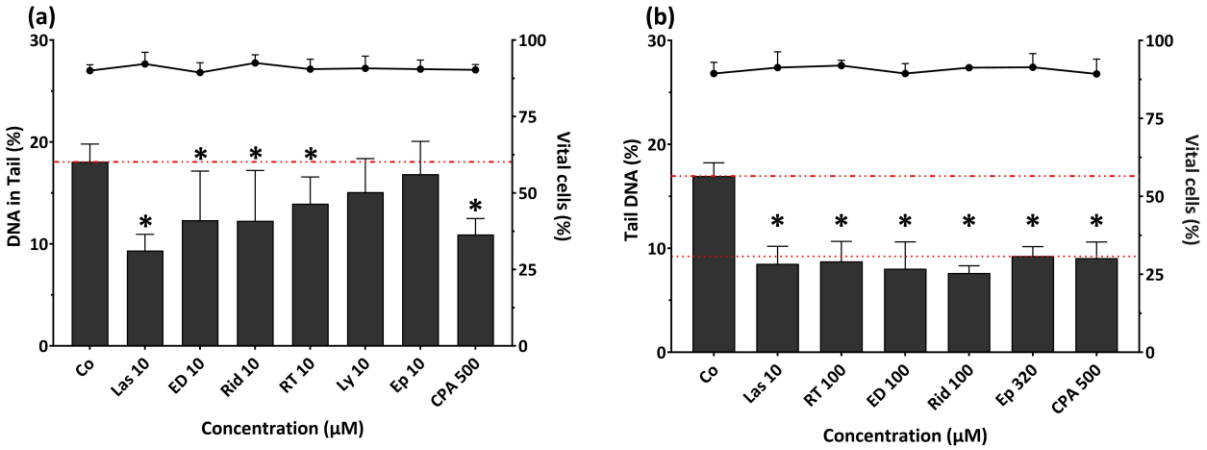

Figure 35: Reduction of hydrogen peroxide (H_2O_2; 100µM; 30 min; Co) induced DNA damage (Tail DNA %) in the crosslink comet assay by pre-treatment with the indicated PAs and cyclophosphamide (CPA; positive control for crosslinking activity). Lasiocarpine (Las), echimidine (ED), riddelliine (Rid), retrorsine (RT), lycopsamine (Ly), europine (Ep) were applied for 24 hours before H_2O_2 treatment. *p<0.05 compared to Co (solvent control). Equimolar PA-concentrations **(a)** and higher PA-concentrations **(b)** were used. The results are displayed as mean ± standard deviation from at least four (4) independent experiments.

5.6 Alkaline comet assay

To further assess the genomic damage associated with selected PAs of different ester-types in HepG2 cells, the alkaline comet assay was applied. Lasiocarpine, echimidine, riddelliine, retrorsine, lycopsamine and europine were used at equimolar and also at high concentrations were applied for 4 hours (4h) and 24 hours (24h). The higher concentrations here were chosen based on micronucleus induction in HepG2 cells observed in this dissertation.

There was no significant change in the percentage of viable cells after PA-treatment, both with equimolar and high PA-concentrations at different exposure (4h and 24h) duration. The percentage viable cells in all groups were more than 89.7% **(Figure 37a-d)**.

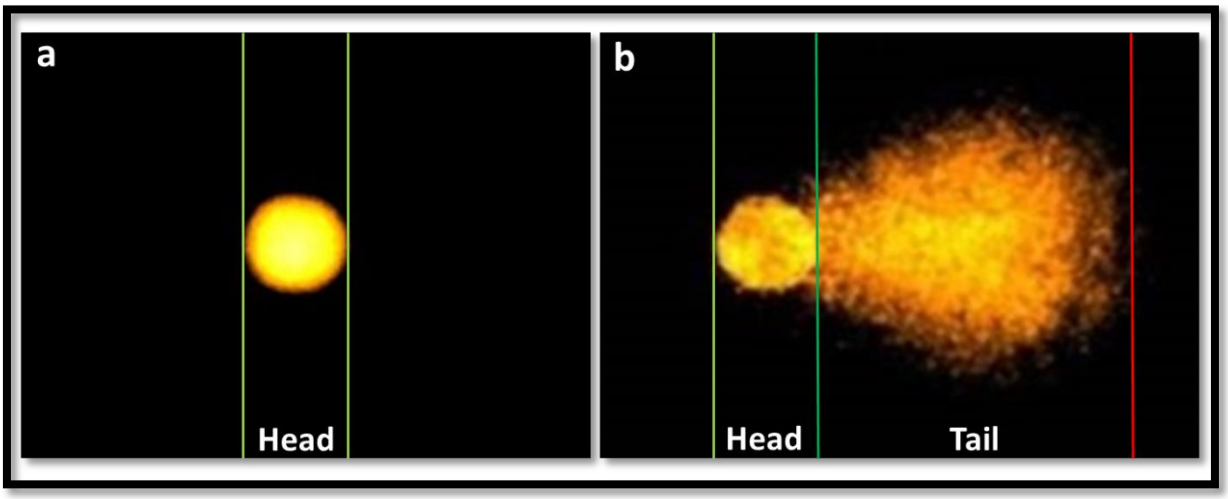

Figure 36: Representative photographs of HepG2 cells in the alkaline comet assay. Undamaged (intact DNA) HepG2 cells treated with solvent control **(a)**; Damaged DNA in HepG2 cells treated with 50 µM H_2O_2 as a positive control for 30 mins **(b).**

After 4h treatment with PA-equimolar concentrations in HepG2 cells **(Figure 37a)**, a significant increase in DNA strand breaks compared to the solvent control was observed with retrorsine and the monoester europine. However, the tail intensity was still far below that of the positive control hydrogen peroxide (H_2O_2 50 µM; 30 mins treatment). No DNA strand breaks (Tail DNA %) were observed after treatment with lasiocarpine, riddelliine, retrorsine, echimidine, lycopsamine and europine at high concentration for 4h duration **(Figure 37b)** nor was there an

effect in equimolar or high concentrations after 24h treatment **(Figure 37c-d)**. The results as an overall picture seem to indicate the absence of the effects of PA in the alkaline comet assay.

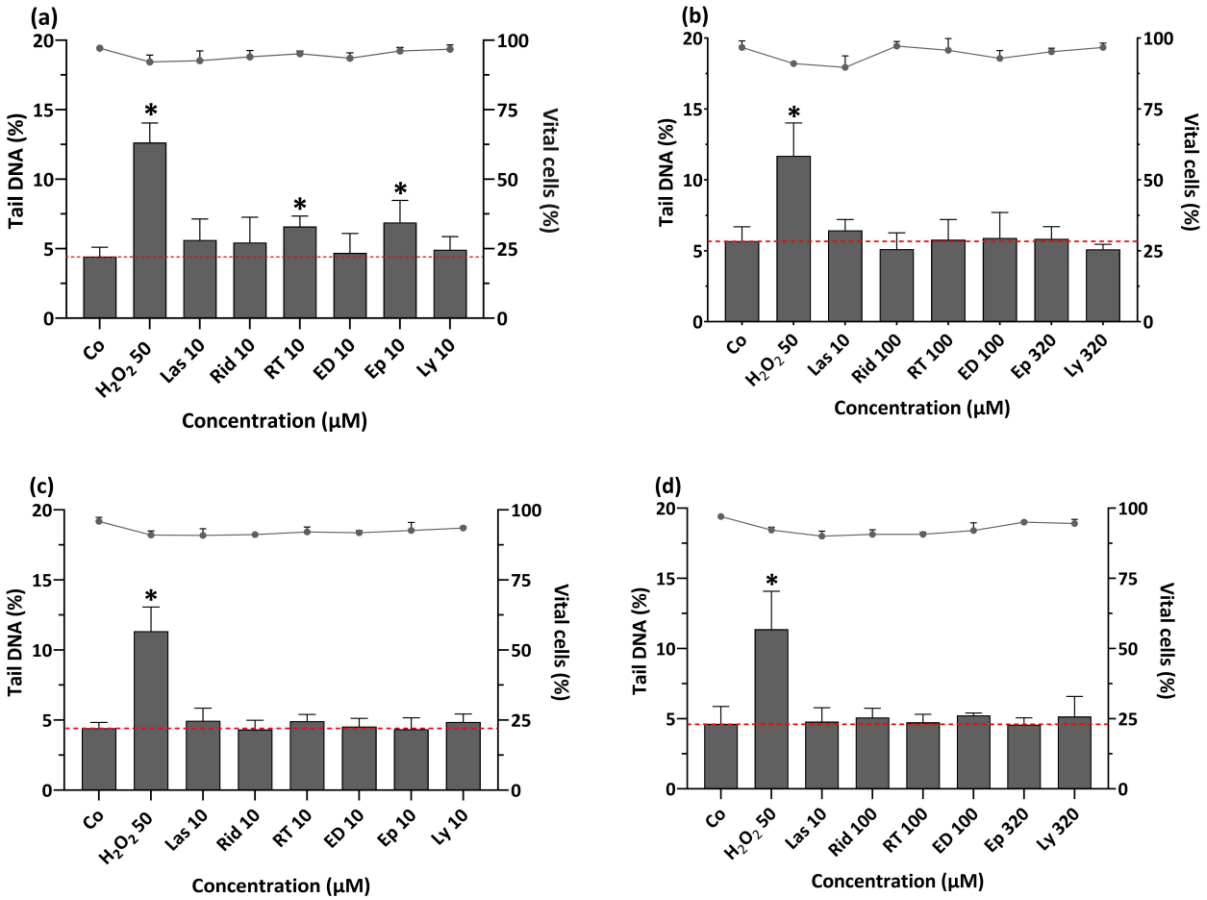

Figure 37: Percentage mean DNA strand breaks (column) and vital cells (line) in HepG2 cells treated with PAs of different ester type at equimolar (a, c) and high concentrations (b, d) for 4 hours (a, b) and 24 hours (c, d) duration. Quantification of comet assay are presented as mean tail DNA and vitals cells in percentage (%) ± STDev from 3 independent experiments; n=3. *p<0.05 against Co (solvent control); H_2O_2 50= hydrogen peroxide 50 µM for 30 minutes treatment; Las 10= lasiocarpine 10 µM (open-diester PA); ED 10= echimidine 10 µM (open-diester PA); Rid 10=riddelliine 10 µM (cyclic-diester PA); RT 10= retrorsine 10 µM (cyclic-diester PA); Ep 10= europine 10 µM (monoester PA); Ly 10= lycopsamine 10 µM (monoester PA).

5.7 Oxidative stress measurement

Oxidative stress induction by PAs was investigated in the HepG2 cells. The intracellular ROS production was analysed using the ROS-sensitive dye dihydroethidium (DHE), which detects superoxide formation. The production of ROS was quantified with ImageJ software and represented as mean DHE fluorescence intensity. The equimolar concentration of 10 µM of

lasiocarpine (open-diester PA), riddelliine (cyclic-diester PA) and europine (monoester) significantly induced ROS production with the highest ROS generation observed after lasiocarpine treatment followed by riddelliine and then europine **(Figure 39)**. No significant increase of ROS production was found with lycopsamine (10 µM; monoester PA) even at higher concentration (320 µM). The representative images can be seen in **Figure 38**.

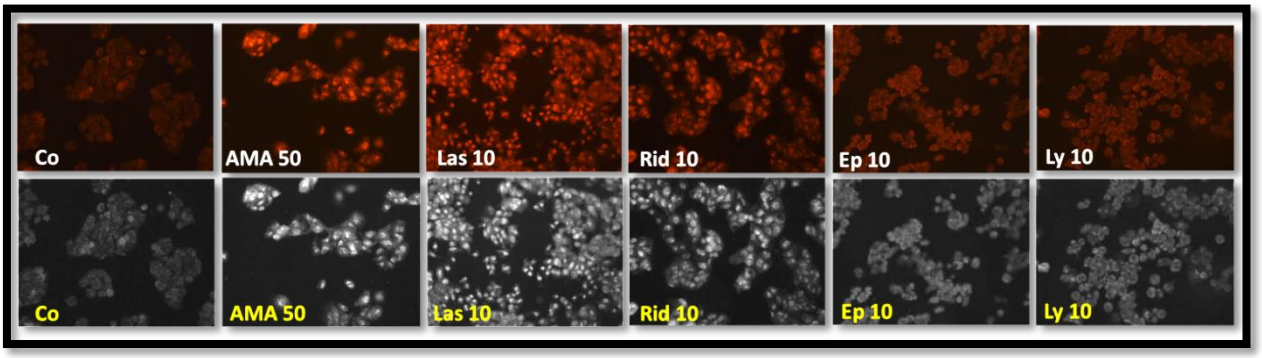

Figure 38: Representative images of DHE stained HepG2 cells treated with their respective test substances. Reactive oxygen species (ROS) formation was visualized by staining HepG2 cells with dihydroethidium (DHE; 10 µM) dye for 15 minutes. The images were later quantified with ImageJ software and represented as mean grey value. Co= solvent control; AMA 50 = antimycin A 50 µM (positive control); Las 10= lasiocarpine 10 µM (open-diester PA); Rid 10= riddelliine 10 µM (cyclic-diester PA); Ep 10= europine 10 µM (monoester PA).

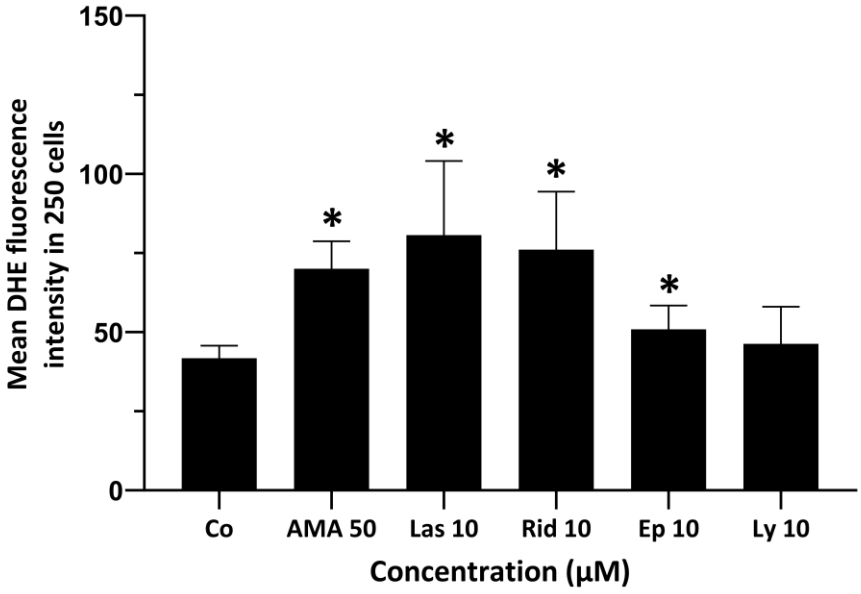

Figure 39: Microscopic detection of intracellular ROS formation using DHE dye in HepG2 cells treated for a total of 75 minutes with PAs of different ester type and 15 minutes with 10 µM DHE. Quantification of DHE fluorescence intensity by measuring the mean grey value of DHE signal from 250 cells using image J software. Data are presented as mean fold change compared to control ± standard deviation (SD) of 4 independent experiment; n=4. *p<0.05 against Co (solvent control); AMA 50= antimycin A 50 µM (positive control); Las 10= lasiocarpine 10 µM (open-diester PA); Rid 10= riddelliine 10 µM (cyclic-diester PA); Ep 10= europine 10 µM (monoester PA); Ly 10= lycopsamine 10 µM (monoester PA).

For confirmation of generation of ROS by PAs in the HepG2 cells, 5 mM of the thiol radical scavenger antioxidant N-acetyl cysteine was combined with lasiocarpine, riddelliine, or europine, and the effect was then assessed by using DHE assay. This analysis yielded a significant decrease in oxidative stress (ROS) after combining N-acetyl cysteine (5 mM) with lasiocarpine, riddelliine, and europine **[Figure 41]**; typical images are illustrated in **Figure 40**.

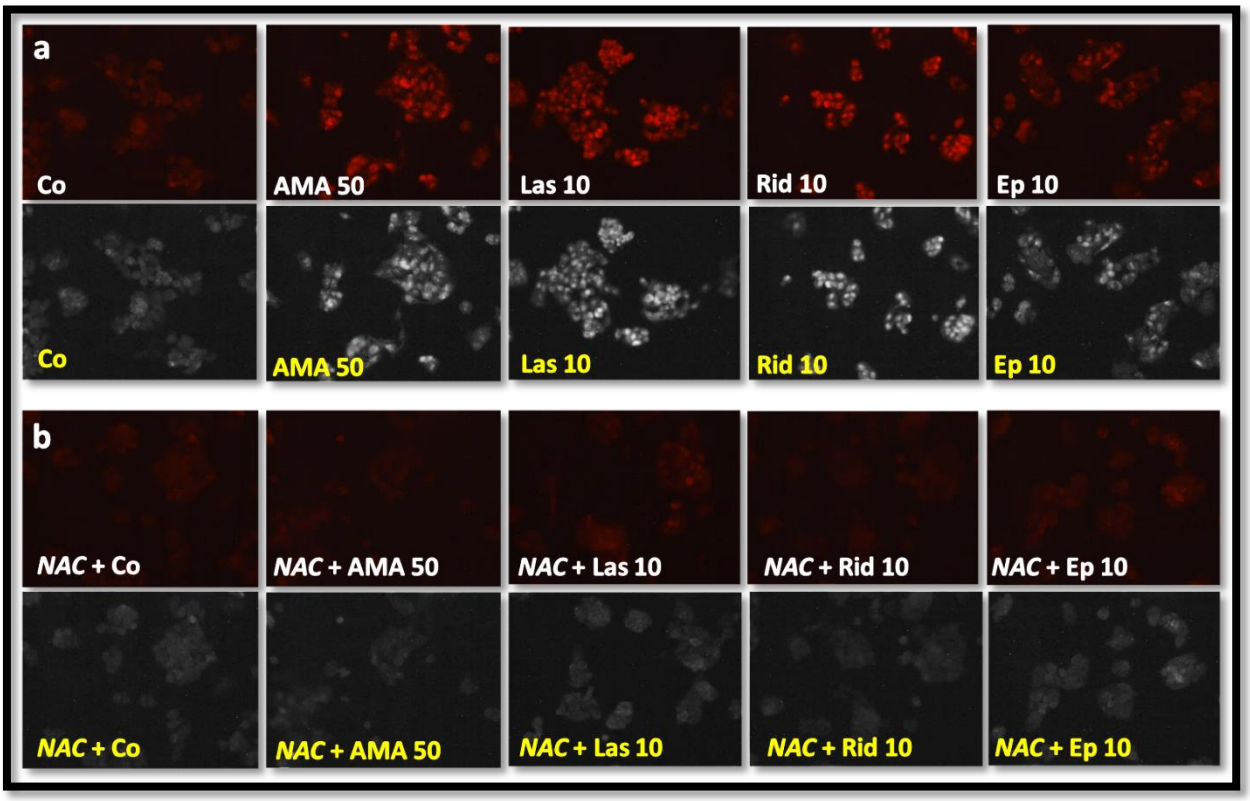

Figure 40: Typical images on the effect of N-acetyl cysteine (NAC; 5 mM) on PA-induced reactive oxygen species (ROS) in HepG2 cells. Images **(a)**: cells were treated with PAs without NAC (5 mM). Images **(b)**: cells were treated with PAs in presence of NAC (5 mM). Co= solvent control; AMA 50 = antimycin A 50 µM (positive control); Las 10= lasiocarpine 10 µM (open-diester PA); Rid 10= riddelliine 10 µM (cyclic-diester PA); Ep 10= europine 10 µM (monoester PA).

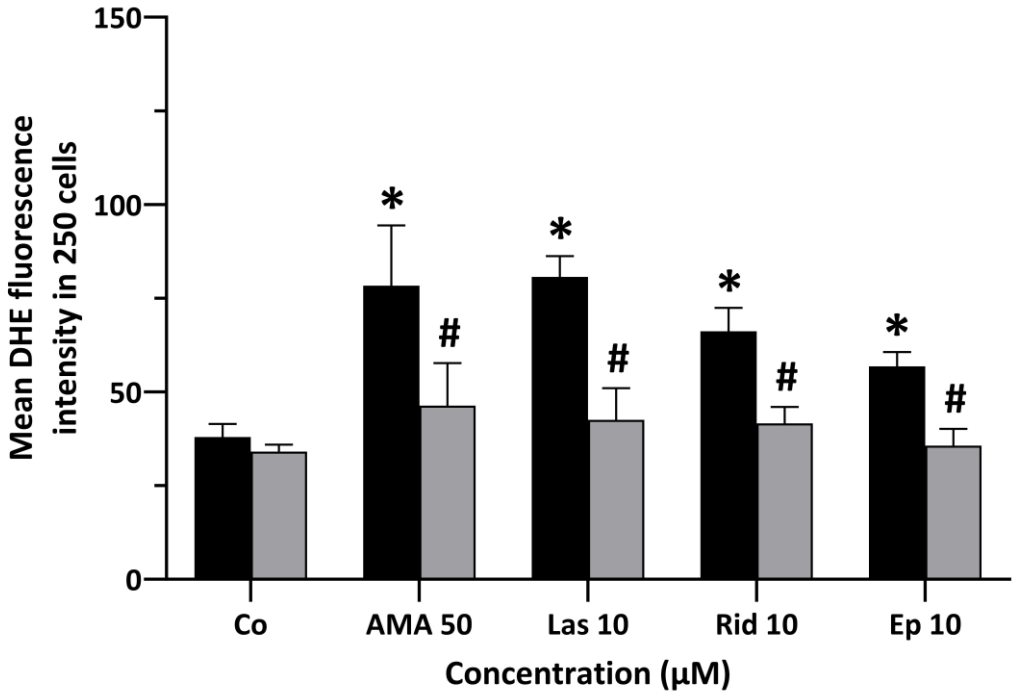

Figure 41: Microscopic detection of intracellular oxidative stress inhibition. HepG2 cells were treated with PAs of different ester type with or without addition of N-acetyl-L-cysteine (NAC), as ROS scavenger. NAC (5 mM) treatment was for a total of 2 hours; PAs treatment was for a total of 75 minutes; and 10 µM DHE was applied for 15 minutes. Quantification of DHE fluorescence intensity was performed by measuring the mean grey value of DHE signal from 250 cells using image J software. Data are presented as mean fold change compared to control ± standard deviation (SD) of 4 independent experiment; n=4. *p<0.05 against Co (solvent control); AMA 50= antimycin A 50 µM (positive control); Las 10= lasiocarpine 10 µM (open-diester PA); Rid 10= riddelliine 10 µM (cyclic-diester PA); Ep 10= europine 10 µM (monoester PA).

To investigate whether mitochondria may be a target for PA, TMRE fluorescence staining was performed. The results showed that the equimolar concentrations of lasiocarpine, riddelliine and europine, induced a loss of mitochondrial membrane potential in HepG2 cells **[Figure 43]**. When HepG2 cells were incubated with the open-diester PA lasiocarpine (10 µM), cyclic-diester PA riddelliine (10 µM), monoester PA europine (10 µM) and positive control antimycin A (50 µM) for 24 hours, the red TMRE fluorescence intensity decreased significantly, which entails the damage of mitochondrial leading to mitochondrial depolarization. The typical images of decreased TMRE red fluorescence in HepG2 cells due to lasiocarpine, riddelliine, europine PAs and the positive control antimycin A are well illustrated in **Figure 42**.

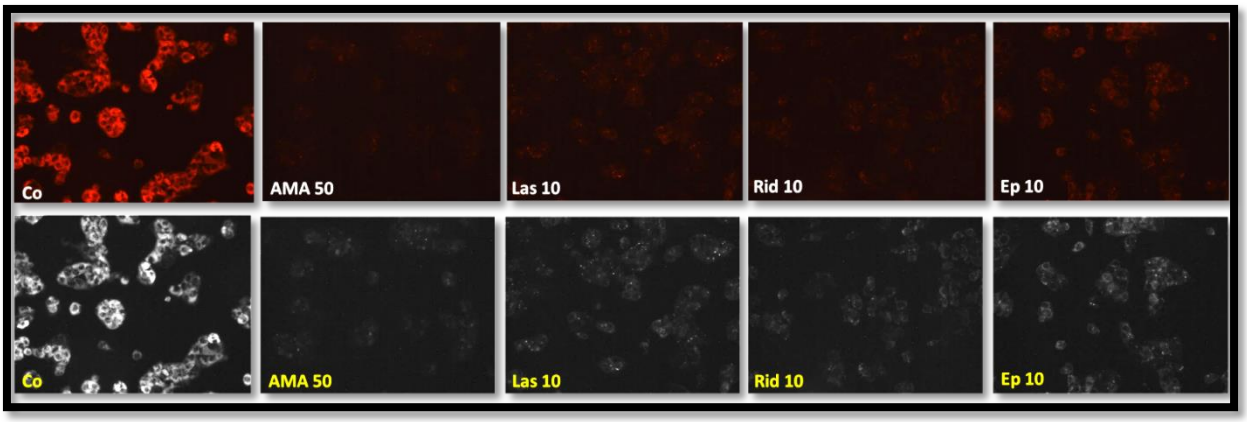

Figure 42: Representative Images of tetramethylrhodamine ethyl ester (TMRE) stained HepG2 cells after treatment with the indicated test substance. Co= solvent control; AMA 50 = antimycin A 50 µM (positive control); Las 10= lasiocarpine 10 µM (open-diester PA); Rid 10= riddelliine 10 µM (cyclic-diester PA); Ep 10= europine 10 µM (monoester PA).

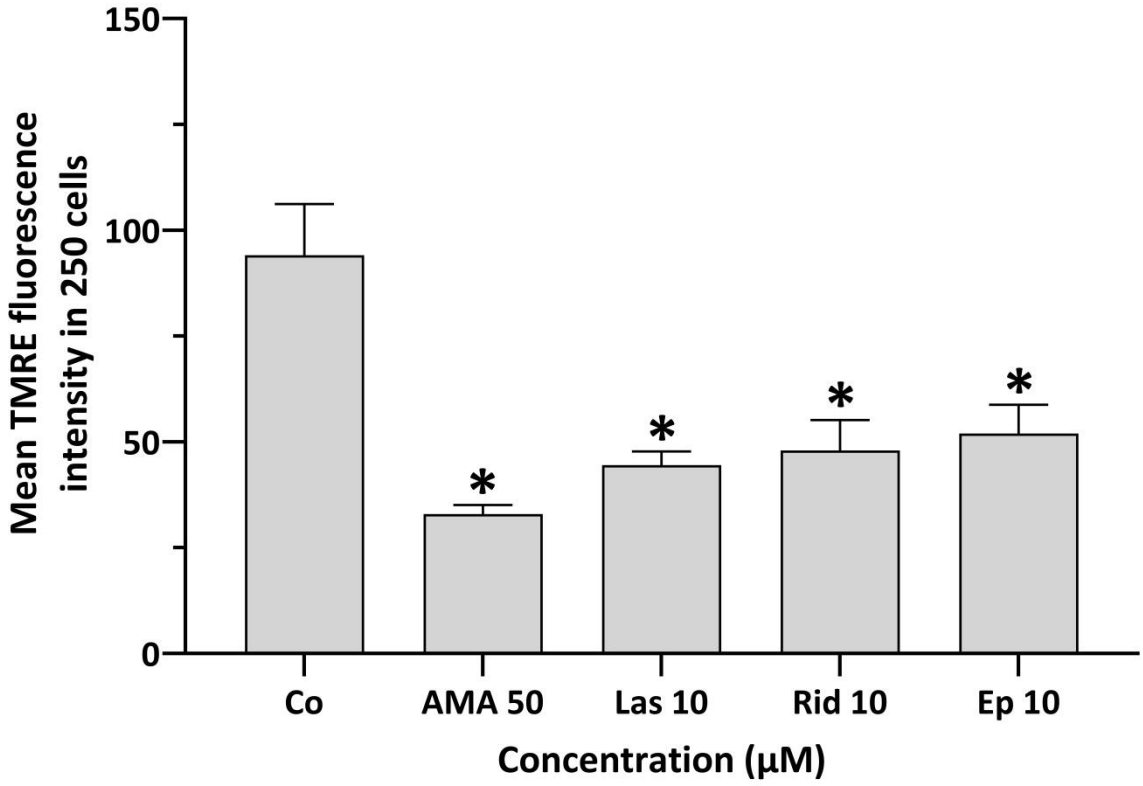

Figure 43: TMRE fluorescence to measure the change in mitochondrial membrane potential in HepG2 cells treated with PAs of different ester type for a total of 75 minute; and 30 nM TMRE dye for 15 minutes. Quantification of TMRE fluorescence intensity by measuring the mean grey value of TMRE signal from 250 cells using image J software. Data are presented as mean fold change compared to control ± STDev of 3 independent experiment; n=3. *$p<0.05$ against Co (solvent control); AMA 50= antimycin A 25 µM or 50 µM (positive control); Las 10= lasiocarpine 10 µM (open-diester PA); Rid 10= riddelliine 10 µM (cyclic-diester PA); Ep 10= europine 10 µM (monoester PA).

5.8 Establishment of a Co-Culture System

The co-culture set up in terms of cell ratio and culture conditions was established. Seeding of 40,000 of HeLa H2B-GFP cells and 150,000 of HepG2 cells in HepG2 culture medium yielded a suitable cell ratio between the two cell lines; which corresponds to 32% HeLa H2B-GFP cells and 68% HepG2 cells at the time of harvest after the experiment **(Figure 44)**. At this cell ratio there was no significant over growth of HeLa H2B-GFP over HepG2 cells. The cell ratio was evaluated with bisbenzimide H33342 staining (all nuclei) and the cells were evaluated (counted) with the use of UV (bisbenzimide H33342, all nuclei) and the FITC filter (HeLaH2B-GPF green fluorescence) using fluorescence microscope; sample images are shown in **Figure 44**.

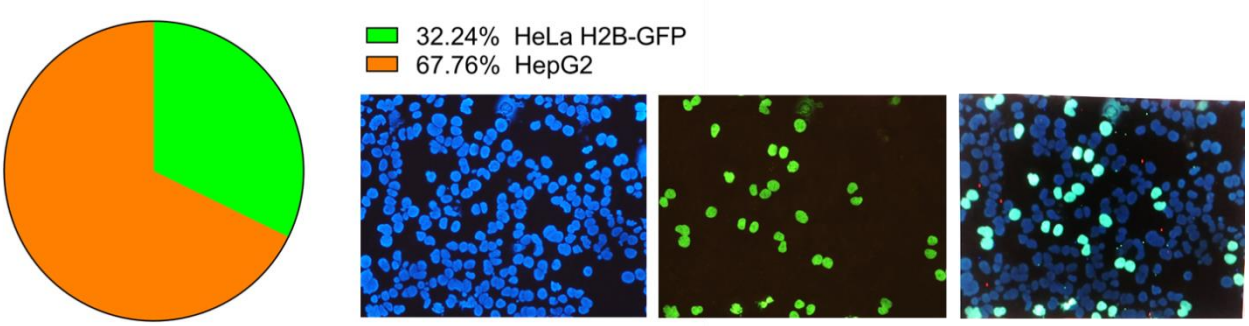

Figure 44: Representative image of the co-culture cell ratio at the time of cell harvest achieved by seeding 40,000 of HeLa H2B-GFP cells (green) and 150,000 of HepG2 cells (blue). Images were taken at × 200-fold magnification and are shown as an overlay of UV excitation and FITC filter. Cells were stained with bisbenzimide (Hoechst 33342) dye (blue) and viewed under an Eclipse 55i florescence microscope.

5.9 Induction of micronuclei by selected PAs in co-culture system

Sample images of micronuclei in HeLa H2B-GFP cells, as used in the co-culture, and of HepG2 cells are shown in **Figure 45**. The quantification of PA-induced micronucleus formation is presented in **Figure 46**. There was a significant induction of micronucleus formation in HeLa H2B-GFP cells in the co-culture treated with PAs compared to the solvent control. However, in the culture of only HeLa H2B-GFP cells, there was no micronucleus formation associated with treatment with PAs, while micronucleus induction was observed with PAs in cultures of only HepG2 cells.

Regarding the proliferation index (CBPI; secondary line graph), there was a decrease in the proliferation index in the co-culture treated with PAs compared to the solvent control of only

HeLa H2B-GFP or the solvent control of the co-culture (HeLa H2B-GFP + HepG2). However, a significant decrease in the proliferation index was found only with lasiocarpine and riddelliine, but not with europine when compared to the solvent control of only HeLa H2B-GFP. Additionally, in the co-culture treated with lasiocarpine (not riddelliine or europine), a significant decrease in the proliferation index was also observed when compared with the solvent control of the co-culture model. This indicates cytotoxicity induced by lasiocarpine and riddelliine but not europine.

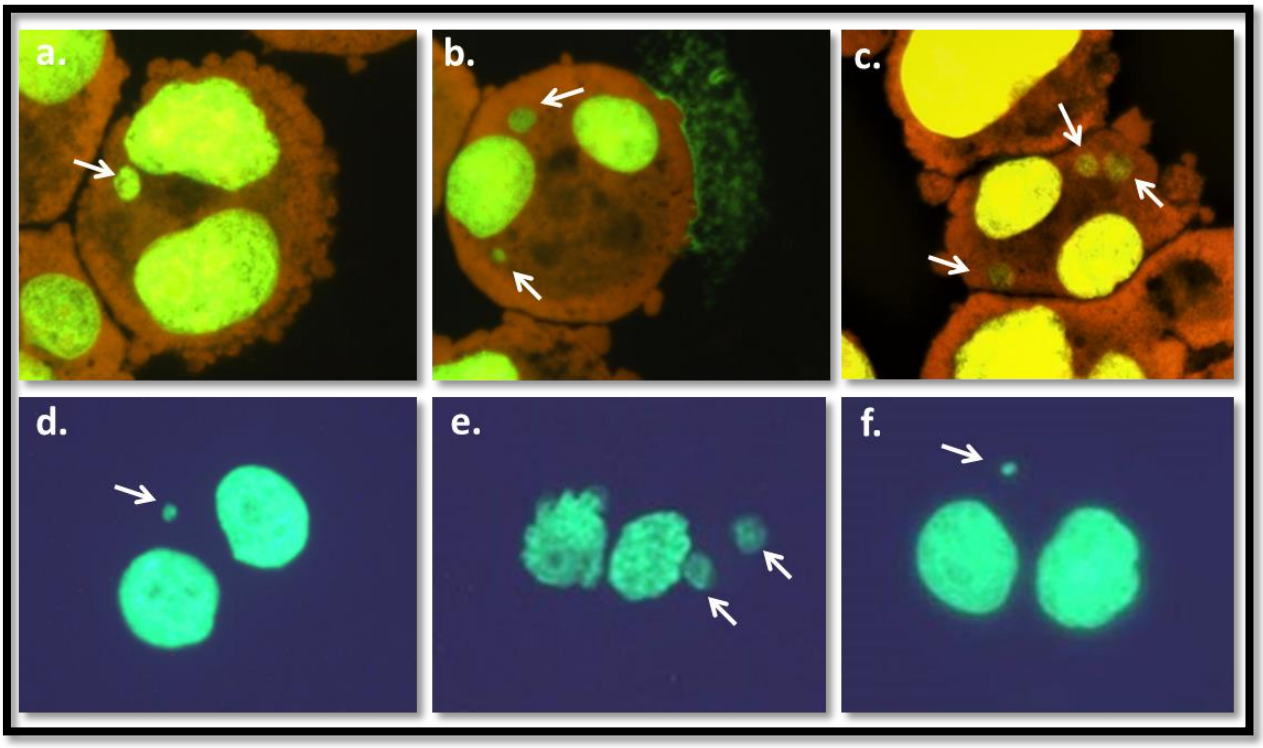

Figure 45: Representative images of HepG2 cells (a, b, and c) and HeLa H2B-GFP cells in co-culture (d, e, and f). The images represent typical micronucleated binucleated cells: a binucleated cell with one micronucleus (a, d, f); a binucleated cell with two micronuclei (b, e); and a binucleated cell with three micronuclei (c). The HepG2 cells were stained with Gel Green, while the HeLa cells in co-culture were mounted only with DABCO without staining.

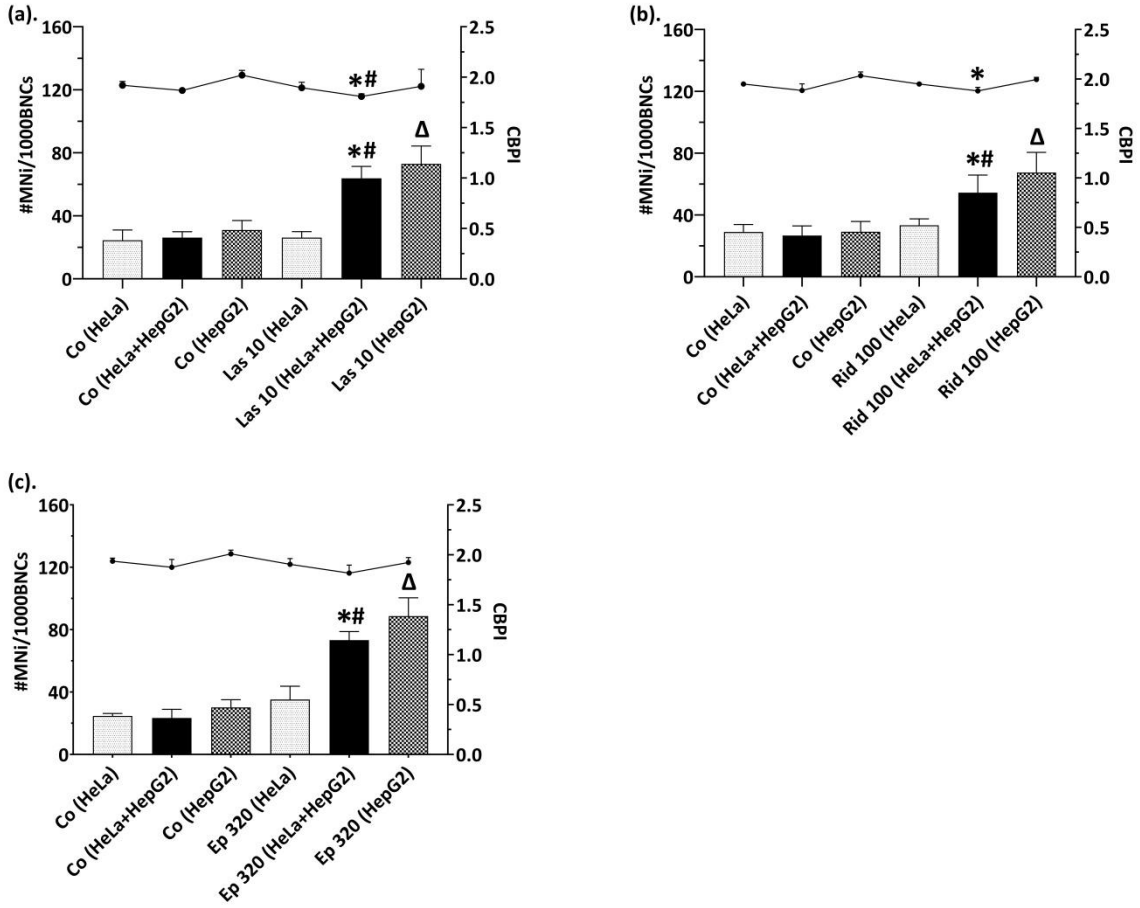

Figure 46: Micronucleus induction (columns) and proliferation index (CBPI; line) in HeLa H2B-GFP only cells, co-culture system and HepG2 only cells after treatment with the indicated pyrrolizidine alkaloids. *p<0.05 compared to solvent control in HeLa H2B-GFP only cultured cells (DMSO; HeLa H2B-GFP). #p<0.05 compared to solvent control in co-culture system (DMSO; combination of HepG2+HeLa H2B-GFP). ΔP<0.05 compared to solvent control in HepG2 cells (DMSO; HepG2). Las 10= lasiocarpine 10 µM (open-diester PA); Rid 100= riddelliine 100 µM (cyclic-diester PA); Ep 320= europine 320 µM (monoester PA); DMSO= dimethyl sulfoxide (solvent control); MNi= micronucleus; BNCs= binucleated cells; CBPI= cytokinesis-block proliferation index; n=3.

5.10 Inhibition of metabolism in the co-culture system

To elucidate the mechanism of genomic damage induced by PAs, a mechanistic investigation was further conducted in the co-culture model using ketoconazole to inhibit the cytochrome P450-3A4 isoenzyme. As shown in **Figure 47**, ketoconazole significantly reduced micronucleus formation induced by lasiocarpine, riddelliine, and europine. However, ketoconazole did not significantly change the proliferation index (CBPI; line graph) of PAs, indicating no cytotoxicity effect.

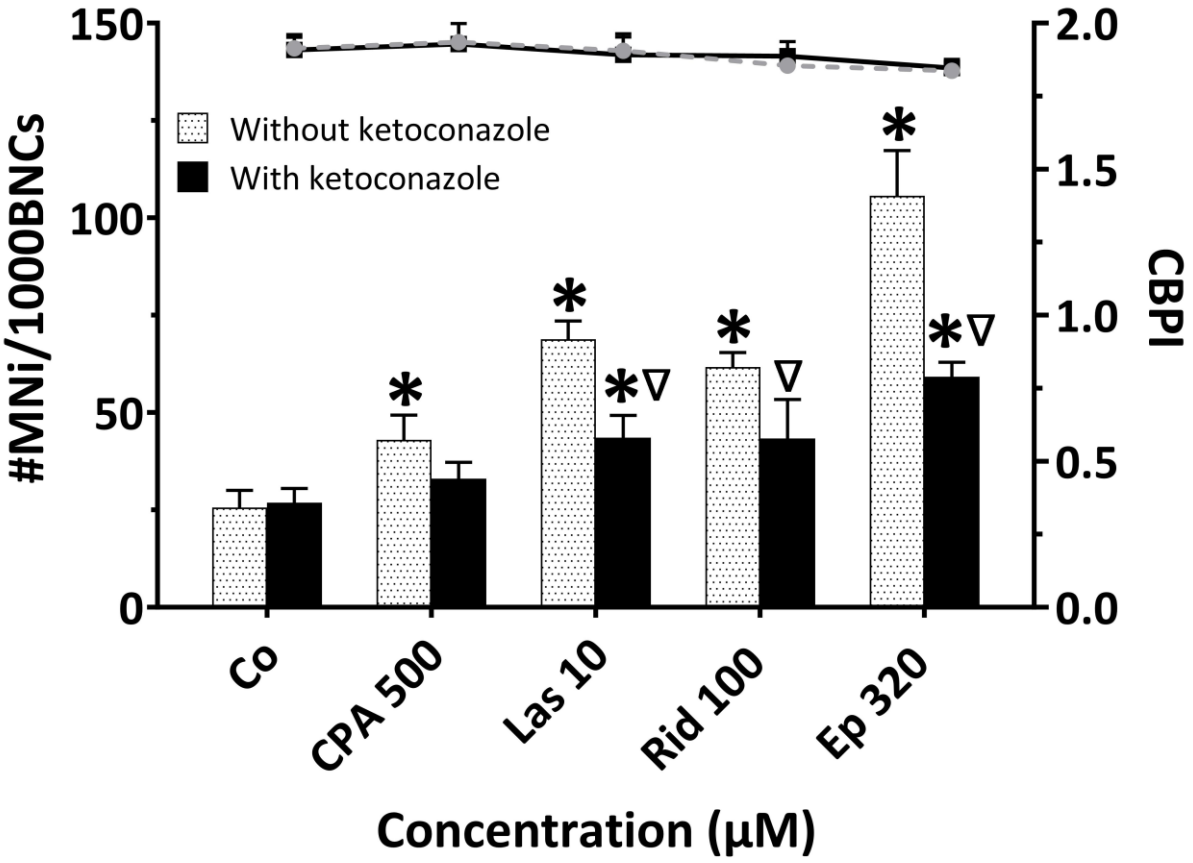

Figure 47: Micronucleus frequency (columns) and proliferation index (CBPI; line) in the co-culture model consisting of HeLa H2B-GFP and HepG2 cells. Cells were pre-treated with ketoconazole for 24 hours, then treated with PAs for 28 hours and compared with the standard protocol without ketoconazole pre-treatment. *p<0.05 compared with solvent control (DMSO), ∇p<0.05 compared with the respective dose without inhibitor pre-treatment. MNi= micronucleus; BNCs= binucleated cells; CBPI= Cytokinesis-block proliferation index; CPA 500 = cyclophosphamide 500 µM (positive control); Las 10= lasiocarpine 10 µM; Rid 100= riddelliine 100 µM; Ep 320= europine 320 µM.

5.11 Inhibitors of efflux- transporters in the co-culture system

The relevance of efflux- membrane transporters for PA-mediated genotoxicity was further investigated in the co-culture system with chemical inhibitors. In co-culture system, impairing the efflux of metabolites from HepG2 cells should reduce their amount available for uptake into HeLa H2B-GFP cells. Therefore, efflux chemical inhibitors were applied in the co-culture system and the micronucleus formation was determined. Both, the inhibitor of MDR1 efflux transporter, verapamil, and the inhibitor of MRP2 efflux transporter, benzbromarone, as well as their combination, significantly reduced lasiocarpine, riddelliine and europine induced

micronucleus formation in HeLa H2B-GFP cells within the co-culture with HepG2 cells **[Figure 48]**. No significant difference in proliferation index (CBPI, line graph) among the groups and when compared to the solvent control was observed, indicating the absence of cytotoxicity.

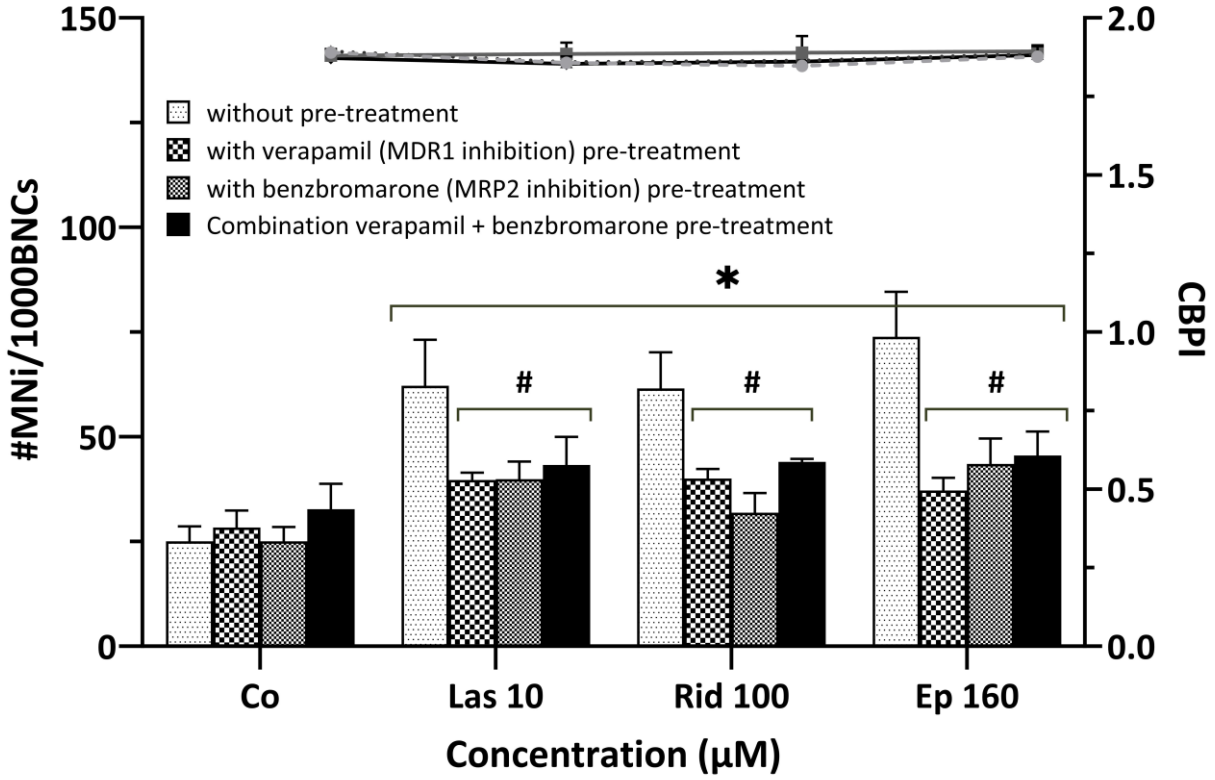

Figure 48: Micronucleus frequency (columns) and proliferation index (CBPI; line) in the co-culture model consisting of HeLa H2B-GFP and HepG2 cells. MDR1 efflux transporter inhibitor verapamil, MRP2 efflux transporter inhibitor benzbromarone and the combination of verapamil and benzbromarone was applied for 24 hours. Then, cells were treated with PAs of different ester type for 28 hours and compared with their standard protocol without inhibitor pre-treatment. *$p<0.05$ compared with solvent control (DMSO), Δ$p<0.05$ compared with the respective dose without inhibitor pre-treatment. MNi= micronucleus; BNCs= binucleated cells; CBPI= Cytokinesis-block proliferation index; Las 10= lasiocarpine 10 µM; Rid 100= riddelliine 100 µM; Ep 160= europine 160 µM.

5.12 Analysis of mitotic figures

The microscopic examination of mitotic figures after PA-treatment of the co-culture, HepG2 and HeLa H2B-GFP cells was performed and expressed as mitotic index as shown in **Figure 50**. The typical images of the microscopic examination of mitotic figures in co-culture, HepG2 and HeLa H2B-GFP cells are illustrated in **Figure 49**.

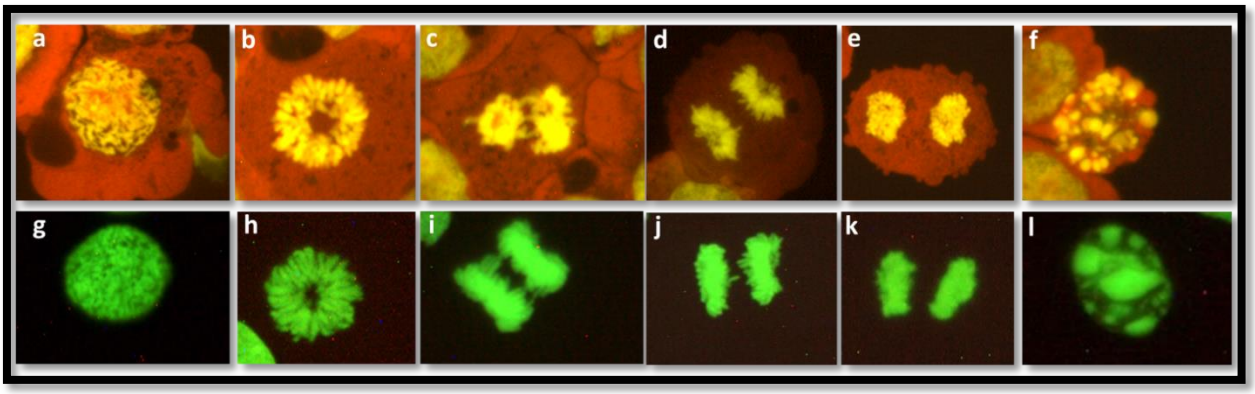

Figure 49: Representative images of mitotic stages and apoptotic cells in HepG2 cells (a, b, c, d, e, and f) and in HeLa H2B-GFP cells of the co-culture system (g, h, i, j, k and l). The cells in co-culture and HeLa H2B-GFP only cultured cells were mounted with DABCO without staining while HepG2 only cultured cells were stained with Gel green then mounted with DABCO. The classified mitotic stages are Prophase (a and g); metaphase (b and h); early anaphase (c and i); late anaphase (d and j); and telophase (e and k); and apoptotic cells (f and l).

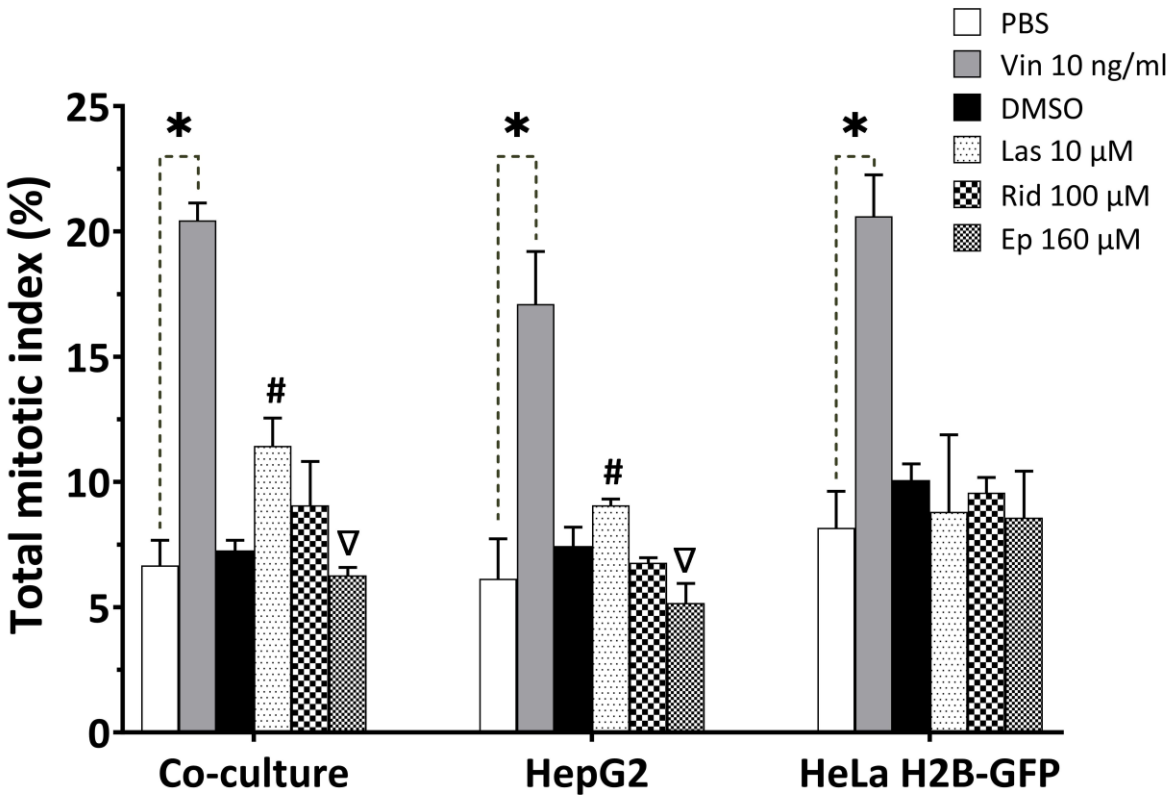

Figure 50: Mitotic index in HeLa H2B-GFP in co-culture and in HepG2 only cells. Results are presented as mean ± standard deviation (SD) of three replicates within the same experiment and *p<0.05 compared to PBS as solvent control; #p<0.05 compared to DMSO as solvent control; ∇p<0.05 significant decrease effect against DMSO as solvent control. PBS= solvent control used for vincristine; DMSO= solvent control used for PAs; Vin 10 ng/ml= vincristine 10 ng/ml; Las 10 µM= lasiocarpine 10 µM; Rid 100 µM= riddelliine 100 µM; Ep 160 µM= europine 160 µM.

Lasiocarpine (10 µM) significantly increased the mitotic index when compared to the solvent control in co-culture and HepG2 only cultured cells but did not alter the mitotic index in HeLa H2B-GFP cells if cultured alone. Riddelliine (100 µM) did not cause significant alterations in the mitotic index. Europine (160 µM) significantly decreased the mitotic index in the co-culture and HepG2 only cultured cells but caused no change in HeLa H2B-GFP only cultured cells.

Concisely, there was no difference in the total mitotic index in HeLa H2B-GFP only cultured cells treated with PAs. These results indicate that PAs require metabolic activation to affect the mitotic processes as disturbances were observed in HeLa H2B-GFP cells of co-culture and in HepG2 cells cultured alone, but not in HeLa H2B-GFP cells cultured alone. In addition, the mitotic index at the different stages prophase, metaphase, anaphase and telophase, and apoptotic cells were also examined microscopically in 1000 nuclei cells and the results are presented in **Appendix IV.**

The most common chromosomal abnormalities associated with PAs were no-congression, no-spindle formation, bridges, lagging chromosomes and multipolar metaphase, as shown in **Figure 52**. The only clear difference in chromosomal abnormalities (mitotic abnormalities) between lasiocarpine, riddelliine and europine, was that the monoester europine induced less ana-/telophase bridges than the two diesters (lasiocarpine and riddelliine).Typical representations of these chromosomal abnormalities during mitosis are illustrated in **Figure 51**.

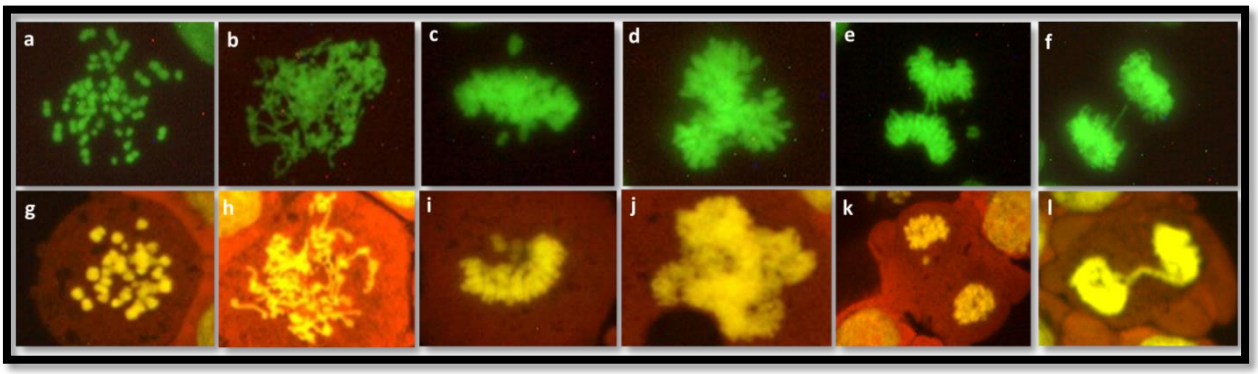

Figure 51: Representative images of mitotic disturbances in HeLa H2B-GFP cells (a, b, c, d, e, and f) and HepG2 cells (g, h, I, j, k, and l). The cells in co-culture and HeLa H2B-GFP only cells were mounted with DABCO without staining while HepG2 cells were stained with Gel green then mounted with DABCO. The classified metaphase disturbances are no-spindle formation (a and g); elongated chromosomes/chromatids (b and h); non-congression (c and i); and multipolar metaphase (d and j); while anaphase-telophase are the lagging chromosome(s)/chromatid(s) (e and k) and bridges (f and l).

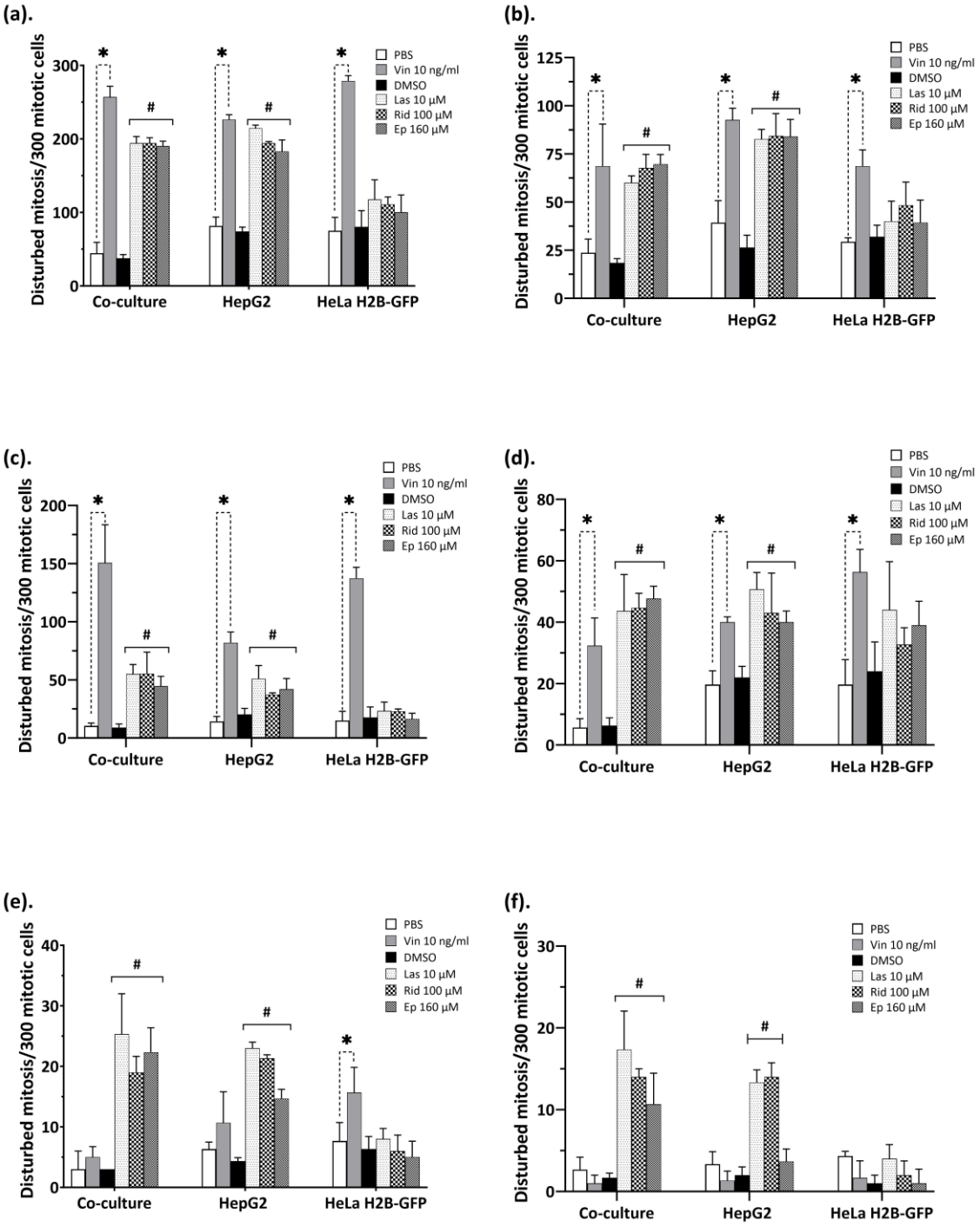

Figure 52: Categories of mitotic disturbances induced by PAs in 300 mitotic cells; HeLa H2B-GFP analysed after co-culture or cultured alone, and HepG2 cells cultured alone. Total mitotic disturbance, graph **a**; non-congression at metaphase, graph **b**; combination of no-spindle formation and elongated chromosomes at metaphase, graph **c**; multipolar effect at metaphase, anaphase and telophase, graph **d**; lagging chromosome(s)/chromatid(s) at anaphase and telophase, graph **e**; bridges at anaphase and telophase, graph **f**. Results are presented as mean ± standard deviation (SD) in three (3) replicates of the same experiment and *p<0.05 against PBS solvent control; #p<0.05 against DMSO solvent control. PBS= solvent control used for vincristine; DMSO= solvent control used for PAs; Vin 10 ng/ml= vincristine 10 ng/ml; Las 10 µM= lasiocarpine 10 µM; Rid 100 µM= riddelliine 100 µM; Ep 160 µM= europine 160 µM.

5.13 Combination of lasiocarpine and riddelliine in HepG2 cells and in the co-culture system

The influence of the combination of lasiocarpine and riddelliine was assessed to determine either synergism or additive effects in HepG2 cells and also in the co-culture system under standard conditions using the CBMN assay. This may indicate whether the same mechanism of action and target biomolecule is shared or whether more than one is affected. Typical appearances of micronuclei (MNi), nuclear buds (NUB), and nuclear bridges (NPB) in binucleated, mitotic, and apoptotic cells in HepG2 only cultured cells and in HeLa H2B-GFP cells of the co-culture model are shown in **Figure 53**.

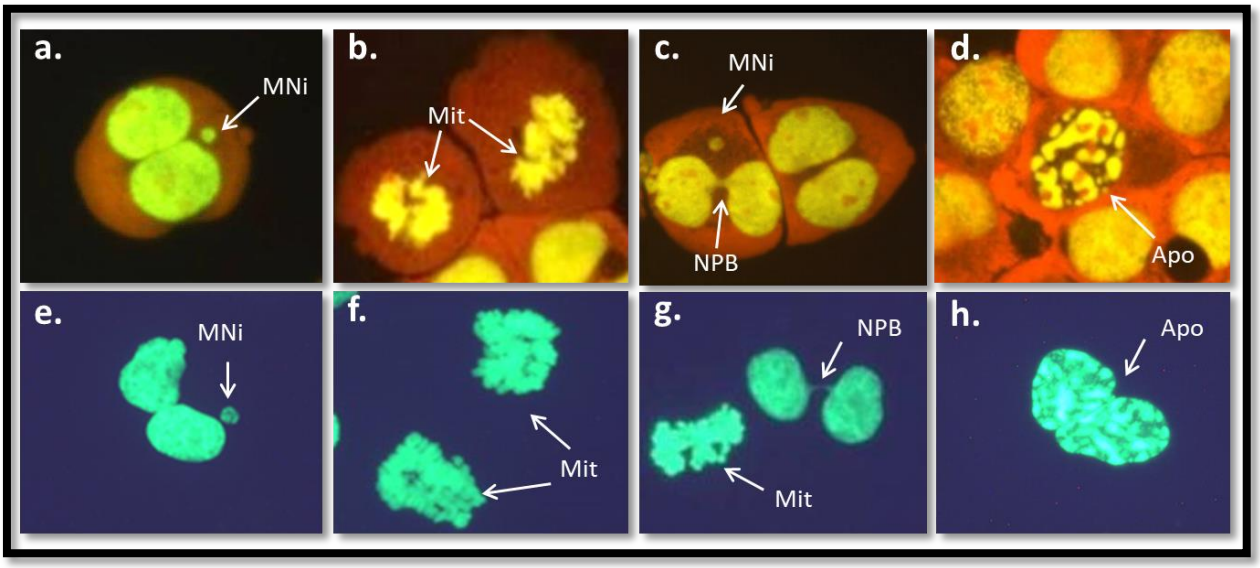

Figure 53: Representative images of HepG2 cells (a, b, c, and d) and HeLa H2B-GFP cells of co-culture model system (e, f, g, and h). The images represent a typical micronuclei formation (MNi; a, and e), mitosis (Mit; b, and f), nuclear bridge (NPB; c, and g), and apoptosis (Apo; d, and h) in HepG2 cells and HeLa H2B-GFP cells of co-culture model system. The HepG2 cells were stained with gel green while the HeLa cells in co-culture model system were mounted with DABCO only without staining.

In HepG2 only cultured cells, no significant difference in micronucleus induction was observed between the combination of lasiocarpine and riddelliine at low and high concentrations compared to the individual PAs **(Figure 54)**. However, when compared to the solvent control, both low and high combinations significantly induced micronuclei in HepG2 only cultured cells. The proliferation index (CBPI; secondary line graph in **Figure 54**), which determines cytotoxicity, was lower (though not significant) in the combination of high concentrations compared to the solvent control and also when compared to the individual PAs. Representative images of

micronuclei (MNi), nuclear buds (NUB), and nuclear bridges (NPB) in binucleated, mitotic, and apoptotic cells in HepG2 only cultured cells are illustrated in **Figure 53a-d**.

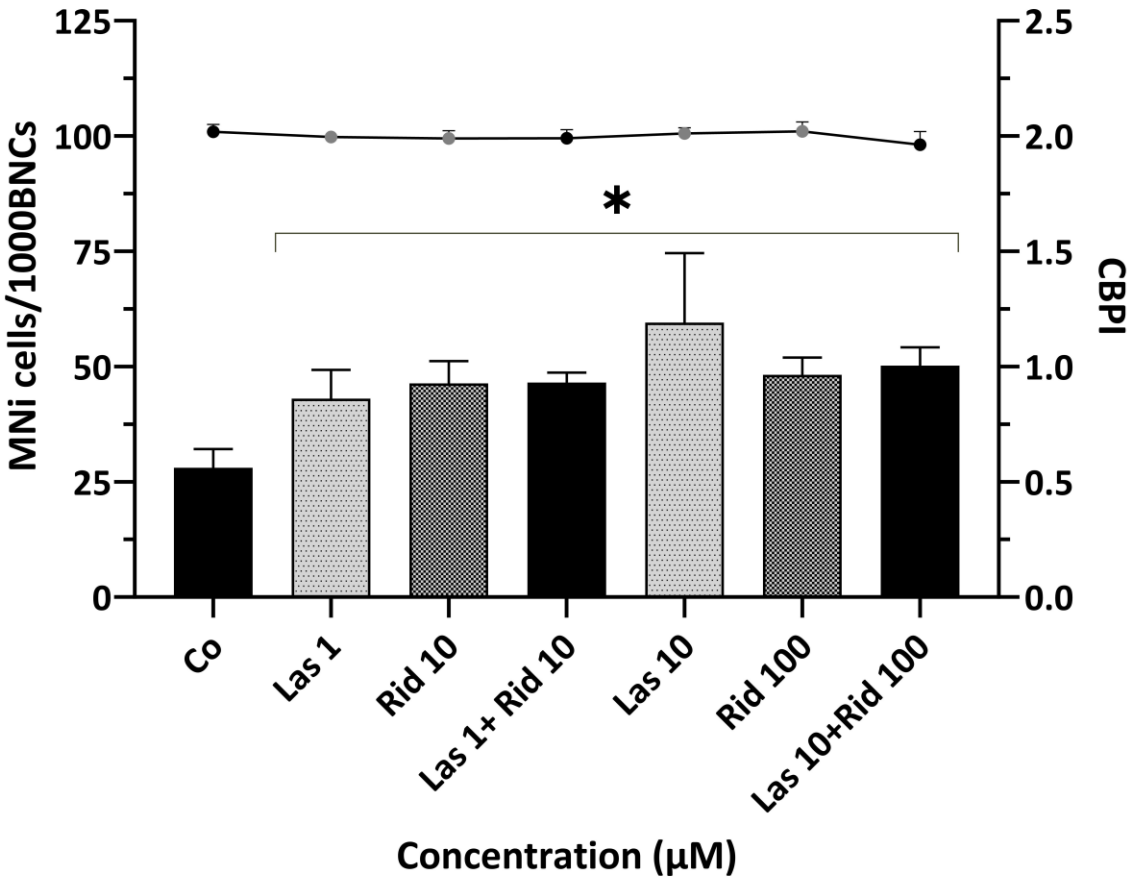

Figure 54: Micronucleus induction (columns) and proliferation index (CBPI; line) in HepG2 cells treated with a combination of lasiocarpine and riddelliine (low and high concentrations). *p<0.05 against Co (solvent control); Las 1= lasiocarpine 1 µM; Rid 10= riddelliine 10 µM; Las 1+Rid 10= combination of lasiocarpine 1 µM and riddelliine 10 µM (combination of low concentration PAs); Las 10= lasiocarpine 10 µM; Rid 100= riddelliine 100 µM; Las 10+Rid 100= combination of lasiocarpine 10 µM and riddelliine 100 µM (combination of high concentration PAs); #MNi= number of micronucleus; BNCs= binucleated cells; CBPI= cytokinesis-block proliferation index. Results are displayed as mean ± standard deviation (SD) from n=3.

Consequently, the combination of lasiocarpine and riddelliine was also assessed in the co-culture system, where the micronuclei were evaluated in HeLa H2B-GFP cells. Typical images of micronuclei, mitosis, nuclear buds, nuclear bridge, and apoptosis in HeLa H2B-GFP cells of co-culture system are illustrated in **Figure 53e-h**.

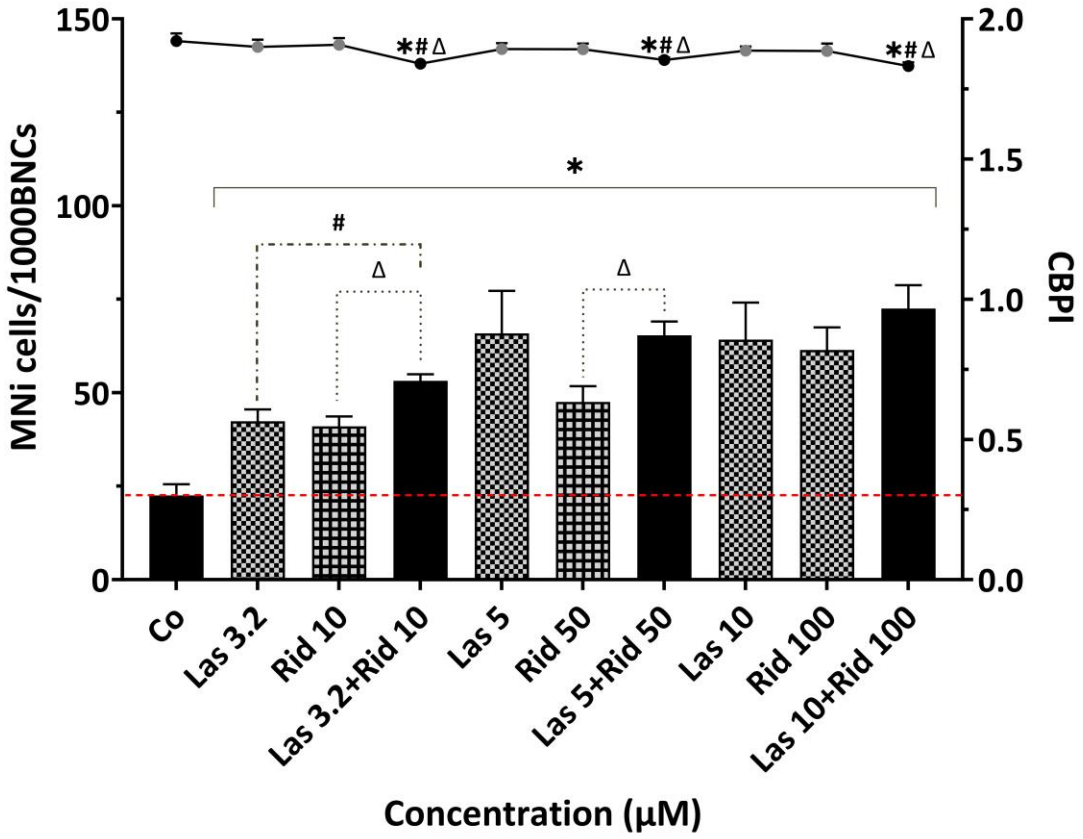

Figure 55: Micronucleus induction (columns) and proliferation index (CBPI; line) in co-culture model system treated with combination of lasiocarpine and riddelliine (low, medium or high concentrations). *p<0.05 against 0.05 against Co (solvent control); Las 3.2= lasiocarpine 3.2 µM; Rid 10µM= riddelliine 10 µM; Las 3.2+Rid 10= combination of lasiocarpine 3.2 µM and riddelliine 10 µM (combination of low concentration PAs); Las 5= lasiocarpine 5 µM; Rid 50= riddelliine 50 µM, Las 5+Rid 50= combination of lasiocarpine 5 µM and riddelliine 50 µM (combination of medium concentration PAs); Las 10= lasiocarpine 10 µM; Rid 100= riddelliine 100 µM; Las 10= lasiocarpine 10 µM; Las 10+Rid 100= combination of lasiocarpine 10 µM and riddelliine 100 µM (combination of high concentration PAs); #MNi= number of micronucleus; BNCs= binucleated cells; CBPI= cytokinesis-block proliferation index. Results are displayed as mean ± standard deviation (SD) from n=3.

The PAs lasiocarpine and riddelliine were combined at low, medium and high concentrations. All treatments induced micronuclei significantly compared to the solvent control as shown in **Figure 55**. Also, a significant increase in micronuclei was found after treatment with the combination of the low concentrations compared to the individual PAs. Using the combination of the high concentrations there was an increase (not significant) in micronuclei compared to the individual PAs. The proliferation index (CBPI; secondary line graph in **Figure 55**) showed significant cytotoxicity in all combination concentrations when compared to the solvent control as well as the individual PA.

CHAPTER SIX

6 DISCUSSION

6.1 In vitro genotoxicity potency of selected PAs in HepG2 cells

The risk assessment with regard to PAs has assumed that all PAs, despite of their different chemical characteristics, have equal potency as riddelliine, which has been considered to be one of the most potent PAs in rats **[196]**. Using the human liver cell line HepG2, we attempted to optimize the standard micronucleus protocol, using a differentiation-reseeding variant, which had been described for HepaRG cells in the literature **[500]**, but was used for the first time for HepG2 cells in this dissertation. This yielded more sensitivity of the system than the regular micronucleus test. We also tried to further improve the method by application of BSO for depletion of glutathione, a method which had been found useful for the testing of the mycotoxin patulin-induced genotoxicity **[501]**. Chen et al. (2009) **[502]** also used the same method to demonstrate that intracellular GSH plays a critical role in regulating the cytotoxicity induced by PAs monocrotaline and senecionine in human normal liver L-02 cells. In the same cell line, Ji et al. (2008) **[503]** also demonstrated the importance of intracellular GSH in PA clovirine-induced toxicity.

Therefore, in this study, BSO worked well when applied alone in the cells. However, in combination with confluent cultured cells, cell viability was reduced. Our study also indicated the influence of intracellular GSH in lasiocarpine-induced genotoxicity. Another option was pre-treatment with rifampicin to induce cytochrome P450 **[416-419]**. This yielded very similar results to the pre-differentiation protocol but only required a three-day pretreatment instead of the two-week pretreatment needed for possible cell differentiation.

Rifampicin has been shown to induce CYP 450-3A4 expression via the pregnane X receptor (PXR) **[504-506]**. Rifampicin binds to PXR in the cell cytoplasm, then enters the nucleus, forming a heterodimer with the retinoic acid receptor. This heterodimer is believed to bind to the promoter of the target gene and activate transcription **[507]**. Similarly, Kobayashi et al. (2019)

[508] used the same method to demonstrate plant extract inhibition of CYP 450-3A4 in rifampicin-pretreated HepG2 cells. They further showed rifampicin inducing CYP 450-3A4 expression in HepG2 cells. However, in our study a combination of CYP 450 induction by rifampicin with glutathione depletion by BSO resulted in reduced cell viability.

Thus, the preferred protocol for the dose-response experiments with the selected PA was pretreatment with rifampicin. We further confirmed if the rifampicin pretreatment in HepG2 cells induced CYP 450 activity. This was investigated based on the metabolism of 17β-estradiol (E2) and estrone (E1). Rifampicin clearly led to increased CYP 450-3A4-mediated metabolism of 17β-estradiol (E2) and estrone (E1), resulting in a 3-fold increase in hydroxylation represented by the formation of the major 16α-hydroxyestrone metabolite. The formation of this metabolite is known to be mainly catalyzed by the CYP 450-3A4 isoenzyme **[509]**.

Consequently, using rifampicin-pretreated HepG2 cells, the selected PAs europine, lycopsamine, retrorsine, riddelliine, seneciphylline, echimidine and lasiocarpine all induced micronuclei to a significant extent. The induction yielded a similar maximal increase for all PA in the range of 1.64-2.0 folds. While the monoesters europine and lycopsamine induced a 1.99x and 1.64x fold increase, the cyclic diesters retrorsine, riddelliine and seneciphylline induced a 1.99x, 2.0x and 1.8x fold increase and the open diesters echimidine and lasiocarpine induced a 1.94x and 1.97x fold increase. According to the lowest concentrations at which significant induction of micronuclei was found, the potency ranking in our investigation was:

Lasiocarpine /riddelliine > retrorsine /echimidine > seneciphylline /europine /lycopsamine

Allemang et al. (2018) **[510]** had found (with seneciphylline not tested):

Lasiocarpine > riddelliine > retrorsine/echimidine > europine > lycopsamine

Louisse et al. (2019) **[196]** had reported:

Lasiocarpine /riddelliine/retrorsine/seneciphylline > echimidine > europine > lycopsamine

Thus, our findings were in excellent agreement with Allemang et al. (2018) and good (but not complete) agreement with Louisse et al. (2019). It has to be remembered that only Allemang et

al. (2018) **[510]** used the same endpoint, micronuclei, while Louisse et al. (2019) **[196]** measured yH2Ax-induction, which may be expected to deviate slightly. While micronuclei are formed during mitosis from misaligned chromatids/chromosomes or from chromosomal fragments, yH2Ax staining reveals sites of DNA (double strand break) repair activity **[91, 196]**.

The shape of the dose-response curves was in agreement with a presumed threshold, i.e. concentrations could be identified which did not induce a detectable significant effect. At higher doses, a saturation of the maximally observed micronucleus frequency was observed, and toxicity occured, which was measured as reduction of the proliferation index CBPI. However, all tested PA induced micronuclei also at non-toxic concentrations.

In addition, one of our colleagues in the working group (Lea Schott) tested the three PAs seneciphylline, europine and lasiocarpine in the liver cell line Huh6. This cell line had not been used much for genotoxicity assessement of metabolically activated compounds, but Knasmüller et al. **[511, 512]** had demonstrated their good metabolic capacity in the micronucleus test. Here, the tested PAs induced a significant elevation of genomic damage. Thus, both human liver cell lines, HepG2 and Huh6, were suitable for the detection of genotoxicity of PA in the in vitro cytokinesis block micronucleus test. This is relevant because other recent publications regarding PA genotoxicity used the rather expensive HepaRG cell system **[196, 510]**. Using HepG2 or Huh6 cells enables an extension of research in this area to more labs.

Based on our CBMN assay results we went further to quantify the mechanistic potency of these PAs of different chemical classes using a modified comet assay. PAs have been reported to induce DNA cross-linking in vivo and in vitro studies **[510, 513-518]** and DNA cross-links are a severe form of DNA damage in cells **[436]**. We used equimolar (equal) concentrations and also higher concentrations of these PAs. Lasiocarpine (open diester PA-type) was the most effective of these PAs causing DNA damage via DNA cross-linking followed by retrorsine (cyclic diester PA-type) and then europine (monoester PA-type) with the least DNA crosslink formation.

Therefore, to induce genomic damage via DNA crosslink by PAs is based on their chemical structure with the open diesters being the most potent followed by cyclic diesters and then monoesters. This ester moiety is relevant in the formation of the toxic pyrrolic moiety **[232,**

252] which causes DNA crosslinks leading to genomic damage. The difference in their chemical structure (ester moiety) may thus play an important role in causing genomic damage. Previous research studies have also investigated the toxicity of different PAs and shown that the monoester intermedine (Im) was less toxic and had a lower carcinogenic risk **[519]**. However, Wang et al. (2021) **[520]** using different mammalian cell lines found that the monoester intermedine was toxic at concentrations (167, 250 and 334 µM). These concentrations were higher than the concentrations used in other experiments **[29]**. Interestingly, at these higher monoester concentrations we also observed micronucleus induction by europine and lycopsamine at concentrations (100µM, 320 µM and 1000 µM) but no DNA cross-linking activity.

6.2 PA-induced oxidative stress in HepG2 cells

To elucidate the mechanism of PA-induced genotoxicity, our study went further to investigate the involvement of PA in causing oxidative stress in the human liver cell line HepG2 cells. It was relevant to study this because oxidative stress reflects an imbalance between reactive oxygen species (ROS) and the ability of the biological cellular system to detoxify the reactive intermediates or to repair the damage caused by oxidative stress **[521]**. These reactive species (ROS) can affect biomolecules in the cells such as DNA, leading to genotoxicity **[522]**. PAs have been reported to induce oxidative stress with liver being the most sensitive organ **[523-525]**. Liang et al. (2009) **[526]** have shown otonecine PA-type clivorine-induced oxidative stress in an in vitro studies using normal human liver L-02 cells. Liu et al. (2010) **[525]** used an in vivo study, reported a retronecine-PA type isoline-induced oxidative stress injury in various mouse tissues. According to the finding of this study, lasiocarpine, riddelliine and europine, but not lycopsamine caused significant elevation of oxidative stress via formation of ROS in HepG2 cells. The strongest magnitude of oxidative stress induction was observed in diesters PA (lasiocarpine and riddelliine), followed by the monoesters europine and lycopsamine.

To confirm if really these tested PAs induced oxidative stress via ROS formation, N-acetyl-L-cysteine (NAC; 5 mM) was applied. NAC is a synthetic precursor of intracellular cysteine which is important in the cellular glutathione synthesis **[443]**. It is also considered as one of the main

sources of sulfhydryl groups which act directly as a free radical scavenger **[443, 444]**. Hence, its anti-ROS activity is from free radical scavenging properties either directly via the redox potential of thiols or secondarily via increasing glutathione levels in cells **[445]**. Due to these facts, NAC is used to confirm the involvement of ROS in drug or chemical –induced ROS leading to cell damage, and inhibit ROS **[527]**.Therefore, in this study, using NAC (5 mM) in presence of PAs significantly reduced the oxidative stress. Hence, it can be clearly deduced that lasiocarpine, riddelliine and europine caused oxidative stress in HepG2 cells.

There are many different organelles in the cell that can generate ROS however; the main sites are mitochondria, the endoplasmic reticulum (ER), plasma membrane and cytosol. The mitochondria are a major source of ROS, especially when damaged. Superoxide (O_2^-) is formed at complexes I and III of the electron transport chain, where fully reduced prosthetic groups can donate electrons directly to molecular oxygen (O_2) **[528]**. It is well known that mitochondria generate a huge percentage (approximately 90%) of the total ROS in the human cell and the mitochondrial electron transport chain is the central source of ROS formation. Mitochondria are vital cellular organelles for energy generation in a cell **[529]** and they serve as a primary target for oxidative stress via ROS formation in human cells leading to induction of genomic damage **[446, 527]**. Their primary role in energy metabolism, as well as their high abundance in hepatocytes, makes them an important target for drug-induced hepatotoxicity. For example, mitochondrial toxicity associated with acute toxicity of PAs has been shown for the PAs clivorine and senecionine **[530]**, retrorsine **[531]**, lasiocarpine **[532]** and dehydromonocrotaline **[533]**. This study therefore may serve as an important basis for understanding the mechanism of PA-inducing genotoxicity and also developing further detoxification approaches for PAs and PA-containing products.

Mitochondrial membrane potential is an early marker event of mitochondria damage leading to ROS generation because, mitochondrial membrane potential is mainly required for ATP production **[529]**. The results with mitochondrial membrane potential (MMP) decrease will cause ATP depletion along with changes in the pH of mitochondrial intermembrane space and matrix. Hence, fluorescent dyes such as TMRE accumulate in healthy mitochondria depend on the pH. Our present results showed significant impact of PAs on the mitochondrial membrane

potential. This is also supported by several studies. For example, based on in vivo and in vitro studies, Wang et al. (2020) **[529]** have shown PA-seneciphylline disrupting mitochondrial homeostasis through mitochondrial membrane potential loss and induction of mitochondrial depolarization leading to hepatotoxicity in mice (70 mg/kg, orally), and also in primary mouse and human hepatocytes (5–50 μM). Wang et al. (2021) **[520]** found that the monoester intermedine caused generation of ROS in HepD cells with significant decrease in mitochondrial membrane potential. Therefore, our current research results uncovered that PAs-lasiocarpine, riddelliine and europine significantly induced the deprivation of mitochondrial membrane potential which may be the cause of the oxidative stress induced by these PAs.

Notably, our results did indicate that the monoester europine induced less ROS formation than the diesters' lasiocarpine and riddelliine, but all three PAs induced almost the same extent of mitochondrial membrane potential damage. Possibly, the diester PAs may be depleting glutathione (GSH) more than the monoester europine hence, resulting in more ROS-mediated damage in cells treated with diester PAs. Basically, intracellular GSH is an important molecule which not only maintains cellular redox homeostasis by scavenging cellular ROS but also neutralizes (detoxifies) certain reactive PA-metabolites (dehydro-PAs) generated by metabolic activation of PAs **[534-536]**. For this reason, GSH is believed to play a crucial role in drug metabolism-induced liver injury **[537]**. Previous studies have shown that PAs could cause significant GSH depletion in cells in vitro and in animals, and the toxicities caused by PAs could be ameliorated by restoration of cellular GSH **[534, 538]**. Also, in our present study, we have illustrated that lasiocarpine-induced micronucleus formation was significantly elevated in GSH depleted HepG2 cells. These results were in good correlation with the findings where the reduced GSH level led to an increased formation of the pyrrole-protein adducts leading to PA-induced genomic damage **[536]**. In addition, our findings also revealed an increased cellular ROS level in HepG2 cells, with a remarkable decrease in ROS in the presence of the anti-oxidant N-acetylcysteine (NAC) in HepG2 cells with PA treatment. These results were consistent with the anti-oxidant role of GSH, because its depletion has been considered as a major reason for induction of cellular ROS and aggravated oxidative stress. Our findings were also in agreement with studies where PAs were demonstrated to significantly decrease cellular GSH in murine

sinusoidal endothelial cells (SECs) **[534]**, HepG2 **[538],** and human L-02 cell **[523]**, and produce concentration-dependent formation of toxicity-related protein adducts in livers of mice and rats **[349, 539]**.

Several studies have highlighted the significance of glutathione (GSH) in mitigating pyrrolizidine alkaloid (PA)-induced toxicity. For instance, He et al. (2020) **[202]** demonstrated that both GSH and cysteine significantly reduce PA-induced hepatotoxicity in rat primary hepatocytes. Additionally, other studies have reported a reduction in PA-induced cytotoxicity in the presence of GSH or GSH precursors **[523, 540]**. Dos Santos et al. (2009) **[541]** further illustrated the depletion of endogenous glutathione by dehydromonocrotaline in isolated rat liver mitochondria.

In this study, we observed a more pronounced DNA crosslinking effect and ROS induction in diester PAs (lasiocarpine and riddelliine) compared to the monoesters europine and lycopsamine. The bioactivation of PAs appears to be correlated with the presence of an unsaturated C1-C2 double bond in the necine base, branched-chain acids, and C-7 and C-9 ester substituents **[252, 292, 542]**. Pyrrolic PAs react with cellular nucleophiles at either or both ester linkages. The highly electrophilic nature of these diester PAs (lasiocarpine and riddelliine) pyrroles ensures their ready reaction with nucleophilic tissue constituents such as DNA **[332, 543]** and proteins **[544]**.

Diester PAs have two electrophilic sites (at C7 and C9 positions), with C7 being more electrophilic in nature than C9, unlike monoester PAs, which have only one electrophilic site (at C9 position). Thus, with such bifunctional electrophilic pyrroles, lasiocarpine and riddelliine can alkylate DNA and subsequently form stronger inter- or intrastrand DNA-DNA crosslinks **[255, 545]**, in contrast to monoester PAs (europine and lycopsamine), which exhibit little to no crosslink effects.

Additionally, our findings revealed potent ROS induction with diester PAs (lasiocarpine and riddelliine) but comparatively weak ROS induction with monoester PAs (europine and lycopsamine). Excessive ROS production in a cell is known to induce crosslinking of cellular macromolecules, including DNA and proteins, leading to genomic damage **[546-548]**. Therefore,

our results support the idea that lasiocarpine and riddelliine induce robust DNA crosslinks due to high ROS levels, while europine and lycopsamine exhibit weaker DNA crosslink effects attributed to lower ROS generation.

Moreover, other potential sources of ROS in the liver during xenobiotic toxicity include CYP450s and various oxidases in both hepatocytes and Kupffer cells **[549]**. PAs are well-known to be metabolically activated by cytochrome P450 enzymes, inducing toxicity. Cytochrome P450 enzymes are primarily membrane-associated proteins abundantly located in the inner membrane of mitochondria and in the endoplasmic reticulum of human cells. One of the primary functions of cytochrome P450 enzymes in humans is the metabolism, bioactivation, and detoxification of xenobiotics. It has been reported that cytochrome P450-mediated metabolism of xenobiotics in the human liver can also generate ROS, leading to an increase in oxidative stress. Therefore, in addition to the bioactivated intermediates or metabolites, cytochrome P450-mediated metabolism activity on xenobiotics may also increase oxidative stress in human liver cells, contributing to liver toxicity **[149, 550-552]**.

The damage to mitochondrial membrane potential could be of the same magnitude in all three PAs because all of them require cytochrome P450, mainly located in the inner membrane of mitochondria, leading to the generation of ROS. However, the amount of GSH depletion by the diester PAs (lasiocarpine and riddelliine) and the monoester PA (europine) may differ, resulting in different levels of ROS.

According to published reports, the metabolic activation of monoesters in human liver microsomes was different from that of diesters and did not result in glutathione (GSH) conjugates and DNA adducts formation. For example, Geburek et al. (2020) **[553]** found higher amounts of metabolites formed with diester PAs than with monoesters europine and lycopsamine, including the levels of DNA-reactive intermediates and DNA adduct formation. Additionally, GSH conjugates were only detectable with diester PAs, with lasiocarpine causing the highest amount. Therefore, this provides another explanation as to why ROS generation at equimolar concentrations of monoesters europine and lycopsamine was much lower than that of diester PAs lasiocarpine and riddelliine in HepG2 cells.

In addition, differences in toxicokinetics among PAs of different ester types can be pointed out. The high lipophilicity of diester PAs favors their general bioactivation, thus leading to the induction of ROS generation in HepG2 cells. However, at the molecular level, the mechanism of these PA-induced ROS production still remains unknown. We speculate that the mechanism could be similar to that of isoline-induced oxidative damage in mouse cells. In that study, the cyclic diester retronecine–PA isoline significantly decreased the activities of total antioxidant capacity, glutathione-S-transferase (GST), glutathione peroxidase (GPx), and catalase (CAT), while significantly increasing the lipid peroxidation (LPO) level in the liver of isoline-treated mice **[525]**.

Another interesting observation reported by Mingatto et al. (2007) **[554]**, which can also be alluded to our findings on PAs inducing oxidative stress. It was demonstrated that exposure of isolated rat liver mitochondria to dehydromonocrotaline, not monocrotaline, caused a concentration-dependent loss of membrane potential and ATP depletion in mitochondria. Additionally, there was a concentration-dependent inhibition of complex I NADH oxidase activity between 100 µM and 250 µM (IC_{50} 62.06 µM) through a non-competitive type of inhibition (K_I=8.1 µM). The same concentration that inhibited complex I activity also resulted in significant oxidation of GSH. This was suggested that the alkylating effect of the PA metabolite dehydromonocrotaline binds to thiol groups of molecules like GSH and proteins, causing oxidation of these molecules. Considering that the activity of complex I has been reported to be regulated by thiol groups **[555, 556]**, and that the reversible oxidation of complex I cysteine thiols causes its inhibition **[557]**, it is noteworthy that complex I presents several cysteine residues **[558]**, whose modification could influence its conformation and function. Therefore, this mechanism could also be speculated in our tested PAs as another mechanism of PA inducing oxidative stress through the generation of ROS, though it warrants further investigations.

Altogether, we can summarize that the PAs tested here, the open-diester lasiocarpine, cyclic-diester riddelliine and monoester europine, induced intracellular oxidative stress and generated excessive ROS, which may have resulted in DNA crosslinking and micronucleus formation.

6.3 Influence of membrane transporters in PA-induced genotoxicity

It is yet unknown how these PAs enter or leave hepatocytes. The role of hepatic transporters is just beginning to be appreciated as a key determinant of PA-induced toxicity. These hepatic transporters are relevant for PA toxicokinetics, mediating the import or export of PAs and their metabolites from hepatocytes—a crucial step for PAs to exert their toxic potential **[559]**. Data are limited, partly due to the many structural differences among PAs. However, influx and efflux transporters have recently been discovered as key contributors to PA toxicity **[352, 354, 365]**. In general, it was assumed that PAs pass through the intestinal and hepatic membranes only by facilitated biological diffusion, as this is the primary mechanism for many xenobiotics **[350, 560]**. In addition to passive diffusion, membrane transporters play a significant role in facilitating or preventing xenobiotic movements **[167]**. Altering the influx or efflux process by applying chemical transporter inhibitors may reduce the intake or elimination of PAs, thus decreasing PA-mediated toxicity or increasing PA-mediated toxicity, respectively.

In vivo, sinusoidal liver epithelial cells are a crucial target for PA-induced toxicity and carcinogenicity. However, PAs need to be activated before reaching these cells because sinusoidal cells are not thought to be metabolically active **[15, 19, 561-566]**. Thus, the question of whether and how PAs are taken up by hepatocytes, and how their metabolites are excreted by them, becomes important in elucidating the carcinogenic mechanism further.

Hepatic membrane transporters are classified as influx (uptake into the cell) and efflux (out of the cell) transporters typically located either at the basolateral or apical membrane in polarized cells such as liver cells **[567]**. Hence, this present study focused on assessing the general mode of action of PA transport in the human hepatoma cell line HepG2 using the PA lasiocarpine as a model substance. Two hepatic uptake and two efflux transporters were targeted with inhibitors to identify their role in the uptake or efflux of PA lasiocarpine in the HepG2 cell line. For this purpose, lasiocarpine-induced micronuclei were assessed using the standard micronucleus assay.

While the organic cationic transporter 1 (OCT1) is mainly expressed in the basolateral membrane of hepatocytes, initiating uptake from the blood **[568-572]**, organic anionic

transporter protein 1B1 (OATP1B1) is mainly expressed on the sinusoidal membrane of human hepatocytes **[573-576]**. These two influx transporters have been reported to be expressed in HepG2 cells **[175, 577]**, and they are highly sensitive to inhibitors **[175]**. Quinidine is an antiarrhythmic agent and a known OCT1 inhibitor **[175]**. Nelfinavir is an antiretroviral drug known to have an inhibitory effect on OATP1B1 transporter in HepG2 cells **[175]**. Both influx inhibitors, quinidine and nelfinavir, reduced lasiocarpine-induced micronucleus formation, but only quinidine to a significant extent. This means that lasiocarpine was taken up into the cells by OATP1B1 and OCT1 influx transporters, with OCT1 being the predominant one of the two. This correlates with other experimental endpoints such as cytotoxicity, where inhibition of the OCT1 influx transporter led to a reduced uptake of retrorsine and senecionine into HepaRG cells **[559]**.

Also, in earlier research, a role of OCT1, for monocrotaline mediated liver cell cytotoxicity was demonstrated **[578]**. In addition to that, Tu et al. (2013 and 2014) **[352, 354]** reported the uptake of the PAs monocrotaline and retrorsine through the basolateral transporter OCT1-influx mediated transporter in MDCK/hOCT1-overexpressing cells and cultured primary rat hepatocytes. In both studies, the OCT1 inhibitor quinidine reduced the uptake of monocrotaline and retrorsine and reduced the cytotoxic effects in primary rat hepatocytes. All these facts emphasize the relevance of OCT1 influx- transporter for PA. However, Yang et al. (2020) **[350]** showed that passive diffusion is a major way of PA intestinal uptake, while efflux transporter-mediated active transport was also involved but to a limited extent. Therefore, we also analyzed the inhibition of these influx transporters using suitable fluorescent dye probe substrates, sodium fluorescein as a reference probe substrate for the OATP1B1 influx transporter, and ethidium bromide as a reference probe substrate for the OCT1 influx transporter. Subsequently, in agreement with our previous results, the OATP1B1 and OCT1 influx transporters were significantly inhibited by their respective reference inhibitors in HepG2 cells, as indicated by a significant decrease in the accumulation of the fluorescent probe substrates in the cells.

Regarding efflux transporters, Louisa, M., et al. (2016) **[175]** reported that hepatoma cells such as HepG2 significantly express MDR1 **[175]** and MRP2 **[579]** transporters. Verapamil, a calcium channel blocker, is a specific first-generation MDR1 efflux transporter inhibitor **[427, 428]**.

Benzbromarone, an anti-gout agent, has been shown to inhibit the efflux transporter MRP2 **[430, 580-582]**, also in HepG2 cells **[429]**. Both efflux transporter inhibitors slightly increased lasiocarpine-induced micronucleus induction in HepG2 cells, with the increase being significant only for benzbromarone. This implies that lasiocarpine could be a substrate of MDR1 and also a substrate of MRP2 efflux-mediated transporters. This is in agreement with studies conducted to investigate the involvement of MDR1 efflux-mediated transporters for PAs. For example, Yang et al. (2020) **[350]**, using the inhibitor verapamil, have shown the involvement of MDR1 transporter in the efflux of PAs in a Caco-2 monolayer model. Meanwhile, Hessel et al. (2014) **[365]** demonstrated the efflux of the PA echimidine by the MDR1 transporter using inhibition with cyclosporine A.

Furthermore, the chemical inhibition of the efflux transporters was also analyzed using suitable reference fluorescent dyes to confirm if the efflux transporters were indeed inhibited by the respective inhibitors used. Consistent with our analysis results using the calcein-AM fluorescent dye, the MDR1 and MRP2 efflux transporters were significantly inhibited by their respective inhibitors in HepG2 cells, as indicated by a significant increase in green calcein fluorescence.

Overall, it seems that transporters, possibly in addition to passive diffusion, mediate cellular PA uptake and elimination. However, we cannot exclude the possibility that other transporters or pumps, not investigated here, are also involved in transporting PAs.

6.4 Influence of metabolic enzymes in PA-induced genomic damage

The human hepatoma cell line HepG2 has been demonstrated as a valuable substitute for primary liver cells in studying metabolism-related cellular effects **[583]**. Chemical inhibitors have also been widely employed in in vitro models to elucidate the metabolism of xenobiotics **[416, 418, 419, 422]**. This allowed us to investigate the effect of chemical inhibitors of metabolism on PA-induced genotoxicity. Some of the treatments with chemical inhibitors were expected to decrease micronucleus frequency, while others were anticipated to increase it.

Loperamide is an anti- diarrhoeal drug and *in vitro* studies have shown it to be a selective competitive carboxylesterase subfamily 2 (CES2) enzyme inhibitor **[157, 494, 584]**. Carboxylesterases (CES) are a family of enzymes found in organisms ranging from bacteria to mammals. They are mainly involved in the hydrolysis of ester, amide, or thioester bonds. A recent genomic analysis clearly defined five distinct mammalian CES subfamilies based on genetic sequence and genomic structure **[152]**, but CES1 and CES2 subfamily proteins are the most extensively studied **[157]** due to their dominance in humans and the fact that their mRNA expression is highest in the liver **[158]**. This suggests an important role of these enzymes in detoxification of xenobiotics **[152]**. A recent study by *Forsch et al.* (2018) **[414]** demonstrated that loperamide inhibited CES enzyme in HepG2 cells at a concentration of 2.5 µM leading to a significant decrease in metabolic activity. In our present study, lasiocarpine-induced micronucleus formation was significantly increased in presence of loperamide. This suggests that the detoxification of lasiocarpine was hindered by the inhibition of the CES2 enzyme by loperamide.

The relevance of CES enzymes regarding PAs was also reported in some previous studies, showing that the differences in esterase activity were responsible for the differences in metabolism of otonecine-PA clivorine in normal human hepatocyte L-02 cells **[585, 586]**. In addition, Wang et al. (2021) **[520]** found that the monoester intermedine produced different toxic responses in different mammalian cells, which could be a result of the different esterase activities. We also conducted an analysis to assess the inhibition of CES2 by loperamide in HepG2 cells using the calcein-AM fluorescent dye. Our findings were consistent with the observed inhibition of CES by loperamide, as evidenced microscopically by an increase in calcein green fluorescence in the cells.

Additionally, we investigated the relevance of CYP450 enzymes in PA-induced genotoxicity in HepG2 cells. Cytochrome P450 (CYP450) enzymes are principal catalysts involved in the metabolism of xenobiotics **[447, 448]**. In humans, they are mainly expressed in the liver and are potential targets in pathways that generate undesirable amounts of metabolites of endogenous chemicals, as well as products of some carcinogenic xenobiotics. Understanding the roles of CYP450 in humans has been crucial for elucidating mechanisms of action and addressing issues

such as achieving bioavailability, preventing drug–drug interactions, and avoiding toxicity **[447, 448]**. PAs are known to require metabolic activation by cytochrome P450 oxidase enzymes, such as CYP3A4, CYP1A2, and CYP2B6 isoenzymes **[587]**.

As a first step, our study focused on the involvement of CYP 450 in the metabolism of lasiocarpine. One in vitro approach to determine the extent of CYP450 metabolism is the use of selective chemical inhibitors for specific CYP450 isoforms. In the pharmaceutical industry, chemical inhibitors are widely employed to assess the contribution of particular CYP 450 isoforms to metabolism in liver microsomes **[588]**. In our present study, the chemical inhibitors were applied at concentrations known to be most effective in inhibiting the intended CYP450 isoenzyme with maximum selectivity, based on published literature.

We tested ketoconazole and furafylline as selective CYP 450 isoenzyme inhibitors. Ketoconazole, an anti-fungal drug, is extensively used as a potent and specific inhibitor of the human CYP 450-3A4 isoenzyme **[417, 482]**. At a 1 µM concentration, it has been commonly used in human hepatocytes to inhibit the CYP 450-3A4 isoenzyme **[416, 418, 419]**. Furafylline has been developed as a potential replacement for theophylline in the treatment of asthma **[421]**. Recent in vitro studies have shown that CYP 450-1A2 activity could be blocked completely with 1 µM furafylline **[419, 422]**. In our present findings, both ketoconazole and furafylline led to a strong or almost complete reduction of lasiocarpine-induced micronucleus formation, with furafylline being less effective than ketoconazole. While both isoenzymes contributed to lasiocarpine-induced genotoxicity, CYP 450-3A4 seems to play a larger role than the CYP 450-1A2 isoenzyme.

The relevance of CYP 450-3A4-mediated metabolic activation of lasiocarpine for its genotoxicity was also recently emphasized by Ebmeyer et al. (2019) **[589]**, who found that lasiocarpine exhibited genotoxicity only in metabolically incompetent V79 hamster cells genetically engineered to harbor human CYP 450-3A4. Our findings are also in line with other previous studies that reported CYP 450-3A isoenzymes in rodents leading to the activation of PA **[230, 232, 590]**. In addition, Mingatto et al. (2007) **[554]** also showed that the reactive metabolite dehydromonocrotaline, not the parent monocrotaline, caused a loss of mitochondrial membrane potential in isolated rat liver mitochondria.

6.5 Analysis of cytochrome P450 activity

In collaboration with the department of Food Chemistry at the University of Wuerzburg, Germany (working group of Prof. Dr. Leane Lehmann), the inhibition and induction of CYP 450-3A4 activity by ketoconazole (1 µM) and rifampicin (20 µM) were analyzed in HepG2 cells using GC/MS and UHLPC/MS. The method was based on the metabolism of 17β-estradiol (E2) and estrone (E1) and is published by our collaborators **[449]**.

In the human liver, 17β-estradiol (E2) and estrone (E1) undergo oxidative metabolism, primarily through hydroxylation and keto formation catalyzed by CYP 450 enzymes. These enzymes mediate the metabolism of 17β-estradiol (E2) through two major pathways, predominantly forming the 2- and 16α-hydroxylation estrogens **[509, 591-594]**. The liver expresses high levels of multiple CYP isoforms such as CYP 450-3A4 and CYP450-1A2 **[593, 595, 596]**. Normally, cytochrome P450-3A family enzymes are the most abundant CYP isoforms present in the human liver, and it is estimated that the CYP 450-3A4 isoenzyme accounts for approximately 30% of the total CYP content in the liver **[136, 597, 598]**. Studies have shown that CYP 450-3A4 has high catalytic activity for the formation of hydroxylated metabolites of E2 and E1 and is involved in the formation of 2- and 16α-hydroxylation of estrone metabolites **[509, 593, 594, 599-601]**.

Based on these findings and the outlined approach, ketoconazole (1 µM) inhibited the CYP 450-3A4 isoenzyme, while rifampicin (20 µM) induced the same isoenzyme. The significant inhibition of CYP 450-3A4 by ketoconazole resulted in a notable reduction in the formation of 2-methoxylestrone (2-MeO-E1) and 16α–hydroxylestrone (16α-OH-E1) metabolites.

Ketoconazole is also a potent inhibitor of the UDP-glucuronosyltransferase (UGT) enzyme, a crucial phase II metabolic enzyme responsible for the formation of glucuronide metabolites. This UGT enzyme is primarily found in the liver **[602]** and has a broad spectrum of substrates, including estradiol, drugs, environmental pollutants, and carcinogenic chemicals **[603, 604]**. Studies using human hepatocytes have demonstrated that ketoconazole can reduce glucuronide formation **[605]**.

Glucuronidation is a vital conjugation pathway that predominantly contributes to phase II biotransformation. It facilitates the elimination of lipophilic xenobiotics or endobiotic

substances, including estrogen, by converting them into more water-soluble compounds. This allows for their elimination through urine or bile. For instance, ketoconazole has been shown to inhibit the glucuronidation of the anti-retroviral drug zidovudine and the short-acting anxiolytic lorazepam by inhibiting the UGT enzyme **[606-609]**. Satoh et al. (2004) **[610]** also demonstrated that ketoconazole inhibits the glucuronidation of estradiol using human liver microsomes. In our analysis of the inhibition of CYP 450-3A4 activity by ketoconazole in HepG2 cells, we observed a significant reduction in estrone glucuronide formation, reaching the lower limit of quantification (<LOQ). This suggests that ketoconazole significantly hinders the phase II metabolism glucuronidation process, likely through the inhibition of UDP-glucuronosyltransferase (UGT) enzymes.

Sulfation is another phase II metabolic step for detoxification, reducing the biological activity of certain steroids, including estrogens or xenobiotics, by increasing water solubility. This enables their excretion from the body via urine and/or bile **[611]**. The sulfation conjugation of the phase II metabolism process is primarily catalyzed by sulfotransferase (SULT) enzymes **[612-615]**. For instance, it has been reported that the sulfotransferase isoform 1E1 (SULT1E1) enzyme exhibits the highest affinity for estrogens among known sulfotransferases and is the primary enzyme responsible for the sulfation of 17β-estradiol and estrone **[616]**. In our analytical results, ketoconazole reduced phase II sulfation metabolites such as estrone sulfate (E1-S; significantly reduced) and estradiol-3-sulfate (E2-3-S; not significantly reduced). This suggests the possibility of ketoconazole favouring the inhibition of sulfation via E1-S metabolite formation rather than E2-3-S metabolites. This observation indicates that ketoconazole may also inhibit the sulfation process through the inhibition of the sulfotransferase enzyme. However, this warrants further investigation as we are the first to report this observation in our analytical results, and no information is available to date in the literature.

With regard to CYP 450 induction by rifampicin, our results significantly favored the formation of estrone (E1) from 17β-estradiol (E2). Rifampicin also increased the formation of the phase I metabolite 16α-hydroxylestrone (16α-HO-E1) by 3-fold, but not the 2-methoxylestrone (2-MeO-E1) metabolites. The 3-fold increase in 16α-HO-E1 metabolites was not deemed significant, possibly due to interexperimental variations. Based on our results, it appears that rifampicin

favors the hydroxylation formation of phase I metabolites rather than methylation. This may explain the increase in 16α-HO-E1 rather than the 2-MeO-E1 metabolites. This observation aligns with studies by Yamazaki et al. (1998) **[509]**, where the authors demonstrated that the CYP 450-3A4 isoenzyme predominantly favors the formation of 16α-hydroxylation metabolites of estrone and estradiol in human liver microsomes. Badawi et al. (2001) **[594]** also reported that 16α-hydroxylation of estrone metabolites is most favored by CYP 450 enzymes using complementary DNA expressed CYP isoforms.

Rifampicin has been shown to induce phase II metabolism glucuronidation of estradiol, naphthol, propofol, and morphine by inducing UGT enzymes in cultured primary human hepatocytes **[617]**. According to our findings, rifampicin significantly increases the formation of the phase II metabolite estrone-3-glucuronide (E1-G) by 2-fold, indicating the induction of UGT enzymes by rifampicin. Additionally, we observed a significant decrease in phase II metabolites estradiol-3-sulfate (E2-3-S) and estrone sulfate (E1-S), consistent with a study reported by Kodama et al. in 2011 **[616]**. This study showed that rifampicin suppresses the transcription of the estrogen sulfotransferase (EST/SULT1E1) gene in human primary hepatocytes and hepatocellular carcinoma cell lines HepG2 and Huh7, via an interaction with nuclear factor 4α (HNF4α), thereby lowering the sulfation of estrone. Therefore, the 3-fold increase in 16α -OH-E1 and a significant increase in E1-G confirm that rifampicin indeed induces CYP 450 enzymes. The induction of CYP 450 activity is further supported by published reports demonstrating rifampicin as a potent PXR activator and CYP 450-3A inducer **[618]**.

The inhibition of the CYP 450-1A2 isoenzyme by furafylline was not analyzed, but it would be worthwhile to explore in future studies. In this dissertation, we assumed, based on the published literature, that 1 µM furafylline is sufficient to inhibit the expression and activity of the CYP 450-1A2 isoenzyme.

Therefore, our analytical study confirms that ketoconazole is an inhibitor of CYP 450-3A4 isoenzyme activity and also inhibits the sulfation and glucuronidation processes of phase II metabolism. We also agree with the literature that rifampicin is an inducer of CYP 450-3A4 isoenzyme activity, as well as the glucuronidation process of phase II metabolism, but a

suppressor of the sulfation process. Hence, the use of these chemicals was relevant in our present study to achieve our objectives.

6.6 PAs-induced genomic damage in Co-Culture System

Numerous studies have highlighted the liver as the principal site of PA toxicity, drawing significant attention to research on liver diseases induced by PAs. The human liver, a crucial organ for the metabolism, bioactivation, and detoxification of exogenous substances, is consistently recognized as the primary target for the toxicity of such substances **[619]**. At an acute level, human exposure to high concentrations of PAs has been considered one of the primary causes of hepatic sinusoidal obstruction syndrome (HSOS). For example, Yang et al. (2017) **[246]** reported PAs inducing HSOS in humans. Earlier, HSOS was referred to as hepatic veno-occlusive disease, a rare hepatic vascular disease associated with a high mortality rate **[620]**. At an early stage, HSOS is characterized by primary hepatic sinusoidal endothelial cells (HSECs) damage, which can later lead to hepatotoxicity and carcinogenicity. However, the mechanism is not yet fully understood because HSECs in the liver lack or express extremely low levels of CYP 450 enzymes **[246, 536, 621]**, which are required to metabolically activate PAs. To date, there is no direct evidence supporting the toxicity of reactive PA metabolites in hepatic sinusoidal endothelial cells (HSECs), and there is no effective therapy for PAs-induced HSOS **[620]**, due to a lack of information regarding the understanding of the toxic mechanism associated with PAs-induced HSOS.

Currently, most research studies on PA-induced HSEC damage mainly depend on animal models of PA-induced HSOS **[622-625]**. The laborious process of isolating HSECs with high purity, especially from animal models that have developed hepatic sinusoidal damage, has limited their use in the toxicity and mechanistic studies of PA-induced HSEC damage. In the field of toxicology, in vitro culture models offer many advantages over animal models for investigating toxicity. However, until now, only limited in vitro studies have been conducted on HSECs. One of the main hindrances that obstructs in vitro studies is the extremely low or lack of CYP 450

expression in human HSECs, preventing the bioactivation of PAs to the reactive pyrrolic metabolites (Dehydro PAs) that can induce toxicity **[623]**.

Another problem that hindered the in vitro study on PA-induced HSECs damage is that the reactive pyrrolic intermediates (Dehydro-PAs) derived from different PAs are all known to be highly unstable and the direct in vitro testing of dehydro-PAs is challenging and complicated **[626]**. To solve these problems our present study came up with a novel co-culture system which mimics the hepatic environment. Therefore, as a first step, a co-culture system was established in which HeLa H2B-GFP (green fluorescent labelled human cervical cancer cells) were brought into close vicinity to potential target cells of the liver represented by the human liver cell line HepG2. HepG2 are a hepatocarcinoma cell line of good metabolically activity, while HeLa H2B-GFP are not metabolically active. In this system, micronucleus induction was evaluated in the target HeLa H2B-GFP cells. In addition, under same conditions each cell line was cultured alone as well and micronucleus induction was assessed in parallel to the co-culture. In the co-culture, PAs were metabolically activated by CYP 450 enzymes in HepG2 cells to generate reactive pyrrolic metabolites, which then reacted with the co-cultured HeLa H2B-GFP cells leading to micronucleus formation. Three representative PAs of different ester type, which were chosen from our selected PAs, the open diester-PA lasiocarpine, the cyclic diester-PA riddelliine and the monoester-PA europine, induced micronucleus formation significantly in HeLa H2B-GFP cells in the co-cultured system and in separately cultured HepG2 cells, but did not cause micronucleus induction in a culture of only HeLa H2B-GFP cells. This observation confirmed that HeLa H2B-GFP cells were not able to bioactivate PAs and thus no micronucleus formation occurred. Therefore, we can deduce that the PAs were bioactivated in HepG2 cells and the metabolites were taken up by the HeLa H2B-GFP cells of the co-culture system, inducing genomic damage. Considering the situation in the human liver, we can hypothesize that PAs are first metabolically activated in the hepatocytes, then move out and are taken-up by their primary target HSECs.

In addition, we used the open diester-lasiocarpine, the cyclic diester-riddelliine, and the monoester-europine in the co-culture system. Our results revealed that the open-diester PA lasiocarpine exhibited the strongest micronucleus induction at the lowest concentration (10 µM). At this concentration, lasiocarpine also displayed significant cytotoxicity, as indicated by

the proliferation index (CBPI). Following this, cyclic-diester riddelliine induced micronucleus formation at a concentration of 100 µM, and the monoester PA europine induced micronucleus formation at a concentration of 320 µM. In other words, micronucleus induction was nearly equivalent for the three PAs but at different concentrations: lasiocarpine (10 µM), riddelliine (100 µM), and europine (320 µM). Additionally, the proliferation index (CBPI) was significantly reduced at the tested concentrations of lasiocarpine (10 µM) and riddelliine (100 µM), but not in the case of europine (320 µM). This clearly indicates that the diesters, lasiocarpine, and riddelliine, were indeed more potent in inducing genomic damage than the monoester europine. This observation is consistent with our results observed in rifampicin-pretreated HepG2 cells **[627]** and aligns with previous studies using HepaRG or HepG2 cells to investigate the relative potency of different ester-type PAs **[2, 29]**.

To sum up, in the present study, we mimicked the hepatic microenvironment and successfully developed a novel co-culture system that utilized two types of cell lines: the metabolically active human hepatoma cell line HepG2 and the non-metabolically active human cervical epithelial cell line HeLa H2B-GFP. This system was designed to study PAs-induced genomic damage in the non-metabolically active target HeLa H2B-GFP cells within the co-culture system, similar to presumed situations of damage to HSEC. Our objective was to investigate whether PA-metabolites could move out of hepatocytes and induce damage in neighboring target cells.

This co-culture system can also be applied for in vitro screening studies of other potential phytotoxins that require metabolic activation before affecting non-metabolically active cells. Previous in vitro studies have demonstrated PA-induced damage to HSECs. For instance, Lu et al. (2019) **[536]** developed a two-layer transwell co-culture model and reported that PA retrorsine, monocrotaline, and clivorine induced hepatic sinusoidal damage. However, their model involved human HepaRG cells and HSECs, while in our case; we used human HepG2 and HeLa H2B-GFP cells. In their case, it might be more direct to explain PA-induced HSEC damage; however, it's worth noting that their use of human liver HepaRG cells, supplied in a predifferentiated state with enhanced expression of metabolic enzymes, is rather expensive **[628, 629]**.

Furthermore, the same authors extended their studies by developing a CYP 450-3A4-transduced human hepatic sinusoidal endothelial cell model, demonstrating that PA retrorsine induced hepatotoxicity via reduced cell viability, depletion of GSH, and increased formation of pyrrole-protein adducts **[621]**. However, in both of their studies, the authors did not demonstrate how membrane transporters might be involved or how the PAs are taken up once metabolized by hepatocytes. Additionally, the relevance of showing PA metabolism in HSECs by transducing them with CYP 450, considering that HSECs lack these enzymes in reality, could be debated. In our co-culture system, we aimed to address questions regarding the mechanism of PA-induced genomic damage, focusing not only on metabolic activation but also on the role of membrane transporters.

It is also worth noting that the concentrations of the three PAs used here, lasiocarpine (10 µM), riddelliine (100 µM) and europine (160 µM), are orders of magnitude higher than the average human exposure. However, metabolic activation may be more efficient in vivo and accumulation of mutagenic adducts in the liver may occur. The elucidation of mechanisms of action is therefore relevant for human risk assessment.

6.7 Influence of inhibition of metabolic enzymes and efflux transporters in PA-induced genotoxicity in the Co-Culture System

Up to this point, our studies have indicated that liver cells are the primary cells responsible for the bioactivation of PAs. Reactive metabolites formed in the liver can move out and cause toxicity in adjacent liver cells. There is also a possibility that these reactive PA metabolites formed in hepatocytes may induce extrahepatic toxicities in various organs throughout the human body. For instance, Liu et al. (2010) **[525]** found that the retronecine-diester PA isoline had different effects on the total oxidant and antioxidant capacity in various organs such as the liver, lung, brain, and heart. The liver recorded the highest oxidative injury among these organs. Additionally, other reports have indicated that diester PAs, such as monocrotaline and trichodesmine, can induce neurotoxicity **[630, 631]**, with monocrotaline being a potent pneumotoxic **[632]** and trichodesmine a potent neurotoxic compound **[631]**. Therefore,

exploring potential toxicity induced by PAs in extrahepatic organs is another aspect that needs consideration.

The role of hepatic membrane transporters is only at the beginning stages of being recognized as a key determinant of PA-induced toxicity. Therefore, the possibility that PAs inflict harm on humans warrants further consideration and research, especially regarding human metabolism and transport, and how PAs are taken into or out of hepatocytes. Subsequently, the open diester lasiocarpine, the cyclic diester riddelliine, and the monoester europine were investigated. The potent cytochrome P450-3A4 inhibitor ketoconazole **[416-419]** significantly reduced micronucleus induction of the three representative PAs in HeLa H2B-GFP cells in the co-culture, possibly due to the inhibition of metabolism via the CYP 450-3A4 isoenzyme in the HepG2 cells. This aligns with our earlier observations in this dissertation on the effect of lasiocarpine-induced genotoxicity in ketoconazole-pretreated HepG2 cells, where we observed a significant increase in genomic damage. Similarly, in parallel with our findings, although not focused on investigating genotoxicity, Lu et al. **[633]** established in a two-layer transwell co-culture model that PAs were metabolized by human HepaRG hepatocytes, and the produced metabolites reacted with HSECs. The three investigated PAs, retrorsine, monocrotaline, and clivorine, induced concentration-dependent cytotoxicity in HSEC.

Therefore, we next employed chemical membrane transporter inhibitors, and considering the co-culture system context, it was reasonable to use inhibitors for efflux transporters to reduce the outward transport of potential PA metabolites from HepG2 cells. Inhibiting influx transporters in this co-culture system could impair PAs from entering HepG2 cells, making it challenging to distinguish from the inhibition of metabolite influx into HeLa H2B-GFP cells or inhibition of metabolic enzymes in HepG2 cells.

Both efflux membrane transporter inhibitors decreased micronucleus formation induced by lasiocarpine, riddelliine, and europine in HeLa H2B-GFP cells in the co-culture system. These findings in the co-culture system regarding efflux membrane transporters were consistent with our earlier results in HepG2 cells, where we tested only one PA, lasiocarpine. In the co-culture system, we tested three PAs of different ester types (lasiocarpine, riddelliine, and europine).

The findings were also in agreement with Hessel et al. (2014) **[365]**, who reported clear apical elimination of the PA echimidine mediated by the MDR1-efflux transporter in Madin-Darby Canine Kidney cells overexpressing human MDR1 (MDCK/hMDR1).

Based on our findings, we can deduce that PAs were primarily bioactivated by the CYP 450-3A4 isoenzyme in HepG2 hepatocytes. The reactive PA metabolites formed were then effluxed out of hepatocytes via MDR1 and MRP2 efflux transporters, causing genomic damage in the HeLa H2B-GFP cells of the co-culture system. Therefore, it is conceivable that PAs are first metabolically activated in hepatocytes and then move out to their primary target, HSECs. The latter have been reported to have a lower basal GSH level and are significantly more susceptible to reactive PA metabolites after severe GSH depletion, leading to pyrrole-protein adduct formation, causing HSOS and hepatotoxicity **[538]**.

Although we found the CYP 450-3A4 isoenzyme to play a key role in PA metabolism, it is important to acknowledge that other CYP 450 isoforms might also contribute to the overall metabolism of PAs. Additionally, while we investigated the MDR1 and MRP2 efflux transporters, it is crucial to remember that other efflux transporters or pumps, not examined in our study, might also contribute to PA-induced toxicity.

6.8 PAs-induced mitotic disturbance in HepG2 only cultured cells and in Co-Culture System

In the course of micronucleus evaluation, disturbances in mitotic figures were detected and subsequently investigated in separate experiments within the co-culture system, a culture of only HepG2 cells, and a culture of only HeLa H2B-GFP cells. All three pyrrolizidine alkaloids (PAs) of different ester types—the open diester PA lasiocarpine, the cyclic diester PA riddelliine, and the monoester PA europine—induced various mitotic disturbances. These included non-congression of chromosomes to the metaphase plate, missing metaphase alignment typical of disturbed spindle formation, lagging chromosomes left at the metaphase plate location after the separation of daughter chromosomes, and multipolar metaphases. A prominent mechanism for mitotic disturbance is the inhibition of spindle formation or disassembly of chromosomes. It

could be hypothesized that PAs react with the tubulin molecule, which possesses many accessible cysteine residues **[634, 635]**. However, substances disturbing the spindle usually lead to an arrest in the metaphase of mitosis, as indicated by an elevated mitotic index, as seen with the positive control and spindle formation inhibitor vincristine. This was observed only to a small extent for lasiocarpine but not for riddelliine or europine.

Consequently, alternative mechanisms for mitotic disturbance may have to be identified. For example, recently in a transcriptomics approach it was shown that five PAs (lasiocarpine, riddelliine, lycopsamine, echimidine, and monocrotaline) interfered with cell cycle regulation and DNA damage repair. Additionally, the authors using microscopic methods reported the mitotic disturbances in form of chromosome congression defects, which is in agreement with our findings in this study **[397]**. The only distinct difference between the three PAs used in our study was that the monoester europine induced less ana-/telophase bridge formation than the diesters' lasiocarpine and riddelliine at concentrations which caused a similar number of micronuclei. Several mechanisms for the formation of chromatin bridges have been suggested. One of them is that chromatin bridges between sister chromatids may reveal the presence of crosslinks in between the DNA strands. Therefore, due to the presence of a strong mechanical traction during anaphase, covalently bound chromatids can give rise to such anaphase chromatin bridges **[636, 637]**. Earlier in this dissertation, we found that diester PAs induced DNA crosslinks but the monoester europine did not **[193]**. Thus, this entails the mechanism of mitotic disturbance may be different for monoester and diester PAs.

Moreover, another study investigating the fate of anaphase bridges in cultured oral squamous cell carcinoma cells in real-time revealed that chromosomes in bridges most of the time resolve by breaking into multiple fragments and frequently, these fragments give rise to micronuclei (MN) at the end of mitosis **[638]**. However, since the induced micronucleus frequency was similar for the three PAs under the same applied conditions; bridge formation may only contribute a small number of micronuclei to the overall frequency. Further support for a difference in mode of action between monoester and open or cyclic diester PAs comes from a study in which effective metabolic degradation by human liver microsomes was observed for diesters, but not for monoesters **[639]** and a published report in which the cyclic diester

riddelliine was described as a more potent DNA-cross linker than heliosupine, which is an open diester **[255]**.

Therefore, with regard to the mode of action, in addition to the reactive intermediates forming DNA adducts, which then lead to mutations, we have described that mitotic disturbances are induced to a large extent. Thus, mitotic disturbances may lead to or contribute to the micronucleus formation caused by PAs.

6.9 In vitro genotoxic effects of combinations of PAs in HepG2 Cells and in the Co-Culture System

It is usually a combination or mixture of PAs that is found as contaminants in foods such as herbal teas and honey, food supplements, and herbal medicines. PA exposures in combinations or in mixtures are one of the additional aspects that need further consideration in the overall risk assessment process. For instance, in a recent study on two common sources of PA exposure, which are honey and tea, it was found that a total of 8-19 PAs (in honey) and 17-28 PAs (in tea) were identified, of which the identified PAs in these products require regulatory monitoring due to their known toxicity nature in humans **[7]**. The risk assessment of mixtures or combinations of phytotoxins is a complex challenge, and there are several suggestions, the most recent coming from the Organization for Economic Co-operation and Development (OECD) and European Food Safety Authority (EFSA) on the assessment of risk from combined exposures to multiple chemicals **[640, 641]**.

The general approach for combined exposure to multiple chemicals is based on either the whole-mixture approach or the component-based approach, depending on the knowledge of the combinations or mixtures. The whole-mixture approach considers the mixture as an individual existence, in contrast to the component-based approach, which considers the exposure and the effect data of the individual mixture components. Therefore, when the individual components of the combination or mixture share a similar mechanism of action, a default component-based approach of dose-addition is applied, where the individual components are assumed to act as if they were dilutions of one another **[642]**. However, much

of the work in this area was focused on the exposure to intentional combinations or mixtures, such as formulated products, or on unintentional exposures to environmental contaminants, such as pesticides and polychlorinated biphenyls, and is commonly conducted retrospectively **[643-645]**.

Thousands of PAs of different chemical features are known to be present in nature **[34]**, and therefore, depending on the plant species from which they are attained, there are many different combinations or mixtures of PAs that could potentially occur. Given the various chemical structure classes of PAs and the resulting difference in their potencies, the combined exposures would include PAs of varying potency. PAs share a common mechanism of action, that is, DNA reactivity of activated PA metabolites leading to DNA adducts. These adducts, if not repaired, can lead to gene mutation and clastogenicity.

Earlier in this present study, we demonstrated that the human hepatoma cell line HepG2 and the co-culture system of HepG2 and HeLa cells are well-suited for genotoxicity studies of PAs, including their mechanisms. Therefore, we used both models to explore whether PA combinations would also follow the general assumption of dose-effect additivity or whether synergistic effect or antagonistic effect should be anticipated in an assessment of their combined exposure. Of late such effects have been immensely examined in the field of toxicology **[646]**. The main concern is whether some chemicals or their active metabolites can enhance the effect of other metabolites, so that they jointly exert a larger effect than predicted. This phenomenon is commonly referred to as synergy **[647]**. Concentration or dose addition is another common reference model that assumes compounds or chemicals, when administered simultaneously, do not interfere with each other at the site of action **[648]**. The third phenomenon is an antagonistic effect, which refers to the biological response to exposure to multiple substances that is less than would be expected if the known effects of the individual substances were added together.

Therefore, combination of two or more PAs is an important question in determining additive or synergistic, or antagonistic effects. We examined the genotoxicity of PA combinations by measuring the formation of micronuclei, in HepG2 cells as well as in the co-culture system. We

designed the combination of PAs using an equipotent concentrations rather than equimolar concentrations approach, with low, medium and high concentrations of the PAs lasiocarpine and riddelliine. This concept of using equipotent concentrations will minimize the bias that highly potent PA component of the combination would introduce if equimolar amounts of PA were tested. Hence, we considered the use of equipotent approach a well-suited for the purpose of understanding dose addition, synergy or antagonistic effect in respect with our genotoxicity endpoint. Simply, this implies that exposure to PAs was equalized by potency so that a low concentration of the PA lasiocarpine would be expected to give a micronucleus response of similar magnitude and this was also done for a medium and high concentration of each PA.

There were no differences in micronucleus formation between the PA combinations compared to the individual PAs. However, cytotoxicity, indicated by the proliferation index (CBPI), was elevated in the PA combinations, significantly in the co-culture system and to a non-significant extent in HepG2. Compared to HepG2 cells, this could be due to a lower basal GSH level in HeLa H2B-GFP cells of the co-culture, which makes these cells more susceptible to the reactive PA metabolites.

Basically, the micronucleus data presented here indicate that the combination of PAs exhibits a dose-addition effect, where the total response can be calculated by adding up the potencies of individual PAs present in a combination. This aligns with the idea that individual PAs act via the same mode of action, probably involving identical DNA adduct formations. Additionally, our combination PA results are consistent with those of Allemang et al. (2022) **[649]**, who recently demonstrated a dose-addition-type genotoxic effect of PA combinations using micronucleus formation in HepaRG human liver cells. Recently, Louisse et al., 2022 **[650]**, using the γH2AX assay in HepaRG cells, evaluated a combination of three PAs with a similar equipotent approach. Like our combination outcomes, their results also showed that PA combinations comply with the principle of additive effects. In conclusion, in this present study using HepG2 cells and the co-culture system, we have shown through an in vitro genotoxicity testing approach that combinations of PAs showed an additive effect. Thus, this study therefore provides support that

the assumption of dose-addition can be applied in the characterization of the genotoxicity risk of PAs present in a mixture.

6.10 Metabolism-dependence of PA-induced genotoxicity

It is considered that the toxicity is not exerted by PA itself but rather by the reactive intermediates formed during hepatic metabolism. The hepatic metabolism of PA is initiated with an oxidation, which is a phase I metabolism catalyzed by cytochrome P450 enzymes. In our observation of reduced lasiocarpine-induced genotoxicity by ketoconazole, it clearly showed that CYP450-3A4 mediates the metabolism of lasiocarpine, forming the reactive intermediates and, hence, inducing genotoxicity. Therefore, the relevance of CYP450-3A4 was distinctly shown to play an important role in lasiocarpine-induced toxicity, as well as in other PAs tested in the co-culture system. This result is in line with previous studies that reported that CYP450-3A enzymes in rodents lead to the activation of PA, leading to the induction of toxicity **[230, 232, 651]**.

Earlier, a few other studies also showed the activation of other PAs by the human CYP450-3A4 isoenzyme. Miranda et al. (1991) **[235]** and Xia et al. (2003) **[652]** demonstrated the formation of electrophilic reactive pyrrolic intermediates of PAs after incubation with human liver microsomes, which were later inhibited in the presence of the CYP450-3A4 inhibitor triacetyloleandomycin. Ruan et al. (2014) **[36]** demonstrated CYP450-3A4–mediated pyrrole-glutathione adduct formation for lasiocarpine and other PAs in experiments with supersomes, while Dai et al. (2010) **[369]** presented similar findings for the PA monocrotaline and retrorsine.

Tu et al. (2014) [351] conducted a cytotoxicity assessment of the PA retrorsine in mock and human CYP450-3A4-expression clone of MDCK cells, indicating that cells without CYP450-3A4 expression were protected from severe toxicity. This indicates the prerequisite for the CYP450-3A4 isoenzyme in the bioactivation of PA retrorsine. However, in their study, the authors did not analyze the molecular mechanisms of toxicity. Thus, in our present study with human hepatoma HepG2 cells and the co-culture system, we substantiate the results of Tu et al. **[354]** for PAs and provide further insights into CYP450-3A4-dependent molecular mechanisms by showing

genotoxicity as a mechanism of CYP450-dependent toxicity. For example, in our experiments, we showed that lasiocarpine-induced genotoxicity was significantly reduced when CYP450-3A4 was inhibited by ketoconazole in human hepatoma HepG2 cells, as well as in other PAs tested in the co-culture system. We also demonstrated the mitotic disturbance induced by PAs in the co-culture system; a system consisting of metabolically active HepG2 cells and non-metabolically active human cervical HeLa H2B-GFP cells. In only HeLa-H2B GFP cell cultures, PAs did not induce mitotic disturbance, but in the HepG2 cells cultured alone and in co-culture, PAs significantly induced mitotic disturbances. This clearly indicated the relevance of CYP450 in the induction of PA-mediated genotoxicity.

These results are supported by Ebmeyer et al. 2019 **[254]** in vitro studies; however, in their experiments, the authors used a different endpoint to demonstrate DNA double-strand breaks induced by lasiocarpine through the detection of phosphorylation of histone H2AX. Allemang et al. (2018) **[29]** demonstrated the genotoxic potential of different PAs using micronucleus induction in an in vitro metabolically competent cell line, HepaRG. The authors observed significant induction of micronuclei by lasiocarpine, echimidine, riddelliine, retrorsine, seneciphylline, europine, and lycopsamine (along with some more tested PAs) at different concentrations, which were in the same order of magnitude as the PA concentrations that induced micronuclei in our experiments using HepG2 cells. However, due to the use of HepaRG cells, which are well-known for their metabolic competency, the authors could not distinguish between metabolism-dependent and metabolism-independent effects. For example, Müller et al. (1992) **[653]** showed metabolism dependence of the clastogenic potential through the analysis of chromosomal aberrations in the Chinese hamster cell line V79 cells after treatment with the PA retrorsine, monocrotaline, and isatidine without and with Aroclor-induced rat S9 mix or primary rat hepatocytes. Our results link the metabolism-dependent genotoxicity of the selected PAs to a specific human enzyme. Remarkably, using lasiocarpine as a model PA, we demonstrated human CYP 450-3A4-, CYP 450-1A2-, and detoxifying enzyme CES2-dependent micronucleus induction. Additionally, we showed CYP 450-3A4 dependent micronucleus induction, also in rifampicin pre-treated HepG2 cells. Another piece of evidence supporting the metabolism dependence of PA in our study was the use of a co-culture system. PAs induced

micronucleus formation in HeLa H2B-GFP cells when co-cultured with HepG2 cells but not in HeLa H2B-GFP cells cultured alone.

Another notable observation in our study was the decrease in the CBPI value, particularly at the highest concentration of each selected PA with different ester types in rifampicin-pretreated HepG2 cells. This observation indicates a CYP-450-3A4-dependent impairment of proliferation, where a decrease in the CBPI signifies an increased proportion of mononuclear cells and, consequently, fewer cells undergoing mitosis. This discovery aligns with the anti-mitotic potential described for lasiocarpine, heliotrine, and monocrotaline in rat liver **[654, 655]**. These findings were further substantiated using the PA metabolite dehydroretronecine in cultured hepatocytes **[656]**.

PAs treatment in vivo has also been shown to induce micronucleus formation **[657, 658]**. Some of these PAs, such as lasiocarpine, have been demonstrated to exhibit the formation of DNA adducts after activation by rat liver microsomes **[396]**. However, Fowler et al. (2012) **[659]** reported that p53-deficient rodent cell lines, such as the Chinese hamster cell line V79, are prone to giving misleading positive results in the micronucleus assay. This means that even for substances that do not exhibit DNA reactivity or genotoxicity in vivo, they can manifest with positive results.

Subsequently, there is strong substantiation that the positive response in our experiments is not due to residual (misleading positive) effects. However, it has to be pointed out that our in vitro model is an artificial system designed to assess the CYP 450- and CES-dependent toxicity of PA lasiocarpine. Therefore, some of the other detoxifying enzymes, such as glutathione S-transferase or GSH, may be suppressed or not functional in the system. The metabolism of PAs is known to consist of activating as well as detoxifying reactions, and the vulnerability towards PA-induced toxicity is assumed to be based on the relative activity of these two reaction types **[660]**. Hence, this balance may differ in the liver of one individual to another as well as compared to the used experimental model **[254]**.

In summary, our results demonstrated that the CYP 450-3A4 isoenzyme is a crucial enzyme for PA metabolism. Human CYP 450-3A4 is capable of toxifying PAs of different ester types, such as

lasiocarpine, riddelliine, and europine, confirming the results from the literature. We also demonstrated the relevance of carboxylesterase (CES) enzyme as a key player in the detoxification of PA lasiocarpine. Hence, we concluded that it is important for human risk assessment to consider PA metabolism as one of the main mechanisms inducing toxicity.

6.11 Structure-dependent Relationship of Selected PAs

Many different PAs are produced by thousands of plant species **[16]**. Some of these PAs are genotoxic and may pose a cancer risk in humans **[15, 16, 223, 661]**. For a long time, there have been attempts to predict the potential toxicity of xenobiotics and their metabolites based on their chemical structural characteristics **[662-664]**. The general structures of PAs include necine base and necine acids. So far, the necine base has been mostly discussed, where the double bond between the C1 and C2 positions in the unsaturated necine base is known to undergo metabolic activation, hence exerting their toxicity. Due to this, the platynecine PA-type containing a saturated necine base has been considered irrelevant to safety assessment.

However, based on the ester-type in the PA-necic acid moiety, Culvenor et al. (1976) **[301]** conducted an in vivo study and reported that the di-ester PAs of heliotridine- and retronecine-types were more toxic than the respective monoester PAs. For example, heliotridine necine-based PA variants were about 2- to 4-fold more toxic than retronecine-based variants **[301]**. Field et al. (2015) **[665]** have demonstrated an in-vitro study suggesting that the necine base, ester type configuration, and saturation contributed to cytotoxicity, with the heliotridine-PA type being associated with higher cytotoxicity.

Consequently, in our present study, the diesters were generally more potent in inducing genomic damage than the monoesters. Lasiocarpine, an open-diester heliotridine-type, exhibited distinctly higher potency than the cyclic-diester retronecine-type and the open-diester retronecine-type (echimidine) in rifampicin-pretreated HepG2 cells. Thus, both open- and cyclic-diester PAs in our studies showed higher potency than monoester PAs of heliotridine or retronecine-type. This difference was clearly depicted at equimolar concentrations, where the

monoester PAs induced oxidative stress, DNA cross-linking effects, and micronucleus formation to a lower extent than the diester PAs.

Our potency order differences were also parallel to previous reports by Wang et al. (2021) **[666]**, who used a cell proliferation assay in human hepatocytes (HepD). They reported that the toxicity of the monoester intermedine was much lower than that of the diester PAs. Similarly, Gao et al. (2020) **[667]** reported much lower cytotoxicity-related EC_{50} values in primary rat hepatocytes for the diester PAs, such as lasiocarpine, echimidine, senecionine, and retrorsine, compared to the monoester PAs europine and lycopsamine. Therefore, the chemical structure characteristics, both the ester-type at the necic acid moiety and structural features in the necine base moiety, seemed to play a vital role in the toxicity associated with the PAs.

It is known that esters are important functional groups in drug delivery systems as they function as prodrugs and decrease the polarity in a compound, thereby increasing lipophilicity. This increase in lipophilicity enhances absorption in tissues, and the release of the compound depends on the hydrolysis rate of the ester group **[668-670]**. Basically, the ester functional group enhances the bioavailability of xenobiotics because it can easily form hydrogen bonds through its oxygen atoms to the hydrogen atoms of water molecules, making a compound hydrophilic. Therefore, di-ester PAs seem to be more absorbed than monoesters, enabling diester PAs to reach the liver faster for bioactivation, leading to genotoxicity. Meanwhile, cyclic-di esters might be more unstable than open-side chain diesters due to the enhanced ring strain facilitating hydrolysis, making the open-chain di-ester (lasiocarpine) higher in potency than the cyclic-di esters (riddelliine, retrorsine, seneciphylline).

Geburek et al. (2020) **[553]** demonstrated indirect evidence for the formation of reactive PA metabolites, mainly by the diester PAs, including lasiocarpine, echimidine, and retrorsine, followed by the monoester PAs, including europine and lycopsamine. For example, the open-chained and cyclic diester PAs formed more GSH conjugates, while the monoester PAs only formed a limited number of GSH metabolites, such as mono-DHP-GSH. Additionally, the authors reported another major difference between the monoester and diester PAs in terms of the proportion of the unknown fraction of metabolites formed; diesters accounted for up to 70%,

while monoester PAs accounted for only 17%. This could suggest that monoesters, in contrast to diesters, form fewer reactive metabolites that bind to tissue constituents to a lesser extent.

Therefore, the good correlation of the amount of the highest number of lasiocarpine metabolites observed by Geburek et al. (2020) **[553]** to its toxicity description may also indicate the potency of open-diester PA lasiocarpine. Henceforth, we can also postulate that the lower extent of binding between monoester PAs and biomolecules, as well as their lower lipophilicity due to their lower polarity in their chemical structure, could account for their lower genotoxicity, as observed in our results.

7 CONCLUSION

In this dissertation, we have demonstrated the suitability of the widely available human hepatoma cell line HepG2 for assessing PAs-induced genotoxicity. The selected PAs studied here induced micronuclei in a dose-dependent manner at micromolar dose ranges, supporting previous published data obtained with other cell lines. Additionally, the shape of the dose-response curve was in agreement with the idea of the existence of a threshold. Existing published potency rankings for these selected PAs could be largely or completely confirmed.

The role of metabolic enzymes in the metabolic activation of PAs is critical for their mechanisms of inducing genotoxicity, and transmembrane transporters contribute to their genotoxic effects, in addition to the passive diffusion of PA transmembrane transport mechanisms. Moreover, the use of a co-culture of metabolically active human hepatoma HepG2 cells with non-metabolically active human cervical epithelial HeLa H2B-GFP cells helped to further support the role of metabolic activation of PAs. This shows that metabolites can reach another, metabolically inactive cell type in the vicinity of the metabolically active cells, and that efflux transporters enable or support the movement of metabolites.

Regarding the mode of action, in addition to the reactive intermediates forming DNA adducts, which then lead to mutations, we describe that mitotic disturbances are induced to a large extent. Mitotic disturbances may lead to or contribute to the micronucleus formation caused by PAs. We also demonstrated that reactive oxygen species (ROS) and DNA cross-links may contribute to the genomic damage induced by PAs, especially for the diester PAs.

Furthermore, the co-culture system, used for the first time in our laboratory, can be suggested as a screening platform for assessing other newly identified PAs or phytotoxins that require metabolically activating enzymes. It can mimic the hepatic environment to some extent, signifying the requirement of metabolic activation in the hepatocytes and the induction of damage to other cells or even organs in the human body. This is particularly relevant in the case of PAs, which induce hepatic sinusoidal endothelial damage.

Additionally, this present study has shown that a combination of PAs resulted in an additive effect. Thus, this provides support for considering the assumption of dose addition in the characterization of the genotoxicity risk of PAs present in natural mixtures.

8 SUMMARY

Cancer is one of the leading causes of death worldwide. Toxic contaminants in human food or medicinal products, such as substances like pyrrolizidine alkaloids (PAs), have been thought to contribute to cancer incidence. PAs are found in many plant species as secondary metabolites, and they may affect humans through contaminated food sources, herbal medicines, and dietary supplements. Hundreds of compounds belonging to PAs have been identified, differing in their chemical structures, either in their necine base moiety or esterification at their necic acid moiety. PAs undergo hepatic metabolism, and after this process, they can induce hepatotoxicity, genotoxicity, and carcinogenicity. However, the mechanism of inducing genotoxicity and carcinogenicity is still unclear and warrants further investigation.

Therefore, the present study aims to investigate the mechanism of genotoxicity induced by selected PAs with different chemical structures in in vitro systems. Primarily, human hepatoma HepG2 cells were utilized, and in co-culture, metabolically active HepG2 cells were combined with non-metabolically active human cervical HeLa H2B-GFP cells.

First, the genotoxicity of the PAs europine, lycopsamine, retrorsine, riddelliine, seneciphylline, echimidine, and lasiocarpine was investigated in the cytokinesis-block micronucleus (CBMN) assay. All seven selected PAs caused the formation of micronuclei in a dose-dependent manner, with the maximal increase of micronucleus formation ranging from 1.64 to 2.0 fold. The lowest concentrations at which significant induction of micronuclei was found were 3.2 µM for lasiocarpine and riddelliine, 32 µM for retrorsine and echimidine, and 100 µM for seneciphylline, europine, and lycopsamine. These results confirmed previously published potency rankings in the micronucleus assay.

The same PAs, with the exception of seneciphylline, were also investigated in a crosslink-modified comet assay, and reduced tail formation after hydrogen peroxide treatment was found in all diester-type PAs. Meanwhile, an equimolar concentration of the monoesters europine and lycopsamine did not significantly reduce DNA migration. Thus, the crosslinking activity was related to the ester type.

Next, the role of metabolic enzymes and membrane transporters in PA-induced genotoxicity was assessed. Ketoconazole (CYP 450-3A4 inhibitor) prevented lasiocarpine-induced micronucleus formation completely, while furafylline (CYP 450-1A2 inhibitor) reduced lasiocarpine-induced micronucleus formation, but did not abolish it completely. This implies that the CYP 450 enzymes play an important role in PA-induced genotoxicity.

Carboxylesterase 2 enzyme (CES 2) is commonly known to be involved in the detoxification of xenobiotics. Loperamide (CES 2 inhibitor) yielded an increased formation of lasiocarpine-induced micronuclei, revealing a possible role of CES-mediated detoxification in the genotoxicity of lasiocarpine. Also, intracellular glutathione (GSH) plays an important role in the detoxification of xenobiotics or toxins in the cells. Cells which had been pretreated with L-buthionine sulfoximine (BSO) to reduce GSH content were significantly more sensitive for the induction of micronucleus formation by lasiocarpine revealing the importance of GSH in PA-induced genotoxicity.

Quinidine (Q) and nelfinavir (NFR) are OCT1 and OATP1B1 influx transporter inhibitors, respectively, which reduced micronucleus induction by lasiocarpine (only quinidine significantly), but not completely, pointing to a relevance of OCT1 for PA uptake in HepG2 cells. Verapamil (V) and benzbromarone (Bz) are MDR1 and MRP2 efflux transporter inhibitors, respectively, and they caused a slightly increased micronucleus induction by lasiocarpine (significant only for benzbromarone) thus, revealing the role of efflux transporters in PA-induced genotoxicity.

The mechanistic approach to PA-induced genotoxicity was further studied based on oxidative stress via the formation of reactive oxygen species (ROS) in HepG2 cells. Overproduction of ROS can cross-link cellular macromolecules such as DNA, leading to genomic damage. An equimolar concentration of 10 µM of lasiocarpine (open-diester PA), riddelliine (cyclic-diester PA), and europine (monoester) significantly induced ROS production, with the highest ROS generation observed after lasiocarpine treatment, followed by riddelliine and then europine. No significant increase in ROS production was found with lycopsamine (10 µM; monoester PA), even at a higher concentration (320 µM). The generation of ROS by these PAs was further analyzed for

confirmation by using 5 mM of the thiol radical scavenger antioxidant N-acetyl cysteine (NAC) combined with lasiocarpine, riddelliine, or europine. This analysis yielded a significant decrease in ROS after combining NAC with lasiocarpine, riddelliine, and europine. In addition, lasiocarpine, riddelliine, and europine induced a loss of mitochondrial membrane potential, pointing to mitochondria as the source of ROS generation.

In vivo, hepatic sinusoidal epithelial cells (HSECs) are known to be damaged first by PAs after hepatic metabolisation, but HSECs themselves do not express the required metabolic enzymes for activation of PAs. To mimic this situation, HepG2 cells were used to metabolically activate PA in a co-culture with HeLa H2B-GFP cells as non-metabolically active neighbours. Due to the green fluorescent GFP label the HeLa cells could be identified easily based in the co-culture. The PAs europine, riddelliine and lasiocarpine induced micronucleus formation in HepG2 cells, and in HeLa H2B-GFP cells co-cultured with HepG2 cells, but not in HeLa H2B-GFP cells cultured alone. Metabolic inhibition of CYP 450 enzymes with ketoconazole abrogated micronucleus formation induced by the same PAs tested in the co-culture. The efflux transporter inhibitors verapamil and benzbromarone reduced the micronucleus formation in the co-culture. Furthermore, mitotic disturbances as an additional genotoxic mechanism of action were observed in HepG2 cells and in HeLa H2B-GFP cells co-cultured with HepG2 cells, but not in HeLa H2B-GFP cells cultured alone. Overall, we were able to show that PAs were activated by HepG2 cells and the metabolites induced genomic damage in co-cultured non-metabolically active green HeLa cells.

Finally, in HepG2 cells as well as the co-culture, combinations of PAs lasiocarpine and riddelliine favoured an additive effect rather than synergism. Thus, this study therefore provides support that the assumption of dose-addition can be applied in the characterization of the genotoxicity risk of PAs present in a mixture.

9 ZUSAMMENFASSUNG

Krebs ist eine der häufigsten Todesursachen weltweit. Toxische Verunreinigungen in Lebensmitteln oder pflanzlichen Arzneimitteln, wie Pyrrolizidinalkaloide (PAs), können zur Krebsinzidenz beitragen. PAs kommen in vielen Pflanzenarten als Sekundärmetabolite vor. Menschen können diese über kontaminierte Nahrungsquellen, pflanzliche Arzneimittel und Nahrungsergänzungsmittel aufnehmen. Eine Vielzahl von Verbindungen, die zu pyrrolizidinalkaloidhaltigen Substanzen (PAs) gehören, wurden identifiziert. Diese unterscheiden sich in ihrer chemischen Struktur entweder durch ihre Necinbaseneinheit oder ihre Veresterung an der Necicsäureeinheit. Nach metabolischer Aktivierung in der Leber können PAs Hepatotoxizität, Genotoxizität und Karzinogenität induzieren. Jedoch ist der Genotoxizitätsmechanismus nicht vollständig aufgeklärt und erfordert weitere Untersuchungen.

Das Ziel dieser Studie liegt in der Untersuchung des Mechanismus der Genotoxizität, die in vitro durch bestimmte PAs mit unterschiedlicher chemischer Struktur induziert wird. Hierbei wurden primär humane Hepatom-HepG2-Zellen verwendet sowie in Co-Kultur metabolisch aktive HepG2-Zellen und nicht-metabolisch aktive humane zervikale HeLa H2B-GFP-Zellen.

Zunächst wurde die Genotoxizität der PAs Europin, Lycopsamin, Retrorsin, Riddelliin, Seneciphyllin, Echimidin und Lasiocarpin im Zytokinese-Block-Mikronukleus-Assay (CBMN) untersucht. Die sieben (7) ausgewählten PAs führten dosisabhängig zur Bildung von Mikrokernen. Der maximale Anstieg der Mikronukleusbildung lag für alle PAs im Bereich des 1,64- bis 2,0-fachen des Ausgangswertes. Die niedrigsten Konzentrationen, bei denen eine signifikante Induktion von Mikrokernen gefunden wurde, waren 3,2 µM für Lasiocarpin und Riddelliin, 32 µM für Retrorsin und Echimidin sowie 100 µM für Seneciphyllin, Europin und Lycopsamin. Diese Ergebnisse bestätigen zuvor veröffentlichte Potenz-Rankings im Mikronukleus-Assay.

Die Genotoxizität der gleichen PAs, mit Ausnahme von Seneciphyllin, wurde zusätzlich mittels eines Crosslink-modifizierten Comet-Assay untersucht. Es wurde eine reduzierte Schweifbildung nach der Behandlung mit Wasserstoffperoxid in allen PAs des Diestertyps gefunden, während eine äquimolare Konzentration der Monoester Europin und Lycopsamin die DNA-Migration

nicht signifikant reduzierte. Dies deutet darauf hin, dass die Vernetzungsaktivität von PAs auf der Ester-Einheit beruht.

Als nächstes wurde die Rolle von Stoffwechselenzymen und Membrantransportern in der PA-induzierten Genotoxizität untersucht. Ketoconazol (CYP 450-3A4-Inhibitor) verhinderte die Lasiocarpin-induzierte Mikronukleusbildung vollständig, während Furafyllin (CYP 450-1A2-Inhibitor) die Lasiocarpin-induzierte Mikronukleusbildung reduzierte, aber nicht vollständig beseitigte. Dies deutet darauf hin, dass CYP 450-Enzyme eine wichtige Rolle bei der PA-induzierten Genotoxizität spielen.

Es ist allgemein bekannt, dass das Enzym Carboxylesterase 2 (CES-2) an der Entgiftung von Xenobiotika beteiligt ist. Loperamid (CES-2-Inhibitor) führte zu einer erhöhten Bildung von Lasiocarpin-induzierten Mikrokernen, was auf eine mögliche Rolle der CES-vermittelten Entgiftung bei der Genotoxizität von Lasiocarpin hindeutet. Auch intrazelluläres Glutathion (GSH) spielt eine wichtige Rolle bei der Entgiftung von Xenobiotika oder Toxinen. Zellen, die mit L-Buthioninsulfoximin (BSO) vorbehandelt worden waren, um den GSH-Gehalt zu reduzieren, waren signifikant empfindlicher für die Induktion der Mikronukleusbildung durch Lasiocarpin, was die Bedeutung von GSH für die PA-induzierte Genotoxizität zeigt.

Chinidin (Q) und Nelfinavir (NFR) sind OCT1- bzw. OATP1B1-Influx-Transporter-Inhibitoren, die die Mikronukleus-Induktion durch Lasiocarpin reduzierten (nur Chinidin signifikant), aber nicht vollständig, was auf eine Relevanz von OCT1 für die PA-Aufnahme in HepG2-Zellen hindeutet.Verapamil (V) und Benzbromaron (Bz) sind MDR1- bzw. MRP2-Efflux-Transporter-Inhibitoren und verursachten eine leicht erhöhte Mikronukleus-Induktion durch Lasiocarpin (signifikant nur für Benzbromaron), was die Rolle von Efflux-Transportern bei der PA-induzierten Genotoxizität aufzeigt.

Der Mechanismus der PA-induzierten Genotoxizität wurde auf der Grundlage von oxidativem Stress durch die Bildung von reaktiven Sauerstoffspezies (ROS) in HepG2-Zellen weiter untersucht. Eine Überproduktion von ROS kann zelluläre Makromoleküle wie DNA vernetzen, was zu genomischen Schäden führt. Eine äquimolare Konzentration von 10 µM von Lasiocarpin (Open-Diester PA), Riddelliin (Cyclic-Diester PA) und Europin (Monoester) induzierte signifikant

die ROS-Produktion, wobei die höchste ROS-Erzeugung nach Lasiocarpin-Behandlung beobachtet wurde, gefolgt von Riddelliin und Europin. Mit Lycopsamin (10 µM; Monoester PA) wurde auch bei höherer Konzentration (320 µM) keine signifikante Steigerung der ROS-Produktion gefunden.

Um die Beteiligung von ROS am Mechanismus der Genotoxizität einzelner PAs genauer zu betrachten und die bisherigen Ergebnisse zu bestätigen, wurden weitere Untersuchungen in Anwesenheit des Sauerstoffradikalfängers N-Acetylcysteine (NAC) in Kombination mit Lasiocarpin, Riddelliin oder Europin durchgeführt. Diese Analyse ergab eine signifikante Abnahme der ROS-Produktion nach der Kombination von NAC mit Lasiocarpin, Riddelliin und Europin. Darüber hinaus induzierten Lasiocarpin, Riddelliin und Europin Veränderungen im mitochondrialen Membranpotenzial. Dies deutet darauf hin, dass ROS vermehrt in den Mitochondrien der Zellen gebildet werden.

Aus in vivo Daten ist bekannt, dass hepatische sinusoidale Epithelzellen (HSECs) die Zelltypen innerhalb der Leber sind, die nach der metabolischen Aktivierung von PAs zuerst geschädigt werden. Jedoch exprimieren HSECs nicht die erforderlichen Stoffwechselenzyme für die Aktivierung von PAs. Um diese Situation nachzuahmen, wurden HepG2-Zellen verwendet, um PAs in einer Kokultur mit HeLa H2B-GFP-Zellen als nicht-metabolisch aktive Nachbarn metabolisch zu aktivieren. Durch die grün fluoreszierende GFP-Markierung konnten die HeLa-Zellen in der Co-Kultur leicht identifiziert werden. Die PAs Europine, Riddelliin und Lasiocarpin induzierten die Bildung von Mikrokernen in HepG2-Zellen und in HeLa H2B-GFP-Zellen, die mit HepG2-Zellen kokultiviert wurden, jedoch nicht in HeLa H2B-GFP-Zellen, die allein kultiviert wurden. Die metabolische Hemmung von CYP 450-Enzymen mit Ketoconazol hob die Mikronukleusbildung, welche durch die zuvor getesteten PAs induziert wurde, auf. Die Efflux-Transporter-Inhibitoren Verapamil und Benzbromaron reduzierten die Mikronukleusbildung in der Kokultur. Darüber hinaus wurden mitotische Störungen als zusätzlicher genotoxischer Wirkmechanismus in der Co-Kultur aus HepG2-Zellen und in HeLa H2B-GFP-Zellen beobachtet, jedoch nicht in HeLa H2B-GFP-Zellen, die allein kultiviert wurden. Zusammengefasst deuten diese Ergebnisse darauf hin, dass PAs durch HepG2-Zellen bioaktiviert werden können und aus

PAs gebildete Metabolite genomische Schäden in kokultivierten, nicht-metabolisch aktiven HeLa-Zellen induzierten.

Abschließend zeigen Kombinationen der PAs Lasiocarpin und Riddelliin sowohl in HepG2-Zellen als auch in der Co-Kultur eher einen additiven Effekt als einen Synergismus. Diese Studie liefert daher Unterstützung für die Annahme, dass die Dosisaddition zur Charakterisierung des genotoxischen Risikos von in einem Gemisch vorhandenen PAs angewendet werden kann.

10 REFERENCES

1. Edgar, J.A., R.J. Molyneux, and S.M. Colegate, Pyrrolizidine alkaloids: potential role in the etiology of cancers, pulmonary hypertension, congenital anomalies, and liver disease. Chemical research in toxicology, 2015. 28(1): p. 4-20.

2. Li, Y.H., et al., Assessment of pyrrolizidine alkaloid-induced toxicity in an in vitro screening model. Journal of Ethnopharmacology, 2013. 150(2): p. 560-567.

3. Almazroo, O.A., M.K. Miah, and R. Venkataramanan, Drug Metabolism in the Liver. Clin Liver Dis, 2017. 21: p. 1-20.

4. Rocha, T., J.S. Amaral, and M.B.P. Oliveira, Adulteration of dietary supplements by the illegal addition of synthetic drugs: a review. Comprehensive reviews in food science and food safety, 2016. 15(1): p. 43-62.

5. Humans, I.W.G.o.t.E.o.C.R.t., I.A.f.R.o. Cancer, and W.H. Organization, Some traditional herbal medicines, some mycotoxins, naphthalene and styrene. Vol. 82. 2002: World Health Organization.

6. Agency, E.M., Public Statement on the Use of Herbal Medicinal Products Containing Toxic, Unsaturated Pyrrolizidine Alkaloids (PAs). 2014.

7. Authority, E.F.S., Dietary exposure assessment to pyrrolizidine alkaloids in the European population. EFSA Journal, 2016. 14(8): p. e04572.

8. Organization, W.H., Safety evaluation of certain food additives and contaminants: supplement 2: pyrrolizidine alkaloids, prepared by the eightieth meeting of the Joint FAO/WHO Expert Committee on Food Additives (JECFA). 2020.

9. Chain, E.P.o.C.i.t.F., Scientific opinion on pyrrolizidine alkaloids in food and feed. EFSA Journal, 2011. 9(11): p. 2406.

10. Risk-Assessment, F.I.f., Pyrrolizidine alkaloids in herbal teas and teas. BfR Berlin (Germany), 2013. 018: p. 1-29.

11. Stegelmeier, B., et al., Pyrrolizidine alkaloid plants, metabolism and toxicity. Journal of natural toxins, 1999. 8(1): p. 95-116.

12. Roeder, E., Medicinal plants in China containing pyrrolizidine alkaloids. Die Pharmazie, 2000. 55: p. 711-726.

13. Roeder, E., Medicinal Plans in Europe Containing Pyrrolizidine Alkaloids. Die Pharmazie, 1995. 50: p. 83-98.

14. Lin, G., Y.-Y. Cui, and E.M. Hawes, Characterization of rat liver microsomal metabolites of clivorine, an hepatotoxic otonecine-type pyrrolizidine alkaloid. Drug metabolism and disposition, 2000. 28(12): p. 1475-1483.

15. Fu, P.P., et al., Pyrrolizidine alkaloids--genotoxicity, metabolism enzymes, metabolic activation, and mechanisms. Drug Metab Rev, 2004. 36(1): p. 1-55.

16. Li, N., et al., Hepatotoxicity and tumorigenicity induced by metabolic activation of pyrrolizidine alkaloids in herbs. Curr Drug Metab, 2011. 12(9): p. 823-34.

17. Ruan, J., et al., Lack of metabolic activation and predominant formation of an excreted metabolite of nontoxic platynecine-type pyrrolizidine alkaloids. Chem Res Toxicol, 2014. 27(1): p. 7-16.

18. Ruan, J., et al., Metabolic activation of pyrrolizidine alkaloids: insights into the structural and enzymatic basis. Chem Res Toxicol, 2014. 27(6): p. 1030-9.

19. Edgar, J.A., R.J. Molyneux, and S.M. Colegate, Pyrrolizidine Alkaloids: Potential Role in the Etiology of Cancers, Pulmonary Hypertension, Congenital Anomalies, and Liver Disease. Chem Res Toxicol, 2015. 28(1): p. 4-20.

20. Mattocks, A., Chemistry and toxicology of pyrrolizidine alkaloids. 1986: Academic Press.

21. Fu, P.P., et al., Genotoxic Pyrrolizidine Alkaloids — Mechanisms Leading to DNA Adduct Formation and Tumorigenicity. International Journal of Molecular Sciences, 2002. 3(9): p. 948-964.

22. Ma, J., et al., Pyrrole–hemoglobin adducts, a more feasible potential biomarker of pyrrolizidine alkaloid exposure. Chemical Research in Toxicology, 2019. 32(6): p. 1027-1039.

23. He, Y., et al., Metabolism-mediated cytotoxicity and genotoxicity of pyrrolizidine alkaloids. Archives of Toxicology, 2021. 95(6): p. 1917-1942.

24. Ma, J., et al., Clinical application of pyrrole–hemoglobin adducts as a biomarker of pyrrolizidine alkaloid exposure in humans. Archives of Toxicology, 2021. 95(2): p. 759-765.

25. Xia, Q., et al., Pyrrolizidine alkaloid-derived DNA adducts as a common biological biomarker of pyrrolizidine alkaloid-induced tumorigenicity. Chemical research in toxicology, 2013. 26(9): p. 1384-1396.

26. Zhu, L., et al., The long persistence of pyrrolizidine alkaloid-derived DNA adducts in vivo: kinetic study following single and multiple exposures in male ICR mice. Archives of toxicology, 2017. 91(2): p. 949-965.

27. He, Y., et al., Mutational signature analysis reveals widespread contribution of pyrrolizidine alkaloid exposure to human liver cancer. Hepatology, 2021. 74(1): p. 264-280.

28. Lin, G., Y.-Y. Cui, and E.M. Hawes, Microsomal formation of a pyrrolic alcohol glutathione conjugate of clivorine: firm evidence for the formation of a pyrrolic metabolite of an otonecine-type pyrrolizidine alkaloid. Drug Metabolism and Disposition, 1998. 26(2): p. 181-184.

29. Allemang, A., et al., Relative potency of fifteen pyrrolizidine alkaloids to induce DNA damage as measured by micronucleus induction in HepaRG human liver cells. Food and Chemical Toxicology, 2018. 121: p. 72-81.

30. Louisse, J., et al., Determination of genotoxic potencies of pyrrolizidine alkaloids in HepaRG cells using the γH2AX assay. Food and chemical toxicology, 2019. 131: p. 110532.

31. World Health, O., S. International Programme on Chemical, and W.H.O.T.G.o.P. Alkaloids, Pyrrolizidine alkaloids / published under the joint sponsorship of the United Nations Environment Programme, the International Labour Organisation, and the World Health Organization. 1988, World Health Organization: Geneva.

32. Organization, W.H., Pyrrolizidine alkaloids: health and safety guide. 1989: World Health Organization.

33. toxicity, C.o., Statement on Pyrrolizidine Alkaloids in Food. Committee on toxicity of chemicals in food, consumer products and the environment. 2008, Committee on Toxicity: Committee on Toxicity.

34. Beuerle, T., et al., Scientific opinion on pyrrolizidine alkaloids in food and feed. EFSA Journal, 2011. 9(11): p. 1-134.

35. Organization, W.H., Safety evaluation of certain food additives and contaminants: supplement 2: pyrrolizidine alkaloids, prepared by the eightieth meeting of the Joint FAO/WHO Expert Committee on Food Additives (JECFA). WHO Food Additive Series, 2020.

36. Ruan, J., et al., Metabolic Activation of Pyrrolizidine Alkaloids: Insights into the Structural and Enzymatic Basis. Chemical Research in Toxicology, 2014. 27(6): p. 1030-1039.

37. Srinivas, U.S., et al., ROS and the DNA damage response in cancer. Redox biology, 2019. 25: p. 101084.

38. Cannan, W.J. and D.S. Pederson, Mechanisms and consequences of double-strand DNA break formation in chromatin. Journal of cellular physiology, 2016. 231(1): p. 3-14.

39. Terradas, M., et al., Genetic activities in micronuclei: is the DNA entrapped in micronuclei lost for the cell? Mutation Research/Reviews in Mutation Research, 2010. 705(1): p. 60-67.

40. Arjunan, K.P., V.K. Sharma, and S. Ptasinska, Effects of atmospheric pressure plasmas on isolated and cellular DNA—a review. International journal of molecular sciences, 2015. 16(2): p. 2971-3016.

41. Luzhna, L., P. Kathiria, and O. Kovalchuk, Micronuclei in genotoxicity assessment: from genetics to epigenetics and beyond. Frontiers in genetics, 2013. 4: p. 131.

42. Baudoin, N.C. and D. Cimini, A guide to classifying mitotic stages and mitotic defects in fixed cells. Chromosoma, 2018. 127(2): p. 215-227.

43. HALLIWELL, B., Oxidative stress and cancer: have we moved forward? Biochem. J, 2007. 401: p. 1-11.

44. Curtin, J.F., M. Donovan, and T.G. Cotter, Regulation and measurement of oxidative stress in apoptosis. Journal of immunological methods, 2002. 265(1-2): p. 49-72.

45. Azad, M.B., Y. Chen, and S.B. Gibson, Regulation of autophagy by reactive oxygen species (ROS): implications for cancer progression and treatment. Antioxidants & redox signaling, 2009. 11(4): p. 777-790.

46. Trachootham, D., J. Alexandre, and P. Huang, Targeting cancer cells by ROS-mediated mechanisms: a radical therapeutic approach? Nature reviews Drug discovery, 2009. 8(7): p. 579-591.

47. Bratic, I. and A. Trifunovic, Mitochondrial energy metabolism and ageing. Biochimica et Biophysica Acta (BBA)-Bioenergetics, 2010. 1797(6-7): p. 961-967.

48. Halasi, M., et al., ROS inhibitor N-acetyl-L-cysteine antagonizes the activity of proteasome inhibitors. Biochemical Journal, 2013. 454(2): p. 201-208.

49. Ozcan, A. and M. Ogun, Biochemistry of reactive oxygen and nitrogen species. Basic principles and clinical significance of oxidative stress, 2015. 3: p. 37-58.

50. Kara, A., et al., Oxidative stress and autophagy. Free Radicals and Diseases, 2016: p. 69-86.

51. Kehrer, J.P., Free radicals as mediators of tissue injury and disease. Critical reviews in toxicology, 1993. 23(1): p. 21-48.

52. Stohs, S.J., The role of free radicals in toxicity and disease. Journal of basic and clinical physiology and pharmacology, 1995. 6(3-4): p. 205-228.

53. Radak, Z., Free radicals in exercise and aging. 2000: Human kinetics.

54. Rice-Evans, C.A., N.J. Miller, and G. Paganga, Structure-antioxidant activity relationships of flavonoids and phenolic acids. Free radical biology and medicine, 1996. 20(7): p. 933-956.

55. Young, I. and J. Woodside, Antioxidants in health and disease. Journal of clinical pathology, 2001. 54(3): p. 176-186.

56. Kükürt, A., et al., Thiols: Role in oxidative stress-related disorders. Accenting Lipid Peroxidation, 2021: p. 27.

57. Finkel, T. and N.J. Holbrook, Oxidants, oxidative stress and the biology of ageing. nature, 2000. 408(6809): p. 239-247.

58. Rossi, R., et al., Cysteinylation and homocysteinylation of plasma protein thiols during ageing of healthy human beings. Journal of cellular and molecular medicine, 2009. 13(9b): p. 3131-3140.

59. Sen, C.K. and L. Packer, Thiol homeostasis and supplements in physical exercise. The American journal of clinical nutrition, 2000. 72(2): p. 653S-669S.

60. W³odek, L., Beneficial and harmful effects of thiols. Pol. J. Pharmacol, 2002. 54: p. 215-223.

61. Cremers, C.M. and U. Jakob, Oxidant sensing by reversible disulfide bond formation. Journal of Biological Chemistry, 2013. 288(37): p. 26489-26496.

62. Turell, L., R. Radi, and B. Alvarez, The thiol pool in human plasma: the central contribution of albumin to redox processes. Free Radical Biology and Medicine, 2013. 65: p. 244-253.

63. Erel, O. and S. Neselioglu, A novel and automated assay for thiol/disulphide homeostasis. Clinical biochemistry, 2014. 47(18): p. 326-332.

64. Gào, X., et al., Serum total thiol levels and the risk of lung, colorectal, breast and prostate cancer: A prospective case–cohort study. International journal of cancer, 2020. 146(5): p. 1261-1267.

65. Sezgin, B., et al., Thiol-disulfide status of patients with cervical cancer. Journal of Obstetrics and Gynaecology Research, 2020. 46(11): p. 2423-2429.

66. Sezgin, B., et al., Assessment of thiol disulfide balance in early-stage endometrial cancer. Journal of Obstetrics and Gynaecology Research, 2020. 46(7): p. 1140-1147.

67. Hizal, M., et al., Evaluation of dynamic serum thiol/disulfide homeostasis in locally advanced and metastatic gastric cancer. Journal of Oncological Sciences, 2018. 4(1): p. 1-4.

68. Lu, S.C., Glutathione synthesis. Biochimica et Biophysica Acta (BBA)-General Subjects, 2013. 1830(5): p. 3143-3153.

69. Hayes, J.D. and L.I. McLellan, Glutathione and glutathione-dependent enzymes represent a co-ordinately regulated defence against oxidative stress. Free radical research, 1999. 31(4): p. 273-300.

70. Masella, R., et al., Novel mechanisms of natural antioxidant compounds in biological systems: involvement of glutathione and glutathione-related enzymes. The Journal of nutritional biochemistry, 2005. 16(10): p. 577-586.

71. Maher, P., et al., A novel approach to enhancing cellular glutathione levels. Journal of neurochemistry, 2008. 107(3): p. 690-700.

72. Ketterer, B., The role of nonenzymatic reactions of glutathione in xenobiotic metabolism. Drug metabolism reviews, 1982. 13(1): p. 161-187.

73. Meister, A., Selective modification of glutathione metabolism. Science, 1983. 220(4596): p. 472-477.

74. REED, D.J., Glutathione depletion and susceptibility. Pharmacol Rev, 1984. 36: p. 25S-33S.

75. Ziegler, D., Role of reversible oxidation-reduction of enzyme thiols-disulfides in metabolic regulation. Annual review of biochemistry, 1985. 54: p. 305-329.

76. Arrigo, A.-P., Gene expression and the thiol redox state. Free Radical Biology and Medicine, 1999. 27(9-10): p. 936-944.

77. Giles, G.I., The redox regulation of thiol dependent signaling pathways in cancer. Current pharmaceutical design, 2006. 12(34): p. 4427-4443.

78. Kachur, A.V., C.J. Koch, and J.E. Biaglow, Mechanism of copper-catalyzed oxidation of glutathione. Free radical research, 1998. 28(3): p. 259-269.

79. Giles, N.M., et al., Metal and redox modulation of cysteine protein function. Chemistry & biology, 2003. 10(8): p. 677-693.

80. Dhakshinamoorthy, A., M. Alvaro, and H. Garcia, Aerobic oxidation of thiols to disulfides using iron metal–organic frameworks as solid redox catalysts. Chemical communications, 2010. 46(35): p. 6476-6478.

81. Dickinson, D.A. and H.J. Forman, Cellular glutathione and thiols metabolism. Biochemical pharmacology, 2002. 64(5-6): p. 1019-1026.

82. Johnson, W.M., A.L. Wilson-Delfosse, and J.J. Mieyal, Dysregulation of glutathione homeostasis in neurodegenerative diseases. Nutrients, 2012. 4(10): p. 1399-1440.

83. Wu, G., et al., Recent Advances in Nutritional Sciences-Glutathione Metabolism and Its Implications for Health. Journal of Nutrition, 2004. 134(3): p. 489-492.

84. Hinson, J.A., D.W. Roberts, and L.P. James, Mechanisms of acetaminophen-induced liver necrosis. Adverse drug reactions, 2010: p. 369-405.

85. Jones, D.P., [11] Redox potential of GSH/GSSG couple: assay and biological significance, in Methods in enzymology. 2002, Elsevier. p. 93-112.

86. Nersesyan, A., et al., Use of the lymphocyte cytokinesis-block micronucleus assay in occupational biomonitoring of genome damage caused by in vivo exposure to chemical genotoxins: Past, present and future. Mutation Research/Reviews in Mutation Research, 2016. 770: p. 1-11.

87. Annangi, B., et al., Biomonitoring of humans exposed to arsenic, chromium, nickel, vanadium, and complex mixtures of metals by using the micronucleus test in lymphocytes. Mutation Research/Reviews in Mutation Research, 2016. 770: p. 140-161.

88. Gonzalez, L. and M. Kirsch-Volders, Biomonitoring of genotoxic effects for human exposure to nanomaterials: the challenge ahead. Mutation Research/Reviews in Mutation Research, 2016. 768: p. 14-26.

89. Kirsch-Volders, M., et al., Report from the in vitro micronucleus assay working group. Mutation Research/Genetic Toxicology and Environmental Mutagenesis, 2003. 540(2): p. 153-163.

90. Hayashi, M., The micronucleus test—most widely used in vivo genotoxicity test—. Genes and Environment, 2016. 38(1): p. 1-6.

91. Fenech, M., Cytokinesis-block micronucleus cytome assay. Nat Protoc, 2007. 2(5): p. 1084-104.

92. Fenech, M., The lymphocyte cytokinesis-block micronucleus cytome assay and its application in radiation biodosimetry. Health physics, 2010. 98(2): p. 234-243.

93. Bolt, H., J. Stewart, and J. Hengstler, A comprehensive review about micronuclei: mechanisms of formation and practical aspects in genotoxicity testing. Archives of toxicology, 2011. 85: p. 861-862.

94. Al-Sabti, K. and C.D. Metcalfe, Fish micronuclei for assessing genotoxicity in water. Mutation Research/Genetic Toxicology, 1995. 343(2-3): p. 121-135.

95. Hovhannisyan, G.G., Fluorescence in situ hybridization in combination with the comet assay and micronucleus test in genetic toxicology. Molecular cytogenetics, 2010. 3(1): p. 1-11.

96. Degrassi, F. and C. Tanzarella, Immunofluorescent staining of kinetochores in micronuclei: a new assay for the detection of aneuploidy. Mutation Research/Environmental Mutagenesis and Related Subjects, 1988. 203(5): p. 339-345.

97. Fenech, M., Cytokinesis-block micronucleus cytome assay. Nature protocols, 2007. 2(5): p. 1084-1104.

98. Ostling, O. and K.J. Johanson, Microelectrophoretic study of radiation-induced DNA damages in individual mammalian cells. Biochemical and biophysical research communications, 1984. 123(1): p. 291-298.

99. Singh, N.P., et al., A simple technique for quantitation of low levels of DNA damage in individual cells. Experimental cell research, 1988. 175(1): p. 184-191.

100. Hartmann, A., et al., Recommendations for conducting the in vivo alkaline Comet assay. Mutagenesis, 2003. 18(1): p. 45-51.

101. Tice, R.R., et al., Single cell gel/comet assay: guidelines for in vitro and in vivo genetic toxicology testing. Environmental and molecular mutagenesis, 2000. 35(3): p. 206-221.

102. Duthie, S.J. and V. Dobson, Dietary flavonoids protect human colonocyte DNA from oxidative attack in vitro. European journal of nutrition, 1999. 38(1): p. 28-34.

103. Crebelli, R., et al., Can sustained exposure to PFAS trigger a genotoxic response? A comprehensive genotoxicity assessment in mice after subacute oral administration of PFOA and PFBA. Regulatory Toxicology and Pharmacology, 2019. 106: p. 169-177.

104. Cordelli, E., et al., No genotoxicity in rat blood cells upon 3-or 6-month inhalation exposure to CeO2 or BaSO4 nanomaterials. Mutagenesis, 2017. 32(1): p. 13-22.

105. Booth, E.D., et al., Regulatory requirements for genotoxicity assessment of plant protection product active ingredients, impurities, and metabolites. Environmental and Molecular Mutagenesis, 2017. 58(5): p. 325-344.

106. Collins, A.R., et al., The comet assay: topical issues. Mutagenesis, 2008. 23(3): p. 143-151.

107. Abbotts, R. and D.M. Wilson III, Coordination of DNA single strand break repair. Free Radical Biology and Medicine, 2017. 107: p. 228-244.

108. Jaeschke, H., et al., Mechanisms of hepatotoxicity. Toxicological sciences, 2002. 65(2): p. 166-176.

109. Patel, M., K.S. Taskar, and M.J. Zamek-Gliszczynski, Importance of hepatic transporters in clinical disposition of drugs and their metabolites. The Journal of Clinical Pharmacology, 2016. 56: p. S23-S39.

110. Roberts, M.S., et al., Enterohepatic circulation. Clinical pharmacokinetics, 2002. 41(10): p. 751-790.

111. Read, A., Clinical physiology of the liver. BJA: British Journal of Anaesthesia, 1972. 44(9): p. 910-917.

112. Kmiec, Z., Cooperation of liver cells in health and disease: with 18 tables. 2001.

113. Goodman, L.S., et al., Goodman & Gilman's pharmacological basis of therapeutics. 2011, McGraw-Hill.

114. Glatt, H., Bioactivation of mutagens via sulfation. The FASEB Journal, 1997. 11(5): p. 314-321.

115. Strange, R.C., et al., Glutathione-S-transferase family of enzymes. Mutation Research/Fundamental and Molecular Mechanisms of Mutagenesis, 2001. 482(1-2): p. 21-26.

116. Zhou, S., et al., Drug bioactivation covalent binding to target proteins and toxicity relevance. Drug metabolism reviews, 2005. 37(1): p. 41-213.

117. Ritter, J.K., Roles of glucuronidation and UDP-glucuronosyltransferases in xenobiotic bioactivation reactions. Chemico-biological interactions, 2000. 129(1-2): p. 171-193.

118. Sallustio, B.C., et al., Hepatic disposition of electrophilic acyl glucuronide conjugates. Current drug metabolism, 2000. 1(2): p. 163-180.

119. Boelsterli, U.A., Xenobiotic acyl glucuronides and acyl CoA thioesters as protein-reactive metabolites with the potential to cause idiosyncratic drug reactions. Current drug metabolism, 2002. 3(4): p. 439-450.

120. Shipkova, M., et al., Acyl glucuronide drug metabolites: toxicological and analytical implications. Therapeutic drug monitoring, 2003. 25(1): p. 1-16.

121. Isin, E.M. and F.P. Guengerich, Complex reactions catalyzed by cytochrome P450 enzymes. Biochimica et Biophysica Acta (BBA)-General Subjects, 2007. 1770(3): p. 314-329.

122. Guengerich, F.P., Intersection of the roles of cytochrome P450 enzymes with xenobiotic and endogenous substrates: relevance to toxicity and drug interactions. Chemical research in toxicology, 2017. 30(1): p. 2-12.

123. Seliskar, M. and D. Rozman, Mammalian cytochromes P450--importance of tissue specificity. Biochim Biophys Acta, 2007. 1770(3): p. 458-66.

124. Neve, E. and M. Ingelman-Sundberg, Intracellular transport and localization of microsomal cytochrome P450. Analytical and bioanalytical chemistry, 2008. 392(6): p. 1075-1084.

125. Peter Guengerich, F., Cytochrome P450: what have we learned and what are the future issues? Drug metabolism reviews, 2004. 36(2): p. 159-197.

126. Nelson, D.R., et al., Comparison of cytochrome P450 (CYP) genes from the mouse and human genomes, including nomenclature recommendations for genes, pseudogenes and alternative-splice variants. Pharmacogenetics and Genomics, 2004. 14(1): p. 1-18.

127. Omura, T., Forty years of cytochrome P450. Biochemical and biophysical research communications, 1999. 266(3): p. 690-698.

128. Hasler, J.A., et al., Human cytochromes P450. Molecular aspects of medicine, 1999. 20(1-2): p. 1-137.

129. Furge, L.L. and F.P. Guengerich, Cytochrome P450 enzymes in drug metabolism and chemical toxicology: An introduction. Biochemistry and Molecular Biology Education, 2006. 34(2): p. 66-74.

130. Rendic, S., Summary of information on human CYP enzymes: human P450 metabolism data. Drug metabolism reviews, 2002. 34(1-2): p. 83-448.

131. Rendic, S. and F.J.D. Carlo, Human cytochrome P450 enzymes: a status report summarizing their reactions, substrates, inducers, and inhibitors. Drug metabolism reviews, 1997. 29(1-2): p. 413-580.

132. Nelson, D.R., et al., P450 superfamily: update on new sequences, gene mapping, accession numbers and nomenclature. Pharmacogenetics, 1996. 6(1): p. 1-42.

133. Wormhoudt, L.W., J.N. Commandeur, and N.P. Vermeulen, Genetic polymorphisms of human N-acetyltransferase, cytochrome P450, glutathione-S-transferase, and epoxide hydrolase enzymes: relevance to xenobiotic metabolism and toxicity. Critical reviews in toxicology, 1999. 29(1): p. 59-124.

134. Rodrigues, A. and T.H. Rushmore, Cytochrome P450 pharmacogenetics in drug development: in vitro studies and clinical consequences. Current drug metabolism, 2002. 3(3): p. 289-309.

135. Domanski, T.L., et al., cDNA cloning and initial characterization of CYP3A43, a novel human cytochrome P450. Molecular Pharmacology, 2001. 59(2): p. 386-392.

136. Shimada, T., et al., Interindividual variations in human liver cytochrome P-450 enzymes involved in the oxidation of drugs, carcinogens and toxic chemicals: Studies with liver microsomes of 30 Japanese and 30 Caucasians. Journal of Pharmacology and Experimental Therapeutics, 1994. 270(1): p. 414-423.

137. Kuehl, P., et al., Sequence diversity in CYP3A promoters and characterization of the genetic basis of polymorphic CYP3A5 expression. Nature genetics, 2001. 27(4): p. 383-391.

138. Westlind-Johnsson, A., et al., Comparative analysis of CYP3A expression in human liver suggests only a minor role for CYP3A5 in drug metabolism. Drug Metabolism and Disposition, 2003. 31(6): p. 755-761.

139. Wrighton, S.A., et al., Studies on the expression and metabolic capabilities of human liver cytochrome P450IIIA5 (HLp3). Molecular pharmacology, 1990. 38(2): p. 207-213.

140. Schuetz, J.D., D.L. Beach, and P.S. Guzelian, Selective expression of cytochrome P450 CYP3A mRNAs in embryonic and adult human liver. Pharmacogenetics, 1994. 4(1): p. 11-20.

141. Komori, M., et al., Fetus-specific expression of a form of cytochrome P-450 in human livers. Biochemistry, 1990. 29(18): p. 4430-4433.

142. Aoyama, T., et al., Cytochrome P-450 hPCN3, a Novel Cytochrome P-450 IIIA Gene Product That Is Differentially Expressed in Adult Human Liver: cDNA and deduced amino acid sequence and distinct specificities of cDNA-expressed hPCN1 and hPCN3 for the metabolism of steroid hormones and cyclosporin. Journal of Biological Chemistry, 1989. 264(18): p. 10388-10395.

143. Guengerich, F.P., Cytochrome P-450 3A4: regulation and role in drug metabolism. Annual review of pharmacology and toxicology, 1999. 39: p. 1.

144. Rebbeck, T.R., et al., Modification of clinical presentation of prostate tumors by a novel genetic variant in CYP3A4. JNCI: Journal of the National Cancer Institute, 1998. 90(16): p. 1225-1229.

145. Shimada, T., et al., Activation of procarcinogens by human cytochrome P450 enzymes expressed in Escherichia coli. Simplified bacterial systems for genotoxicity assays. Carcinogenesis, 1994. 15(11): p. 2523-2529.

146. Thummel, K.E., et al., Oral first-pass elimination of midazolam involves both gastrointestinal and hepatic CYP3A-mediated metabolism. Clinical Pharmacology & Therapeutics, 1996. 59(5): p. 491-502.

147. Zhou, S.-F., et al., Clinically important drug interactions potentially involving mechanism-based inhibition of cytochrome P450 3A4 and the role of therapeutic drug monitoring. Therapeutic drug monitoring, 2007. 29(6): p. 687-710.

148. Dai, D., et al., Identification of variants of CYP3A4 and characterization of their abilities to metabolize testosterone and chlorpyrifos. Journal of Pharmacology and Experimental Therapeutics, 2001. 299(3): p. 825-831.

149. Bhattacharyya, S., K. Sinha, and P. C Sil, Cytochrome P450s: mechanisms and biological implications in drug metabolism and its interaction with oxidative stress. Current drug metabolism, 2014. 15(7): p. 719-742.

150. Lindahl, T., Instability and decay of the primary structure of DNA. nature, 1993. 362(6422): p. 709-715.

151. Moloney, J.N. and T.G. Cotter. ROS signalling in the biology of cancer. in Seminars in cell & developmental biology. 2018. Elsevier.

152. Williams, E.T., et al., Genomic analysis of the carboxylesterases: identification and classification of novel forms. Mol Phylogenet Evol, 2010. 57(1): p. 23-34.

153. Redinbo, M.R. and P.M. Potter, Keynote review: Mammalian carboxylesterases: From drug targets to protein therapeutics. Drug discovery today, 2005. 10(5): p. 313-325.

154. Rautio, J., et al., Prodrugs: design and clinical applications. Nature reviews Drug discovery, 2008. 7(3): p. 255-270.

155. Liu, S.-Y., et al., An activity-based fluorogenic probe enables cellular and in vivo profiling of carboxylesterase isozymes. Analytical Chemistry, 2020. 92(13): p. 9205-9213.

156. Hosokawa, M., Structure and catalytic properties of carboxylesterase isozymes involved in metabolic activation of prodrugs. Molecules, 2008. 13(2): p. 412-431.

157. Williams, E.T., et al., Characterization of the expression and activity of carboxylesterases 1 and 2 from the beagle dog, cynomolgus monkey, and human. Drug Metab Dispos, 2011. 39(12): p. 2305-13.

158. TETSUO SATOH, P.T., WILLIAM F. BOSRON, SONAL P. SANGHANI, MASAKIYO HOSOKAWA, and A.B.N.L. DU, Current Progress on Esterases-From Molecular Structure to Function by satoh2002.pdf. DRUG METABOLISM AND DISPOSITION, 2002. Vol. 30, No. 5(30): p. 488–493.

159. Xu, G., et al., Human carboxylesterase 2 is commonly expressed in tumor tissue and is correlated with activation of irinotecan. Clinical Cancer Research, 2002. 8(8): p. 2605-2611.

160. Na, K., et al., Human plasma carboxylesterase 1, a novel serologic biomarker candidate for hepatocellular carcinoma. Proteomics, 2009. 9(16): p. 3989-3999.

161. Shaojun, C., et al., Expression of Topoisomerase 1 and carboxylesterase 2 correlates with irinotecan treatment response in metastatic colorectal cancer. Cancer Biology & Therapy, 2018. 19(3): p. 153-159.

162. Ohtsuka, K., et al., Intracellular conversion of irinotecan to its active form, SN-38, by native carboxylesterase in human non-small cell lung cancer. Lung Cancer, 2003. 41(2): p. 187-198.

163. Uchida, K., et al., Clinical implications of CES2 RNA expression in neuroblastoma. Journal of Pediatric Surgery, 2013. 48(3): p. 502-509.

164. Park, S.J., et al., A carboxylesterase-selective ratiometric fluorescent two-photon probe and its application to hepatocytes and liver tissues. Chemical science, 2016. 7(6): p. 3703-3709.

165. Hakamata, W., et al., Multicolor imaging of endoplasmic reticulum-located esterase as a prodrug activation enzyme. ACS medicinal chemistry letters, 2014. 5(4): p. 321-325.

166. Potter, M.J.H.P.M., Carboxylesterase inhibitors by hatfield2011.pdf. informa healthcare, 2011. 21(8): p. 1159-1171.

167. Ho, R.H. and R.B. Kim, Transporters and drug therapy: implications for drug disposition and disease. Clin Pharmacol Ther, 2005. 78(3): p. 260-77.

168. Nakata, K., et al., Nuclear receptor-mediated transcriptional regulation in Phase I, II, and III xenobiotic metabolizing systems. Drug metabolism and pharmacokinetics, 2006. 21(6): p. 437-457.

169. Eloranta, J.J. and G.A. Kullak-Ublick, Coordinate transcriptional regulation of bile acid homeostasis and drug metabolism. Archives of biochemistry and biophysics, 2005. 433(2): p. 397-412.

170. You, G. and M.E. Morris, Drug transporters: molecular characterization and role in drug disposition. 2014: Wiley-Blackwell.

171. Pan, G., Roles of hepatic drug transporters in drug disposition and liver toxicity. Drug Transporters in Drug Disposition, Effects and Toxicity, 2019: p. 293-340.

172. Li, P., et al., Liver transporters in hepatic drug disposition: an update. Current drug metabolism, 2009. 10(5): p. 482-498.

173. Klaas Nico Faber , M.M., Peter L.M. Jansen, Drug transport proteins in the liver by faber2003.pdf. Advanced Drug Delivery Reviews 2003. 55: p. 107-124.

174. Shitara, Y., T. Horie, and Y. Sugiyama, Transporters as a determinant of drug clearance and tissue distribution. Eur J Pharm Sci, 2006. 27(5): p. 425-46.

175. Louisa, M., et al., Differential expression of several drug transporter genes in HepG2 and Huh-7 cell lines. Adv Biomed Res, 2016. 5: p. 104.

176. Shitara, Y., T. Horie, and Y. Sugiyama, Transporters as a determinant of drug clearance and tissue distribution. European journal of pharmaceutical sciences, 2006. 27(5): p. 425-446.

177. Evers, R. and X.-Y. Chu, Role of the murine organic anion-transporting polypeptide 1b2 (Oatp1b2) in drug disposition and hepatotoxicity. Molecular pharmacology, 2008. 74(2): p. 309-311.

178. Kalliokoski, A. and M. Niemi, Impact of OATP transporters on pharmacokinetics. British journal of pharmacology, 2009. 158(3): p. 693-705.

179. Lee, E.J.D., C.B. Lean, and L.M.G. Limenta, Role of membrane transporters in the safety profile of drugs. Expert opinion on drug metabolism & toxicology, 2009. 5(11): p. 1369-1383.

180. Abe, T., et al., LST-2, a human liver-specific organic anion transporter, determines methotrexate sensitivity in gastrointestinal cancers. Gastroenterology, 2001. 120(7): p. 1689-1699.

181. Hagenbuch, B. and P.J. Meier, Organic anion transporting polypeptides of the OATP/SLC21 family: phylogenetic classification as OATP/SLCO superfamily, new nomenclature and molecular/functional properties. Pflügers Archiv, 2004. 447(5): p. 653-665.

182. Hagenbuch, B. and C. Gui, Xenobiotic transporters of the human organic anion transporting polypeptides (OATP) family. Xenobiotica, 2008. 38(7-8): p. 778-801.

183. König, J.r., et al., A novel human organic anion transporting polypeptide localized to the basolateral hepatocyte membrane. American Journal of Physiology-Gastrointestinal and Liver Physiology, 2000. 278(1): p. G156-G164.

184. König, J.r., et al., Localization and genomic organization of a new hepatocellular organic anion transporting polypeptide. Journal of Biological Chemistry, 2000. 275(30): p. 23161-23168.

185. Kindla, J., M.F. Fromm, and J. König, In vitro evidence for the role of OATP and OCT uptake transporters in drug–drug interactions. Expert opinion on drug metabolism & toxicology, 2009. 5(5): p. 489-500.

186. Hirohashi, T., et al., Hepatic expression of multidrug resistance-associated protein-like proteins maintained in Eisai hyperbilirubinemic rats. Molecular Pharmacology, 1998. 53(6): p. 1068-1075.

187. Kool, M., et al., Expression of human MRP6, a homologue of the multidrug resistance protein gene MRP1, in tissues and cancer cells. Cancer Research, 1999. 59(1): p. 175-182.

188. Borst, P., et al., The multidrug resistance protein family. Biochimica et Biophysica Acta (BBA)-Biomembranes, 1999. 1461(2): p. 347-357.

189. Lecureur, V., et al., Expression and regulation of hepatic drug and bile acid transporters. Toxicology, 2000. 153(1-3): p. 203-219.

190. John A. Edgar, E.R., and Russell J. Molyneux, Honey from Plants Containing Pyrrolizidine Alkaloids: A Potential Threat to Health. J. Agric. Food Chem. , 2002. 50: p. 2719−2730.

191. Reimann, A., et al., Repeated evolution of the pyrrolizidine alkaloid-mediated defense system in separate angiosperm lineages. Plant Cell, 2004. 16(10): p. 2772-84.

192. Gluck, J., et al., Pyrrolizidine Alkaloids Induce Cell Death in Human HepaRG Cells in a Structure-Dependent Manner. Int J Mol Sci, 2020. 22(1).

193. Hadi, N.S.A., et al., Genotoxicity of selected pyrrolizidine alkaloids in human hepatoma cell lines HepG2 and Huh6. Mutat Res, 2021. 861-862: p. 503305.

194. Molyneux, R.J., et al., Pyrrolizidine alkaloid toxicity in livestock: a paradigm for human poisoning? Food Addit Contam Part A Chem Anal Control Expo Risk Assess, 2011. 28(3): p. 293-307.

195. Xiaobo He, Q.X., Qiangen Wu, William H. Tolleson, Ge Lin, Peter P. Fu,, Primary and Secondary Pyrrolic Metabolites of Pyrrolizidine Alkaloids Form DNA Adducts in Human A549 Cells. Toxicology in Vitro, 2018.

196. Louisse, J., et al., Determination of genotoxic potencies of pyrrolizidine alkaloids in HepaRG cells using the gammaH2AX assay. Food Chem Toxicol, 2019. 131: p. 110532.

197. Agency, E.M., Public statement on the use of herbal medicinal products1 containing toxic, unsaturated pyrrolizidine alkaloids (PAs) including recommendations regarding contamination of herbal medicinal products with PAs. Science Medicines Health, 2021.

198. Reimann, A., et al., Repeated evolution of the pyrrolizidine alkaloid-mediated defense system in separate angiosperm lineages. Plant Cell, 2004. 16(10): p. 2772-84.

199. Kempf, M., et al., Pyrrolizidine alkaloids in honey: risk analysis by gas chromatography-mass spectrometry. Molecular nutrition & food research, 2008. 52(10): p. 1193-1200.

200. Kakar, F., et al., An outbreak of hepatic veno-occlusive disease in Western Afghanistan associated with exposure to wheat flour contaminated with pyrrolizidine alkaloids. Journal of toxicology, 2010. 2010.

201. Zhu, L., et al., Contamination of hepatotoxic pyrrolizidine alkaloids in retail honey in China. Food Control, 2018. 85: p. 484-494.

202. He, X., et al., Effects of glutathione and cysteine on pyrrolizidine alkaloid-induced hepatotoxicity and DNA adduct formation in rat primary hepatocytes. Journal of Environmental Science and Health, Part C, 2020. 38(2): p. 109-123.

203. Stillman, A.E., et al., Hepatic veno-occlusive disease due to pyrrolizidine (Senecio) poisoning in Arizona. Gastroenterology, 1977. 73(2): p. 349-352.

204. Fu, P.P., et al., Detection, hepatotoxicity, and tumorigenicity of pyrrolizidine alkaloids in Chinese herbal plants and herbal dietary supplements. Journal of Food and Drug Analysis, 2007. 15(4).

205. Lin, G., et al., Hepatic sinusoidal obstruction syndrome associated with consumption of Gynura segetum. Journal of hepatology, 2011. 54(4): p. 666-673.

206. Zhu, L., et al., Tu-San-Qi (Gynura japonica): the culprit behind pyrrolizidine alkaloid-induced liver injury in China. Acta Pharmacologica Sinica, 2021. 42(8): p. 1212-1222.

207. Nations, W.H.O.F.a.A.O.o.t.U., Safety evaluation of certain food additives and contaminants: supplement 2: pyrrolizidine alkaloids, prepared by the eightieth meeting of the Joint FAO/WHO Expert Committee on Food Additives (JECFA). WHO Food additives series ; 71-S2, 2020.

208. Hoogenboom, L.A., et al., Carry-over of pyrrolizidine alkaloids from feed to milk in dairy cows. Food Addit Contam Part A Chem Anal Control Expo Risk Assess, 2011. 28(3): p. 359-72.

209. Bodi, D., et al., Determination of pyrrolizidine alkaloids in tea, herbal drugs and honey. Food Additives & Contaminants: Part A, 2014. 31(11): p. 1886-1895.

210. Flade, J., et al., Occurrence of nine pyrrolizidine alkaloids in Senecio vulgaris L. depending on developmental stage and season. Plants, 2019. 8(3): p. 54.

211. Hartmann, T. and L. Witte, Chemistry, biology and chemoecology of the pyrrolizidine alkaloids, in Alkaloids: chemical and biological perspectives. 1995, Elsevier. p. 155-233.

212. Moreira, R., et al., Pyrrolizidine Alkaloids: Chemistry, Pharmacology, Toxicology and Food Safety. Int J Mol Sci, 2018. 19(6).

213. Hartmann, T. and L. Witte, Chapter Four - Chemistry, Biology and Chemoecology of the Pyrrolizidine Alkaloids, in Alkaloids: Chemical and Biological Perspectives, S.W. Pelletier, Editor. 1995, Pergamon. p. 155-233.

214. Gottschalk, C., et al., Pyrrolizidine alkaloids in natural and experimental grass silages and implications for feed safety. Animal Feed Science and Technology, 2015. 207: p. 253-261.

215. Wang, Y.-P., P.P. Fu, and M.W. Chou, Metabolic activation of the tumorigenic pyrrolizidine alkaloid, retrorsine, leading to DNA adduct formation in vivo. International Journal of Environmental Research and Public Health, 2005. 2(1): p. 74-79.

216. Zhou, Y., et al., A new approach for simultaneous screening and quantification of toxic pyrrolizidine alkaloids in some potential pyrrolizidine alkaloid-containing plants by using ultra performance liquid chromatography–tandem quadrupole mass spectrometry. Analytica chimica acta, 2010. 681(1-2): p. 33-40.

217. Chen, T., N. Mei, and P.P. Fu, Genotoxicity of pyrrolizidine alkaloids. Journal of Applied Toxicology: An International Journal, 2010. 30(3): p. 183-196.

218. Rowell-Rahier, M., et al., Sequestration of plant pyrrolizidine alkaloids by chrysomelid beetles and selective transfer into the defensive secretions. Chemoecology, 1991. 2(1): p. 41-48.

219. de Fresno, Á.M.V., Farmacognosia general. 1999.

220. These, A., et al., Structural screening by multiple reaction monitoring as a new approach for tandem mass spectrometry: presented for the determination of pyrrolizidine alkaloids in plants. Analytical and bioanalytical chemistry, 2013. 405(29): p. 9375-9383.

221. Opinion, B., Pyrrolizidine alkaloids in herbal teas and teas. Bundesinstitut für Risikobewertung, 2013: p. 1-29.

222. Mattocks, A.R., et al., Metabolism and toxicity of synthetic analogues of macrocyclic diester pyrrolizidine alkaloids. Chemico-Biological Interactions, 1986. 58: p. 95-108.

223. Peter P. Fu, Q.X., 1 Ge Lin,2 and Ming W. Chou1 Genotoxic pyrrolizidine alkaloids-mechanism leading to DNA Adduct formation and tumorigenicity by Fu 2002.pdf. nt. J. Mol. Sci I, 2002 3: p. 948-964.

224. Bruneton, J., Farmacognosia, fitoquímica, plantas medicinales. 2001.

225. da Cunha, A.P. and J.A.B. da Graça, Farmacognosia e fitoquímica. 2005.

226. Hessel-Pras, S., et al., The pyrrolizidine alkaloid senecionine induces CYP-dependent destruction of sinusoidal endothelial cells and cholestasis in mice. Archives of Toxicology, 2020. 94(1): p. 219-229.

227. Lafranconi, W.M. and R.J. Huxtable, Hepatic metabolism and pulmonary toxicity of monocrotaline using isolated perfused liver and lung. Biochem Pharmacol, 1984. 33(15): p. 2479-84.

228. Roeder, E., Medicinal plants in Europe containing pyrrolizidine alkaloids. Pharmazie, 1995. 50(2): p. 83-98.

229. Mattocks, A., et al., Metabolism and toxicity of synthetic analogues of macrocyclic diester pyrrolizidine alkaloids. Chemico-biological interactions, 1986. 58: p. 95-108.

230. Kasahara, Y., et al., Bioactivation of monocrotaline by P-450 3A in rat liver. Journal of cardiovascular pharmacology, 1997. 30(1): p. 124-129.

231. Dueker, S., M. Lame, and H. Segall, Hydrolysis rates of pyrrolizidine alkaloids derived from Senecio jacobaea. Archives of toxicology, 1995. 69(10): p. 725-728.

232. Fu, P.P., et al., Pyrrolizidine alkaloids—genotoxicity, metabolism enzymes, metabolic activation, and mechanisms. Drug metabolism reviews, 2004. 36(1): p. 1-55.

233. Forsch, K., et al., Development of an in vitro screening method of acute cytotoxicity of the pyrrolizidine alkaloid lasiocarpine in human and rodent hepatic cell lines by increasing susceptibility. Journal of ethnopharmacology, 2018. 217: p. 134-139.

234. Dueker, S.R., et al., Guinea pig and rat hepatic microsomal metabolism of monocrotaline. Drug Metab Dispos, 1992. 20(2): p. 275-80.

235. Miranda, C.L., et al., Role of cytochrome P450IIIA4 in the metabolism of the pyrrolizidine alkaloid senecionine in human liver. Carcinogenesis, 1991. 12(3): p. 515-519.

236. Chung, W.-G., C. Miranda, and D. Buhler, A cytochrome P4502B form is the major bioactivation enzyme for the pyrrolizidine alkaloid senecionine in guinea pig. Xenobiotica, 1995. 25(9): p. 929-939.

237. Williams, D., et al., Bioactivation and detoxication of the pyrrolizidine alkaloid senecionine by cytochrome P-450 enzymes in rat liver. Drug metabolism and disposition, 1989. 17(4): p. 387-392.

238. Williams, D.E., et al., Bioactivation and detoxication of the pyrrolizidine alkaloid senecionine by cytochrome P-450 enzymes in rat liver. Drug metabolism and disposition: the biological fate of chemicals, 1989. 17(4): p. 387-392.

239. Williams, D.E., et al., The role of flavin-containing monooxygenase in the N-oxidation of the pyrrolizidine alkaloid senecionine. Drug metabolism and disposition: the biological fate of chemicals, 1989. 17(4): p. 380-386.

240. Chou, M.W., et al., Riddelliine N-oxide is a phytochemical and mammalian metabolite with genotoxic activity that is comparable to the parent pyrrolizidine alkaloid riddelliine. Toxicology Letters, 2003. 145(3): p. 239-247.

241. Yan, J., et al., Metabolic activation of retronecine and retronecine N-oxide – formation of DHP-derived DNA adducts. Toxicology and Industrial Health, 2008. 24(3): p. 181-188.

242. Wang, Y.-P., et al., Human liver microsomal reduction of pyrrolizidine alkaloid N-oxides to form the corresponding carcinogenic parent alkaloid. Toxicology Letters, 2005. 155(3): p. 411-420.

243. Mattocks, A.R., Hepatotoxic Effects due to Pyrrolizidine Alkaloid N-Oxides. Xenobiotica, 1971. 1(4-5): p. 563-565.

244. Harris, P.N. and K. Chen, Development of hepatic tumors in rats following ingestion of Senecio longilobus. Cancer Research, 1970. 30(12): p. 2881-2886.

245. Fu, P., et al., Genotoxic pyrrolizidine alkaloids and pyrrolizidine alkaloid N-oxides—mechanisms leading to DNA adduct formation and tumorigenicity. Journal of Environmental Science and Health, Part C, 2001. 19(2): p. 353-385.

246. Yang, M., et al., First evidence of pyrrolizidine alkaloid N-oxide-induced hepatic sinusoidal obstruction syndrome in humans. Archives of toxicology, 2017. 91: p. 3913-3925.

247. Fu, P.P., et al., Pyrrolizidine alkaloids--genotoxicity, metabolism enzymes, metabolic activation, and mechanisms. Drug metabolism reviews, 2004. 36(1): p. 1-55.

248. Chung, W.G. and D.R. Buhler, The Effect of Spironolactone Treatment on the Cytochrome P450-Mediated Metabolism of the Pyrrolizidine Alkaloid Senecionine by Hepatic Microsomes from Rats and Guinea Pigs. Toxicology and Applied Pharmacology, 1994. 127(2): p. 314-319.

249. Chung, W.-G., C.L. Miranda, and D.R. Buhler, A cytochrome P4502B form is the major bioactivation enzyme for the pyrrolizidine alkaloid senecionine in guinea pig. Xenobiotica, 1995. 25(9): p. 929-939.

250. Kasahara, Y., et al., Bioactivation of monocrotaline by P-450 3A in rat liver. J Cardiovasc Pharmacol, 1997. 30(1): p. 124-9.

251. Reid, M.J., et al., Involvement of cytochrome P450 3A in the metabolism and covalent binding of 14C-monocrotaline in rat liver microsomes. Journal of biochemical and molecular toxicology, 1998. 12(3): p. 157-166.

252. Mattocks, A., Toxicity of pyrrolizidine alkaloids. Nature, 1968. 217(5130): p. 723-728.

253. Mattocks, A.R. and R. Jukes, Trapping and measurement of short-lived alkylating agents in a recirculating flow system. Chemico-biological interactions, 1990. 76(1): p. 19-30.

254. Ebmeyer, J., et al., Human CYP3A4-mediated toxification of the pyrrolizidine alkaloid lasiocarpine. Food and Chemical Toxicology, 2019. 130: p. 79-88.

255. Hincks, J.R., et al., DNA cross-linking in mammalian cells by pyrrolizidine alkaloids: structure-activity relationships. Toxicology and applied pharmacology, 1991. 111(1): p. 90-98.

256. Kim, H.-Y., F.R. Stermitz, and R.A. Coulombe Jr, Pyrrolizidine alkaloid-induced DNA-protein cross-links. Carcinogenesis, 1995. 16(11): p. 2691-2697.

257. Yang, Y.-C., et al., Metabolic activation of the tumorigenic pyrrolizidine alkaloid, riddelliine, leading to DNA adduct formation in vivo. Chemical research in toxicology, 2001. 14(1): p. 101-109.

258. Fu, P.P., et al., Genotoxic pyrrolizidine alkaloids—mechanisms leading to DNA adduct formation and tumorigenicity. International Journal of Molecular Sciences, 2002. 3(9): p. 948-964.

259. Eastman, D., G. Dimenna, and H. Segall, Covalent binding of two pyrrolizidine alkaloids, senecionine and seneciphylline, to hepatic macromolecules and their distribution, excretion, and transfer into milk of lactating mice. Drug Metabolism and Disposition, 1982. 10(3): p. 236-240.

260. Chou, M.W. and P.P. Fu, Formation of DHP-derived DNA adducts in vivo from dietary supplements and Chinese herbal plant extracts containing carcinogenic pyrrolizidine alkaloids. Toxicology and industrial health, 2006. 22(8): p. 321-327.

261. Prakash, A.S., et al., Pyrrolizidine alkaloids in human diet. Mutation Research/Genetic Toxicology and Environmental Mutagenesis, 1999. 443(1): p. 53-67.

262. Xia, Q., et al., 7-Glutathione pyrrole adduct: a potential DNA reactive metabolite of pyrrolizidine alkaloids. Chemical research in toxicology, 2015. 28(4): p. 615-620.

263. Zhao, Y., et al., Reaction of dehydropyrrolizidine alkaloids with valine and hemoglobin. Chemical Research in Toxicology, 2014. 27(10): p. 1720-1731.

264. Seawright, A. Potential Toxicity Problems with Herbal Medicines and Food-New Observations with Pyrrolizidine Alkaloids. in PROCEEDINGS-NUTRITION SOCIETY OF AUSTRALIA. 1992. NUTRITION SOCIETY OF AUSTRALIA.

265. Prakash, A.S., et al., Pyrrolizidine alkaloids in human diet. Mutation Research/Genetic Toxicology and Environmental Mutagenesis, 1999. 443(1-2): p. 53-67.

266. Huxtable, R., et al., Sulfur conjugates as putative pneumotoxic metabolites of the pyrrolizidine alkaloid, monocrotaline. Biological Reactive Intermediates IV, 1991: p. 605-612.

267. He, X., et al., 7-N-Acetylcysteine-pyrrole conjugate—A potent DNA reactive metabolite of pyrrolizidine alkaloids. journal of food and drug analysis, 2016. 24(4): p. 682-694.

268. He, X., et al., 7-cysteine-pyrrole conjugate: A new potential DNA reactive metabolite of pyrrolizidine alkaloids Part C Environmental carcinogenesis & ecotoxicology reviews. 2016.

269. (CONTAM), E.P.o.C.i.t.F.C., Scientific Opinion on Pyrrolizidine alkaloids in food and feed. EFSA Journal ;, 2011. 9(11): p. 2406.

270. Diaz, G.J., L.X. Almeida, and D.R. Gardner, Effects of dietary Crotalaria pallida seeds on the health and performance of laying hens and evaluation of residues in eggs. Research in veterinary science, 2014. 97(2): p. 297-303.

271. Gardner, D., et al., Detection of dehydropyrrolizidine alklaoids in honey, pollen, eggs and the associated Senecio species. Planta Medica, 2014. 80(10): p. PV5.

272. Mulder, P.P., et al., Transfer of pyrrolizidine alkaloids from various herbs to eggs and meat in laying hens. Food Additives & Contaminants: Part A, 2016. 33(12): p. 1826-1839.

273. Willmot, F. and G. Robertson, Senecio disease, or cirrhosis of the liver due to Senecio poisoning. The Lancet, 1920. 196(5069): p. 848-849.

274. Fox, D.W., et al., Pyrrolizidine (Senecio) intoxication mimicking Reye syndrome. The Journal of pediatrics, 1978. 93(6): p. 980-982.

275. Huxtable, R.J., Herbal teas and toxins: novel aspects of pyrrolizidine poisoning in the United States. Perspectives in Biology and Medicine, 1980. 24(1): p. 1-14.

276. Zuckerman, M., V. Steenkamp, and M. Stewart, Hepatic veno-occlusive disease as a result of a traditional remedy: confirmation of toxic pyrrolizidine alkaloids as the cause, using an in vitro technique. Journal of clinical pathology, 2002. 55(9): p. 676-679.

277. Steenkamp, V., M.J. Stewart, and M. Zuckerman, Clinical and analytical aspects of pyrrolizidine poisoning caused by South African traditional medicines. Therapeutic Drug Monitoring, 2000. 22(3): p. 302-306.

278. Birecka, H., J. Catalfamo, and R. Eisen, A sensitive method for detection and quantitative determination of pyrrolizidine alkaloids. Phytochemistry, 1981. 20(2): p. 343-344.

279. Schroff, F., et al. Acute liver failure after accidental intake of pyrrolizidine-containing plants. in CLINICAL TOXICOLOGY. 2013. INFORMA HEALTHCARE 52 VANDERBILT AVE, NEW YORK, NY 10017 USA.

280. FURUYA, T., M. HIKICHI, and Y. IITAKA, Fukinotoxin, a new pyrrolizidine alkaloid from Petasites japonicus. Chemical and Pharmaceutical Bulletin, 1976. 24(5): p. 1120-1122.

281. Hirono, I., et al., Carcinogenic activity of petasitenine, a new pyrrolizidine alkaloid isolated from Petasites japonicus Maxim. Journal of the National Cancer Institute, 1977. 58(4): p. 1155-1157.

282. Adamczak, A., et al., Content of pyrrolizidine alkaloids in the leaves of coltsfoot (Tussilago farfara L.) in Poland. Acta Societatis Botanicorum Poloniae, 2013. 82(4).

283. Nedelcheva, A., N. Kostova, and A. Sidjimov, Pyrrolizidine alkaloids in Tussilago farfara from Bulgaria. Biotechnology & Biotechnological Equipment, 2015. 29(sup1): p. S1-S7.

284. Kopp, T., M. Abdel-Tawab, and B. Mizaikoff, Extracting and analyzing pyrrolizidine alkaloids in medicinal plants: A review. Toxins, 2020. 12(5): p. 320.

285. Kumana, C., et al., Herbal tea induced hepatic veno-occlusive disease: quantification of toxic alkaloid exposure in adults. Gut, 1985. 26(1): p. 101-104.

286. Mohabbat, O., et al., An outbreak of hepatic veno-occlusive disease in north-western Afghanistan. The Lancet, 1976. 308(7980): p. 269-271.

287. Roulet, M., et al., Hepatic veno-occlusive disease in newborn infant of a woman drinking herbal tea. The Journal of pediatrics, 1988. 112(3): p. 433-436.

288. Tandon, B.N., et al., An epidemic of veno-occlusive disease of liver in central India. The Lancet, 1976. 308(7980): p. 271-272.

289. Mattocks, A., Hepatotoxic effects due to pyrrolizidine alkaloid N-oxides. Xenobiotica, 1971. 1(4-5): p. 563-565.

290. Mattocks, A., Toxicity and metabolism of Senecio alkaloids. Phytochemical ecology, 1972: p. 179-200.

291. Culvenor, C., et al., Pyrrolizidine alkaloids as alkylating and antimitotic agents. Annals of the New York Academy of Sciences, 1969. 163(2): p. 837-847.

292. Bull, L.B., C.t. Culvenor, and A. Dick, The pyrrolizidine alkaloids: their chemistry, pathogenicity and other biological properties. The pyrrolizidine alkaloids: their chemistry, pathogenicity and other biological properties., 1968(9).

293. Bull, L., A. Dick, and J. McKenzie, The acute toxic effects of heliotrine and lasiocarpine, and their N-oxides, on the rat. The Journal of Pathology and Bacteriology, 1958. 75(1): p. 17-25.

294. Downing, D. and J. Peterson, Quantitative assessment of the persistent antimitotic effect of certain hepatotoxic pyrrolizidine alkaloids on rat liver. Australian Journal of Experimental Biology and Medical Science, 1968. 46(5): p. 493-502.

295. Dalefield, R., et al., Determination of the single-dose 72-hour oral gavage LD50 values of monocrotaline and riddelliine in male Han Wistar rats using the up-and-down procedure. J. Herbal Med. Toxicol, 2012. 6: p. 153-165.

296. Dalefield, R.R., M.A. Gosse, and U. Mueller, A 28-day oral toxicity study of echimidine and lasiocarpine in Wistar rats. Regulatory Toxicology and Pharmacology, 2016. 81: p. 146-154.

297. Panel, E.C., EFSA Panel on Contaminants in the Food Chain. 2011. Scientific opinion on tolerable weekly intake for cadmium. EFSA J, 1975. 9.

298. Wang, C., et al., The comparative pharmacokinetics of two pyrrolizidine alkaloids, senecionine and adonifoline, and their main metabolites in rats after intravenous and oral administration by UPLC/ESIMS. Analytical and bioanalytical chemistry, 2011. 401(1): p. 275-287.

299. Cheeke, P. and L. Shull, Natural toxicants in feeds and livestock. West Port: AVI Publishing Inc, 1985: p. 1-2.

300. Jago, M.V., A method for the assessment of the chronic hepatoxicity of pyrrolizidine alkaloids. Australian Journal of Experimental Biology and Medical Science, 1970. 48(1): p. 93-103.

301. Culvenor, C., et al., Hepato-and pneumotoxicity of pyrrolizidine alkaloids and derivatives in relation to molecular structure. Chemico-biological interactions, 1976. 12(3-4): p. 299-324.

302. He, Y., et al., Lung injury induced by pyrrolizidine alkaloids depends on metabolism by hepatic cytochrome P450s and blood transport of reactive metabolites. Arch Toxicol, 2021. 95(1): p. 103-116.

303. Xiao, R., et al., Monocrotaline pyrrole induces pulmonary endothelial damage through binding to and release from erythrocytes in lung during venous blood reoxygenation. Am J Physiol Lung Cell Mol Physiol, 2019. 316(5): p. L798-l809.

304. Chan, P., NTP technical report on the toxicity studies of Riddelliine (CAS No. 23246-96-0) Administered by Gavage to F344 Rats and B6C3F1 Mice. Toxicity report series, 1993. 27: p. 1-D9.

305. Chan, P., et al., Toxicity and carcinogenicity of riddelliine following 13 weeks of treatment to rats and mice. Toxicon, 1994. 32(8): p. 891-908.

306. Chen, L., et al., Risk assessment for pyrrolizidine alkaloids detected in (herbal) teas and plant food supplements. Regulatory Toxicology and Pharmacology, 2017. 86: p. 292-302.

307. Alkaloids, P., Health and Safety Guide No. 26. World Health Organization, Geneva, 1989.

308. Cancer, I.A.f.R.o., Some naturally occurring substances. Vol. 10. 1976: International Agency for Research on Cancer.

309. Humans, I.W.G.o.t.E.o.t.C.R.o.C.t., I.A.f.R.o. Cancer, and W.H. Organization, Some Food Additives, Feed Additives and Naturally Occurring Substances. Vol. 31. 1983: World Health Organization.

310. Cancer, I.A.f.R.o., Overall evaluations of carcinogenicity: an updating of IARC monographs volumes 1 to 42. 1987: IARC Lyon, France:.

311. Ruan, J., et al., Lack of metabolic activation and predominant formation of an excreted metabolite of nontoxic platynecine-type pyrrolizidine alkaloids. Chemical research in toxicology, 2014. 27(1): p. 7-16.

312. Hirono, I., et al., Induction of hepatic tumors in rats by senkirkine and symphytine. Journal of the National Cancer Institute, 1979. 63(2): p. 469-472.

313. Kuhara, K., et al., Carcinogenic activity of clivorine, a pyrrolizidine alkaloid isolated from Ligularia dentata. Cancer letters, 1980. 10(2): p. 117-122.

314. Schoental, R., Pancreatic islet-cell and other tumors in rats given heliotrine, a monoester pyrrolizidine alkaloid, and nicotinamide. Cancer research, 1975. 35(8): p. 2020-2024.

315. Schoental, R., G. Hard, and S. Gibbard, Histopathology of renal lipomatous tumors in rats treated with the “natural” products, pyrrolizidine alkaloids and α, β-unsaturated aldehydes. Journal of the National Cancer Institute, 1971. 47(5): p. 1037-1044.

316. Schoental, R. and J. Cavanagh, Brain and spinal cord tumors in rats treated with pyrrolizidine alkaloids. Journal of the National Cancer Institute, 1972. 49(3): p. 665-671.

317. Schoental, R., M.A. Head, and P. Peacock, Senecio alkaloids: primary liver tumours in rats as a result of treatment with (1) a mixture of alkaloids from S. jacobaea Lin.;(2) retrorsine;(3) isatidine. British journal of cancer, 1954. 8(3): p. 458.

318. Rao, M. and J. Reddy, Malignant neoplasms in rats fed lasiocarpine. British journal of cancer, 1978. 37(2): p. 289-293.

319. Chou, M.W., et al., Correlation of DNA adduct formation and riddelliine-induced liver tumorigenesis in F344 rats and B6C3F1 mice [Cancer Lett. 193 (2003) 119–125]. Cancer letters, 2004. 207(1): p. 119-125.

320. Yang, Y.-C., et al., Development of a 32P-postlabeling/HPLC method for detection of dehydroretronecine-derived DNA adducts in vivo and in vitro. Chemical research in toxicology, 2001. 14(1): p. 91-100.

321. Wang, Y.-P., et al., Metabolic activation of the tumorigenic pyrrolizidine alkaloid, monocrotaline, leading to DNA adduct formation in vivo. Cancer letters, 2005. 226(1): p. 27-35.

322. Yan, J., et al., Detection of riddelliine-derived DNA adducts in blood of rats fed riddelliine. International Journal of Molecular Sciences, 2002. 3(9): p. 1019-1026.

323. Mirsalis, J.C., In vivo measurement of unscheduled DNA synthesis and S-phase synthesis as an indicator of hepatocarcinogenesis in rodents. Cell Biology and Toxicology, 1987. 3(2): p. 165-173.

324. Mirsalis, J.C., et al., Evaluation of the potential of riddelliine to induce unscheduled DNA synthesis, S-phase synthesis, or micronuclei following in vivo treatment with multiple doses. Environmental and molecular mutagenesis, 1993. 21(3): p. 265-271.

325. Program, N.T., Toxicology and carcinogenesis studies of riddelliine (CAS No. 23246-96-0) in F344/N rats and B6C3F1 mice (gavage studies). National Toxicology Program technical report series, 2003(508): p. 1-280.

326. Griffin, D. and H. Segall, Genotoxicity and cytotoxicity of selected pyrrolizidine alkaloids, a possible alkenal metabolite of the alkaloids, and related alkenals. Toxicology and applied pharmacology, 1986. 86(2): p. 227-234.

327. Mori, H., et al., Genotoxicity of a variety of pyrrolizidine alkaloids in the hepatocyte primary culture-DNA repair test using rat, mouse, and hamster hepatocytes. Cancer research, 1985. 45(7): p. 3125-3129.

328. Williams, G.M., et al., Genotoxicity of pyrrolizidine alkaloids in the hepatocyte primary culture/DNA-repair test. Mutation Research/Genetic Toxicology, 1980. 79(1): p. 1-5.

329. Coulombe, R.A., G.L. Drew, and F.R. Stermitz, Pyrrolizidine Alkaloids Crosslink DNA with Actin. Toxicology and Applied Pharmacology, 1999. 154(2): p. 198-202.

330. Hincks, J.R., et al., DNA cross-linking in mammalian cells by pyrrolizidine alkaloids: Structure-activity relationships. Toxicology and Applied Pharmacology, 1991. 111(1): p. 90-98.

331. Kim, H.-Y., et al., Comparative DNA cross-linking by activated pyrrolizidine alkaloids. Food and chemical toxicology, 1999. 37(6): p. 619-625.

332. Petry, T.W., et al., Characterization of hepatic DNA damage induced in rats by the pyrrolizidine alkaloid monocrotaline. Cancer research, 1984. 44(4): p. 1505-1509.

333. Coulombe Jr, R.A., G.L. Drew, and F.R. Stermitz, Pyrrolizidine alkaloids crosslink DNA with actin. Toxicology and applied pharmacology, 1999. 154(2): p. 198-202.

334. Pereira, T.N., et al., Dehydromonocrotaline generates sequence-selective N-7 guanine alkylation and heat and alkali stable multiple fragment DNA crosslinks. Nucleic acids research, 1998. 26(23): p. 5441-5447.

335. Reed, R.L., et al., Crosslinking of DNA by dehydroretronecine, a metabolite of pyrrolizidine alkaloids. Carcinogenesis, 1988. 9(8): p. 1355-1361.

336. White, I. and A. Mattocks, Reaction of dihydropyrrolizines with deoxyribonucleic acids in vitro. Biochemical Journal, 1972. 128(2): p. 291-297.

337. Silva-Neto, J., et al., Genotoxicity and morphological changes induced by the alkaloid monocrotaline, extracted from Crotalaria retusa, in a model of glial cells. Toxicon, 2010. 55(1): p. 105-117.

338. Uhl, M., C. Helma, and S. Knasmüller, Evaluation of the single cell gel electrophoresis assay with human hepatoma (Hep G2) cells. Mutation Research/Genetic Toxicology and Environmental Mutagenesis, 2000. 468(2): p. 213-225.

339. Sanderson, B. and A. Clark, Micronuclei in adult and foetal mice exposed in vivo to heliotrine, urethane, monocrotaline and benzidine. Mutation Research/Fundamental and Molecular Mechanisms of Mutagenesis, 1993. 285(1): p. 27-33.

340. Müller-Tegethoff, K., et al., Application of the in vitro rat hepatocyte micronucleus assay in genetic toxicology testing. Mutation Research/Genetic Toxicology and Environmental Mutagenesis, 1997. 392(1-2): p. 125-138.

341. Takanashi, H., M. Umeda, and I. Hirono, Chromosomal aberrations and mutation in cultured mammalian cells induced by pyrrolizidine alkaloids. Mutation Research/Genetic Toxicology, 1980. 78(1): p. 67-77.

342. Organization, W.H., Pyrrolizidine alkaloids. 1988: World Health Organization.

343. Mei, N., et al., Differential mutagenicity of riddelliine in liver endothelial and parenchymal cells of transgenic big blue rats. Cancer letters, 2004. 215(2): p. 151-158.

344. Mei, N., et al., Mutations induced by the carcinogenic pyrrolizidine alkaloid riddelliine in the liver cII gene of transgenic big blue rats. Chemical research in toxicology, 2004. 17(6): p. 814-818.

345. Rubiolo, P., et al., Mutagenicity of pyrrolizidine alkaloids in the Salmonella typhimurium/mammalian microsome system. Mutation Research Letters, 1992. 281(2): p. 143-147.

346. Yamanaka, H., et al., Mutagenicity of pyrrolizidine alkaloids in the Salmonella/mammalian-microsome test. Mutation Research/Genetic Toxicology, 1979. 68(3): p. 211-216.

347. Wehner, F., P. Thiel, and S. Van Rensburg, Mutagenicity of alkaloids in the Salmonella/microsome system. Mutat. Res, 1979. 66: p. 187-190.

348. Edgar, J., et al., Pyrrolizidine alkaloids in food: a spectrum of potential health consequences. Food Additives & Contaminants: Part A, 2011. 28(3): p. 308-324.

349. Yang, X., et al., Comparative Study of Hepatotoxicity of Pyrrolizidine Alkaloids Retrorsine and Monocrotaline. Chemical Research in Toxicology, 2017. 30(2): p. 532-539.

350. Yang, M., et al., Absorption difference between hepatotoxic pyrrolizidine alkaloids and their N-oxides–Mechanism and its potential toxic impact. Journal of ethnopharmacology, 2020. 249: p. 112421.

351. Widjaja, F., Y. Alhejji, and I.M. Rietjens, The Role of Kinetics as Key Determinant in Toxicity of Pyrrolizidine Alkaloids and Their N-Oxides. Planta medica, 2022. 88(02): p. 130-143.

352. Tu, M., et al., Organic cation transporter 1 mediates the uptake of monocrotaline and plays an important role in its hepatotoxicity. Toxicology, 2013. 311(3): p. 225-230.

353. Koepsell, H. and H. Endou, The SLC22 drug transporter family. Pflügers Archiv, 2004. 447(5): p. 666-676.

354. Tu, M., et al., Involvement of organic cation transporter 1 and CYP3A4 in retrorsine-induced toxicity. Toxicology, 2014. 322: p. 34-42.

355. Evans, D., et al., Measurement of gastrointestinal pH profiles in normal ambulant human subjects. Gut, 1988. 29(8): p. 1035-1041.

356. McConnell, E.L., A.W. Basit, and S. Murdan, Measurements of rat and mouse gastrointestinal pH, fluid and lymphoid tissue, and implications for in-vivo experiments. Journal of Pharmacy and Pharmacology, 2008. 60(1): p. 63-70.

357. Yang, M., et al., Intestinal and hepatic biotransformation of pyrrolizidine alkaloid N-oxides to toxic pyrrolizidine alkaloids. Archives of Toxicology, 2019. 93(8): p. 2197-2209.

358. Powis, G., M.M. Ames, and J.S. Kovach, Metabolic conversion of indicine N-oxide to indicine in rabbits and humans. Cancer Research, 1979. 39(9): p. 3564-3570.

359. Chu, P.-S., M.W. Lamé, and H. Segall, In vivo metabolism of retrorsine and retrorsine-N-oxide. Archives of toxicology, 1993. 67(1): p. 39-43.

360. Jago, M.V., et al., Metabolic conversion of heliotridine-based pyrrolizidine alkaloids to dehydroheliotridine. Molecular pharmacology, 1970. 6(4): p. 402-406.

361. Phillipson, J. and S. Handa, Alkaloid N-oxides. A review of recent developments. Lloydia, 1978. 41(5): p. 385-431.

362. Chen, L., et al., Use of physiologically based kinetic modelling-facilitated reverse dosimetry to convert in vitro cytotoxicity data to predicted in vivo liver toxicity of lasiocarpine and riddelliine in rat. Food and Chemical Toxicology, 2018. 116: p. 216-226.

363. Lester, C., et al., Intrinsic relative potency of a series of pyrrolizidine alkaloids characterized by rate and extent of metabolism. Food and Chemical Toxicology, 2019. 131: p. 110523.

364. Suparmi, S., S. Wesseling, and I.M. Rietjens, Monocrotaline-induced liver toxicity in rat predicted by a combined in vitro physiologically based kinetic modeling approach. Archives of toxicology, 2020. 94(9): p. 3281-3295.

365. Hessel, S., et al., Structure–activity relationship in the passage of different pyrrolizidine alkaloids through the gastrointestinal barrier: ABCB1 excretes heliotrine and echimidine. Molecular nutrition & food research, 2014. 58(5): p. 995-1004.

366. Jewell, C., et al., Specificity of procaine and ester hydrolysis by human, minipig, and rat skin and liver. Drug Metabolism and Disposition, 2007. 35(11): p. 2015-2022.

367. Dueker, S.R., et al., Guinea pig and rat hepatic microsomal metabolism of monocrotaline. Drug metabolism and disposition, 1992. 20(2): p. 275-280.

368. Williams, D.E., et al., The role of flavin-containing monooxygenase in the N-oxidation of the pyrrolizidine alkaloid senecionine. Drug metabolism and disposition, 1989. 17(4): p. 380-386.

369. Dai, J., F. Zhang, and J. Zheng, Retrorsine, but not monocrotaline, is a mechanism-based inactivator of P450 3A4. Chemico-Biological Interactions, 2010. 183(1): p. 49-56.

370. Gordon, G.J., W.B. Coleman, and J.W. Grisham, Induction of cytochrome P450 enzymes in the livers of rats treated with the pyrrolizidine alkaloid retrorsine. Experimental and molecular pathology, 2000. 69(1): p. 17-26.

371. Luckert, C., et al., Hepatotoxic pyrrolizidine alkaloids: Structure-dependent activation of PXR and PXR-mediated induction of CYP3A4 expression. Toxicology Letters, 2016(258): p. S256.

372. Luckert, C., et al., PXR: Structure-specific activation by hepatotoxic pyrrolizidine alkaloids. Chemico-Biological Interactions, 2018. 288: p. 38-48.

373. Reid, M., et al., Effect of monocrotaline metabolites on glutathione levels in human and bovine pulmonary artery endothelial cells. Research communications in molecular pathology and pharmacology, 1998. 99(1): p. 53-68.

374. Yan, C.C. and R.J. Huxtable, Relationship between glutathione concentration and metabolism of the pyrrolizidine alkaloid, monocrotaline, in the isolated, perfused liver. Toxicology and applied pharmacology, 1995. 130(1): p. 132-139.

375. Yan, C.C. and R.J. Huxtable, Effects of monocrotaline, a pyrrolizidine alkaloid, on glutathione metabolism in the rat. Biochemical pharmacology, 1996. 51(3): p. 375-379.

376. Medeiros, R.M.T., S.L. Górniak, and J.L. Guerra, Fetotoxicity and reproductive effects of monocrotaline in pregnant rats. Journal of ethnopharmacology, 2000. 69(2): p. 181-188.

377. Sandini, T.M., et al., Prenatal exposure to integerrimine N-oxide impaired the maternal care and the physical and behavioral development of offspring rats. International Journal of Developmental Neuroscience, 2014. 36: p. 53-63.

378. Medeiros, R., S. Górniak, and J. Guerra, Comparative study of prenatal and postnatal monocrotaline effects in rats. Toxic plants and other natural toxicants, 1998: p. 312-316.

379. Sandini, T.M., et al., Prenatal exposure to integerrimine N-oxide enriched butanolic residue from Senecio brasiliensis affects behavior and striatal neurotransmitter levels of rats in adulthood. International Journal of Developmental Neuroscience, 2015. 47: p. 157-164.

380. Hueza, I., et al. A Postnatal Evaluation of the Immunotoxic Effect of Integerrimine N-oxide Exposure during Gestation to Rats. in BIRTH DEFECTS RESEARCH PART A-CLINICAL AND MOLECULAR TERATOLOGY. 2011. WILEY-BLACKWELL COMMERCE PLACE, 350 MAIN ST, MALDEN 02148, MA USA.

381. Hueza, I.M., et al., Low doses of monocrotaline in rats cause diminished bone marrow cellularity and compromised nitric oxide production by peritoneal macrophages. Journal of Immunotoxicology, 2009. 6(1): p. 11-18.

382. Benassi, J., et al., Comparative study of monocrotaline toxicity on peritoneal macrophage activity when dosed for 14 or 28 days, in Poisoning by plants, mycotoxins and related toxins. 2011, CABI Wallingford UK. p. 572-576.

383. Elias, F., et al., Haematological and immunological effects of repeated dose exposure of rats to integerrimine N-oxide from Senecio brasiliensis. Food and chemical toxicology, 2011. 49(9): p. 2313-2319.

384. Deyo, J.A. and N.I. Kerkvliet, Immunotoxicity of the pyrrolizidine alkaloid monocrotaline following subchronic administration to C57B16 mice. Fundamental and Applied Toxicology, 1990. 14(4): p. 842-849.

385. Deyo, J.A. and N.I. Kerkvliet, Tier-2 studies on monocrotaline immunotoxicity in C57BL/6 mice. Toxicology, 1991. 70(3): p. 313-325.

386. Coll, C., et al., Effect of Monocrotaline on Blood-BrainBarrier Permeability in Rats. Latin American Journal of Pharmacy, 2011. 30(2): p. 412-6.

387. Wang, C.-C., et al., Metabolic activation of pyrrolizidine alkaloids leading to phototoxicity and photogenotoxicity in human HaCaT keratinocytes. Journal of Environmental Science and Health, Part C, 2014. 32(4): p. 362-384.

388. Zhao, Y., et al., Photoirradiation of dehydropyrrolizidine alkaloids—formation of reactive oxygen species and induction of lipid peroxidation. Toxicology letters, 2011. 205(3): p. 302-309.

389. WHO-IPCS, Pyrrolizidine alkaloids. Environmental Health Criteria 80, 1988: p. 1-345.

390. Chow, L.-H., et al., Low serum 25-hydroxyvitamin in hereditary hemochromatosis: relation to iron status. Gastroenterology, 1985. 88(4): p. 865-869.

391. COT, COT statement on pyrrolizidine alkaloids in food. 2008.

392. Bundesgesundheitsamt, Bekanntmachung über die Zulassung und Registrierung von Arzneimitteln (Abwehr von Arzneimittelrisiken–Stufe II). Bundesanzeiger, 1992. 111: p. 4805-4807.

393. REGULATION, H.A.T., Council Regulation (EEC) No 315/93 of 8 February 1993 laying down Community procedures for contaminants in food. Official Journal L, 1993. 37(13/02): p. 0001-0003.

394. Kempf, M., A. Reinhard, and T. Beuerle, Pyrrolizidine alkaloids (PAs) in honey and pollen-legal regulation of PA levels in food and animal feed required. Molecular nutrition & food research, 2010. 54(1): p. 158-168.

395. Smith, L. and C. Culvenor, Plant sources of hepatotoxic pyrrolizidine alkaloids. Journal of Natural Products, 1981. 44(2): p. 129-152.

396. Xia, Q., et al., Formation of DHP-derived DNA adducts from metabolic activation of the prototype heliotridine-type pyrrolizidine alkaloid, lasiocarpine. Cancer Letters, 2006. 231(1): p. 138-145.

397. Abdelfatah, S., et al., Pyrrolizidine alkaloids cause cell cycle and DNA damage repair defects as analyzed by transcriptomics in cytochrome P450 3A4-overexpressing HepG2 clone 9 cells. Cell biology and toxicology, 2022. 38(2): p. 325-345.

398. Williams, L., et al., Toxicokinetics of Riddelliine, a Carcinogenic Pyrrolizidine Alkaloid, and Metabolites in Rats and Mice. Toxicology and Applied Pharmacology, 2002. 182(2): p. 98-104.

399. Kim, H., et al., Structural influences on pyrrolizidine alkaloid-induced cytopathology. Toxicology and applied pharmacology, 1993. 122(1): p. 61-69.

400. Bruggeman, I.M. and J.C.M. van der Hoeven, Induction of SCEs by some pyrrolizidine alkaloids in V79 Chinese hamster cells co-cultured with chick embryo hepatocytes. Mutation Research Letters, 1985. 142(4): p. 209-212.

401. Wang, Z., et al., Combined Hepatotoxicity and Toxicity Mechanism of Intermedine and Lycopsamine. Toxins, 2022. 14(9): p. 633.

402. Kanda, T., K.F. Sullivan, and G.M. Wahl, Histone–GFP fusion protein enables sensitive analysis of chromosome dynamics in living mammalian cells. Current Biology, 1998. 8(7): p. 377-385.

403. Utani, K.-i., et al., Emergence of micronuclei and their effects on the fate of cells under replication stress. PloS one, 2010. 5(4): p. e10089.

404. Reimann, H., H. Stopper, and H. Hintzsche, Long-term fate of etoposide-induced micronuclei and micronucleated cells in Hela-H2B-GFP cells. Archives of toxicology, 2020. 94(10): p. 3553-3561.

405. Papermaster, B.R.a.B.W., Membrane Properties Of Living Mammalian Cells As Studied By Enzymatic Hydrolysis Of Fluorogenic Esters. Biochemistry, 1966. 55: p. 134-141.

406. (2013), B., Safety Report for GelRed and GelGreen. Nucleic acid detection technologies. Accessed Oct 2014(http://www.biotium.com).

407. Anjomshoa, M. and M. Torkzadeh-Mahani, Competitive DNA-Binding Studies between Metal Complexes and GelRed as a New and Safe Fluorescent DNA Dye. J Fluoresc, 2016. 26(4): p. 1505-10.

408. Crisafuli, F.A., E.B. Ramos, and M.S. Rocha, Characterizing the interaction between DNA and GelRed fluorescent stain. Eur Biophys J, 2015. 44(1-2): p. 1-7.

409. OECD, Test No. 487: In Vitro Mammalian Cell Micronucleus Test. 2016.

410. Luckert, C., et al., Comparative analysis of 3D culture methods on human HepG2 cells. Arch Toxicol, 2017. 91(1): p. 393-406.

411. Badolo, L., et al., Evaluation of 309 molecules as inducers of CYP3A4, CYP2B6, CYP1A2, OATP1B1, OCT1, MDR1, MRP2, MRP3 and BCRP in cryopreserved human hepatocytes in sandwich culture. Xenobiotica, 2015. 45(2): p. 177-87.

412. Nagai, M., et al., Establishment of In Silico Prediction Models for CYP3A4 and CYP2B6 Induction in Human Hepatocytes by Multiple Regression Analysis Using Azole Compounds. Drug Metab Dispos, 2016. 44(8): p. 1390-8.

413. Yang, K. and K.H. koh, Induction of CYP2B6 and CYP3A4 Expression by 1Aminobenzotriazole (ABT) in Human Hepatocytes by yang2010.pdf. Drug MetabLett

2010. 4(3): p. 129-33.

414. Forsch, K., et al., Development of an in vitro screening method of acute cytotoxicity of the pyrrolizidine alkaloid lasiocarpine in human and rodent hepatic cell lines by increasing susceptibility. J Ethnopharmacol, 2018. 217: p. 134-139.

415. Yang, K., K.H. Koh, and H. Jeong, Induction of CYP2B6 and CYP3A4 expression by 1-aminobenzotriazole (ABT) in human hepatocytes. Drug Metab Lett, 2010. 4(3): p. 129-33.

416. Araki, N., et al., Inhibition of CYP3A4 by 6',7'-dihydroxybergamottin in human CYP3A4 over-expressed hepG2 cells. J Pharm Pharmacol, 2012. 64(12): p. 1715-21.

417. Novotna, A., et al., Dual effects of ketoconazole cis-enantiomers on CYP3A4 in human hepatocytes and HepG2 Cells. PLoS One, 2014. 9(10): p. e111286.

418. Weemhoff, J.L., et al., Apparent mechanism-based inhibition of human CYP3A in-vitro by lopinavir. J Pharm Pharmacol, 2003. 55(3): p. 381-6.

419. Westerink, W.M. and W.G. Schoonen, Cytochrome P450 enzyme levels in HepG2 cells and cryopreserved primary human hepatocytes and their induction in HepG2 cells. Toxicol In Vitro, 2007. 21(8): p. 1581-91.

420. Dorothea Sesardic, A.R.B., B. P. Murray, S. Murray, J. Segura, R. De La Torre & D. S. Davies, Furafylline is a potent and selective inhibitor of cytochrome P450IA2 in man by sesardic1990.pdf. Br. J. clin. Pharmac., 1990. 29: p. 651-663.

421. Jordi Segura, I.G., Emili Tarrus, Some pharmacokinetic of furafylline, a new 1,3,8-trisubsituted xanthin by segura1986.pdf. J. Pharm. Pharmacol. , 1986. 38: p. 615-618.

422. Trager, K.L.K.a.W.F., Isoform-selective mechanism-based inhibition of human cytochrome P450 1A2 by furafylline by kunze1993.pdf. Chem. Res. Toxicol. 1993,6, 649-656 1993. 6: p. 649-656.

423. Griffith, O.W. and A. Meister, Potent and specific inhibition of glutathione synthesis by buthionine sulfoximine (Sn-butyl homocysteine sulfoximine). Journal of Biological Chemistry, 1979. 254(16): p. 7558-7560.

424. Drew, R. and J.O. Miners, The effects of buthionine sulphoximine (BSO) on glutathione depletion and xenobiotic biotransformation. Biochemical pharmacology, 1984. 33(19): p. 2989-2994.

425. Chen, Y., et al., Glutathione defense mechanism in liver injury: insights from animal models. Food and chemical toxicology, 2013. 60: p. 38-44.

426. C. Muller, F.G., E. Ferrandis, I. Cornil-Scharwtz, J. D. Bailly, C. Bordier, J. Benard, B. I. Sikic, And G. Laurent, Evidence for Transcriptional Control of Human MDR l Gene expression

by verapamil in Multidrug-resistant leukimic cells by MULLER 1995.pdf. MOLECULAR PHARMACOLOGY, 1995. 47: p. 51-56.

427. Donmez, Y., et al., Effect of MDR modulators verapamil and promethazine on gene expression levels of MDR1 and MRP1 in doxorubicin-resistant MCF-7 cells. Cancer Chemother Pharmacol, 2011. 67(4): p. 823-8.

428. S. Nobili, I.L., B. Giglioni and E. Mini, Pharmacological Strategies for Overcoming Multidrug Resistance by nobili2006.pdf. Current Drug Targets, 2006. 7: p. 861-879.

429. Sinclair, D.S. and I.H. Fox, The pharmacology of hypouricemic effect of benzbromarone. J Rheumatol, 1975. 2(4): p. 437-45.

430. M. T. Huisman, J.S., J. Monbaliu, M. Martens, V. Sekar, A. Raoof, in_vitro_studies_investigating_the_mechanism_of_interaction_between_tmc435_and_hepatic_transporters_2010.pdf. Poster presented at the 61st AASLD Meeting, Boston, MA, USA, 2010.

431. Tice, R.R., et al., Single cell gel/comet assay: guidelines for in vitro and in vivo genetic toxicology testing. Environmental and molecular mutagenesis, 2000. 35(3): p. 206-221.

432. Hartmann, G.S.a.A., The Comet Assay: A Sensitive Genotoxicity Test for the Detection of DNA Damage. Methods in Molecular Biology, 2005. 291.

433. Collins, A.R., The Comet Assay for DNA Damage and Repair. MOLECULAR BIOTECHNOLOGY, 2004. 26: p. 249-261.

434. Narendra P. Singh, M.T.M., Raymond R. Tice and Edward L. Schneider, A Simple Technique for Quantitation of Low Levels of DNA Damage in Individual Cells. Experimental Cell Research 1988. 175: p. 184-191.

435. Wolf, S.P.a.H.U., Detection of DNA-Crosslinking Agents With the Alkaline Comet Assay. Environmental and Molecular Mutagenesis 1996. 27: p. 196-201.

436. Swift, L.P., L. Castle, and P.J. McHugh, Analysis of DNA Interstrand Cross-Links and their Repair by Modified Comet Assay. Methods Mol Biol, 2020. 2119: p. 79-88.

437. Mukhopadhyay, R., P. Dubey, and S. Sarkar, Structural changes of DNA induced by mono- and binuclear cancer drugs. J Struct Biol, 2005. 150(3): p. 277-83.

438. Brulikova, L., J. Hlavac, and P. Hradil, DNA interstrand cross-linking agents and their chemotherapeutic potential. Curr Med Chem, 2012. 19(3): p. 364-85.

439. Pfuhler, S. and H.U. Wolf, Detection of DNA-crosslinking agents with the alkaline comet assay. Environ Mol Mutagen, 1996. 27(3): p. 196-201.

440. Trachootham, D., J. Alexandre, and P. Huang, Targeting cancer cells by ROS-mediated mechanisms: a radical therapeutic approach? Nature reviews. Drug discovery, 2009. 8(7): p. 579-591.

441. Azad, M.B., Y. Chen, and S.B. Gibson, Regulation of autophagy by reactive oxygen species (ROS): implications for cancer progression and treatment. Antioxidants & redox signaling, 2009. 11(4): p. 777-790.

442. Lu, J., et al. A novel and compact review on the role of oxidative stress in female reproduction. Reproductive biology and endocrinology : RB&E, 2018. 16, 80 DOI: 10.1186/s12958-018-0391-5.

443. Kelly, G.S., Clinical applications of N-acetylcysteine. Alternative medicine review : a journal of clinical therapeutic, 1998. 3(2): p. 114-127.

444. Gillissen, A. and D. Nowak, Characterization of N-acetylcysteine and ambroxol in anti-oxidant therapy. Respiratory medicine, 1998. 92(4): p. 609-623.

445. Sun, S.-Y., N-acetylcysteine, reactive oxygen species and beyond. Cancer biology & therapy, 2010. 9(2): p. 109-110.

446. Bratic, I. and A. Trifunovic, Mitochondrial energy metabolism and ageing. Biochimica et Biophysica Acta (BBA) - Bioenergetics, 2010. 1797(6): p. 961-967.

447. Guengerich, F.P., Cytochrome P450 enzymes in the generation of commercial products. Nat Rev Drug Discov, 2002. 1(5): p. 359-66.

448. Rendic, S. and F.J. Di Carlo, Human cytochrome P450 enzymes: a status report summarizing their reactions, substrates, inducers, and inhibitors. Drug Metab Rev, 1997. 29(1-2): p. 413-580.

449. Kleider, C., et al., Validation of a GC-and LC-MS/MS based method for the quantification of 22 estrogens and its application to human plasma. Steroids, 2022. 186: p. 109077.

450. Holló, Z., et al., Calcein accumulation as a fluorometric functional assay of the multidrug transporter. Biochimica et biophysica acta, 1994. 1191(2): p. 384-388.

451. Vellonen, K.-S., P. Honkakoski, and A. Urtti, Substrates and inhibitors of efflux proteins interfere with the MTT assay in cells and may lead to underestimation of drug toxicity. European journal of pharmaceutical sciences : official journal of the European Federation for Pharmaceutical Sciences, 2004. 23(2): p. 181-188.

452. Essodaigui, M., H.J. Broxterman, and A. Garnier-Suillerot, Kinetic analysis of calcein and calcein-acetoxymethylester efflux mediated by the multidrug resistance protein and P-glycoprotein. Biochemistry, 1998. 37(8): p. 2243-2250.

453. Polli, J.W., et al., Rational use of in vitro P-glycoprotein assays in drug discovery. The Journal of pharmacology and experimental therapeutics, 2001. 299(2): p. 620-628.

454. Hynes, J., et al., Fluorescence-based cell viability screening assays using water-soluble oxygen probes. Journal of biomolecular screening, 2003. 8(3): p. 264-272.

455. Tiberghien, F. and F. Loor, Ranking of P-glycoprotein substrates and inhibitors by a calcein-AM fluorometry screening assay. Anti-cancer drugs, 1996. 7(5): p. 568-578.

456. Saengkhae, C., C. Loetchutinat, and A. Garnier-Suillerot, Kinetic analysis of fluorescein and dihydrofluorescein effluxes in tumour cells expressing the multidrug resistance protein, MRP1. Biochemical Pharmacology, 2003. 65(6): p. 969-977.

457. De Bruyn, T., et al., Sodium fluorescein is a probe substrate for hepatic drug transport mediated by OATP1B1 and OATP1B3. J Pharm Sci, 2011. 100(11): p. 5018-30.

458. Sweet, D.H., et al., Organic anion and cation transporter expression and function during embryonic kidney development and in organ culture models. Kidney Int, 2006. 69(5): p. 837-45.

459. Cqrazon D. Bucana, R.G., Rajiv Nayar,Catherine A. 0' Ian, Christopher Seid, Laura E. Earnest, Apjd Dominic Fan, Retention of Vital Dyes Correlates Inversely with the multidrug-Resistant Phenotype of Adriamycin-Selected Murine Fibrosarcoma Variants. Experimental Cell Research, 1990. 190: p. 69-75.

460. Lee, W.K., et al., Organic cation transporters OCT1, 2, and 3 mediate high-affinity transport of the mutagenic vital dye ethidium in the kidney proximal tubule. Am J Physiol Renal Physiol, 2009. 296(6): p. F1504-13.

461. Montermini, D., C.P. Winlove, and C. Michel, Effects of perfusion rate on permeability of frog and rat mesenteric microvessels to sodium fluorescein. J Physiol, 2002. 543(Pt 3): p. 959-75.

462. Lee, W.-K., et al., Organic cation transporters OCT1, 2, and 3 mediate high-affinity transport of the mutagenic vital dye ethidium in the kidney proximal tubule. American Journal of Physiology-Renal Physiology, 2009. 296(6): p. F1504-F1513.

463. Bauer, B., D.S. Miller, and G. Fricker, Compound profiling for P-glycoprotein at the blood-brain barrier using a microplate screening system. Pharmaceutical research, 2003. 20(8): p. 1170-1176.

464. Evers, R., et al., Inhibitory effect of the reversal agents V-104, GF120918 and Pluronic L61 on MDR1 Pgp-, MRP1- and MRP2-mediated transport. British journal of cancer, 2000. 83(3): p. 366-374.

465. Homolya, L., et al., Fluorescent cellular indicators are extruded by the multidrug resistance protein. The Journal of biological chemistry, 1993. 268(29): p. 21493-21496.

466. Eneroth, A., et al., Evaluation of a vincristine resistant Caco-2 cell line for use in a calcein AM extrusion screening assay for P-glycoprotein interaction. European journal of pharmaceutical sciences : official journal of the European Federation for Pharmaceutical Sciences, 2001. 12(3): p. 205-214.

467. Kuncharoenwirat, N., W. Chatuphonprasert, and K. Jarukamjorn, Effects of Phenol Red on Rifampicin-Induced Expression of Cytochrome P450s Enzymes. Pharmacophore, 2020. 11(3): p. 13-20.

468. Chen, J. and K. Raymond, Roles of rifampicin in drug-drug interactions: underlying molecular mechanisms involving the nuclear pregnane X receptor. Ann Clin Microbiol Antimicrob, 2006. 5: p. 3.

469. Hesse, L.M., et al., Effect of bupropion on CYP2B6 and CYP3A4 catalytic activity, immunoreactive protein and mRNA levels in primary human hepatocytes: comparison with rifampicin. Journal of Pharmacy and Pharmacology, 2003. 55(9): p. 1229-1239.

470. Kobayashi, T., et al., Peppermint (Mentha piperita L.) extract effectively inhibits cytochrome P450 3A4 (CYP3A4) mRNA induction in rifampicin-treated HepG2 cells. Biosci Biotechnol Biochem, 2019. 83(7): p. 1181-1192.

471. Gashaw, I., et al., Cytochrome P450 3A4 messenger ribonucleic acid induction by rifampin in human peripheral blood mononuclear cells: Correlation with alprazolam pharmacokinetics. Clinical Pharmacology & Therapeutics, 2003. 74(5): p. 448-457.

472. Matsuda, H., et al., Taurine modulates induction of cytochrome P450 3A4 mRNA by rifampicin in the HepG2 cell line. Biochim Biophys Acta, 2002. 1593(1): p. 93-8.

473. Glaeser, H., et al., Influence of rifampicin on the expression and function of human intestinal cytochrome P450 enzymes. British Journal of Clinical Pharmacology, 2005. 59(2): p. 199-206.

474. Loos, U., et al., Pharmacokinetics of oral and intravenous rifampicin during chronic administration. Klin Wochenschr, 1985. 63(23): p. 1205-11.

475. Kliewer, S.A. and T.M. Willson, Regulation of xenobiotic and bile acid metabolism by the nuclear pregnane X receptor. J Lipid Res, 2002. 43(3): p. 359-64.

476. Waxman, D.J. and L. Azaroff, Phenobarbital induction of cytochrome P-450 gene expression. Biochem J, 1992. 281 (Pt 3)(Pt 3): p. 577-92.

477. Schuetz, E.G., W.T. Beck, and J.D. Schuetz, Modulators and substrates of P-glycoprotein and cytochrome P4503A coordinately up-regulate these proteins in human colon carcinoma cells. Mol Pharmacol, 1996. 49(2): p. 311-8.

478. Pelkonen, O., et al., Inhibition and induction of human cytochrome P450 enzymes: current status. Archives of toxicology, 2008. 82(10): p. 667-715.

479. Vermeer, L.M., et al., Evaluation of Ketoconazole and Its Alternative Clinical CYP3A4/5 Inhibitors as Inhibitors of Drug Transporters: The In Vitro Effects of Ketoconazole, Ritonavir, Clarithromycin, and Itraconazole on 13 Clinically-Relevant Drug Transporters. Drug Metab Dispos, 2016. 44(3): p. 453-9.

480. Greiner, B., et al., The role of intestinal P-glycoprotein in the interaction of digoxin and rifampin. J Clin Invest, 1999. 104(2): p. 147-53.

481. Li, L., et al., The contribution of human OCT1, OCT3, and CYP3A4 to nitidine chloride-induced hepatocellular toxicity. Drug Metab Dispos, 2014. 42(7): p. 1227-34.

482. Karthik Venkatakrishnan, L.L.v.M.a.D.J.G., Effects of the Antifungal Agents on Oxidative Drug Metabolism by venkatakrishnan2000.pdf. Clin Pharmacokinet, 2000. 38(2): p. 111-180.

483. Ohyama, K., et al., A Significant Role of Human Cytochrome P450 2C8 in Amiodarone N-Deethylation: An Approach to Predict the Contribution with Relative Activity Factor. Drug Metabolism and Disposition, 2000. 28(11): p. 1303-1310.

484. Elsherbiny, M.E., A.O. El-Kadi, and D.R. Brocks, The metabolism of amiodarone by various CYP isoenzymes of human and rat, and the inhibitory influence of ketoconazole. J Pharm Pharm Sci, 2008. 11(1): p. 147-59.

485. Greenblatt, H.K. and D.J. Greenblatt, Liver injury associated with ketoconazole: review of the published evidence. J Clin Pharmacol, 2014. 54(12): p. 1321-9.

486. Greenblatt, D.J., Evidence-based choice of ritonavir as index CYP3A inhibitor in drug-drug interaction studies. J Clin Pharmacol, 2016. 56(2): p. 152-6.

487. Greenblatt, D.J., The ketoconazole legacy. Clinical Pharmacology in Drug Development, 2014. 3(1): p. 1-3.

488. Zhang, H., G. Ya, and H. Rui, Inhibitory Effects of Triptolide on Human Liver Cytochrome P450 Enzymes and P-Glycoprotein. Eur J Drug Metab Pharmacokinet, 2017. 42(1): p. 89-98.

489. Arzuk, E., F. Karakuş, and H. Orhan, Bioactivation of clozapine by mitochondria of the murine heart: Possible cause of cardiotoxicity. Toxicology, 2020. 447: p. 152628.

490. Kalgutkar, A.S., et al., N-(3,4-dimethoxyphenethyl)-4-(6,7-dimethoxy-3,4-dihydroisoquinolin-2[1H]-yl)-6,7-dimethoxyquinazolin-2-amine (CP-100,356) as a "chemical knock-out equivalent" to assess the impact of efflux transporters on oral drug absorption in the rat. J Pharm Sci, 2009. 98(12): p. 4914-27.

491. Pelkonen, O., et al., Inhibition and induction of human cytochrome P450 enzymes: current status. Arch Toxicol, 2008. 82(10): p. 667-715.

492. S. V. Nikulin, E.A.T., and A. A. Poloznikova, Effect of ketoconazole on the transport and metabolism of drugs in the human liver cell model. Russian Chemical Bulletin, 2017. 66(1): p. 150—155.

493. Zou, L.W., et al., Carboxylesterase Inhibitors: An Update. Curr Med Chem, 2018. 25(14): p. 1627-1649.

494. Quinney, S.K., et al., Hydrolysis of capecitabine to 5'-deoxy-5-fluorocytidine by human carboxylesterases and inhibition by loperamide. J Pharmacol Exp Ther, 2005. 313(3): p. 1011-6.

495. Lagas, J.S., et al., P-glycoprotein, multidrug-resistance associated protein 2, Cyp3a, and carboxylesterase affect the oral availability and metabolism of vinorelbine. Mol Pharmacol, 2012. 82(4): p. 636-44.

496. Hatfield, M.J. and P.M. Potter, Carboxylesterase inhibitors. Expert Opinion on Therapeutic Patents, 2011. 21(8): p. 1159-1171.

497. Wandel, C., et al., Interaction of morphine, fentanyl, sufentanil, alfentanil, and loperamide with the efflux drug transporter P-glycoprotein. Anesthesiology, 2002. 96(4): p. 913-920.

498. Kamencic, H., et al., Monochlorobimane fluorometric method to measure tissue glutathione. Analytical biochemistry, 2000. 286(1): p. 35-37.

499. Rice, G.C., et al., Quantitative analysis of cellular glutathione by flow cytometry utilizing monochlorobimane: some applications to radiation and drug resistance in vitro and in vivo. Cancer research, 1986. 46(12 Pt 1): p. 6105-6110.

500. Le Hegarat, L., et al., Performance of comet and micronucleus assays in metabolic competent HepaRG cells to predict in vivo genotoxicity. Toxicol Sci, 2014. 138(2): p. 300-9.

501. Glaser, N. and H. Stopper, Patulin: Mechanism of genotoxicity. Food Chem Toxicol, 2012. 50(5): p. 1796-801.

502. Chen, Y., et al., Intracellular glutathione plays important roles in pyrrolizidine alkaloids-induced growth inhibition on hepatocytes. Environmental Toxicology and Pharmacology, 2009. 28(3): p. 357-362.

503. Ji, L., Y. Chen, and Z. Wang, Intracellular glutathione plays important roles in pyrrolizidine alkaloid clivorine-induced toxicity on L-02 hepatocytes. Toxicology Mechanisms and Methods, 2008. 18(8): p. 661-664.

504. Lehmann, J.M., et al., The human orphan nuclear receptor PXR is activated by compounds that regulate CYP3A4 gene expression and cause drug interactions. The Journal of clinical investigation, 1998. 102(5): p. 1016-1023.

505. Lemaire, G., G. de Sousa, and R. Rahmani, A PXR reporter gene assay in a stable cell culture system: CYP3A4 and CYP2B6 induction by pesticides. Biochemical pharmacology, 2004. 68(12): p. 2347-2358.

506. Goodwin, B., E. Hodgson, and C. Liddle, The orphan human pregnane X receptor mediates the transcriptional activation of CYP3A4 by rifampicin through a distal enhancer module. Molecular pharmacology, 1999. 56(6): p. 1329-1339.

507. Chen, J. and K. Raymond, Roles of rifampicin in drug-drug interactions: underlying molecular mechanisms involving the nuclear pregnane X receptor. Annals of clinical microbiology and antimicrobials, 2006. 5: p. 1-11.

508. Kobayashi, T., et al., Peppermint (Mentha piperita L.) extract effectively inhibits cytochrome P450 3A4 (CYP3A4) mRNA induction in rifampicin-treated HepG2 cells. Bioscience, Biotechnology, and Biochemistry, 2019.

509. Yamazaki, H., et al., Roles of cytochromes P450 1A2 and 3A4 in the oxidation of estradiol and estrone in human liver microsomes. Chemical research in toxicology, 1998. 11(6): p. 659-665.

510. Allemang, A., et al., Relative potency of fifteen pyrrolizidine alkaloids to induce DNA damage as measured by micronucleus induction in HepaRG human liver cells. Food Chem Toxicol, 2018. 121: p. 72-81.

511. Misik, M., et al., Cytome micronucleus assays with a metabolically competent human derived liver cell line (Huh6): A promising approach for routine testing of chemicals? Environ Mol Mutagen, 2019. 60(2): p. 134-144.

512. Waldherr, M., et al., Use of HuH6 and other human-derived hepatoma lines for the detection of genotoxins: a new hope for laboratory animals? Arch Toxicol, 2018. 92(2): p. 921-934.

513. Hea-Young Kim, F.R.S.a. and R. A.CoulombeJr., Pyrrolizidine alkaloid-induced DNA-protein cross-links. Carcinogenesis, 1995. 16: p. 2691-2697.

514. Maria Uhl, C.H., Siegfried Knasmu¨ller, Evaluation of the single cell gel electrophoresis assay with human hepatoma (Hep G2) cells. Mutation Research, 2000: p. 213–225.

515. Qingsu Xia, M.W.C., Fred. F. Kadlubar, Po-Cheun Chan, and and Peter P. Fu, Human Liver Microsomal Metabolism and DNA Adduct Formation of the Tumorigenic Pyrrolizidine Alkaloid, Riddelliine. Chem. Res. Toxicol., 2003. 16: p. 66-73.

516. Chen, T., N. Mei, and P.P. Fu, Genotoxicity of pyrrolizidine alkaloids. J Appl Toxicol, 2010. 30(3): p. 183-96.

517. NTP, Toxicology and carcinogenesis studies of riddelliine (CAS No. 23246-96-0) in F344/N rats and B6C3F1 mice (gavage studies). Natl Toxicol Program Tech Rep Ser, 2003(508): p. 1-280.

518. Xia, Q., et al., Formation of DHP-derived DNA adducts from metabolic activation of the prototype heliotridine-type pyrrolizidine alkaloid, lasiocarpine. Cancer Lett, 2006. 231(1): p. 138-45.

519. Glück, J., et al., Pyrrolizidine alkaloids induce cell death in human heparg cells in a structure-dependent manner. International Journal of Molecular Sciences, 2020. 22(1): p. 202.

520. Wang, Z., et al., Hepatotoxicity of pyrrolizidine alkaloid compound intermedine: Comparison with other pyrrolizidine alkaloids and its toxicological mechanism. Toxins, 2021. 13(12): p. 849.

521. Betteridge, D.J., What is oxidative stress? Metabolism, 2000. 49(2): p. 3-8.

522. Sies, H., Biochemistry of oxidative stress. Angewandte Chemie International Edition in English, 1986. 25(12): p. 1058-1071.

523. Ji, L., et al., Protective mechanisms of N-acetyl-cysteine against pyrrolizidine alkaloid clivorine-induced hepatotoxicity. Journal of Cellular Biochemistry, 2009. 108(2): p. 424-432.

524. Amin, K.A., et al., Oxidative hepatotoxicity effects of monocrotaline and its amelioration by lipoic acid, S-adenosyl methionine and vitamin E. Journal of Complementary and Integrative Medicine, 2014. 11(1): p. 35-41.

525. Liu, T.-Y., et al., Pyrrolizidine alkaloid isoline-induced oxidative injury in various mouse tissues. Experimental and Toxicologic Pathology, 2010. 62(3): p. 251-257.

526. Liang, Q., et al., Pyrrolizidine alkaloid clivorine-induced oxidative stress injury in human normal liver L-02 cells. pathways, 2009. 6(8): p. 9.

527. Halasi, M., et al., ROS inhibitor N-acetyl-L-cysteine antagonizes the activity of proteasome inhibitors. The Biochemical journal, 2013. 454(2): p. 201-208.

528. Murphy, M.P., How mitochondria produce reactive oxygen species. Biochemical journal, 2009. 417(1): p. 1-13.

529. Wang, W., et al., Seneciphylline, a main pyrrolizidine alkaloid in Gynura japonica, induces hepatotoxicity in mice and primary hepatocytes via activating mitochondria-mediated apoptosis. Journal of Applied Toxicology, 2020. 40(11): p. 1534-1544.

530. Ji, L., et al., Involvement of Bcl-xL degradation and mitochondrial-mediated apoptotic pathway in pyrrolizidine alkaloids-induced apoptosis in hepatocytes. Toxicology and Applied Pharmacology, 2008. 231(3): p. 393-400.

531. Gordon, G.J., W.B. Coleman, and J.W. Grisham, Bax-mediated apoptosis in the livers of rats after partial hepatectomy in the retrorsine model of hepatocellular injury. Hepatology, 2000. 32(2): p. 312-320.

532. Armstrong, S.J., A.J. Zuckerman, and R.G. Bird, Induction of morphological changes in human embryo liver cells by the pyrrolizidine alkaloid lasiocarpine. Br J Exp Pathol, 1972. 53(2): p. 145-9.

533. Mingatto, F.E., et al., Dehydromonocrotaline inhibits mitochondrial complex I. A potential mechanism accounting for hepatotoxicity of monocrotaline. Toxicon, 2007. 50(5): p. 724-730.

534. DeLeve, L.D., et al., Toxicity of azathioprine and monocrotaline in murine sinusoidal endothelial cells and hepatocytes: the role of glutathione and relevance to hepatic venoocclusive disease. Hepatology, 1996. 23(3): p. 589-599.

535. Ma, J., et al., Pyrrole-protein adducts – A biomarker of pyrrolizidine alkaloid-induced hepatotoxicity. Journal of Food and Drug Analysis, 2018. 26(3): p. 965-972.

536. Lu, Y., J. Ma, and G. Lin, Development of a two-layer transwell co-culture model for the in vitro investigation of pyrrolizidine alkaloid-induced hepatic sinusoidal damage. Food and Chemical Toxicology, 2019. 129: p. 391-398.

537. DeLeve, L.D. and N. Kaplowitz, Glutathione metabolism and its role in hepatotoxicity. Pharmacology & Therapeutics, 1991. 52(3): p. 287-305.

538. Yang, M., et al., Cytotoxicity of pyrrolizidine alkaloid in human hepatic parenchymal and sinusoidal endothelial cells: Firm evidence for the reactive metabolites mediated pyrrolizidine alkaloid-induced hepatotoxicity. Chemico-Biological Interactions, 2016. 243: p. 119-126.

539. Ruan, J., et al., Blood pyrrole-protein adducts—a biomarker of pyrrolizidine alkaloid-induced liver injury in humans. Journal of Environmental Science and Health, Part C, 2015. 33(4): p. 404-421.

540. Neuman, M.G., A.Y. Jia, and V. Steenkamp, Senecio latifolius induces in vitro hepatocytotoxicity in a human cell line. Canadian journal of physiology and pharmacology, 2007. 85(11): p. 1063-1075.

541. dos Santos, A.B., et al., Dehydromonocrotaline induces cyclosporine A-insensitive mitochondrial permeability transition/cytochrome c release. Toxicon, 2009. 54(1): p. 16-22.

542. McLean, E.K., The toxic actions of pyrrolizidine (Senecio) alkaloids. Pharmacological reviews, 1970. 22(4): p. 429-483.

543. Robertson, K.A., Alkylation of N 2 in deoxyguanosine by dehydroretronecine, a carcinogenic metabolite of the pyrrolizidine alkaloid monocrotaline. Cancer Research, 1982. 42(1): p. 8-14.

544. Robertson, K., et al., Covalent interaction of dehydroretronecine, a carcinogenic metabolite of the pyrrolizidine alkaloid monocrotaline, with cysteine and glutathione. Cancer Research, 1977. 37(9): p. 3141-3144.

545. Wagner, J., T. Petry, and R. Roth, Characterization of monocrotaline pyrrole-induced DNA cross-linking in pulmonary artery endothelium. American Journal of Physiology-Lung Cellular and Molecular Physiology, 1993. 264(5): p. L517-L522.

546. Bhattacharya, S., Reactive oxygen species and cellular defense system. Free radicals in human health and disease, 2015: p. 17-29.

547. Klaunig, J.E., Oxidative stress and cancer. Current pharmaceutical design, 2018. 24(40): p. 4771-4778.

548. Arfin, S., et al., Oxidative stress in cancer cell metabolism. Antioxidants, 2021. 10(5): p. 642.

549. Jaeschke, H., M.R. McGill, and A. Ramachandran, Oxidant stress, mitochondria, and cell death mechanisms in drug-induced liver injury: lessons learned from acetaminophen hepatotoxicity. Drug metabolism reviews, 2012. 44(1): p. 88-106.

550. Liu, L., R.J. Bridges, and C.L. Eyer, Effect of cytochrome P450 1A induction on oxidative damage in rat brain. Molecular and cellular biochemistry, 2001. 223: p. 89-94.

551. Zangar, R.C., D.R. Davydov, and S. Verma, Mechanisms that regulate production of reactive oxygen species by cytochrome P450. Toxicology and applied pharmacology, 2004. 199(3): p. 316-331.

552. Veith, A. and B. Moorthy, Role of cytochrome P450s in the generation and metabolism of reactive oxygen species. Current opinion in toxicology, 2018. 7: p. 44-51.

553. Geburek, I., D. Schrenk, and A. These, In vitro biotransformation of pyrrolizidine alkaloids in different species: part II—identification and quantitative assessment of the metabolite profile of six structurally different pyrrolizidine alkaloids. Archives of toxicology, 2020. 94: p. 3759-3774.

554. Mingatto, F.E., et al., Dehydromonocrotaline inhibits mitochondrial complex I. A potential mechanism accounting for hepatotoxicity of monocrotaline. Toxicon, 2007. 50(5): p. 724-730.

555. Shivakumar, B.R., S. Kolluri, and V. Ravindranath, Glutathione and protein thiol homeostasis in brain during reperfusion after cerebral ischemia. Journal of Pharmacology and Experimental Therapeutics, 1995. 274(3): p. 1167-1173.

556. Balijepalli, S., M.R. Boyd, and V. Ravindranath, Inhibition of mitochondrial complex I by haloperidol: the role of thiol oxidation. Neuropharmacology, 1999. 38(4): p. 567-577.

557. Jha, N., et al., Glutathione Depletion in PC12 Results in Selective Inhibition of Mitochondrial Complex I Activity: IMPLICATIONS FOR PARKINSON' S DISEASE. Journal of Biological Chemistry, 2000. 275(34): p. 26096-26101.

558. Schilling, B., et al., Rapid purification and mass spectrometric characterization of mitochondrial NADH dehydrogenase (Complex I) from rodent brain and a dopaminergic neuronal cell line. Molecular & Cellular Proteomics, 2005. 4(1): p. 84-96.

559. Enge, A.-M., et al., Active transport of hepatotoxic pyrrolizidine alkaloids in HepaRG cells. International Journal of Molecular Sciences, 2021. 22(8): p. 3821.

560. Chhabra, R.S., Intestinal absorption and metabolism of xenobiotics. Environmental health perspectives, 1979. 33: p. 61-69.

561. Chojkier, M., Hepatic sinusoidal-obstruction syndrome: toxicity of pyrrolizidine alkaloids. Journal of Hepatology, 2003. 39(3): p. 437-446.

562. Field, R.A., et al., An in vitro comparison of the cytotoxic potential of selected dehydropyrrolizidine alkaloids and some N-oxides. Toxicon, 2015. 97: p. 36-45.

563. Gao, H., et al., Blood pyrrole-protein adducts as a diagnostic and prognostic index in pyrrolizidine alkaloid-hepatic sinusoidal obstruction syndrome. Drug Des Devel Ther, 2015. 9: p. 4861-8.

564. Lin, G., et al., Hepatic sinusoidal obstruction syndrome associated with consumption of Gynura segetum. J Hepatol, 2011. 54(4): p. 666-73.

565. Ruan, J., et al., Blood Pyrrole-Protein Adducts--A Biomarker of Pyrrolizidine Alkaloid-Induced Liver Injury in Humans. J Environ Sci Health C Environ Carcinog Ecotoxicol Rev, 2015. 33(4): p. 404-21.

566. Yang, M., et al., First evidence of pyrrolizidine alkaloid N-oxide-induced hepatic sinusoidal obstruction syndrome in humans. Arch Toxicol, 2017. 91(12): p. 3913-3925.

567. Sugiyama, K.M.G.a.Y., Membrane transporters and drug response. The pharmacological basis 2006. Chapter 2.

568. Konig, J., et al., Double-transfected MDCK cells expressing human OCT1/MATE1 or OCT2/MATE1: determinants of uptake and transcellular translocation of organic cations. Br J Pharmacol, 2011. 163(3): p. 546-55.

569. Meyer zu Schwabedissen, H.E., et al., Human multidrug and toxin extrusion 1 (MATE1/SLC47A1) transporter: functional characterization, interaction with OCT2 (SLC22A2), and single nucleotide polymorphisms. Am J Physiol Renal Physiol, 2010. 298(4): p. F997-F1005.

570. Muller, F., et al., Role of organic cation transporter OCT2 and multidrug and toxin extrusion proteins MATE1 and MATE2-K for transport and drug interactions of the antiviral lamivudine. Biochem Pharmacol, 2013. 86(6): p. 808-15.

571. Sato, T., et al., Transcellular transport of organic cations in double-transfected MDCK cells expressing human organic cation transporters hOCT1/hMATE1 and hOCT2/hMATE1. Biochem Pharmacol, 2008. 76(7): p. 894-903.

572. Brosseau, N. and D. Ramotar, The human organic cation transporter OCT1 and its role as a target for drug responses. Drug Metab Rev, 2019. 51(4): p. 389-407.

573. Bonnie Hsiang, Y.Z., Zhaoqing Wang, Yuli Wu, Vito Sasseville, Wen-Pin Yang, and and T.G. Kirchgessner, A novel human hepatic organic anion transporting polypeptide (OATP2) by hsiang1999.pdf. THE JOURNAL OF BIOLOGICAL CHEMISTRY, 1999. 274(52): p. 37161–37168.

574. Jorg Konig, Y.C., Anne T. Nies, And Dietrich Keppler, A novel human organic anion transporting polypeptide localized to the basolateral hepatocyte membrane by konig 2000.pdf. Am. J. Physiol. Gastrointest. Liver Physiol., 2000. 278: p. 156–164.

575. Kalliokoski, A. and M. Niemi, Impact of OATP transporters on pharmacokinetics. Br J Pharmacol, 2009. 158(3): p. 693-705.

576. Takaaki Abe, M.K., Taro Tokui, Rie Nakagomi, Toshiyuki Nishio,, H.N. Daisuke Nakai*, Michiaki Unnoi, Masanori Suzukii, Takeshi Naitohi,, and a.H.Y. Seiki Matsunoi, Identification of a novel gene family encoding human liver-specific organic anion transporter LST-1 by abe1999.pdf. THE JOURNAL OF BIOLOGICAL CHEMISTRY, 1999. 274(24): p. 17159–17163.

577. Hilgendorf, C., et al., Expression of thirty-six drug transporter genes in human intestine, liver, kidney, and organotypic cell lines. Drug Metab Dispos, 2007. 35(8): p. 1333-40.

578. Tu, M., et al., Organic cation transporter 1 mediates the uptake of monocrotaline and plays an important role in its hepatotoxicity. Toxicology, 2013. 311(3): p. 225-30.

579. Tocchetti, G.N., et al., Inhibition of multidrug resistance-associated protein 2 (MRP2) activity by the contraceptive nomegestrol acetate in HepG2 and Caco-2 cells. Eur J Pharm Sci, 2018. 122: p. 205-213.

580. Huang, J., et al., Interactions Between Emodin and Efflux Transporters on Rat Enterocyte by a Validated Ussing Chamber Technique. Front Pharmacol, 2018. 9: p. 646.

581. Jemnitz, K., et al., Biliary efflux transporters involved in the clearance of rosuvastatin in sandwich culture of primary rat hepatocytes. Toxicol In Vitro, 2010. 24(2): p. 605-10.

582. Kidron, H., et al., Impact of probe compound in MRP2 vesicular transport assays. Eur J Pharm Sci, 2012. 46(1-2): p. 100-5.

583. Gerets, H.H., et al., Characterization of primary human hepatocytes, HepG2 cells, and HepaRG cells at the mRNA level and CYP activity in response to inducers and their predictivity for the detection of human hepatotoxins. Cell Biol Toxicol, 2012. 28(2): p. 69-87.

584. Laurent P. Rivory , M.R.B., Jacques Robert? and Susan M. Pond, Conversion of Irinotecan (CPT-11) to Its Active metabolites in human liver carboxylesterase by rivory1996.pdf. Biochemical Pharmacology, 1996 Vol. 52: p. 1103-l 111.

585. Ji, L., T. Liu, and Z. Wang, Pyrrolizidine alkaloid clivorine induced oxidative injury on primary cultured rat hepatocytes. Human & experimental toxicology, 2010. 29(4): p. 303-309.

586. Godin, S.J., et al., Species differences in the in vitro metabolism of deltamethrin and esfenvalerate: differential oxidative and hydrolytic metabolism by humans and rats. Drug metabolism and disposition, 2006. 34(10): p. 1764-1771.

587. Fu, P.P., et al., Genotoxic Pyrrolizidine Alkaloids — Mechanisms Leading to DNA Adduct Formation and Tumorigenicity. 2002. 3(9): p. 948.

588. Williams, J.A., et al., Reaction phenotyping in drug discovery: moving forward with confidence? Current drug metabolism, 2003. 4(6): p. 527-534.

589. Ebmeyer, J., et al., Human CYP3A4-mediated toxification of the pyrrolizidine alkaloid lasiocarpine. Food Chem Toxicol, 2019. 130: p. 79-88.

590. Reid, M., et al., Involvement of cytochrome P450 3A in the metabolism and covalent binding of 14C-monocrotaline in rat liver microsomes. Journal of biochemical and molecular toxicology, 1998. 12(3): p. 157-166.

591. Martucci, C.P. and J. Fishman, P450 enzymes of estrogen metabolism. Pharmacology & therapeutics, 1993. 57(2-3): p. 237-257.

592. Zhu, B.T. and A.H. Conney, Functional role of estrogen metabolism in target cells: review and perspectives. Carcinogenesis, 1998. 19(1): p. 1-27.

593. Lee, A.J., et al., Characterization of the oxidative metabolites of 17β-estradiol and estrone formed by 15 selectively expressed human cytochrome P450 isoforms. Endocrinology, 2003. 144(8): p. 3382-3398.

594. Badawi, A.F., E.L. Cavalieri, and E.G. Rogan, Role of human cytochrome P450 1A1, 1A2, 1B1, and 3A4 in the 2-, 4-, and 16 [alpha]-hydroxylation of 17 [beta]-estradiol. Metabolism-Clinical and Experimental, 2001. 50(9): p. 1001-1003.

595. Ball, P. and R. Knuppen, Formation of 2- and 4-hydroxyestrogens by brain, pituitary, and liver of the human fetus. The Journal of clinical endocrinology and metabolism, 1978. 47(4): p. 732-737.

596. Zhu, B.T., et al., Conversion of estrone to 2- and 4-hydroxyestrone by hamster kidney and liver microsomes: implications for the mechanism of estrogen-induced carcinogenesis. Endocrinology, 1994. 135(5): p. 1772-1779.

597. Guengerich, F.P., CYTOCHROME P-450 3A4: Regulation and Role in Drug Metabolism. Annual Review of Pharmacology and Toxicology, 1999. 39(1): p. 1-17.

598. Thummel, K.E. and G.R. Wilkinson, In vitro and in vivo drug interactions involving human CYP3A. Annual review of pharmacology and toxicology, 1998. 38: p. 389-430.

599. AOYAMA, T., et al., Estradiol Metabolism by Complementary Deoxyribonucleic Acid-Expressed Human Cytochrome P450s. Endocrinology, 1990. 126(6): p. 3101-3106.

600. Kerlan, V., et al., Nature of cytochromes P450 involved in the 2-/4-hydroxylations of estradiol in human liver microsomes. Biochemical pharmacology, 1992. 44(9): p. 1745-1756.

601. Guengerich, F.P., et al., Characterization of rat and human liver microsomal cytochrome P-450 forms involved in nifedipine oxidation, a prototype for genetic polymorphism in oxidative drug metabolism. The Journal of biological chemistry, 1986. 261(11): p. 5051-5060.

602. Miners, J.O. and P.I. Mackenzie, Drug glucuronidation in humans. Pharmacology & therapeutics, 1991. 51(3): p. 347-369.

603. Tukey, R.H. and C.P. Strassburg, Human UDP-glucuronosyltransferases: metabolism, expression, and disease. Annual review of pharmacology and toxicology, 2000. 40(1): p. 581-616.

604. Rajaonarison, J.F., et al., In vitro glucuronidation of 3'-azido-3'-deoxythymidine by human liver. Role of UDP-glucuronosyltransferase 2 form. Drug metabolism and disposition, 1991. 19(4): p. 809-815.

605. Ayrton, A. and P. Morgan, Role of transport proteins in drug absorption, distribution and excretion. Xenobiotica, 2001. 31(8-9): p. 469-497.

606. Yong, W.P., et al., Effects of ketoconazole on glucuronidation by UDP-glucuronosyltransferase enzymes. Clinical Cancer Research, 2005. 11(18): p. 6699-6704.

607. Sawamura, R., et al., Inhibitory effect of azole antifungal agents on the glucuronidation of lorazepam using rabbit liver microsomes in vitro. Biological and Pharmaceutical Bulletin, 2000. 23(5): p. 669-671.

608. Sampol, E., et al., Comparative effects of antifungal agents on zidovudine glucuronidation by human liver microsomes. British journal of clinical pharmacology, 1995. 40(1): p. 83-86.

609. Asgari, M., et al., Effect of Azoles on the Glucuronidation of Zidovudine by Human Liver UDP-Glucuronosyltransferase [with Reply]. The Journal of infectious diseases, 1995. 172(6): p. 1634-1636.

610. Satoh, T., et al., Studies on the interactions between drugs and estrogen. III. Inhibitory effects of 29 drugs reported to induce gynecomastia on the glucuronidation of estradiol. Biological and Pharmaceutical Bulletin, 2004. 27(11): p. 1844-1849.

611. Riches, Z., et al., Quantitative evaluation of the expression and activity of five major sulfotransferases (SULTs) in human tissues: the SULT “pie”. Drug metabolism and disposition, 2009. 37(11): p. 2255-2261.

612. Glatt, H., Sulfotransferases in the bioactivation of xenobiotics. Chemico-biological interactions, 2000. 129(1-2): p. 141-170.

613. Chapman, E., et al., Sulfotransferases: structure, mechanism, biological activity, inhibition, and synthetic utility. Angewandte Chemie International Edition, 2004. 43(27): p. 3526-3548.

614. Kauffman, F.C., Sulfonation in pharmacology and toxicology. Drug metabolism reviews, 2004. 36(3-4): p. 823-843.

615. Mueller, J.W., et al., The regulation of steroid action by sulfation and desulfation. Endocrine reviews, 2015. 36(5): p. 526-563.

616. Kodama, S., et al., Liganded pregnane X receptor represses the human sulfotransferase SULT1E1 promoter through disrupting its chromatin structure. Nucleic acids research, 2011. 39(19): p. 8392-8403.

617. Soars, M.G., et al., An assessment of UDP-glucuronosyltransferase induction using primary human hepatocytes. Drug Metabolism and Disposition, 2004. 32(1): p. 140-148.

618. Zhang, H., et al., Rat pregnane X receptor: molecular cloning, tissue distribution, and xenobiotic regulation. Archives of biochemistry and biophysics, 1999. 368(1): p. 14-22.

619. Cheeke, P.R., Toxicity and metabolism of pyrrolizidine alkaloids. Journal of Animal Science, 1988. 66(9): p. 2343-2350.

620. Xu, J., et al., Pyrrolizidine alkaloids: An update on their metabolism and hepatotoxicity mechanism. Liver Research, 2019. 3(3-4): p. 176-184.

621. Lu, Y., et al., Establishment of a novel CYP3A4-transduced human hepatic sinusoidal endothelial cell model and its application in screening hepatotoxicity of pyrrolizidine alkaloids. Journal of Environmental Science and Health, Part C, 2020. 38(2): p. 169-185.

622. Chen, M.-Y., et al., Reliable experimental model of hepatic veno-occlusive disease caused by monocrotaline. Hepatobiliary & pancreatic diseases international: HBPD INT, 2008. 7(4): p. 395-400.

623. DeLeve, L.D., Liver sinusoidal endothelial cells and liver injury, in Drug-Induced Liver Disease. 2013, Elsevier. p. 135-146.

624. DeLeve, L.D., et al., Embolization by sinusoidal lining cells obstructs the microcirculation in rat sinusoidal obstruction syndrome. American Journal of Physiology-Gastrointestinal and Liver Physiology, 2003. 284(6): p. G1045-G1052.

625. DeLeve, L.D., et al., Characterization of a reproducible rat model of hepatic veno-occlusive disease. Hepatology, 1999. 29(6): p. 1779-1791.

626. Cooper, R.A. and R.J. Huxtable, A simple procedure for determining the aqueous half-lives of pyrrolic metabolites of pyrrolizidine alkaloids. Toxicon, 1996. 34(5): p. 604-607.

627. Hadi, N.S.A., et al., Genotoxicity of selected pyrrolizidine alkaloids in human hepatoma cell lines HepG2 and Huh6. Mutation Research/Genetic Toxicology and Environmental Mutagenesis, 2021. 861: p. 503305.

628. Jessen, B.A., et al., Assessment of hepatocytes and liver slices as in vitro test systems to predict in vivo gene expression. Toxicol Sci, 2003. 75(1): p. 208-22.

629. Kitamura, S., K. Maeda, and Y. Sugiyama, Recent progresses in the experimental methods and evaluation strategies of transporter functions for the prediction of the pharmacokinetics in humans. Naunyn Schmiedebergs Arch Pharmacol, 2008. 377(4-6): p. 617-28.

630. Huxtable, R., et al., Physicochemical and metabolic basis for the differing neurotoxicity of the pyrrolizidine alkaloids, trichodesmine and monocrotaline. Neurochemical research, 1996. 21: p. 141-146.

631. Cooper, R.A. and R.J. Huxtable. The relationship between reactivity of metabolites of pyrrolizidine alkaloids and extrahepatic toxicity. in Proceedings of the Western Pharmacology Society. 1999. Seattle, Wash.: The Society.

632. Kay, J. and D. Heath, Crotalaria spectabilis: The Pulmonary Hypertension Plant. 1969. Thomas, Springfield, IL.

633. Lu, Y., J. Ma, and G. Lin, Development of a two-layer transwell co-culture model for the in vitro investigation of pyrrolizidine alkaloid-induced hepatic sinusoidal damage. Food and chemical toxicology : an international journal published for the British Industrial Biological Research Association, 2019. 129: p. 391-398.

634. Weber, G.F., DNA damaging drugs, in Molecular therapies of cancer. 2015, Springer. p. 9-112.

635. Mohan, L., et al., Indirubin, a bis-indole alkaloid binds to tubulin and exhibits antimitotic activity against HeLa cells in synergism with vinblastine. Biomedicine & Pharmacotherapy, 2018. 105: p. 506-517.

636. Rizzoni, M., et al., Chromatin bridges between sister chromatids induced in late G2 mitosis in CHO cells by trimethylpsoralen+ UVA. Experimental cell research, 1993. 209(1): p. 149-155.

637. Botta, R. and B. Gustavino, Relationship between chromatin bridges in anaphase and chromosomal aberrations induced by TMP + UVA (365 nm) in CHO cells. Mutation research, 1997. 374(2): p. 253-259.

638. Hoffelder, D.R., et al., Resolution of anaphase bridges in cancer cells. Chromosoma, 2004. 112(8): p. 389-397.

639. Geburek, I., et al., In vitro metabolism of pyrrolizidine alkaloids–Metabolic degradation and GSH conjugate formation of different structure types. Food and Chemical Toxicology, 2020. 135: p. 110868.

640. Authority, E.F.S., International frameworks dealing with human risk assessment of combined exposure to multiple chemicals. Efsa Journal, 2013. 11(7): p. 3313.

641. OECD, Considerations for assessing the risks of combined exposure to multiple chemicals, series on testing and assessment no. 296. 2018, Environment, Health and Safety Division, Environment Directorate.

642. Committee, E.S., et al., Guidance on harmonised methodologies for human health, animal health and ecological risk assessment of combined exposure to multiple chemicals. Efsa journal, 2019. 17(3): p. e05634.

643. Graillot, V., et al., Genotoxicity of pesticide mixtures present in the diet of the French population. Environmental and molecular mutagenesis, 2012. 53(3): p. 173-184.

644. Ermler, S., M. Scholze, and A. Kortenkamp, Seven benzimidazole pesticides combined at sub-threshold levels induce micronuclei in vitro. Mutagenesis, 2013. 28(4): p. 417-426.

645. Kopp, B., et al., Genotoxicity and mutagenicity assessment of food contaminant mixtures present in the French diet. Environmental and Molecular Mutagenesis, 2018. 59(8): p. 742-754.

646. Tallarida, R.J., Revisiting the isobole and related quantitative methods for assessing drug synergism. J Pharmacol Exp Ther, 2012. 342(1): p. 2-8.

647. Cedergreen, N., Quantifying synergy: a systematic review of mixture toxicity studies within environmental toxicology. PLoS One, 2014. 9(5): p. e96580.

648. Ritz, C. and J.C. Streibig, From additivity to synergism – A modelling perspective. Synergy, 2014. 1(1): p. 22-29.

649. Allemang, A., C. Mahony, and S. Pfuhler, The in vitro genotoxicity potency of mixtures of pyrrolizidine alkaloids can be explained by dose addition of the individual mixture components. Environmental and Molecular Mutagenesis, 2022. 63(8-9): p. 400-407.

650. Louisse, J., et al., Bioassay-directed analysis-based identification of relevant pyrrolizidine alkaloids. Archives of Toxicology, 2022. 96(8): p. 2299-2317.

651. Reid, M.J., et al., Involvement of cytochrome P450 3A in the metabolism and covalent binding of 14C-monocrotaline in rat liver microsomes. J Biochem Mol Toxicol, 1998. 12(3): p. 157-66.

652. Xia, Q., et al., Human Liver Microsomal Metabolism and DNA Adduct Formation of the Tumorigenic Pyrrolizidine Alkaloid, Riddelliine. Chemical Research in Toxicology, 2003. 16(1): p. 66-73.

653. Müller, L., P. Kasper, and G. Kaufmann, The clastogenic potential in vitro of pyrrolizidine alkaloids employing hepatocyte metabolism. Mutation Research Letters, 1992. 282(3): p. 169-176.

654. Allen, J.R., I.-C. Hsu, and L.A. Carstens, Dehydroretronecine-induced Rhabdomyosarcomas in Rats1. Cancer Research, 1975. 35(4): p. 997-1002.

655. Culvenor, C.C.J., et al., Pyrrolizidine alkaloids as alkylating and antimitotic agents. Annals of the New York Academy of Sciences, 1969. 163(2): p. 837-847.

656. Mattocks, A.R. and R.F. Legg, Antimitotic activity of dehydroretronecine, a pyrrolizidine alkaloid metabolite, and some analogous compounds, in a rat liver parenchymal cell line. Chemico-Biological Interactions, 1980. 30(3): p. 325-336.

657. Sanderson, B.J.S. and A.M. Clark, Micronuclei in adult and foetal mice exposed in vivo to heliotrine, urethane, monocrotaline and benzidine. Mutation Research/Fundamental and Molecular Mechanisms of Mutagenesis, 1993. 285(1): p. 27-33.

658. Takashima, R., et al., Micronucleus induction in rat liver and bone marrow by acute vs. repeat doses of the genotoxic hepatocarcinogen monocrotaline. Mutation Research/Genetic Toxicology and Environmental Mutagenesis, 2015. 780-781: p. 64-70.

659. Fowler, P., et al., Reduction of misleading (“false”) positive results in mammalian cell genotoxicity assays. I. Choice of cell type. Mutation Research/Genetic Toxicology and Environmental Mutagenesis, 2012. 742(1): p. 11-25.

660. Wiedenfeld, H., Plants containing pyrrolizidine alkaloids: toxicity and problems. Food additives & contaminants. Part A, Chemistry, analysis, control, exposure & risk assessment, 2011. 28(3): p. 282-292.

661. Knutsen, H.K., et al., Risks for human health related to the presence of pyrrolizidine alkaloids in honey, tea, herbal infusions and food supplements. EFSA Journal, 2017. 15(7).

662. Golberg, L., Structure-activity correlation as a predictive tool in toxicology: fundamentals, methods, and applications. Chemical Industry Institute of Toxicology, 1983.

663. McKinney, J.D., et al., The practice of structure activity relationships (SAR) in toxicology. Toxicological Sciences, 2000. 56(1): p. 8-17.

664. Wang, J., L. Lai, and Y. Tang, Structural features of toxic chemicals for specific toxicity. Journal of chemical information and computer sciences, 1999. 39(6): p. 1173-1189.

665. Field, R.A., et al., An in vitro comparison of the cytotoxic potential of selected dehydropyrrolizidine alkaloids and some N-oxides. Toxicon, 2015. 97: p. 36-45.

666. Wang, Z., et al., Hepatotoxicity of Pyrrolizidine Alkaloid Compound Intermedine: Comparison with Other Pyrrolizidine Alkaloids and Its Toxicological Mechanism. Toxins (Basel), 2021. 13(12).

667. Gao, L., L. Rutz, and D. Schrenk, Structure-dependent hepato-cytotoxic potencies of selected pyrrolizidine alkaloids in primary rat hepatocyte culture. Food and Chemical Toxicology, 2020. 135: p. 110923.

668. Beaumont, K., et al., Design of ester prodrugs to enhance oral absorption of poorly permeable compounds: challenges to the discovery scientist. Current drug metabolism, 2003. 4(6): p. 461-485.

669. Hajnal, K., et al., Prodrug strategy in drug development. Acta Marisiensis-Seria Medica, 2016. 62(3): p. 356-362.

670. Jana, S., S. Mandlekar, and P. Marathe, Prodrug design to improve pharmacokinetic and drug delivery properties: challenges to the discovery scientists. Current medicinal chemistry, 2010. 17(32): p. 3874-3908.

11 ACKNOWLEDGEMENTS

First and foremost, I would like to send my sincere thanks to my supervisor, Prof. Dr. Helga Stopper, who provided me with the opportunity to engage in this thrilling and inspiring research project. I express deep gratitude for her guidance, support, encouragement, patience, and inspiration throughout my entire PhD study. Her knowledge, energy, and enthusiasm were crucial contributors to the success of my research. I truly consider myself fortunate to have completed my PhD study under her supervision.

I extend my appreciation to my PhD thesis committee members, Prof. Dr. Leane Lehmann and Prof. Dr. Markus Christmann, who have consistently been available and contributed valuable suggestions to this work during our annual progress report meetings.

I would like to express my gratitude to Dr. Carolin Kleider, a member of the working group led by Prof. Dr. Leane Lehmann in the Department of Food Chemistry at the University of Wuerzburg, Germany. Dr. Kleider conducted gas chromatography–mass spectrometry (GC/MS) and ultra-performance liquid chromatography-mass spectrometry (UHLC-MS/MS) for this study.

I express my gratitude to the National Research Fund (NRF) under the Kenyan Ministry of Higher Education and the DAAD for their financial support during my PhD studies in Germany. Specifically, I received support through the DAAD/NRF fellowship under the Kenyan-German Postgraduate Training Programme (ID no. 57343411).

I am deeply grateful for the research grants and valuable scientific input generously provided by Steigerwald Arzneimittelwerk GmbH and Bayer Consumer Health, located in Darmstadt, Germany, as well as by PhytoLab GmbH & Co. KG, situated in Vestenbergsgreuth, Germany. Their support has been instrumental in advancing my research and achieving the goals of this study.

I extend my heartfelt gratitude to the Graduate School of Life Sciences (GSLS) at the University of Wuerzburg for their unwavering support during my PhD journey. Thanks to their invaluable courses, workshops, and travel grants, I was able to not only enhance my academic knowledge

but also actively engage in international conferences, contributing to my overall growth and development as a researcher.

I would also like to extend my immense gratitude to my colleagues and lab mates in Prof. Dr. Stopper's working group for fostering a wonderful working environment and providing unwavering support. I am especially thankful to Dr. Ezgi Eyluel Bankoglu for generously offering her valuable time, support, and guidance during scientific discussions throughout my PhD journey. Additionally, I would like to express my appreciation to Mrs. Gabriele Curtaz-Wolz for her kind support and for nurturing a friendly atmosphere during my time in the lab.

I am grateful to the Institute of Pharmacology and Toxicology, led by Prof. Dr. Kristina Lorenz, for their unwavering support and the insightful weekly institute seminars, which greatly contributed to my PhD program. I would also like to extend my thanks to Mr. Joachim Schäffer for his invaluable technical support, and to Mrs. Heike Keim-Heusler for her assistance in the lab.

I am profoundly thankful to the School of Health and Human Sciences and the entire Pwani University in Kenya for their patience, steadfast support, and granting me study leave, which enabled me to pursue a PhD program in Germany.

Finally, I would like to express my heartfelt gratitude to my family. Sincerely, I owe an immense debt of thanks to my parents, my wife, Dr. Aziza Majid Swaleh El-Busaidy, and my lovely children, Rania and Manal, as well as to my brothers and sisters. Their continuous and unconditional love, emotional support, patience, and encouragement have been invaluable, enabling me to overcome all the challenges throughout my PhD journey.

- To my wife Aziza, your unwavering moral support and boundless love have been the cornerstone of my strength and resilience, guiding me through every challenge.
- To my beloved children, Rania and Manal, I cherish you both deeply. I express my heartfelt appreciation for your love, patience, and understanding during my pursuit of this doctoral degree. Your patience and understanding during my periods of intense study have been invaluable, serving as a constant source of motivation and joy. I am

deeply grateful for your love, patience, encouragement, and for creating a supportive environment at home throughout this journey, especially during the writing of this dissertation.

- Lastly, to my mother, Mrs. Maryam Omar Naji, and my late father, Mr. Said Aboud Hadi, I dedicate this work and my achievements to you. I am committed to continually striving to meet your expectations and realize your aspirations. Dad, may your spirit always accompany me and provide guidance throughout my future endeavors.

DEDICATION

This dissertation is dedicated to

My Family

13. APPENDIX

I). Tables on Dose Response of selected PAs in Rifampicin-pretreated HepG2 cells

Figure 19a: Europine (Ep)

GROUPS	Total MNi ± SD	#MNi ± SD	CBPI ± SD	Apo cells ± SD	Mit cells ± SD	Other cells ± SD
Co	31 ± 3.57	33 ± 3.88	1.858 ± 0.10	9 ± 4.13	12 ± 3.38	11 ± 4.19
Ep 1	29 ± 10.96	31 ± 11.31	1.882 ± 0.05	5 ± 2.47	16 ± 8.13	12 ± 4.24
Ep 3.2	36 ± 4.24	40 ± 6.36	1.802 ± 0.10	10 ± 1.41	14 ± 4.60	14 ± 2.47
Ep 10	42 ± 9.26	44 ± 10.32	1.814 ± 0.05	9 ± 4.87	15 ± 4.11	16 ± 2.10
Ep 32	45 ± 10.87	48 ± 12.42	1.801 ± 0.05	8 ± 5.31	11 ± 3.84	17 ± 2.14
Ep 100	62 ± 9.42*	71 ± 11.33*	1.822 ± 0.07	14 ± 6.75	15 ± 3.03	21 ± 6.79
Ep 320	67 ± 9.49*	76 ± 14.34*	1.704 ± 0.04*	14 ± 6.75	16 ± 2.97	15 ± 4.42
Ep 1000	55 ± 7.65*	71 ± 12.80*	1.422 ± 0.08*	28 ± 11.15*	6 ± 5.11	11 ± 5.87

Note: Europine (Ep; monoester PA) in rifampicin-pretreated HepG2 cells *p<0.05 compared to Co (solvent control). Concentrations of europine are in micromolar (µM). Total MNi= number of cells containing micronucleus in a 1000 binucleated cells; #MNi= number of micronucleus in 1000 binucleated cells; CBPI= cytokinesis-block proliferation index; Apo cells= number of apoptotic cells in 1000 cells; Mit cells= number of mitotic cells in 1000 cells; and other cells= represent abnormal cells in terms of their shapes, nuclear buds and/or nuclear bridges. Results are displayed as mean ± standard deviation (SD) from n=5.

Figure 19b: Lycopsamine (Ly)

GROUPS	Total MNi ± SD	#MNi ± SD	CBPI ± SD	Apo cells ± SD	Mit cells ± SD	Other cells ± SD
Co	33 ± 4.77	35 ± 5.39	1.877 ± 0.10	8 ± 3.01	13 ± 2.81	11 ± 4.03
Ly 1	28 ± 4.60	30 ± 5.30	1.935 ± 0.07	7 ± 1.41	17 ± 3.54	12 ± 0.35
Ly 3.2	33 ± 4.24	34 ± 3.89	1.864 ± 0.03	10 ± 2.12	15 ± 5.30	13 ± 4.95
Ly 10	37 ± 2.25	41 ± 3.61	1.828 ± 0.08	7 ± 3.19	12 ± 4.57	12 ± 2.99
Ly 32	39 ± 5.76	44 ± 6.50	1.818 ± 0.10	10 ± 5.52	10 ± 3.84	13 ± 3.09
Ly 100	40 ± 3.82*	46 ± 4.57*	1.871 ± 0.07	10 ± 4.17	13 ± 3.75	15 ± 3.57
Ly 320	53 ± 7.27*	58 ± 8.59*	1.832 ± 0.09	11 ± 3.62	14 ± 7.97	14 ± 2.40
Ly 1000	54 ± 4.66*	60 ± 5.10*	1.655 ± 0.02*	20 ± 9.06*	17 ± 7.34	14 ± 4.09

Note: Lycopsamine (Ly; monoester PA) in rifampicin-pretreated HepG2 cells *p<0.05 compared to Co (solvent control). Concentrations of lycopsamine are in micromolar (µM). Total MNi= number of cells containing micronucleus in a 1000 binucleated cells; #MNi= number of micronucleus in 1000 binucleated cells; CBPI= cytokinesis-block proliferation index; Apo cells= number of apoptotic cells in 1000 cells; Mit cells= number of mitotic cells in 1000 cells; and other cells= represent abnormal cells in terms of their shapes, nuclear buds and/or nuclear bridges. Results are displayed as mean ± standard deviation (SD) from n=5.

Figure 19c: Retrorsine (RT)

GROUPS	Total MNi ± SD	#MNi ± SD	CBPI ± SD	Apo cells ± SD	Mit cells ± SD	Other cells ± SD
Co	27 ± 3.06	31 ± 5.30	1.911 ± 0.04	2 ± 0.58	10 ± 1.61	12 ± 3.51
RT 1	32 ± 4.19	35 ± 4.75	1.808 ± 0.05	4 ± 1.00	8 ± 3.77	13 ± 3.79
RT 3.2	37 ± 8.22	41 ±8.55	1.842 ± 0.02	4 ± 1.32	9 ± 2.18	8 ± 0.87
RT 10	44 ± 9.00*	51 ± 12.62	1.811 ± 0.05	5 ± 1.00	7 ± 2.29	12 ± 1.61
RT 32	52 ± 1.89*	60 ± 3.69*	1.842 ± 0.04	8 ± 2.84*	6 ± 1.44	12 ± 3.55
RT 100	54 ± 12.87*	62 ± 16.69*	1.825 ± 0.02*	6 ± 1.32*	10 ± 4.37	13 ± 4.16

Note: Retrorsine (RT; cyclic-diester PA) in rifampicin-pretreated HepG2 cells *p<0.05 compared to Co (solvent control). Concentrations of retrorsine are in micromolar (µM). Total MNi= mean number of cells containing micronucleus in a 1000 binucleated cells; #MNi= mean number of micronucleus in 1000 binucleated cells; CBPI= cytokinesis-block proliferation index; Apo cells= mean number of apoptotic cells in 1000 cells; Mit cells= mean number of mitotic cells in 1000 cells; and Other cells= represent abnormal cells in terms of their shapes, nuclear buds and/or nuclear bridges. Results are displayed as mean ± standard deviation (SD) from n=3.

Figure 19d: Riddelliine (Rid)

GROUPS	Total MNi ± SD	#MNi ± SD	CBPI ± SD	Apo cells ± SD	Mit cells ± SD	Other cells ± SD
Co	27 ± 3.06	31±5.30	1.911 ± 0.04	2 ± 0.58	10 ± 1.61	12 ± 3.51
Rid 1	29 ± 3.97	32±6.35	1.868 ± 0.03	4 ± 0.58*	10 ± 2.08	7 ± 2.65
Rid 3.2	35 ± 4.27	40±1.80*	1.832 ± 0.05	3 ± 2.02	10 ± 2.47	6 ± 1.04
Rid 10	38 ± 0.76*	45±3.82*	1.851 ± 0.03	4 ± 0.50*	10 ± 3.04	8 ± 2.00
Rid 32	53 ± 11.62*	60±16.63*	1.840 ± 0.03	5 ± 1.26*	9 ± 5.13	7 ± 1.53
Rid 100	55 ± 7.05*	61 ± 6.11*	1.807 ± 0.03*	5 ± 1.76*	9 ± 0.29	8 ± 4.54

Note: Riddelliine (Rid; cyclic-diester PA) in rifampicin-pretreated HepG2 cells *p<0.05 compared to Co (solvent control). Concentrations of riddelliine are in micromolar (µM). Total MNi= number of cells containing micronucleus in a 1000 binucleated cells; #MNi= number of micronucleus in 1000 binucleated cells; CBPI= cytokinesis-block proliferation index; Apo cells= number of apoptotic cells in 1000 cells; Mit cells= number of mitotic cells in 1000 cells; and other cells= represent abnormal cells in terms of their shapes, nuclear buds and/or nuclear bridges. Results are displayed as mean ± standard deviation (SD) from n=3.

Figure 19e: Seneciphylline (Sc)

GROUPS	Total MNi ± SD	#MNi ± SD	CBPI ± SD	Apo cells ± SD	Mit cells ± SD	Other cells ± SD
Co	26 ± 6.38	28 ± 7.42	1.854 ± 0.05	3 ± 2.02	8 ± 4.36	11 ± 4.19
Sc 1	29 ± 0.76	32 ± 1.15	1.810 ± 0.07	5 ± 1.73	10 ± 3.04	11 ± 7.37
Sc 3.2	35 ± 4.36	41 ± 6.83	1.802 ± 0.05	5 ± 2.50	10 ± 5.07	9 ± 1.53
Sc 10	34 ± 2.52	38 ± 3.82	1.820 ± 0.05	4 ± 2.29	9 ± 1.61	15 ± 3.18
Sc 32	35 ± 4.36	38 ± 4.00	1.801 ± 0.05	8 ± 5.01	12 ± 4.01	8 ± 3.51
Sc 100	47 ± 6.01*	53 ± 6.33*	1.764 ± 0.07	8 ± 4.37	11 ± 2.57	16 ± 4.19

Note: Seneciphylline (Sc; cyclic-diester PA) in rifampicin-pretreated HepG2 cells *p<0.05 compared to Co (solvent control). Concentrations of seneciphylline are in micromolar (µM). Total MNi= number of cells containing micronucleus in a 1000 binucleated cells; #MNi= number of micronucleus in 1000 binucleated cells; CBPI= cytokinesis-block proliferation index; Apo cells= number of apoptotic cells in 1000 cells; Mit cells= number of mitotic cells in 1000 cells; and other cells= represent abnormal cells in terms of their shapes, nuclear buds and/or nuclear bridges. Results are displayed as mean ± standard deviation (SD) from n=3.

Figure 19f: Echimidine (ED)

GROUPS	Total MNi ± SD	#MNi ± SD	CBPI ± SD	Apo cells ± SD	Mit cells ± SD	Other cells ± SD
Co	27±4.60	28±5.26	1.849±0.05	3±1.64	9±3.44	11±3.21
ED 1	30±4.92	34±4.28	1.785±0.04	6±1.52*	11±2.31	13±5.56
ED 3.2	33±3.15	36±4.01	1.809±0.05	7±2.15*	9±2.93	14±5.18
ED 10	44±15.70	49±19.36	1.794±0.03	7±1.29*	10±5.61	15±4.65
ED 32	41±3.44*	46±7.59*	1.765±0.09	9±2.72*	10±4.19	13±5.23
ED 100	44±7.82*	47±8.60*	1.802±0.04	12±3.95*	10±2.38	13±4.59
ED 320	51±3.18*	59±5.66*	1.752±0.04	10±1.53*	10±0.71	15±1.77

Note: Echimidine (ED; open chain-diester PA) in rifampicin-pretreated HepG2 cells *p<0.05 compared to Co (solvent control). Concentrations of echimidine are in micromolar (µM). Total MNi= number of cells containing micronucleus in a 1000 binucleated cells; #MNi= number of micronucleus in 1000 binucleated cells; CBPI= cytokinesis-block proliferation index; Apo cells= number of apoptotic cells in 1000 cells; Mit cells= number of mitotic cells in 1000 cells; and other cells= represent abnormal cells in terms of their shapes, nuclear buds and/or nuclear bridges. Results are displayed as mean ± standard deviation (SD) from n=5.

Figure 19g: Lasiocarpine (Las)

GROUPS	Total MNi ± SD	#MNi ± SD	CBPI ± SD	Apo cells ± SD	Mit cells ± SD	Other cells ± SD
Co	27±4.09	29±3.51	1.944±0.07	2±1.3	17±7.55	10±3.28
Las 0.1	30±1.73	33±0.76	1.872±0.07	2±0.8	12±1.61	9±3.21
Las 0.32	33±3.00	37±3.97	1.870±0.09	3±1.5	10±5.35	11±1.04
Las 1	35±4.65	38±5.06	1.836±0.08	3±0.0	16±5.80	10±2.60
Las 3.2	51±4.93*	56±5.41*	1.814±0.09	4±1.5	15±5.11	9±3.51
Las 10	52±9.29*	59±9.73*	1.784±0.00*	6±1.0*	13±4.93	6±2.52

Note: Lasiocarpine (Las; open chain-diester PA) in rifampicin-pretreated HepG2 cells *p<0.05 compared to Co (solvent control). Concentrations of lasiocarpine are in micromolar (µM). Total MNi= number of cells containing micronucleus in a 1000 binucleated cells; #MNi= number of micronucleus in 1000 binucleated cells; CBPI= cytokinesis-block proliferation index; Apo cells= number of apoptotic cells in 1000 cells; Mit cells= number of mitotic cells in 1000 cells; and other cells= represent abnormal cells in terms of their shapes, nuclear buds and/or nuclear bridges. Results are displayed as mean ± standard deviation (SD) from n=3.

II). Cross-reactivity analysis of chemical inhibitors on Influx-mediated transporters

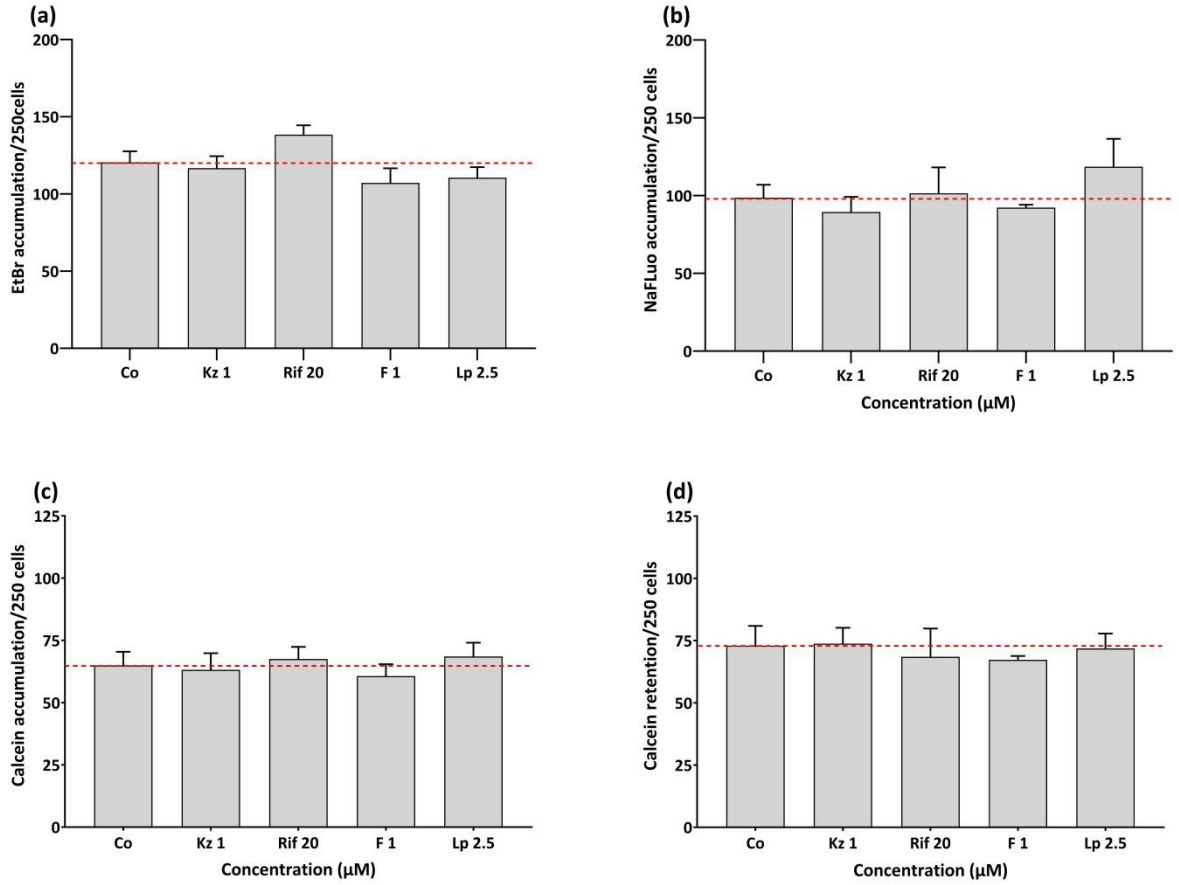

Figure 56: Cross-reactivity analysis of chemical inhibitors on membrane transporters based on accumulation and/or retention of the probe substrate dyes. Graph **(a)**: analysis of OCT1-influx mediated transporter based on the uptake of probe substrate dye ethidium bromide (EtBr; for OCT1).. Graph **(b)**: analysis of OATP1B1 -influx mediated transporters based on uptake of probe substrate dye sodium fluorescein (NaFLuo; for OATP1B1).Graph **(c)**: analysis of MDR1 -efflux mediated transporter based on accumulation of probe substrate dye calcein-AM (MDR1). Graph **(d)**: analysis of MRP2 -efflux mediated transporter based on retention of probe substrate dye calcein (for MRP2). Co= solvent control; Kz 1= ketoconazole 1 µM; Rif 20: rifampicin 20 µM; F1: furafylline 1 µM; and Lp 2.5= loperamide 2.5 µM.

III). Tables on PAs of different ester type in HeLa H2B-GFP only cultured cells, co-culture system, and HepG2 only cultured cells

Figure 46a: Lasiocarpine (Las)

GROUPS	Total MNi ± SD	#MNi ± SD	CBPI ± SD	Apo cells ± SD	Mit cells ± SD	Others cells ± SD
Co (HeLa)	23 ± 5.70	24 ± 6.50	1.919 ± 0.04	65 ± 38.84	62 ± 29.28	10 ± 5.49
Co (HepG2+HeLa)	24 ± 3.72	26 ± 3.79	1.868 ± 0.03	37 ± 7.96	88 ± 11.75	10 ± 4.87
Co (HepG2)	28 ± 4.25	31 ± 6.00	2.020 ± 0.05	5 ± 1.53	21 ± 1.80	47 ± 26.25
Las 10 (HeLa)	24 ± 3.17	26 ± 3.83	1.895 ± 0.05	76 ± 54.52	66 ± 21.00	10 ± 4.80
Las 10 (HepG2+HeLa)	56 ± 5.92*#	64 ± 7.56*#	1.809 ± 0.03*#	44 ± 4.52	87 ± 5.34	11 ± 5.85
Las 10 (HepG2)	60 ± 6.25Δ	73 ± 11.30Δ	1.909 ± 0.17	7 ± 4.44	24 ± 8.13	44 ± 24.03

Note: Lasiocarpine (Las; open chain-diester PA) in HeLa H2B-GFP only cultured cells (HeLa), co-culture system (HeLa+HepG2) and HepG2 only cultured cells (HepG2). *p<0.05 compared to solvent control in HeLa H2B-GFP only cultured cells (DMSO; HeLa H2B-GFP). #p<0.05 compared to solvent control in co-culture system (DMSO; combination of HepG2+HeLa H2B-GFP). ΔP<0.05 compared to solvent control in HepG2 cells (DMSO; HepG2). Co= solvent control; Las= lasiocarpine 10 µM. Results are displayed as mean ± standard deviation (SD) from n=3.

Figure 46b: Riddelliine (Rid)

GROUPS	Total MNi ± SD	#MNi ± SD	CBPI ± SD	Apo cells ± SD	Mit cells ± SD	Other cells ± SD
Co (HeLa)	26 ± 4.57	29 ± 4.82	1.949 ± 0.02	50 ± 11.17	90 ± 23.46	12 ± 6.54
Co (HepG2+HeLa)	24 ± 6.24	27 ± 6.25	1.883 ± 0.07	27 ± 15.23	74 ± 17.76	7 ± 1.89
Co (HepG2)	26 ± 5.51	29 ± 6.64	2.033 ± 0.04	5 ± 3.12	95 ± 52.76	22 ± 8.58
Rid 100 (HeLa)	30 ± 3.06	33 ± 4.16	1.949 ± 0.01	56 ± 19.40	64 ± 7.97	13 ± 6.08
Rid 100 (HeLa+HepG2)	45 ± 5.11*#	55 ± 11.13*#	1.879 ± 0.04*	30 ± 8.25	24 ± 4.19*#	7 ± 3.25
Rid 100 (HepG2)	56 ± 10.56Δ	67 ± 13.07Δ	1.995 ± 0.02	7 ± 1.32	26 ± 5.86	33 ± 15.60

Note: Riddelliine (Rid; cyclic-diester PA) in HeLa H2B-GFP only cultured cells (HeLa), co-culture system (HeLa+HepG2) and HepG2 only cultured cells (HepG2). *p<0.05 compared to solvent control in HeLa H2B-GFP only cultured cells (DMSO; HeLa H2B-GFP). #p<0.05 compared to solvent control in co-culture system (DMSO; combination of HepG2+HeLa H2B-GFP). ΔP<0.05 compared to solvent control in HepG2 cells (DMSO; HepG2). Co= solvent control; Rid 100= riddelliine 100 µM. Results are displayed as mean ± standard deviation (SD) from n=3.

Figure 46c: Europine (Ep)

GROUPS	Total MNi ± SD	#MNi ± SD	CBPI ± SD	Apo cells ± SD	Mit cells ± SD	Others cells ± SD
Co (HeLa)	23 ± 1.04	25 ± 1.61	1.936 ± 0.03	45 ± 5.11	84 ± 17.50	11 ± 8.95
Co (HepG2+HeLa)	19 ± 2.27	23 ± 5.58	1.874 ± 0.08	35 ± 11.47	65 ± 23.15	10 ± 0.29
Co (HepG2)	28 ± 4.04	30 ± 4.91	2.009 ± 0.04	4 ± 2.93	26 ± 4.16	23 ± 2.36
Ep 320 (HeLa)	32 ± 6.61	35 ± 8.55	1.905 ± 0.06	36 ± 3.55	79 ± 7.42	8 ± 3.88
Ep 320 (HepG2+HeLa)	61 ± 2.02*#	73 ± 5.48*#	1.816 ± 0.08	33 ± 13.86	78 ± 2.90	11 ± 3.77
Ep 320 (HepG2)	76 ± 9.18Δ	89 ± 11.72Δ	1.923 ± 0.05Δ	9 ± 3.50	17 ± 1.89Δ	24 ± 9.30

Note: Europine (Ep; monoester PA) in HeLa H2B-GFP only cultured cells (HeLa), co-culture system (HeLa+HepG2) and HepG2 only cultured cells (HepG2). *p<0.05 compared to solvent control in HeLa H2B-GFP only cultured cells (DMSO; HeLa H2B-GFP). #p<0.05 compared to solvent control in co-culture system (DMSO; combination of HepG2+HeLa H2B-GFP). ΔP<0.05 compared to solvent control in HepG2 cells (DMSO; HepG2). Co= solvent control; Ep 320= europine 320 µM. Results are displayed as mean ± standard deviation (SD) from n=3.

IV). Mitotic Stages Indexes

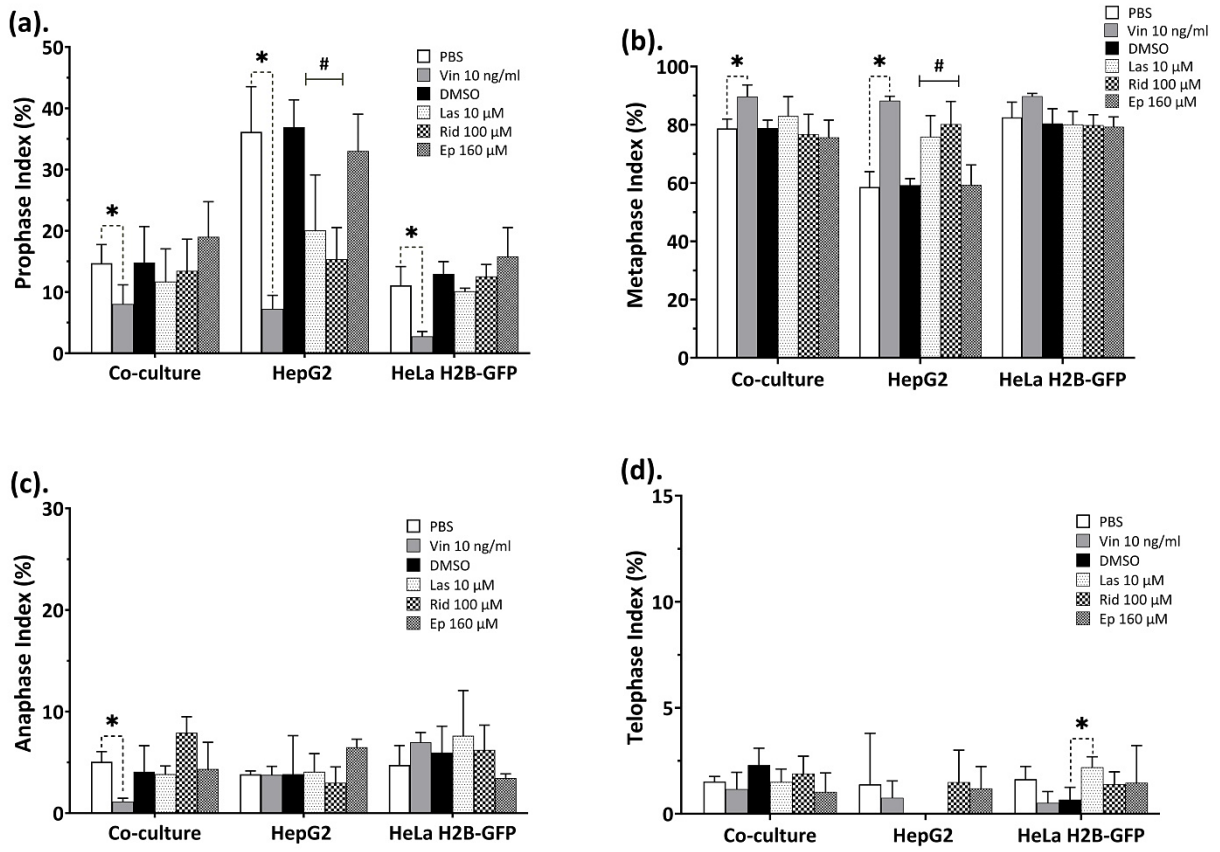

Figure 57: Mitotic stages index in HeLa H2B-GFP cells in co-culture, HepG2 only cultured cells, and HeLa H2B-GFP only cultured cells. Graph (a); represent prophase. Graph (b); represent metaphase index. Graph (c); represent anaphase index. Graph (d); represent telophase index. Each mitotic stage index is represented in percentage (%) against a total number of mitotic cells counted in a 1000 nuclei cells. Results are presented as mean ± standard deviation (SD) of three replicates within the same experiment and *p<0.05 compared to PBS as solvent control; #p<0.05 compared to DMSO as solvent control; ∇p<0.05 significant decrease effect against DMSO as solvent control. PBS= solvent control used for vincristine; DMSO= solvent control used for PAs; Vin 10 ng/ml= vincristine 10 ng/ml; Las 10 µM= lasiocarpine 10 µM; Rid 100 µM= riddelliine 100 µM; Ep 160 µM= europine 160 µM.

14. PERMISSIONS FOR THE USE OF PUBLISHED DATA IN THIS DISSERTATION

i. Permission acquired from Springer Nature Group to use contents of the research article published in the journal Archives of Toxicology for the following paper:

Naji Said Aboud Hadi, Ezgi Eyluel Bankoglu, and Helga Stopper. "Genotoxicity of Pyrrolizidine Alkaloids in Metabolically Inactive Human Cervical Cancer Hela Cells Co-Cultured with Human Hepatoma HepG2 Cells." Archives of Toxicology 97, no. 1 **(2023)**: 295-306.

Dear Dr. Hadi,

Thank you for contacting Springer Nature.

I can confirm that you can use it without permission from Springer Nature since you are also the author and the article is published as open access.

If you have any questions, please do not hesitate to contact us quoting your Ticket ID [#8533540].

With kind regards,
--
Conilyn Llander Llander Ocampo
Global Open Research Support Specialist
Author Service

Springer Nature Group
www.springernature.com

ii. Permission acquired from ELSEVIER to use contents of the research article published in the journal Mutation Research/Genetic Toxicology and Environmental Mutagenesis for the following paper:

Naji Said Aboud Hadi, Ezgi Eyluel Bankoglu, and Helga Stopper. "Genotoxicity of Pyrrolizidine Alkaloids in Metabolically Inactive Human Cervical Cancer Hela Cells Co-Cultured with Human Hepatoma HepG2 Cells." Archives of Toxicology 97, no. 1 (2023): 295-306.

Dear Naji Said Aboud Hadi,

Thank you so much for contacting us.

Please note that, as one of the authors of this article, you retain the right to reuse it in your thesis/dissertation. You do not require formal permission to do so. You are permitted to post this Elsevier article online if it is embedded within your thesis subject to proper acknowledgment;

Our preferred acknowledgement wording will be:

Example: “This article/chapter was published in Publication title, Vol number, Author(s), Title of article, Page Nos, Copyright Elsevier (or appropriate Society name) (Year).”

All the best for your thesis submission!

Kind regards,

Kaveri Thakuria

Senior Copyrights Coordinator

ELSEVIER | HCM - Health Content Management

Visit Elsevier Permissions

15. PUBLICATIONS

The following publications are relevant for this dissertation

i. **Hadi, Naji Said Aboud**, Ezgi Eyluel Bankoglu, and Helga Stopper. "Genotoxicity of Pyrrolizidine Alkaloids in Metabolically Inactive Human Cervical Cancer Hela Cells Co-Cultured with Human Hepatoma HepG2 Cells." Archives of Toxicology 97, no. 1 **(2023)**: 295-306.

ii. **Hadi, Naji Said Aboud**, Ezgi Eyluel Bankoglu, Lea Schott, Eva Leopoldsberger, Vanessa Ramge, Olaf Kelber, Hartwig Sievers, and Helga Stopper. "Genotoxicity of Selected Pyrrolizidine Alkaloids in Human Hepatoma Cell Lines HepG2 and Huh6." Mutation Research/Genetic Toxicology and Environmental Mutagenesis **(2021)**. 861-862:p. 503305.

16. CURRICULUM VITAE

17. AFFIDAVIT

I hereby confirm that my thesis entitled 'In vitro studies on the genotoxicity of selected pyrrolizidine alkaloids' is the result of my own work. I did not receive any help or support from commercial consultants. All sources and / or materials applied are listed and specified in the thesis.

Furthermore, I confirm that this thesis has not yet been submitted as part of another examination process neither in identical nor in similar form.

Wuerzburg, 28.03.2024 Signature

Eidesstattliche Erklärung

Hiermit erkläre ich an Eides statt, die Dissertation 'In-vitro-Studien zur Genotoxizität ausgewählter Pyrrolizidinalkaloide' eigenständig, d.h. insbesondere selbständig und ohne Hilfe eines kommerziellen Promotionsberaters, angefertigt und keine anderen als die von mir angegebenen Quellen und Hilfsmittel verwendet zu haben.

Ich erkläre außerdem, dass die Dissertation weder in gleicher noch in ähnlicher Form bereits in einem anderen Prüfungsverfahren vorgelegen hat.

Würzburg, 28.03.2024 Unterschrift